AMRL-TR-77-33

RESEARCH AND SIMULATION IN SUPPORT OF NEAR REAL TIME / REAL TIME RECONNAISSANCE RPV SYSTEMS

GILBERT KUPERMAN
SYSTEMS RESEARCH LABORATORIES, INC.
2800 INDIAN RIPPLE ROAD
DAYTON, OHIO 45440

WILLIAM N. KAMA
AEROSPACE MEDICAL RESEARCH LABORATORY

JOSEPH FRAGGIOTTI
JOHN KETTLEWELL
SYSTEMS RESEARCH LABORATORIES, INC.

JUNE 1977

AEROSPACE MEDICAL RESEARCH LABORATORY
AEROSPACE MEDICAL DIVISION
AIR FORCE SYSTEMS COMMAND
WRIGHT-PATTERSON AIR FORCE BASE, OHIO 45433

NOTICES

When US Government drawings, specifications, or other data are used for any purpose other than a definitely related Government procurement operation, the Government thereby incurs no responsibility nor any obligation whatsoever, and the fact that the Government may have formulated, furnished, or in any way supplied the said drawings, specifications, or other data, is not to be regarded by implication or otherwise, as in any manner licensing the holder or any other person or corporation, or conveying any rights or permission to manufacture, use, or sell any patented invention that may in any way be related thereto.

Please do not request copies of this report from Aerospace Medical Research Laboratory. Additional copies may be purchased from:

National Technical Information Service
5285 Port Royal Road
Springfield, Virginia 22161

Federal Government agencies and their contractors registered with Defense Documentation Center should direct requests for copies of this report to:

Defense Documentation Center
Cameron Station
Alexandria, Virginia 22314

TECHNICAL REVIEW AND APPROVAL

AMRL-TR-77-33

This report has been reviewed by the Information Office (OI) and is releasable to the National Technical Information Service (NTIS). At NTIS, it will be available to the general public, including foreign nations.

This technical report has been reviewed and is approved for publication.

FOR THE COMMANDER

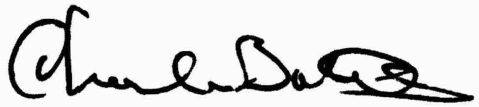

CHARLES BATES, JR.
Chief
Human Engineering Division
Aerospace Medical Research Laboratory

AIR FORCE/56780/25 August 1977 — 125

DISCLAIMER NOTICE

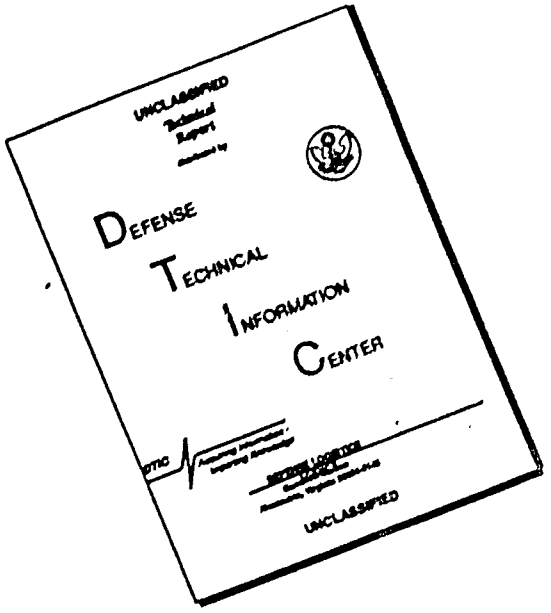

THIS DOCUMENT IS BEST QUALITY AVAILABLE. THE COPY FURNISHED TO DTIC CONTAINED A SIGNIFICANT NUMBER OF PAGES WHICH DO NOT REPRODUCE LEGIBLY.

SECURITY CLASSIFICATION OF THIS PAGE (When Data Entered)

REPORT DOCUMENTATION PAGE

READ INSTRUCTIONS BEFORE COMPLETING FORM

1. REPORT NUMBER: AMRL-TR-77-33	2. GOVT ACCESSION NO.
3. RECIPIENT'S CATALOG NUMBER	
4. TITLE (and Subtitle): RESEARCH AND SIMULATION IN SUPPORT OF NEAR REAL TIME/REAL TIME RECONNAISSANCE RPV SYSTEMS	5. TYPE OF REPORT & PERIOD COVERED: Technical report for the period Dec 75-Jun 76
	6. PERFORMING ORG. REPORT NUMBER
7. AUTHOR(s): Gilbert Kuperman, (SRL)* John Kettlewell (SRL); William N. Kama, (AMRL); Joseph Fraggiotti (SRL)	8. CONTRACT OR GRANT NUMBER(s): In part under F33615-75-C-0127
9. PERFORMING ORGANIZATION NAME AND ADDRESS: Aerospace Medical Research Laboratory, Aerospace Medical Division, Air Force Systems Command, Wright-Patterson Air Force Base, Ohio 45433	10. PROGRAM ELEMENT, PROJECT, TASK AREA & WORK UNIT NUMBERS: 62202F; 7184-04-28
11. CONTROLLING OFFICE NAME AND ADDRESS	12. REPORT DATE: June 1977
	13. NUMBER OF PAGES: 262
14. MONITORING AGENCY NAME & ADDRESS (if different from Controlling Office)	15. SECURITY CLASS. (of this report): UNCLASSIFIED
	15a. DECLASSIFICATION/DOWNGRADING SCHEDULE

16. DISTRIBUTION STATEMENT (of this Report)

Approved for public release; distribution unlimited

17. DISTRIBUTION STATEMENT (of the abstract entered in Block 20, if different from Report)

18. SUPPLEMENTARY NOTES

*The work reported herein was performed, in part, by Systems Research Laboratories, Inc., 2800 Indian Ripple Road, Dayton, Ohio 45440. A portion of this work was performed at the request of the Remotely Piloted Vehicle Special Project Office, Aeronautical Systems Division, WPAFB, OH.

19. KEY WORDS (Continue on reverse side if necessary and identify by block number)

Real time reconnaissance
Target acquisition performance
Sensor evaluation
Simulation
RPV
Operator performance

20. ABSTRACT (Continue on reverse side if necessary and identify by block number)

A facility was developed for assessing operator performance in target recognition and interpretation tasks using real time and near real time electro-optical sensor imagery. A programmable image scanner was upgraded to generate simulated sensor imagery under operational flight profiles. A study was performed to compare operator performance against three candidate sensors. The study utilized two V/H levels, the operationally preferred and the

DD FORM 1 JAN 73 1473 EDITION OF 1 NOV 65 IS OBSOLETE

SECURITY CLASSIFICATION OF THIS PAGE (When Data Entered)

00

Continuation of Item 20:

minimum commensurate with RPV survivability. Significant findings were developed for the dependent measures of: percent of targets detected, time on display until detection, ground range at detection, slant range at detection, and displayed image scale at detection. Accuracy of interpretation and interpreter confidence did not yield significant results. These results were combined with analytically based performance measures to produce a sensor comparison table in which twelve criteria, weighted by their respective operational impact, were used. A slewable television camera, equipped with zoom optics, and supported by a near real time playback capability achieved the highest performance score. Additionally, seventeen areas were identified in which future investigations could provide operationally important findings to the RPV Special Project Office.

PREFACE

This report documents a series of investigations conducted by the Visual Display Systems Branch, Human Engineering Division of the Aerospace Medical Research Laboratory. A portion of the work was requested by the Remotely Piloted Vehicle Special Projects Office. The effort was supported, in part, by Systems Research Laboratories, Inc., Dayton, Ohio, under Air Force contract F33615-75-C-0127. Mr. Thomas A. Furness III, Chief, Visual Display Systems branch, is the Air Force project officer.

The research covered herein was accomplished during the period: December 1975-June 1976. The authors express their appreciation to the following people who contributed to the success of the project: Capt J. D. Silliman (Control Systems Group, Aeronautical Systems Division [ASD], Program Manager for Near Real Time Reconnaissance); Mr. Eugene Wolanski (Photographic Branch, ASD, liaison at RPV SPO); Mr. Frederick Bodine (Systems Research Laboratories, Inc., electronic support); and Mrs. Katherine Berisford (SRL, data analysis). Special acknowledgments are extended to Mr. Leonard C. Crouch (Dynamics and Environmental Evaluation Branch, AF Avionics Laboratory), who assisted us in locating the imagery used in the sensor simulations; and to Lt Col Robert Hilgendorf (Recon/Strike SPO, ASD), who reviewed and refined the experimental design.

TABLE OF CONTENTS

TABLE OF CONTENTS (cont'd)

TABLE OF CONTENTS

LIST OF ILLUSTRATIONS

APPENDIX
LIST OF ILLUSTRATIONS

APPENDIX
LIST OF ILLUSTRATIONS (Cont'd)

APPENDIX

LIST OF ILLUSTRATIONS (Cont'd)

LIST OF TABLES

APPENDIX
LIST OF TABLES

Section 1

INTRODUCTION

GENERAL

An overview of the entire effort and analyses of sensor and operator trade-off considerations of the real time, daylight reconnaissance remotely piloted vehicle (RPV) mission and of system performance evaluation criteria is presented. Appendices A-C present detailed descriptive and analytic treatments of the three sensors studied during this project. Appendix D presents the analytic considerations required to implement simulations of these sensors on the Programmable Image Scanner (PIS).

BACKGROUND

The purpose of this effort was to provide engineering design criteria and trade-off data to assist the Remotely Piloted Vehicle Special Project Office (RPV SPO) in (1) choosing an optimum operational daylight near real time/real time (NRT/RT) reconnaissance system, and (2) designing and developing advanced near real time systems.

The objectives of the AMRL NRT/RT Reconnaissance RPV Program were predicated on both immediate and future requirements of the RPV SPO. They were (1) short-term, FY76, perform an assessment of the operator's target acquisition capability, comparing tracking and overflight sensors; and (2) long-term, FY78, provide an advanced simulation capability for postulated NRT/RT reconnaissance system requirement.

The short-term objective was accomplished within the context of the BGM-34C vehicle (low altitude, high subsonic) profile, and included consideration of the KA-98 laser line scan, the Teledyne-Brown Engineering gated video, and a typical slewable video (including tracker) sensor. Emphasis was placed on daylight reconnaissance although generalization to night mission capabilities was considered where possible. Satisfaction of the short-term requirement formed the basis for accomplishing the long-term objective. The technical approach involved four stages:

1. Systems Analysis: The concept of operations for the RPV and the technical specifications of the candidate sensor systems were studied and analyzed to determine realistic scenarios for simulation, capabilities required in the simulation facility, and criteria against which to evaluate target acquisition performance.

2. Systems Simulation Capability: The available image generation sources were evaluated against simulation requirements, and the PIS was upgraded to satisfy the short-term objective.

3. Target Acquisition: A series of man-in-the-loop experiments were designed, conducted, and analyzed to assess operator performance in target acquisition and first phase interpretation tasks. The candidate sensors were compared by operationally significant dependent measures.

4. Plan for Future Investigations: Based on the systems analysis, the results of the simulations, and interaction with both the RPV SPO and system operator, a series of future experiments were to be formulated and proposed. The plan was to include refinement of the simulation capability to support advanced/additional sensors and image processing/enhancement/transmission characteristics.

Systems Analysis

Background material for the systems analysis was obtained in three ways. A literature search and review was performed which included program documentation, test and evaluation reports, concepts of operation for both the collection and exploitation systems, projected requirements for real time reconnaissance, image interpretation reporting requirements, and information display and human engineering studies. Briefings were attended which encompassed program planning, operational experience, sensor capabilities and planned developments, and ground imagery exploitation facilities. In addition, the analysis team participated as observers in sensor flight tests of the Teledyne-Brown camera.

Systems Simulation Capability

Because of simulation requirements, the AMRL/HEA PIS was selected as the image generation source. The PIS was designed for 5 inch format strip photography and was significantly upgraded to satisfy the requirements for resolution, footprint shape, raster generation, and image scale ranges imposed by the sensor and mission characteristics. Key features of the upgrading are identified below:

1. Image Generation: New 5 and 10 inch diameter flying spot scanner tubes were utilized. The larger diameter tube permitted greater electronic and optical demagnification at increased resolution, while both tubes provided a smaller spot size than was previously obtainable. New high voltage and focus voltage power supplies were utilized to minimize noise. Installation of the large tube required new precision sweep deflection yoke, focus coil, and custom designed tube mounting and coil micropositioners.

2. Optical/Mechanical: New high resolution, large aperture lenses (210, 102, and 58mm focal lengths) were acquired. Manually adjustable mounts and lens positioners were fabricated. An automatic lens changer was designed and fabricated (to simulate the change in modes of operation for the Teledyne-Brown sensor). A new film transport (9-1/2, 5 inch and 70mm formats), with digital control

and readout of film position, was designed and fabricated. A new, 16 inch diameter, 21 inch focal length, condenser lens was acquired and mounted. The optical table was upgraded to accommodate the new components.

3. Electronic: A new photomultiplier tube and power supply provided increased sensitivity and reduced noise. New analog sweep circuits were developed to simulate the unrectilinearized, wide field of view (FOV) KA-98 sensor. Analog sweep circuits were modified to simulate the Teledyne-Brown NAV mode and the slewable television sensors. New digital sweep and sweep control circuits were developed to simulate the Teledyne-Brown RECON mode. New video amplification and processing circuitry was developed to enhance the video signal-to-noise ratio (SNR) and permit simulation of a horizon and of far-field imagery.

4. Imagery: The imagery holdings of AMRL were screened to determine if film was available which provided the required combination of scale, lateral coverage, resolution, and target types. In addition, DIA, DMA, RADC, and AFAL were contacted for support in this area. Nine inch format, strip photography (KA-18, six inch focal length) which satisfied the requirements of these simulations was obtained from AFAL.

5. Overall Capability: The PIS now provides a highly versatile image generation capability for sensor system simulation. It affords the user interactive, dynamic control of displayed scene perspective over a wide range of sensor and aircraft characteristics. Areas of application include sensor comparisons, image metrics studies, system sensitivity investigation (weather, flight profiles, counter-measures, etc.), enhancement technique development, and mission/test planning. The PIS upgrading and capabilities are described in Section 4.

Target Acquisition Experiments

In order to investigate the man/machine capabilities and limitations of NRT/RT reconnaissance, a sequence of related operator target acquisition experiments were deemed necessary. Much of the performance data exploited in the comparison of candidate sensors (Section 6) were developed through these studies.

A two-factor, repeated measures, experimental design was used. The two factors of interest were sensor type and altitude (AGL). Three levels of sensor type were used. Level I was a laser line scan sensor (KA-98), Level II was a slewable TV sensor, and Level III was an overflight TV sensor (Teledyne-Brown). Table 7 presents the salient specifications for these three sensors. Two levels of altitude were used. Level I was 500 feet and Level II was 1,000 feet.

Significant effects ($p < .05$, where p is the probability that the effect was due solely to chance) were established for the dependent measures of percent of targets detected, time on display until detection, ground range at detection, slant range at detection, and displayed image scale at detection. Post hoc statistical analyses were used to locate the cause of each significant effect. Additional analyses were employed to study the sensors at 500 feet AGL, the reference altitude of the sensor performance comparison.

Plan for Future Investigations

Seventeen areas for potential experimental study were identified to the RPV SPO for consideration. These areas were judged to be of program or operational significance based on one or more of the following:

1. Analytic studies
2. Empirical data
3. Program management documentation
4. Operational briefings
5. Interaction with the RPV SPO

These areas and their underlying operational significance are identified and proposed investigative procedures are described in Section 7.

Section 2
SENSOR SYSTEM REQUIREMENTS

MISSION REQUIREMENTS

The requirements for an aircraft/RPV mission determine the types of sensors to be used, and the sensors define the inputs to the display. The mission requirements also determine the tasks that the human operator must perform when using the display, and his required level of proficiency.

The basic requirement of any imaging system for airborne applications is to provide the information necessary for target detection, recognition, and location. An image forming sensor must be capable of discerning small contrast differences so that a large variety of tactical targets can be detected from their backgrounds. The sensor must provide the necessary spatial resolution so that the detected targets can be recognized and interpreted. Also, the collected data must usually be displayed with sufficient accuracy, and with ancillary data, so that the location of the target can be readily determined.

The major mission/scenario factors which are related to target acquisition include:

- o Size and mobility characteristics of the targets of interest
- o Degree to which natural or man-made cover provides concealment for the targets
- o Range of target/background contrast ratios
- o Degree to which the terrain limits flight altitudes and reconnaissance tactics
- o Frequency and degrees of adverse weather conditions
- o Level of conflict and anticipated enemy tactics
- o Threat in terms of types, number, and placement of surface-to-air defenses

In selecting system characteristics for meeting the operational requirements, such factors as available technology and system complexity must be

considered. Since most system parameters are interrelated, trade-offs are always necessary, based upon the overall requirements of performance, cost, and schedule.

INTERPRETATION CONSIDERATIONS

Image interpretation is concerned with the development of new information for updating of the intelligence data base. The task of the image interpreter is to extract militarily significant intelligence data from various kinds of aerially obtained imagery. From a psychological standpoint, transformation of information from recorded or displayed images into intelligence information falls within the domains of sensation, perception, and cognition.

Analyses to enhance the effectiveness of image interpretation must deal with many variables. There is concern not only with the type of imagery (television, infrared, laser, etc.) but also how the terrain was viewed (vertical, oblique, panoramic). Images differ in scale and quality dimensions. They also differ in content: they may depict different types of terrain (jungle, mountains, swamp, desert); they may have been obtained under different degrees of enemy deployment in terms of target type and density. With respect to the interpreter, there are differences in ability, background, experience, and training. In addition, the information requirements differ as a function of the combat level, the user organization, and echelon.

How well the image interpreter performs his assigned task of extracting the Essential Elements of Information (EEI's) requires evaluation of at least the three following performance indices: accuracy, completeness, and timeliness of information. One research (Birnbaum, 1969) indicates that while cumulative completeness increases as a function of time, cumulative accuracy decreases. Furthermore, accuracy can be traded for completeness, and vice versa. Various other trade-offs involving accuracy, completeness, and interpretation time can be made.

SENSOR CONSIDERATIONS

The first decision that the designer must make is the selection of the sensor, or sensors, to collect the intelligence data. This selection is based upon the quality and quantity of information that must be obtained from the target area, the types of targets and their signatures, the collection conditions (all-weather, day/night, overt/covert, RPV characteristics, etc.), and installation and cost constraints. Sensors can be categorized many different ways. One method is by their spatial coverage relative to the air vehicle.

Down Looking Sensors

These sensors provide maximum target unmasking and can produce good ground resolution, both of which are very important in situations involving a high degree of cover and the requirements for resolving small target details. A stable platform may be needed to achieve the desired level of performance. Moreover, it is necessary that the sensor overfly the entire line of coverage or point target under surveillance. Thus, the probability of survival of the RPV could be unacceptably low in some encounter situations. Another shortcoming stems from the fact that often just one frame of imagery containing the target is acquired. As a consequence, the improvement in target detection which results from a varying aspect angle is not realized. In addition, target tracking (required for recce/strike operation) cannot be accomplished.

Both line scan and raster scan electro-optical sensors have been employed in down looking configurations. Infrared line scan (DLIR) and laser line scan (DLLLS) sensors have been developed. The laser line scan sensor is typified by the KA-98 system; the downward looking raster scan sensor is exemplified by the RECON mode of the Teledyne-Brown television system.

Slewable (Variable Pointing) Sensors

These types of sensors are valuable for providing:

- o The capability for offset/standoff and orbital tactics as well as flyover.
- o More than one look (or more than one frame at TV rates) at the same target from different aspect angles.
- o More time on the display for targets in low masking situations. This increases the probability of detection and recognition of some targets, as well as the opportunity of redirection of the flight path prior to target flyover.
- o The capability for viewing underneath vegetation and camouflage.
- o Information concerning the vertical dimension or upright sides of targets. (The importance of vertical dimension/height cues as aids in target detection and recognition has been demonstrated.)
- o Information for use in navigation checkpointing and position updating, an important function in areas where few prominent/unique checkpoints are available but precision navigation is required.
- o Early threat detection and avoidance.
- o A more natural view of objects than with nadir-viewing systems.

Electro-optical sensors which have been employed with gimbaled mounts include raster scan infrared (FLIR), and both conventional and low-light-level television (LLLTV) systems.

Forward Looking/Side Looking Sensors

Fixed ("strap down") forward looking and side looking sensors exhibit some of the attributes of the slewable sensor; however, their mission flexibility is greatly decreased. For example, deviations from the prebriefed flight plan normally cannot be tolerated. The NAV mode of the Teledyne-Brown system falls in this category.

DISPLAY CONSIDERATIONS

The video display is a critical interface with the image interpreter in the airborne target search and identification mission. An information display system consists of both the sensor video display and the visual system of the interpreter. The visual system characteristics will limit the total system performance, as will the video display.

There has been a steady, rapid increase in the performance of airborne image forming sensors in the last few years, and the resolution and image quality of sensors used for reconnaissance has improved substantially. In addition, new sensors, such as FLIR, have been developed.

During this same time period, however, there have been few major improvements and new approaches for airborne displays that can match the performance of these sensors. The problem of displaying the sensor output is compounded in many system applications by requirements for alternately displaying the output of several sensors, each with a different format and frame rate, on a single time-shared display. In addition, computer driven symbology for such functions as air vehicle steering must often be simultaneously presented.

Visual Acuity

Visual acuity is operationally defined as the reciprocal of the angle in minutes of arc subtended by the smallest detail which can be resolved by the human eye under a given set of viewing conditions. Values of visual acuity vary as a function of the type of visual target presented, the type of display system used to present it, the environmental conditions under which it is viewed, and the method of measurement employed. Five measures of acuity are in use: minimum visible, minimum perceptible, minimum separable, vernier, and stereoscopic. Minimum separable acuity is the measure most useful for display design purposes. Minimum separable acuity is defined as the minimum amount of separation necessary for two light sources (or two nonluminous images, i.e., parallel bars) to be perceived as distinct objects.

The human eye, under ideal conditions, can resolve details as small as 0.3 seconds of arc; however, the eye is not a perfect optical system and does not normally view stimuli under perfect conditions. For this reason, the normalized value of one minute of arc is commonly accepted as the minimum resolvable limit of the eye; but, this value is invalid unless the operational and environmental conditions to which it is to be applied are specified.

Mathematical expressions defining the detection threshold of the eye as a function of such variables as display brightness, target contrast, number of sensor resolution elements across target, target angular size, search patterns, and observation time have been developed by a number of investigators. One such study (Bruns, 1970) found that the discriminative factors which contribute to rapid target identification are large size, high contrast, low jaggedness (shape), and low blur--in that order.

Display Types

At present, the best device for displaying the video information generated by electro-optical sensors is the cathode ray tube (CRT). A number of solid state displays are under development. These include such diverse techniques as electroluminesence, light emitting diodes, planer gas discharge, and liquid crystals.

Display system resolution is operationally defined as the quantification of the smallest discernible detail presented on the display. In a CRT display, the smallest discernible unit is the CRT spot size, while in a solid state display it is the size of the individual emitter. A number of system parameters interact to determine the size of the CRT spot and the apparent size of the solid state emitter.

PERFORMANCE REQUIREMENTS

It is the operator's task to acquire and interpret the targets of interest by evaluating the displayed imagery. To do this he must first make a literal identification of the target from its appearance on the display.

Many analytical and empirical studies have been conducted which indicate that operator performance is affected by a combination of equipment, observer, mission, and environmental variables. For convenience, these variables can be divided into two classes.

The first class might be called enabling variables. These parameters determine whether or not the target image appears on the display in recognizable form. The major variables in this case are resolution, contrast, and image size. They are enabling in the sense that certain minimum resolutions, contrast, and image sizes must be achieved in order for a literal identification to be made. Appearance of the target on the display in recognizable form is no guarantee that the observer will find it and identify it as a target. Therefore, the second set of variables bear upon the operator's ability to identify the target once a reasonable image is presented on the video display.

Considerable variation has been found among the experimental results of programs designed to predict operator performance under field conditions. This is due in part to the fact that variables affecting operator performance are many and interactive, while the number of variables which can be controlled during a given series of experiments is limited. Consequently, a mathematical model has not yet been developed to accurately describe the determinants of target imagery as it relates to the psychophysics of target identification.

Some general conclusions concerning target acquisition range are noted below (Self, 1971).

1. The size, contrast, and resolution of details in a target image influence how quickly and at what slant ranges a target can be found and identified. The background is also an important determinant.
2. Targets are frequently missed even though the displayed image is large and clearly resolved. When targets are found, their images are usually 1/3 to 1/2 the way down the display, despite the observer's attempts to acquire targets at long slant ranges.
3. Even at helicopter speeds, targets are usually at surprisingly close slant ranges when detected. When air vehicle speeds are high,

system performance is further reduced. When the displayed image is moving rapidly, the observer cannot perform the display scan task fast enough. This difficulty is largely due to the small angular field of clear vision at any one eye fixation plus lack of clear vision when the eye is in motion.

4. Real time target acquisition requires a minimum number of resolved TV lines across the target image. The number required is in the range of 6 to 10; i.e., the smallest detail of the target that is resolved is 1/6 to 1/10 of the target's maximum dimension. This is true despite the fact that one (or less) displayed resolution element can be seen by the observer. Unless attention is directed to the specific spot, among the many spots on the display, target acquisition cannot be accomplished in any meaningful sense. A spot must have enough form to call it a target.
5. Target identification requires 12-20 TV type resolution elements across the target image. This means that not only is the target image spread across the several TV lines but that details are resolved.
6. The maximum dimension of the target image on the display should subtend an angle of 10-20 minutes of arc at the observer's eye. Smaller images, even if containing fine details, lead to long detection times, short acquisition ranges, and low percentages of targets detected.
7. The above rules on resolution determine, with a given sensor and display, the maximum acquisition and identification ranges, but do not mean that acquisition will occur at the given maximum ranges. The nature of the human observer is such that, on the average, acquisition ranges will be much less than the maximum permitted by displayed target image size and resolution.
8. The number of resolved TV lines required across the target for acceptable detection, identification, and speed of observer response, combined with the rather small total number of available TV lines on displays, means that the ground swath width coverage has to be very narrow. This shortcoming can be alleviated by increasing the raster lines from the conventional 525 to a higher value, such as 875 or 1029.

Some of the more important factors, parameters, and their relationships are discussed herein. As can be seen, the results of various investigations related to airborne target acquisition have not all been in agreement. Consequently, the reference data presented during the following discussion is intended only to show the parametric relationships that must be considered during the design of a real time/near real time reconnaissance system. Additional reference material must be employed to assure that an optimum sensor system design is identified for meeting the specified mission requirements.

Figure 1 depicts many of the parameters which have been demonstrated to exercise a significant effect on operator performance.

FIELD OF VIEW

Selection of the sensor FOV depends primarily on determining an acceptable compromise between the requirements for good angular resolution and scale factor, and hence maximum detection/recognition range on one hand, and greater ground coverage for sufficient orientation and target time on the display on the other.

For sensors such as television and infrared, there are a finite number of resolution elements across the format. As a consequence, selection of a shorter optical focal length to increase the FOV, and therefore ground coverage, will reduce the angular resolution. Decreasing the focal length also decreases the scale, which causes the displayed target image to become smaller.

Use of a slewable sensor system would permit the operator to monitor a larger swath width by employing a smaller FOV, with its attendent improvement in angular resolution and scale. However, a point would be reached where, depending upon the RPV velocity/altitude ratio, a further decrease in the FOV would require sensor slewing at a rate which did not provide sufficient time on display for interpretation. An attempt by the operator to alleviate this problem by tracking during the search function would cause holidays (areas not covered by sensor) in the scan pattern. Improving the navigation accuracy

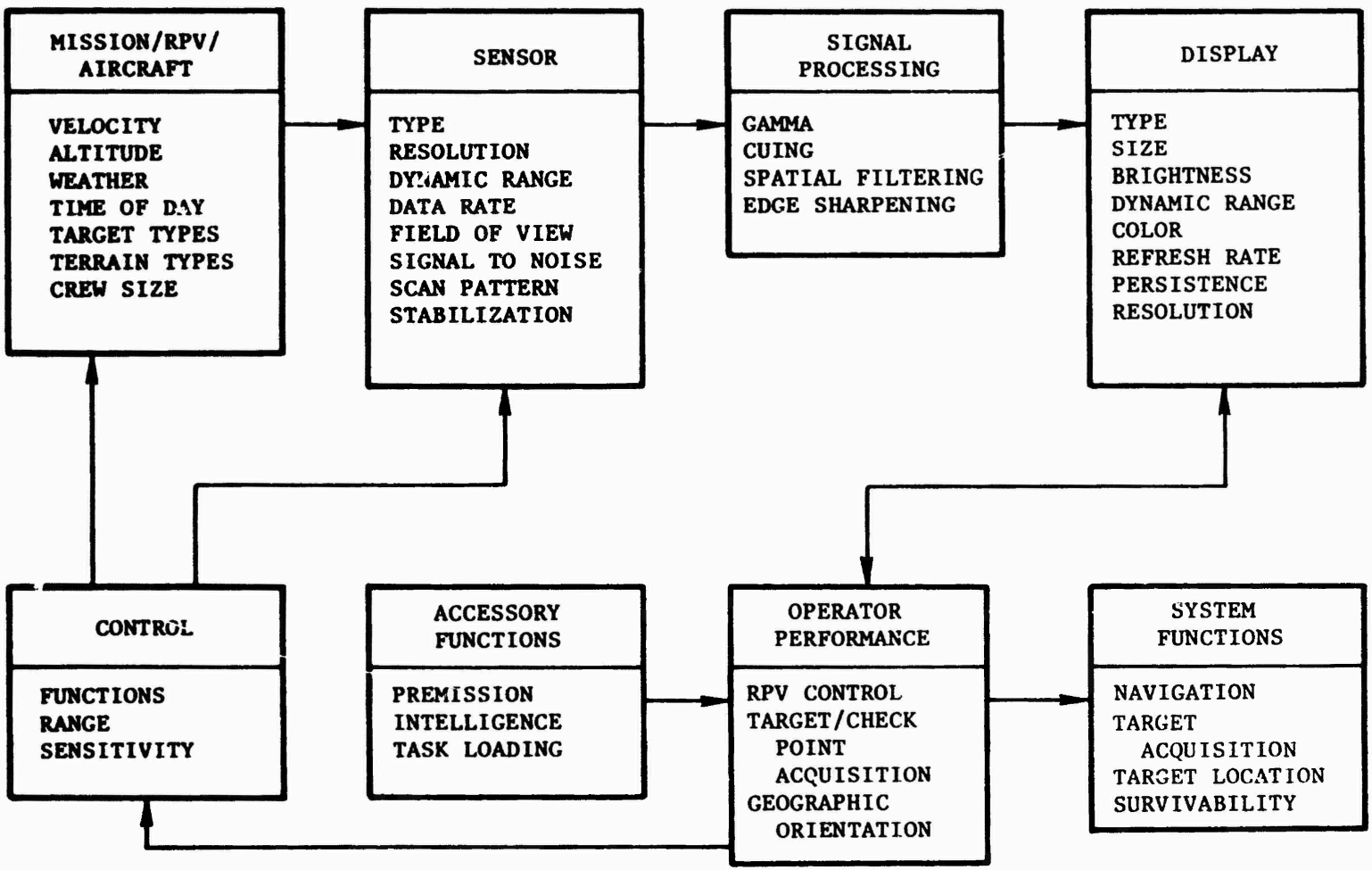

Figure 1. Critical System Parameters

reduces the scan pattern requirements and thus would permit use of a smaller FOV without the need for tracking.

SPATIAL RESOLUTION

The results of tests by various investigators have indicated a relationship between the number of resolution elements projected across the target and the decisions of detection, recognition, and identification. By orienting the resolved line pairs so that they were aligned with the critical target dimension, Johnson (1958) found that the minimum resolution required for a particular decision was a constant for nine military targets within a maximum error excursion of 25 percent. The results are presented in Table 1.

TABLE 1. RESOLUTION REQUIRED AT THE TARGET FOR THE TYPICAL LEVELS OF DECISION PERFORMED BY THE IMAGE INTERPRETER [1]

Target (Broadside View)	Resolution Per Minimum Dimension		
	Detection	Recognition	Identification
Truck	0.9	4.5	8.0
M-48 Tank	0.75	3.5	7.0
Stalin Tank	0.75	3.3	6.0
Centurian Tank	0.75	3.5	6.0
Half-Track	1.0	4.0	5.0
Jeep	1.2	4.5	5.5
Command Car	1.2	4.3	5.5
Soldier (Standing)	1.5	3.8	8.0
105mm Howitzer	1.0	4.8	6.0
Average (LP/MM)	1.0 ± 0.25	4.0 ± 0.8	6.4 ± 1.5

[1]This table was adapted from Johnson's work and appears widely in the literature.

Based upon experimental data by Brainard (1965) the probability of recognition as a function of the number of resolution elements projected across the target is presented in Figure 2. Notice that eight resolution elements will normally yield a probability of recognition of about 90 percent under ideal conditions. However, in practice, the actual number of resolution elements required depends upon additional factors such as the complexity of the target's shape, the image interpreter's ability, intercept (aspect) angle, and the degree of camouflage and concealment.

Perhaps the most significant requirements are those based upon the results actually experienced by image interpreters under combat conditions. The minimum scale required for the tasks of recognition and identification of typical tactical targets is presented in Table 2. The scales were computed for photographic cameras having an average dynamic resolution of 15 to 20 line pairs per millimeter. For this data to be useful in determining the performance of electro-optical sensors, the ground spot size corresponding to the scales and dynamic resolution employed in Table 2 will be calculated as follows.

Ground spot size (s) at the nadir can be found by

$$s = \alpha H \tag{1}$$

where

α = angular resolution (radians)

H = altitude AGL (feet)

The angular resolution (α) is defined by

$$\alpha = 2 \tan \frac{d}{2F}$$

$$\approx d/F \text{ radians} \tag{2}$$

where

d = elemental spot size at the image plane (mm)

F = focal length (mm)

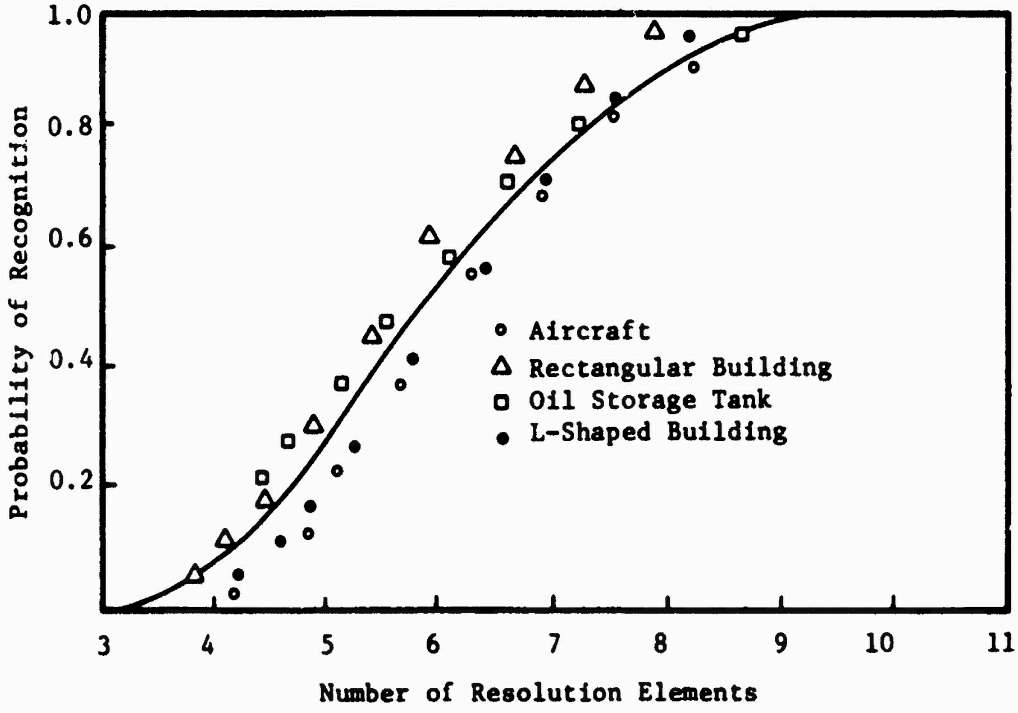

Figure 2. Probability of Recognition as a Function of Number of Resolution Elements Across Minimum Target Dimension

TABLE 2. MINIMUM SCALE FOR RECOGNITION AND IDENTIFICATION

Subject	Breakdown	Minimum Scale for	
		Recognition	Identification
Airfields	Major	1/30,000	1/10,000
	Auxiliary	1/30,000	1/10,000
Defensive Positions	Strong Points, Bunkers	1/10,000	1/5,000
	Trenches	1/15,000	1/5,000
	Foxholes	1/5,000	1/2,000
Military Equipment	Aircraft		
	Wing span under 60 ft	1/10,000	1/2,000
	Wing span 60-100 ft	1/15,000	1/2,000
	Wing span over 100 ft	1/20,000	1/5,000
	Antitank Missile Launcher	1/5,000	1/2,000
	Howitzers	1/5,000	1/2,000
	Helicopters	1/12,000	1/2,000
	Medium AA	1/8,000	1/2,000
	Surface-to-Air Missiles	1/10,000	1/2,000
	Surface-to-Surface Missiles	1/10,000	1/2,000
	Tanks, Trucks	1/8,000	1/2,000
Military Installations	Permanent	1/30,000	1/10,000
	Field	1/20,000	1/5,000
	Supply Dumps	1/30,000	1,10,000
Radar	Fixed	1/10,000	1/2,000
	Mobile	1/5,000	1/2,000
Transportation	Rail, Roads	1/30,000	1/8,000
	Inland Waterways	1/30,000	1/10,000
	Bridges over 100 ft	1/30,000	1/10,000
	Marshalling Yards	1/30,000	1/15,000
	Railway Cars	1/20,000	1/5,000
	Port Facilities	1/12,000	1/5,000
Industry	Major	1/30,000	1/12,000
	Minor	1/10,000	1/5,000
Utilities	Thermal Power Plants		
	Industrial	1/15,000	1/8,000
	Hydroelectric	1/30,000	1/10,000
	Municipal	1/30,000	1/10,000

The element spot size (d) is related to the dynamic film resolution (R_D) by

$$d = \frac{1}{2R_D} \quad \text{mm} \tag{3}$$

where

R_D = dynamic film resolution (ℓp/mm)

Thus, Eq. (2) can be written as

$$\alpha = \frac{1}{2R_D F} \quad \text{radians} \tag{4}$$

Reciprocal scale at the nadir (S_R) is given by

$$S_R = H/F$$

or

$$H = FS_R \tag{5}$$

When the above discussed relationships are inserted into Eq. (1), the ground spot size is related to reciprocal scale and dynamic resolution as indicated by the following equation.

$$s = \frac{S_R}{2R_D} \tag{6}$$

Since R_D was given as 17.5 ℓp/mm nominal

$$s = \frac{S_R}{2(17.5)(25.4)(12)}$$

$$s = 9.4 \times 10^{-5} S_R \quad \text{feet}$$

This relationship is plotted in Figure 3. The minimum ground spot size required for recognizing and identifying the typical targets shown in Table 2 are presented in Table 3.

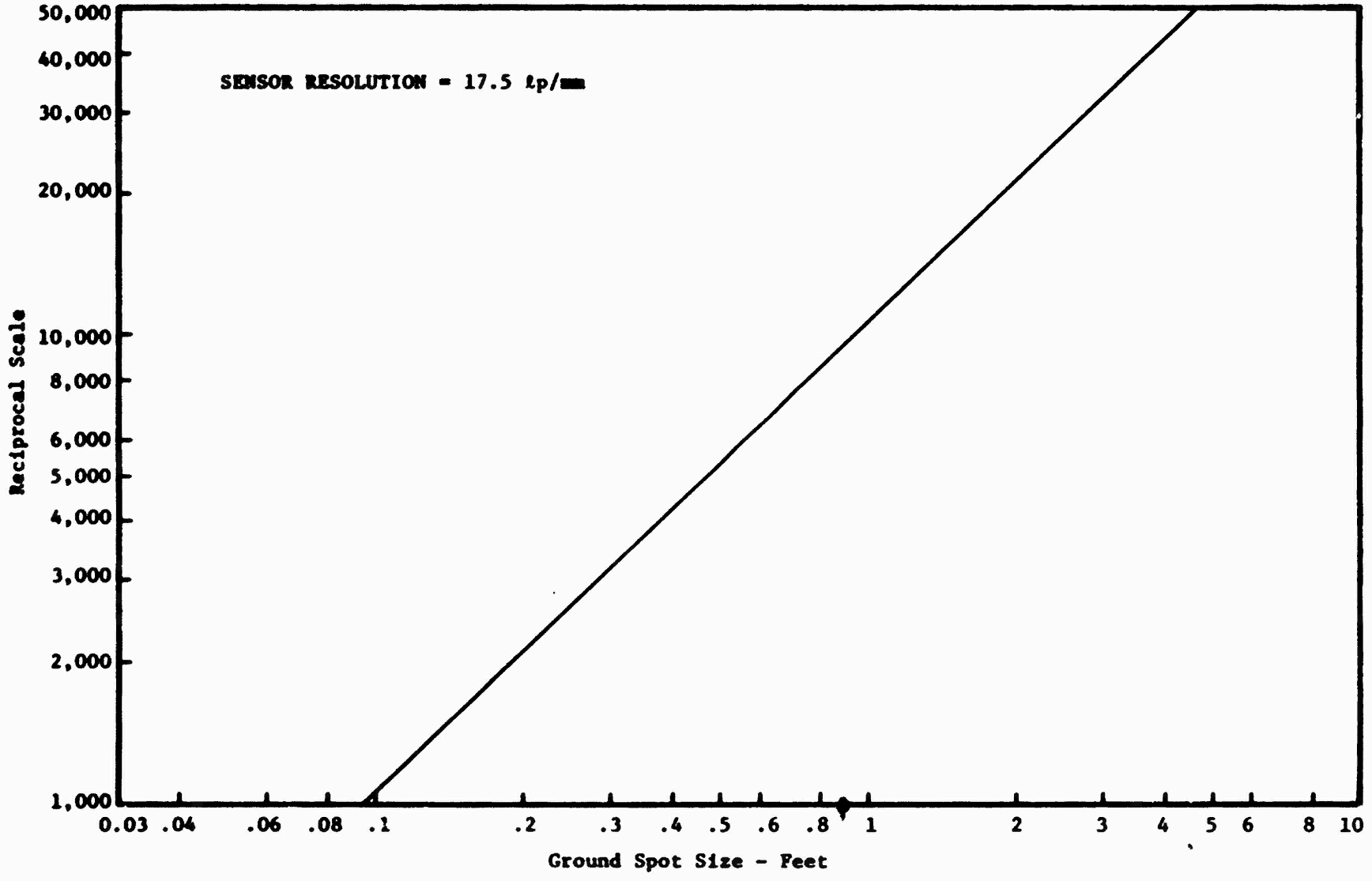

Figure 3. Conversion of Reciprocal Scale to Ground Spot Size

TABLE 3. MINIMUM SPOT SIZE (FEET) FOR RECOGNITION AND IDENTIFICATION*

Subject	Breakdown	Minimum Spot Size for	
		Recognition	Identification
Airfields	Major	3	1
	Auxiliary	3	1
Defensive Positions	Strong Points, Bunkers	1	0.5
	Trenches	1.5	0.5
	Foxholes	0.5	0.2
Military Equipment	Aircraft		
	Wing span under 60 ft	1	0.2
	Wing span 60-100 ft	1.5	0.2
	Wing span over 100 ft	2	0.5
	Antitank Missile Launcher	0.5	0.2
	Howitzers	0.5	0.2
	Helicopters	1.2	0.2
	Medium AA	0.8	0.2
	Surface-to-Air Missiles	1	0.2
	Surface-to-Surface Missiles	1	0.2
	Tanks, Trucks	0.8	0.2
Military Installations	Permanent	3	1
	Field	2	0.5
	Supply Dumps	3	1
Radar	Fixed	1	0.2
	Mobile	0.5	0.2
Transportation	Rail, Roads	3	0.8
	Inland Waterways	3	1
	Bridges over 100 ft	3	1
	Marshalling Yards	3	1.5
	Railway Cars	2	0.5
	Port Facilities	1.2	0.5
Industry	Major		
	Minor		
Utilities	Thermal Power Plants		
	Industrial	1.5	0.8
	Hydroelectric	3	1
	Municipal	3	1

*Source: Naval Air Systems Command

CONTRAST

A target image on the display is not visible to the observer unless some minimum contrast ratio is exceeded. The specific value depends on both image and observer characteristics, as well as how the visual threshold is determined. Within limits, increasing the contrast facilitates the tasks of target detection and recognition while decreasing the false alarm rate.

The results of a study by Fowler and Jones (1972) are plotted in Figure 4. Note that the probability of detection was strongly contrast-dependent for both briefed and unbriefed targets. However, as shown in the figure, higher probabilities were obtained in the briefed mode for a given contrast level.

The displayed contrast required to yield a given level of target detection is a function of such factors as target size, color, duration, and background complexity. In the case of a uniformly luminuous stimulus seen on a uniformly luminous background, the contrast (C) is defined as the difference between the luminance of the stimulus (B_t) and the luminance of the background (B_o) divided by the luminance of the background. Thus

$$C = \frac{B_t - B_o}{B_o}$$

Stimuli lighter than the background can vary in contrast between zero and infinity, and stimuli darker than the background can vary between zero and minus one. It has been found in a number of studies, notably those conducted at the Tiffany Foundation and reported by Blackwell (1946), that over a wide range of conditions positive and negative stimuli of the same numerical value are about equally detectable irrespective of sign.

TIME ON DISPLAY

The time required to acquire a target is a function of factors such as the target size and shape, its contrast with the background, the size of the area to be searched, and the total information content of the scene. A practical minimum limit for detecting a large-scale, high contrast target in

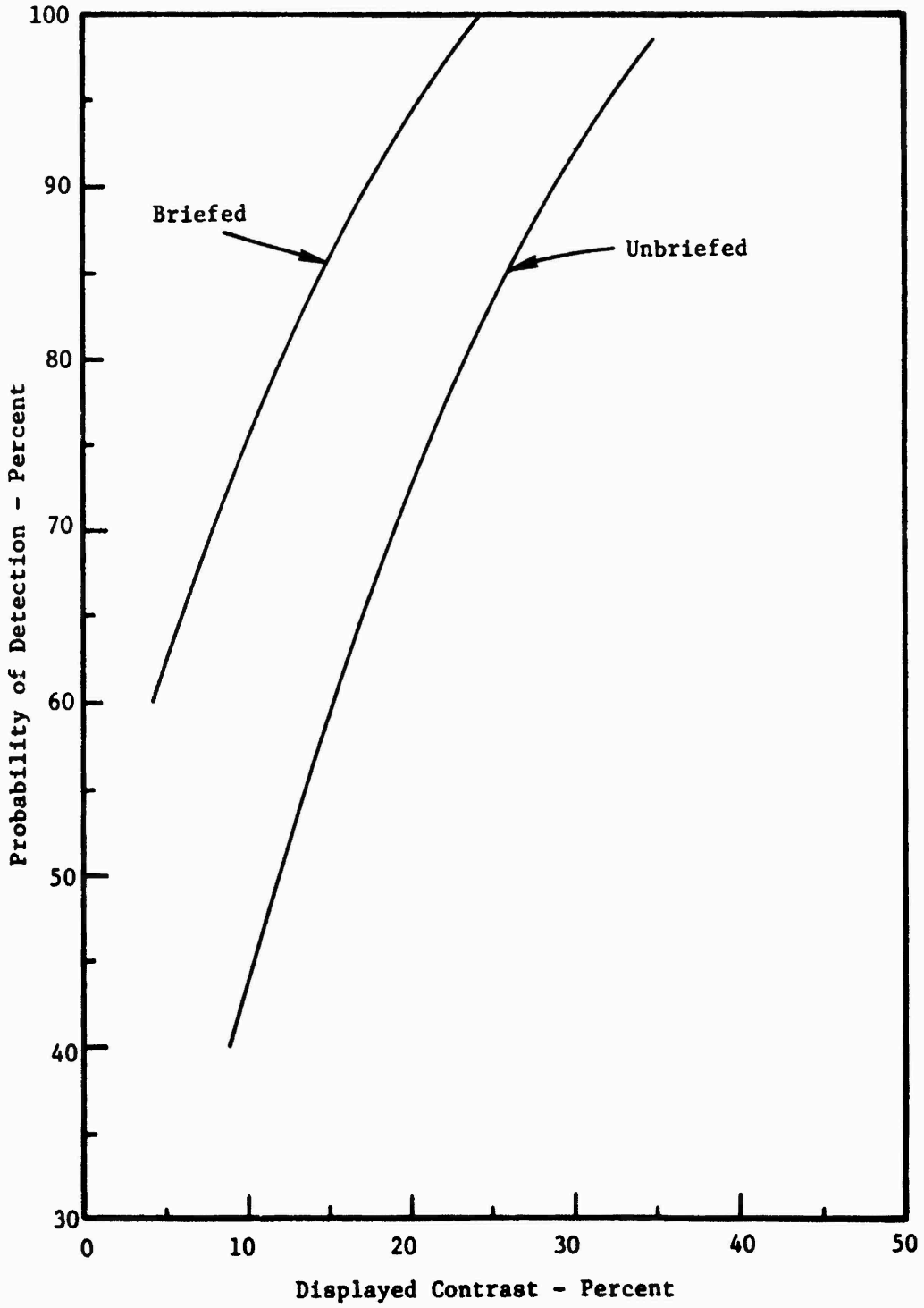

Figure 4. Probability of Detection as a Function of Contrast

an uncluttered background is 3 to 5 seconds. However, more realistic interpretation tasks can require 30 to 40 seconds.

RASTER LINES ACROSS IMAGE/IMAGE PROJECTED ANGLE

The number of raster lines across the displayed image and the size of the angle projected to the interpreter's eyes are intimately related to the ability of the interpreter to perform the functions of target detection and recognition. If the sensor moves closer to the target, or if the FOV is decreased, the image on the monitor will become larger. Not only will the number of scan lines making up the target image increase, but the angular subtense of the image to the interpreter's eyes will also increase. Thus, these two quantities are inversely related to scale.

Tests were conducted by Erickson (1969) to investigate the factors of image projected angle and number of scan lines across the image as they related to image size. Mean performance against vehicles (side view) is shown in Figure 5 as a function of the number of TV raster lines across the target, for three subtended angles per target height. Performance at all three angular subtenses improved rapidly as the lines per vehicle increased from 3.7 to 12, except that no change occurred above 7 lines for the 4.4 minute of arc condition. This indicates that at 4.4 minutes of arc, target angular resolution subtense is the limiting identification factor rather than the number of scan lines.

Erickson (1969) also determined the ability of interpreters to identify vehicles (oblique view) as a function of background type as well as the number of scan lines and angular subtense (Figure 6). Note that performance drops off rapidly when the number of scan lines across the vehicle decreases below 10. Improvements in performance are not large when the number of lines is increased from 10 to 15 per vehicle. Note also that the sandy background was more difficult than the foliage background. This was believed to be due to the fact that highlights on the vehicles had about the same luminance as the background. Hence, there was no contrast against the background and the total form was not visible as a unit.

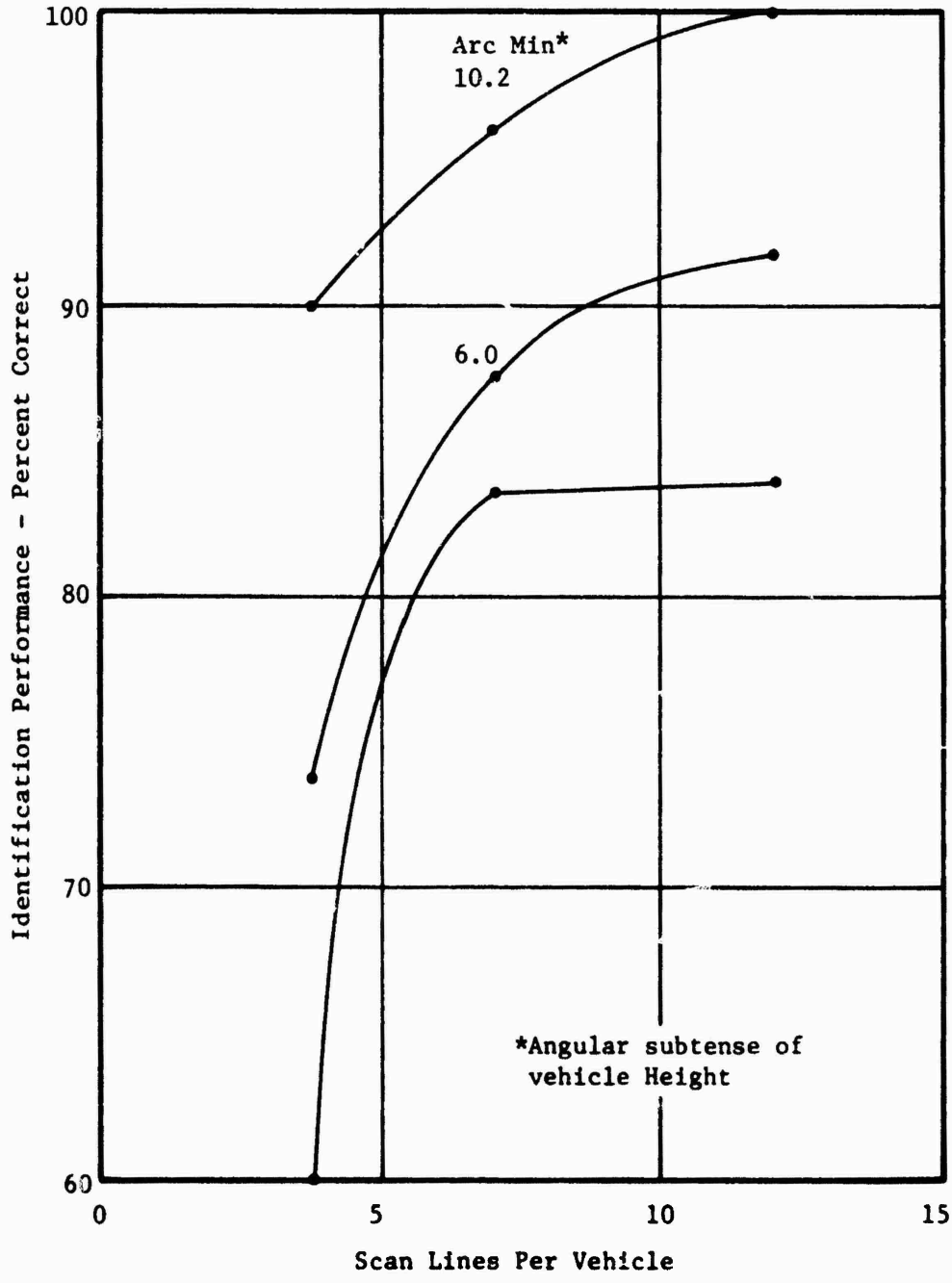

Figure 5. Vehicle Identification Performance on Television

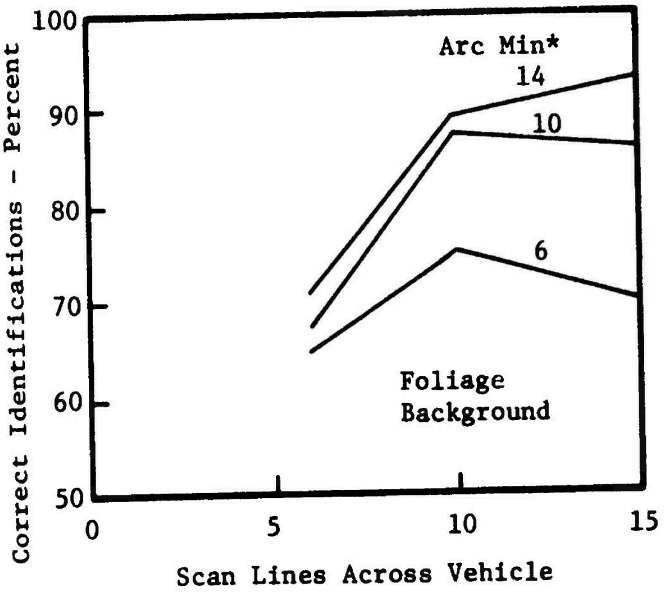

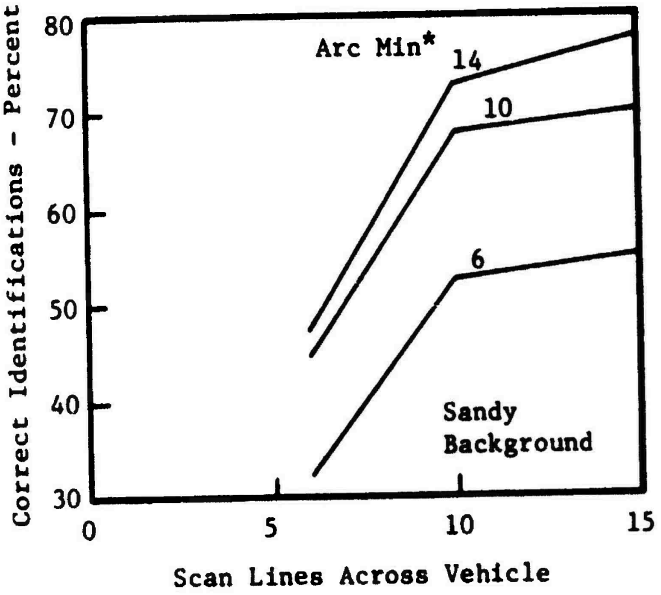

*Angular subtense of vehicle height

Figure 6. Results of Vehicle Identification Test

DISPLAY SIZE

Increasing the display size enhances the tasks of target detection and recognition until a point is reached where the eye can resolve the individual display resolution elements; i.e., the sensor system is no longer eye/display limited. As the display is made larger above this point, studies have shown that both detection time increases and percent detection decreases (Krebs and Graf, 1973). Recognition time, however, decreases slightly for the larger display and accuracy is essentially unchanged.

When target size is increased by display magnification alone, i.e., the number of sensor resolution elements across the target remains unchanged, performance does not improve.

ASPECT ANGLE

Aspect angle as used here is that angle formed by the lines connecting a sensor lens to ground nadir and to the target base facing nadir. Experiments conducted under controlled laboratory conditions (Wallace et al., 1968) indicated that recognition performance can be improved significantly by imaging the target at least five degrees from the nadir. Overall time and efficiency varied significantly over the aspect angles evaluated.

A Newman-Keules test for differences between specific aspect angles for overall time showed 7 and 10 degrees to be different from each other and both to be different from all remaining angles. The two-degree angle produced lower performance than zero degrees, and both yielded poorer results than did the other angles evaluated (0 to 20 degrees). An aspect angle of 7 degrees was found to be superior to all other angles tested.

IMAGE MOTION

Apparent terrain motion of the displayed scene can reduce the interpreter's ability to extract information: (1) the sensor system's dynamic resolution can become degraded, which results in a blurred image on the

display; and (2) the interpreter's dynamic visual acuity can be adversely affected. The elimination of sensor system blur is often very expensive; hence, it is desirable to determine the effect of image blur on interpretability so that cost-versus-performance trade-offs can be made.

Apparent terrain motion may be one of three types. If the airborne sensor system is moving parallel to the ground, the terrain will "flow" through the display from top to bottom (assuming that the display FOV has not been rotated) and objects in the picture will become larger as they move toward the bottom of the display. If the sensor system is descending along a straight line toward a target which appears in the center of the display, the target will grow in size and objects other than the target will exit the display. Finally, air turbulence or deliberate movement of the RPV's attitude control surfaces will induce roll, pitch, and/or yaw motions into an unstabilized sensor; this will result in erratic motions of the target.

Miller and Ludvig (1962) found that visual acuity remained nearly constant when looking at an object subtending two minutes of arc at angular velocities from 10 to 30 degrees per second, but that acuity deteriorated rapidly at higher velocities. Apparent target motion on an airborne display will usually not exceed 30 degrees per second. However, Van Den Brink (1969) has found that the sharpness of an image on a television screen is determined in part by the summating properties of the retina. He found that the brightness of luminous bands had to be raised as the angular velocity increased in order to distinguish the intermediate dark band. This factor indicates that a stationary low contrast target which is just above visual threshold would drop below threshold if motion were present, since reducing the displayed target contrast raises the detection and identification thresholds.

The relationship between visual acuity and angular velocity can be represented by the semi-empirical equation suggested by Ludvig et al. (1953)

$$\alpha_f = a + b\dot{\theta}^3 \quad \text{minutes of arc} \tag{7}$$

where

α_f = critical detail resolved at the fovea (arc minutes)

$\dot{\theta}$ = angular velocity of the target (degrees/second)

a and b are parameters characteristic of an individual's static visual acuity (SVA) and dynamic visual acuity (DVA)

Examination of the a and b parameters for each individual within one age group has shown that, although there is a small positive correlation between SVA and DVA, it is not statistically significant. A person with good static acuity may or may not have good dynamic acuity; a subject with poor static acuity cannot have good dynamic acuity. Thus a relationship exists, and good static acuity is necessary but not a sufficient condition for good dynamic visual acuity.

Figure 7 shows the relationship between foveal visual acuity during ocular pursuit and angular velocity. Visual acuity deteriorates markedly and progressively as the angular velocity of the target increases.

SCENE ROTATION

Scene rotation is defined as rotation of the sensor line-of-sight (LOS), and therefore the displayed scene, nonisomorphically with the "out-the-window" horizon when the aircraft is flying straight and level. This effect results from the necessity to have a gimbaled sensor for acquisition and tracking of targets offset from the RPV's flight path. Some two-dimensional gimbal orders result in heightened rotational effects, while other gimbal orders result in only "natural" rotations of the LOS on the display. One series of tests (Freitag and MacLeod, 1974) indicated that the nonrotated targets were recognized at statistically significantly longer ranges than were the rotated targets. Work load conditions did not produce a statistically significant difference in error or recognition slant range.

The effects of scene rotation on the ability of an airborne observer to track a ground target by means of an electro-optical (television) display were also evaluated during the above referenced program. The results of this

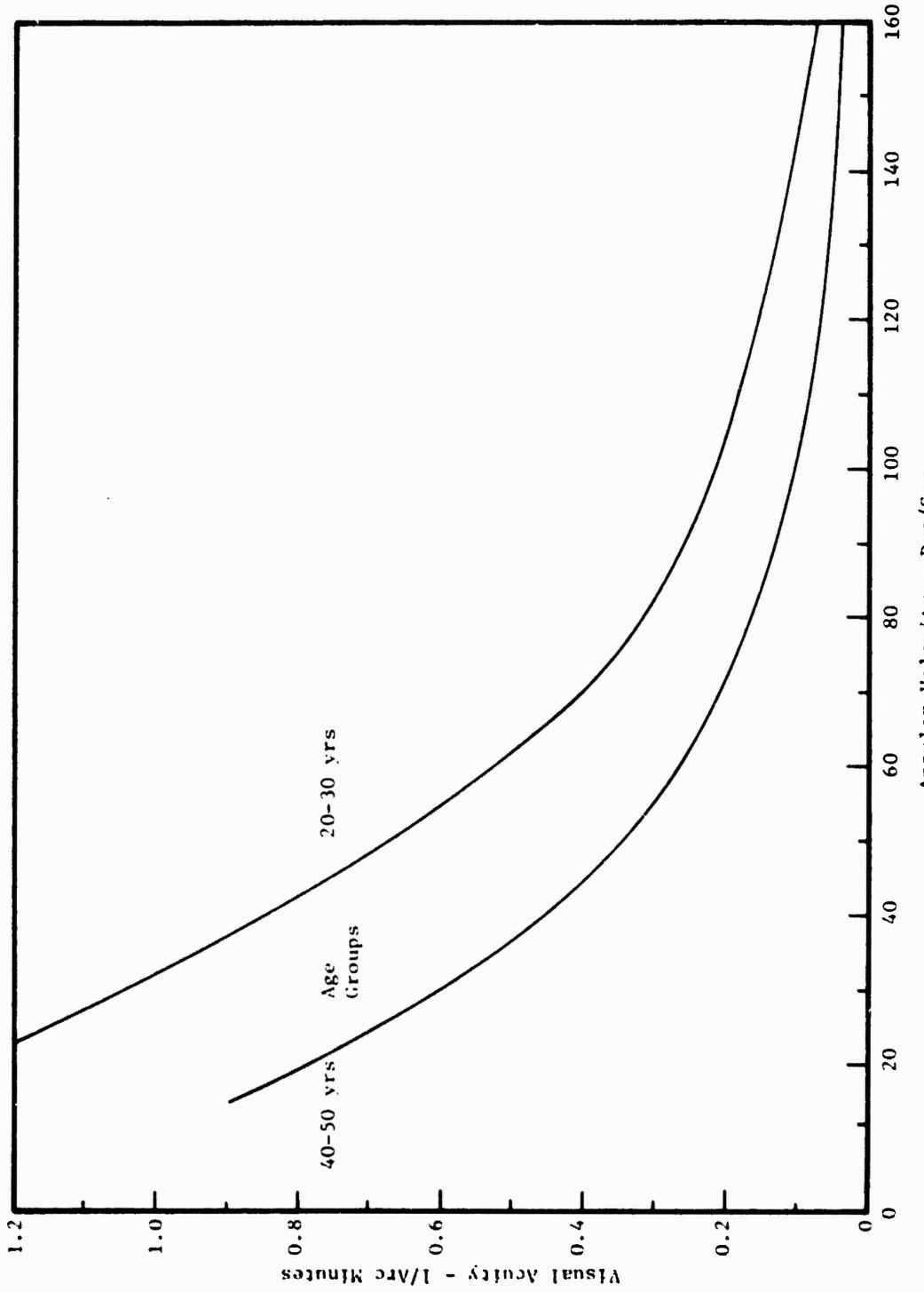

Figure 7. Relationship Between Foveal Visual Acuity and Angular Velocity

study indicated that a yaw-pitch gimbal order resulted in the best performance, as evidenced by the mean tracking error scores. Roll-pitch sensor gimbal order with yaw-pitch tracking had significantly higher error scores at the beginning of testing, decreasing rapidly after a few trials to almost the same level as the yaw-pitch gimbal order. The roll-pitch sensor gimbal order with roll-pitch tracking was an order of magnitude worse than the other two conditions with no learning manifested.

Besides degrading the performance of an airborne target acquisition and tracking system, a displayed scene that rolls nonisomorphically with what would be seen out of the aircraft's window can cause physiological disturbances such as motion sickness and disorientation effects associated with a conflict between visual and proprioceptive cues. In summary, the findings of this study (and others) indicate the desirability of stabilizing the imagery of an electro-optical system if the observer must recognize and/or track ground targets at long ranges and with high accuracy.

SIGNAL-TO-NOISE RATIO

Image quality in terms of the displayed SNR affects operator performance at lower levels. The results of one study (Naval Weapons Center, 1971) indicated that as the SNR dropped from 20 to 4 dB, target acquisition time doubled from about 4 to 8 seconds (see Figure 8). Performance did not significantly improve for SNR's greater than 20 dB.

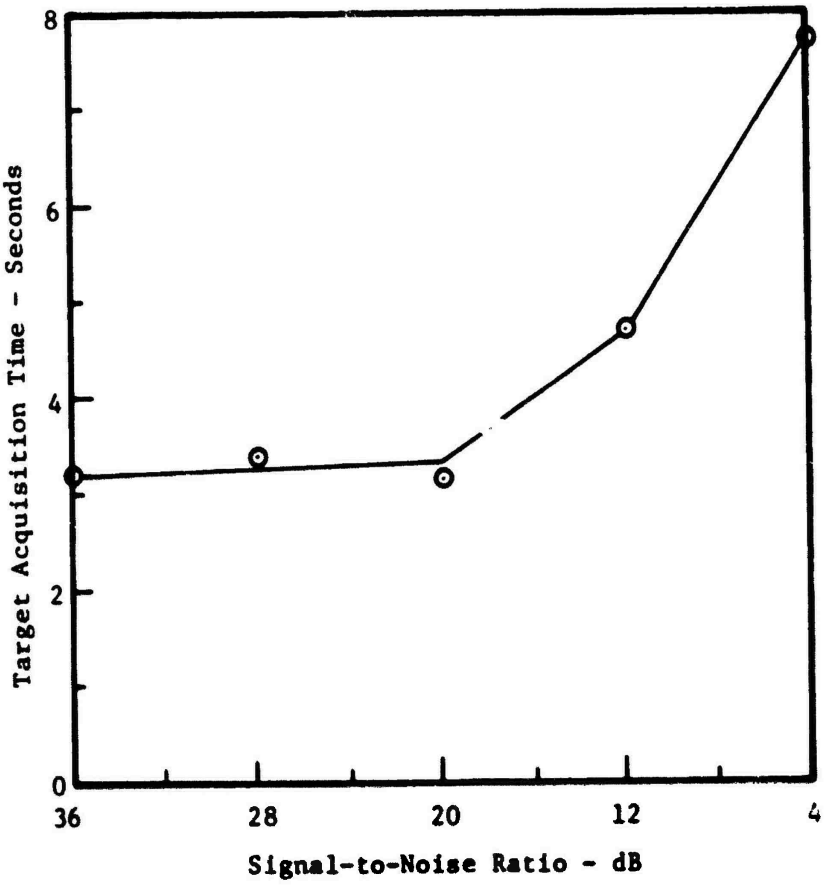

Figure 8. Target Acquisition Time as a Function of Signal-to-Noise Ratio

Section 3
NRT/RT RECONNAISSANCE MISSION

GENERAL

To this point the specific requirements of the real time reconnaissance RPV system have not been identified. The remainder of this technical report is developed in the context of the BGM-34C real time reconnaissance system.

OPERATIONAL SCENARIO

The basic mission profile of the BGM-34C reconnaissance RPV is determined by an onboard program. The vehicle is launched at medium to high altitude, descends to low altitude, penetrates the FEBA, and proceeds to each target location, making any heading changes that are required, before returning for recovery. Under idealized conditions and depending on the specific sensor, operator intervention would be required only to initiate imagery acquisition and to optimize the take by controlling the mode of sensor utilization (e.g., sensor pointing, zoom) at the target. The onboard sensor may be utilized to verify that the RPV is at the correct location/orientation prior to a preprogrammed heading change and/or to confirm that such a maneuver has been correctly accomplished. In both of these applications, waypoints of opportunity can be exploited in support of maintaining navigation accuracy. Also, each of these functions can be facilitated, if necessary and if commensurate with survivability, by having the vehicle "pop up" to a higher altitude, thus increasing the amount of ground coverage encompassed by the sensor FOV.

The intelligence collection requirement to be addressed by this system is the satisfaction of EEI pertaining to fixed and other targets whose locations can be established on an a priori basis. A sortie then consists of a sequence of legs with each leg containing one (or more) prebriefed targets. Target acquisition is accomplished in real time, and imagery exploitation is carried out by the sensor operator in real or near real time. Each of the video sensors proposed for the RPV offers a forward looking, wide FOV capability (NAV mode) for use during target acquisition. In this mode, the image scale is reduced to acquire additional downtrack and swath width coverage.

Upon acquisition and identification of the target, the operator attempts to optimize the imagery obtained for exploitation. In the overflight system, he employs a steering cursor to skid the vehicle heading over the target. In the slewable sensor case, he begins to zoom the camera while maintaining the target in the available FOV. In general, reconnaissance imagery of the target is obtained at the largest scale possible. Interpretations are made based on the specific EEI's to be responded to. It is obvious that, if desired, the system's reconnaissance capabilities can be applied to targets of opportunity, including fixed, mobile, and fleeting types. The process of target acquisition can also be enhanced by a "pop up" during the approach, again, if commensurate with survivability, and if jamming permits man to be in the loop constantly.

The exploitation of the real time imagery (as opposed to collection) is accomplished in one of two ways. It may be accomplished onboard the DC-130 and the image-derived information transmitted to a ground station, or it may be be performed on the ground and the imagery itself transmitted. The ground exploitation facility supporting the BGM-34C system is to be the Reconnaissance Reporting Facility (RRF) developed under the ASD Quick Strike Reconnaissance (QSR) program. The interface of the BGM-34C system with the RRF will be the AN/TYQ-6 Compass Sight data link receiving van. Under QSR, the RRF will support the real time interpretation of AAD-5 line scan infrared and APQ-9 FLIR sensors. Support of the BGM-34C sensor system is essentially identical to exploitation of the QSR imagery. Figure 9 presents a function/flow diagram of the BGM-34C reconnaissance RPV system. Two external phenomena can modify the exploitation process. In the event that severe jamming precludes effective transmission of imagery from the RPV to the DC-130, up to 20 minutes of imagery can be recorded on video tape for later transmission. An airborne recording capability can also be utilized in the event that the RRF is currently servicing the QSR aircraft. Figure 10 presents the alternative actions in the exploitation of imagery. Figure 11 depicts the design configuration of the RRF, a modified TIPI imagery interpretation van. Figures 12 and 13 show the interpretation flow within the RRF.

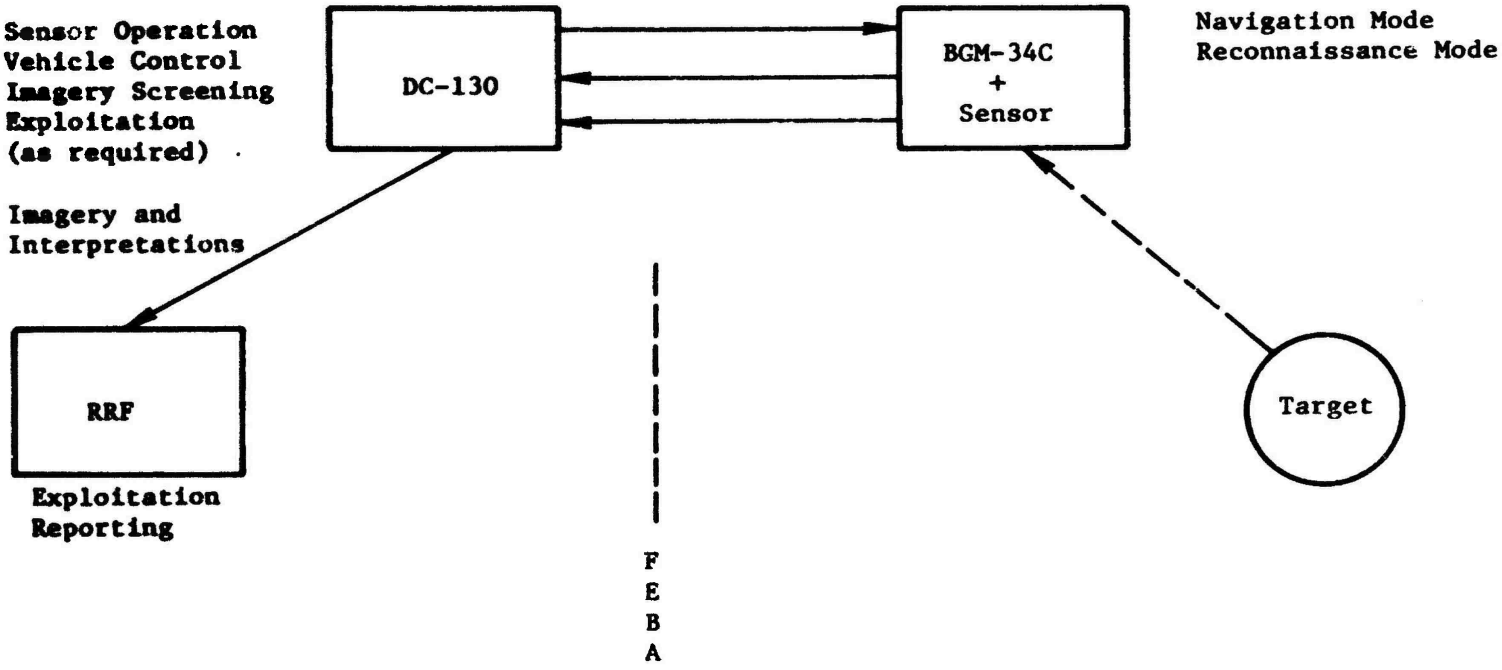

Figure 9. Reconnaissance RPV Function/Flow Diagram

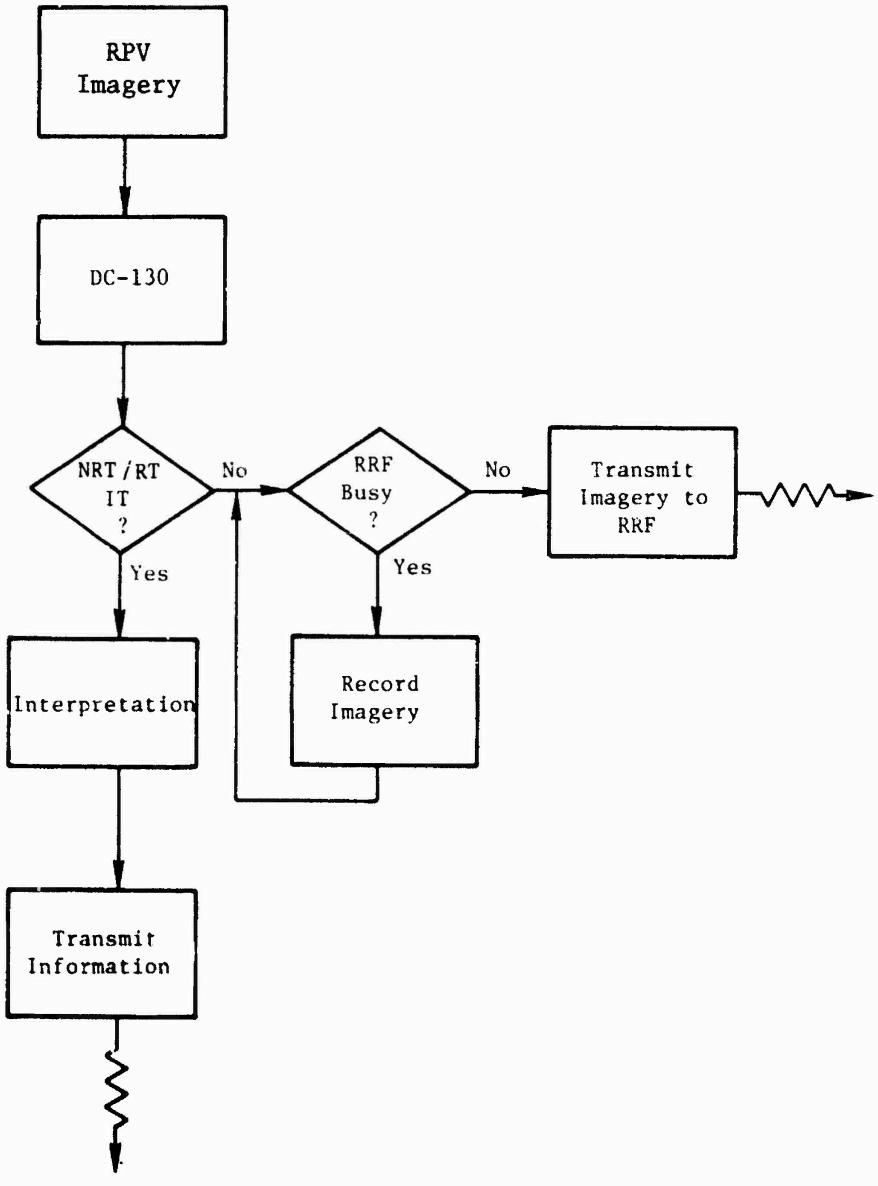

Figure 10. Exploitation Logic

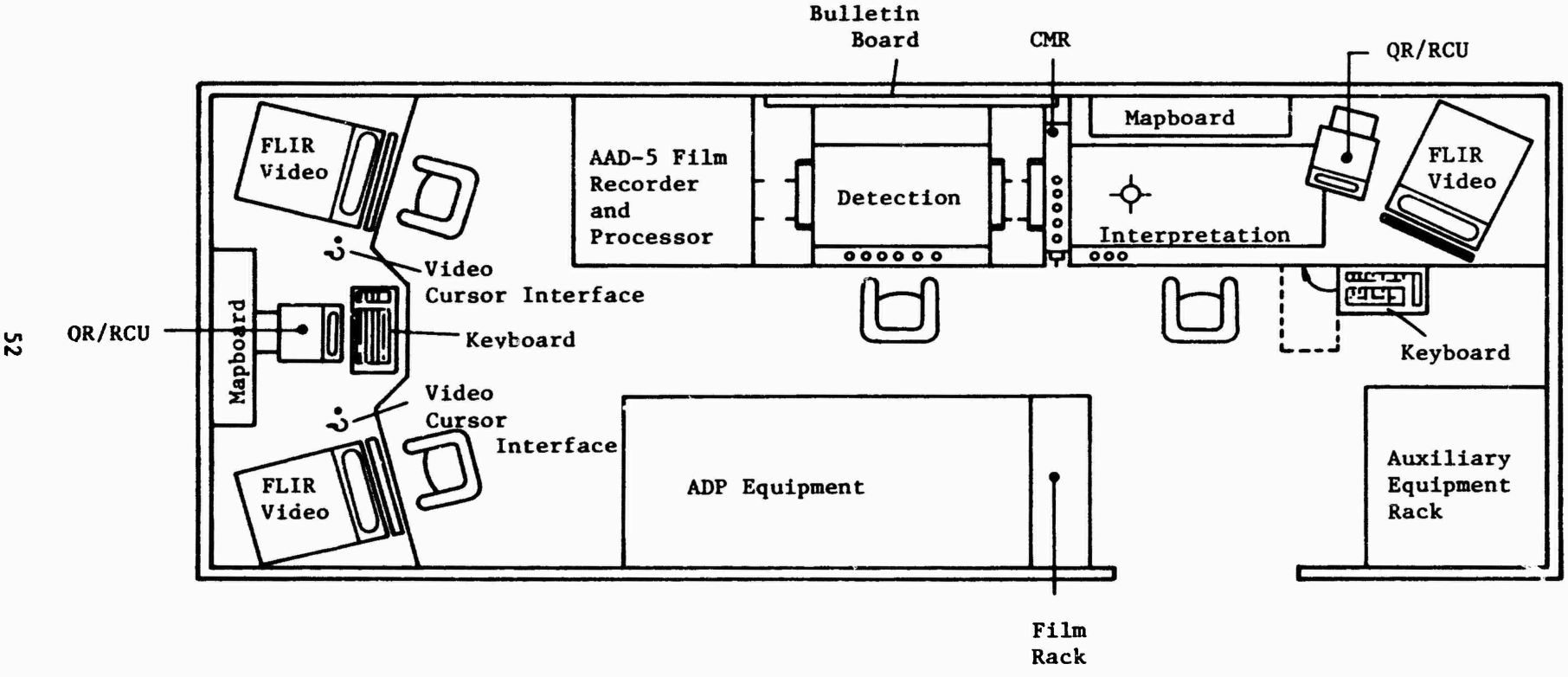

Figure 11. Reconnaissance Reporting Facility

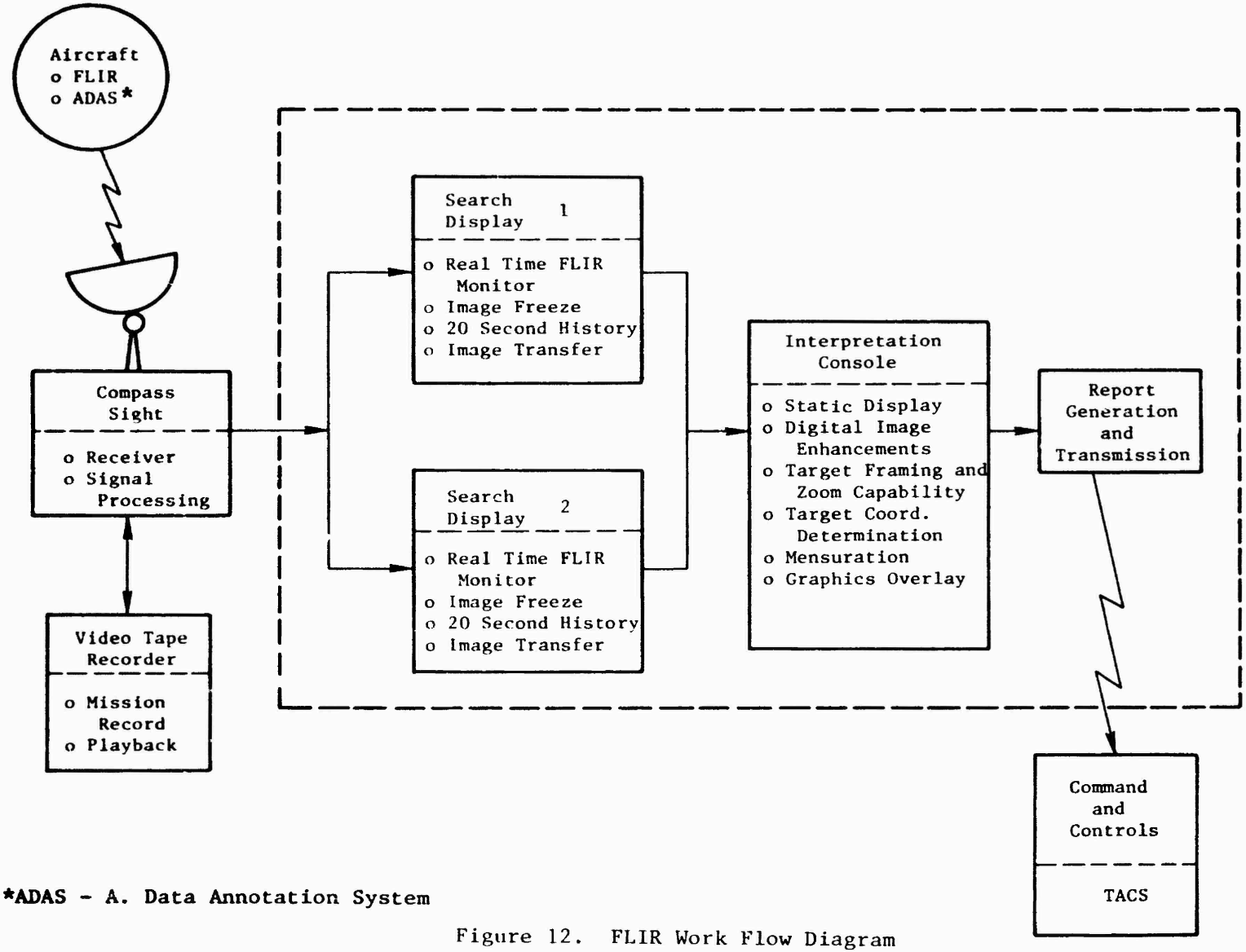

*ADAS - A. Data Annotation System

Figure 12. FLIR Work Flow Diagram

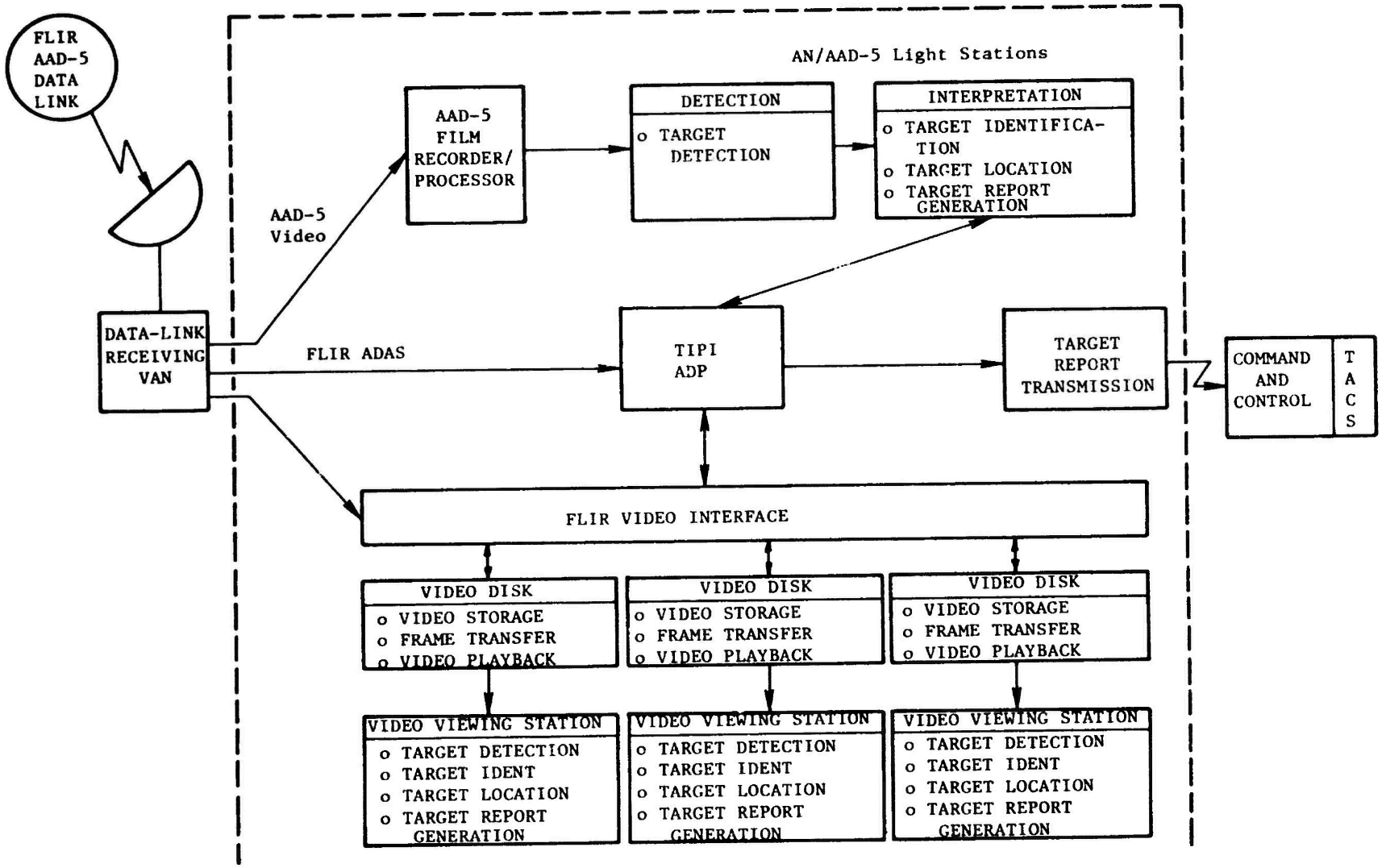

Figure 13. FLIR/IR Work Flow Diagram

The requirements for reporting information derived from this reconnaissance system apply equally to any tactical imagery collection system. AFM 200-50, Image Interpretation Handbook, defines the purpose of this function as follows:

> Image interpretation reports serve two parallel objectives: maximum exploitation of the information they contain and timely dissemination of intelligence to the user.

It should also be recalled that this system is to be applied against prebriefed (prelocated) targets and locations. Because of the (near) real time capability, it can be assumed that operational emphasis would be on (Initial Photo Interpretation Report (IPIR) level dissemination. This type of report is characterized as ". . . a first phase exploitation report used to provide information on approved mission objectives. It may also provide new and perishable intelligence" (AFM 200-50). Subsequent exploitation of imagery collected by this system can also be used in preparing Supplemental Photo Interpretation Report (SUPIR) level reports based on second phase interpretation. A typical outline for IPIR contents is shown in Table 4.

TABLE 4. OUTLINE OF TYPICAL IPIR *

I.	Mission Track
II.	Airfields
	A. New or Changed Information
	B. No Significant Change
III.	Electronics
IV.	Weapons
V.	Military Areas
VI.	Road and Rails
VII.	Surface and Seaborne

* Source: Naval Reconnaissance Technology Support Center

More detailed reporting requirements are set forth in the 58 series of Defense Intelligence Agency manuals on intelligence collection. Order of battle information is divided into seven categories (similar to Table 4). They are: ground, artillery, naval, electronic, air, missile, and nonmilitary equipment. The status of the target, with respect to the most recent previous observation, is (also) to be reported as one of five allowable categories: new installation, significant change, minor change, no change, and unknown as to change. The status or activity of the target itself is also to be reported. Categories for this item are: under construction, completed, operational, abandoned, removed, destroyed, not operational, damaged, occupied, unoccupied, transitory, negated, and unknown. The interpreter is also required to report the validity, or level of assurance, of his interpretations. Validity categories are: confirmed, probable, and possible.

The EEI are questions about the enemy, posed by the operational command, and included in the intelligence collection plan. They may be the objectives and desired results stated in the Fragmentary (Frag) Orders which underlie the mission planning of a BGM-34C reconnaissance sortie or they may, for the basic intelligence requirements pertinent to some target and installation types, take the form of commonly used, standard checklists. (An example of a checklist is given in Table 5.) Frag Order requirements and EEI checklists are complementary. They may be further augmented by the requirements of the operational command (e.g., NATO, PACAF, USAFE, and CENTAG Reporting Guides).

TABLE 5. EEI CHECKLIST FOR MISSILE SITE REPORTING

A. Type: (Offensive or Defensive)
B. Site: (Temporary or Permanent)
C. Launch Site:
    (1) Number of Firing Points or Pads
    (2) Construction (Concrete, Revetted, U/C)
D. List Any Auxiliary Equipment (Transporters, Prime Movers, Launchers, etc.)
E. Number and Type of Antenna: (Guidance and/or Acquisition Radar)
F. Defenses (AAA)

Section 4

PROGRAMMABLE IMAGE SCANNER

DEVELOPING THE SIMULATION CAPABILITY

One of the major tasks accomplished was the specification and development of a real time reconnaissance RPV simulation facility. Immediate application of this facility was in the comparison of the three day sensors discussed in the Appendices. The facility was also required to be capable of application against requirements engendered by mission growth and advanced RPV systems. The approach followed in establishing the facility was based on the use of a flying spot scanner system and advanced video control and processing techniques.

GENERAL DESCRIPTION

The Programmable Image Scanner (PIS) is a special purpose flying spot scanner capable of generating simulated airborne sensor imagery over a wide range of aircraft and sensor performance parameters. A simplified functional diagram of the system is shown in Figure 14 and a photograph of the overall PIS appears in Figure 15. A high resolution CRT is used to generate a small spot of light that is scanned across and down the CRT to form a raster similar to that seen in a standard television tube. The light is optically projected onto moving film imagery. The condenser lens collects the transmitted light, which has now been intensity modulated by the film imagery, and concentrates it at the window of a photomultiplier tube (PMT). The output of the PMT is a current that varies linearly with the intensity of the light at the window. This current is converted to a voltage which is amplified, mixed with appropriate synchronization signals and presented to the television monitor as a composite video signal.

Figure 16 illustrates the process by which the apparent perspective of film imagery can be varied to meet the needs of sensor simulation. In this figure the circles represent the CRT on which the small spot of light generates a raster shown as five lines within the circle. The two thicker

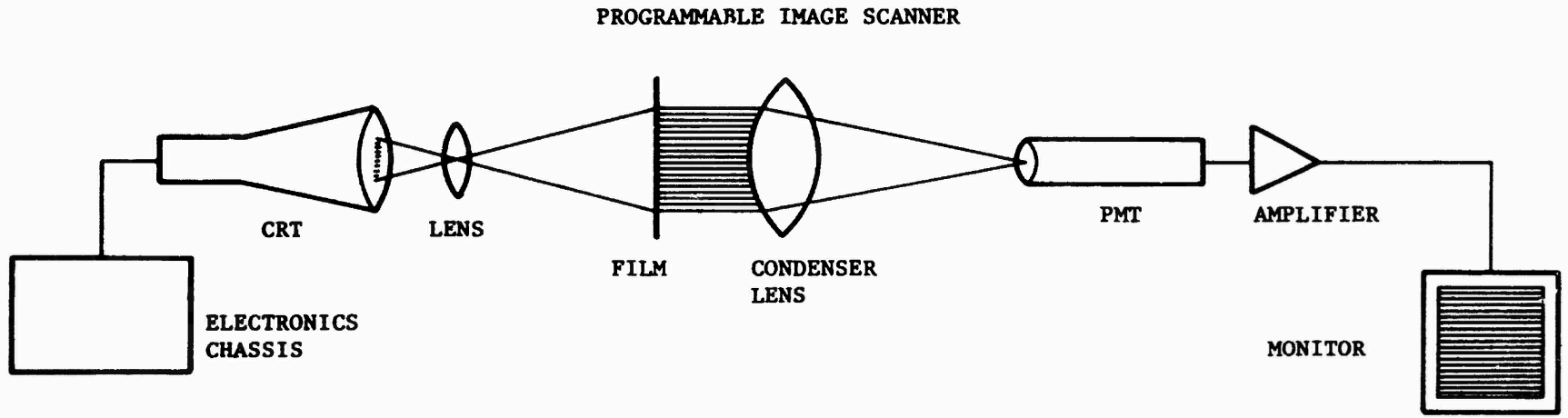

Figure 14. Simplified Functional Diagram of the Programmable Image Scanner

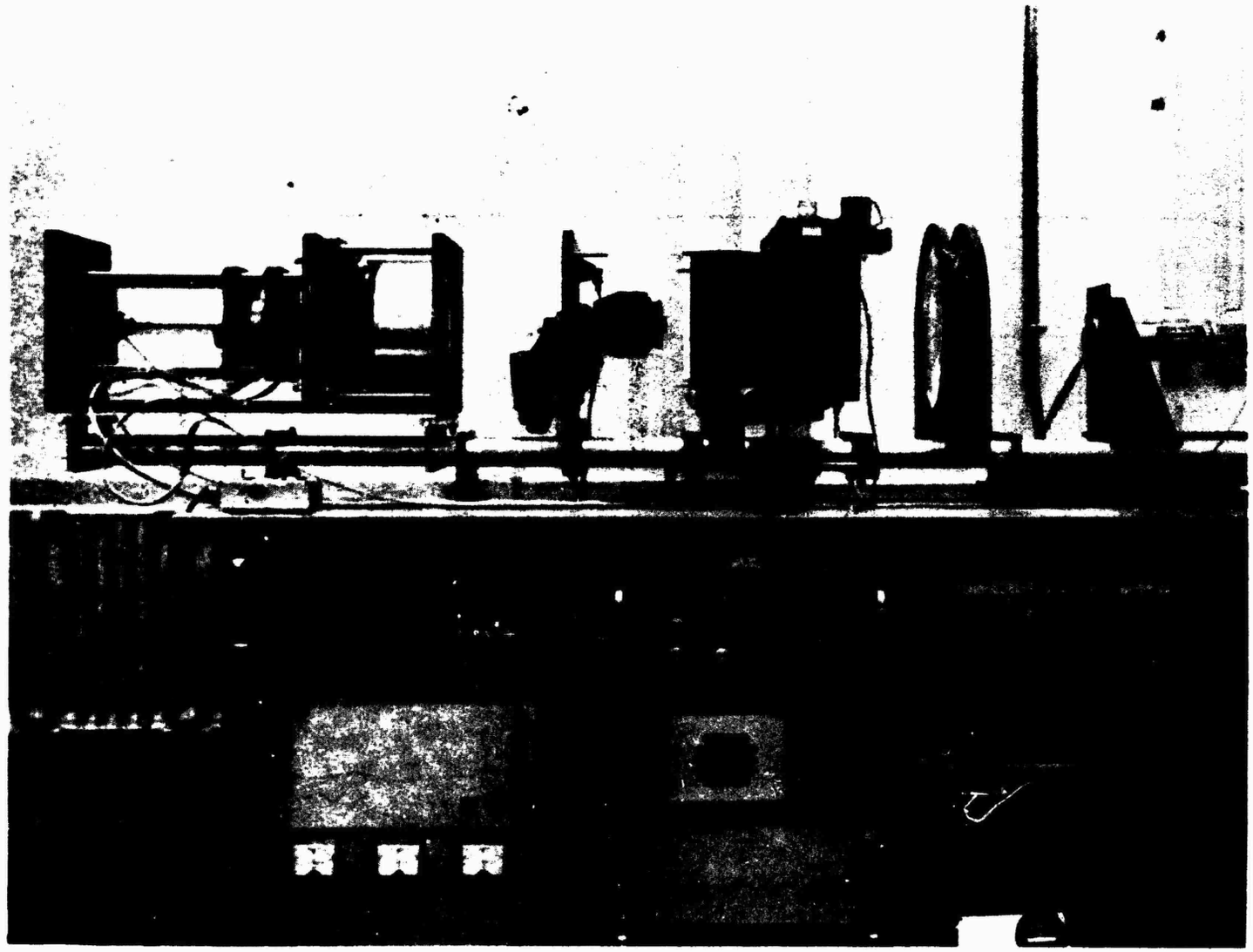

Figure 15. Programmable Image Scanner

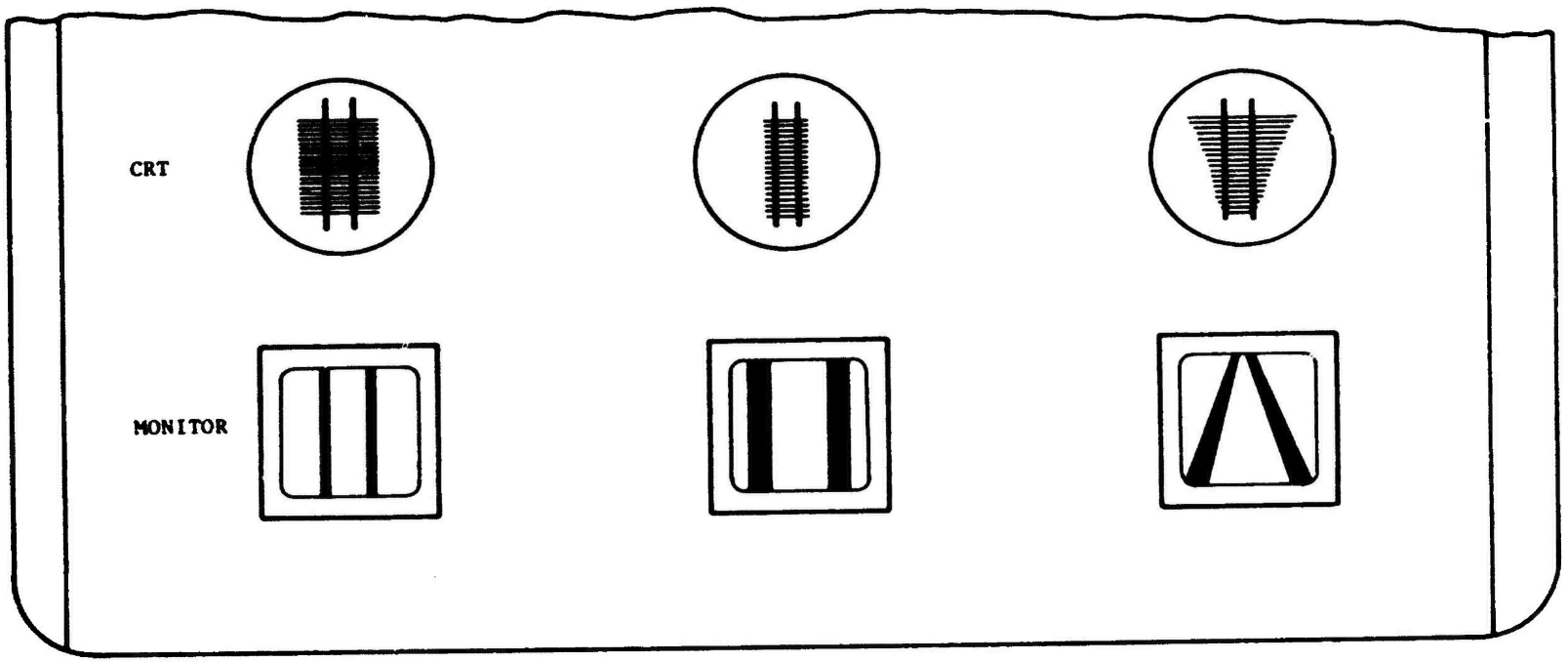

Figure 16. Raster/Display Perspective

dark lines represent the film imagery being scanned. The squares represent the TV monitor on which video pictures are presented. To understand how the altered raster changes the monitor's presentation, it must be kept in mind that the CRT and monitor rasters must be kept in time synchronization; that is, a horizontal line on the CRT raster, regardless of its length, requires the same time interval as a horizontal line on the monitor picture tube.

Referring to the left-most CRT raster, note that the two heavy lines are scanned by the spot of light as it passes through the one-third and two-thirds points in its linear horizontal sweep. The monitor thus shows two bars in a similar arrangement on its screen. In the center CRT raster, the spot of light has been made to move horizontally at a slower velocity; therefore, the two bars appear closer to the edge of the raster and their width becomes a larger percentage of the horizontal line. This change is reflected in the monitor as an apparent reduction in range. In the right-most CRT raster, the length of the horizontal lines is reduced as the spot moves down the screen. It can be seen that the effect in the monitor now is one of apparent convergence of the horizontal lines with the accompanying impression of apparent perspective. Control of the raster affords control of scale, orientation, coverage dimensions, and perspective line at the monitor. Combined with control of film direction and velocity, the PIS simulates dynamic sensor/vehicle characteristics.

DETAILED SYSTEM DESCRIPTION

The PIS was originally developed for the purpose of screening 5 inch format strip photography on a TV monitor. A standard 3:4 aspect raster could be electronically zoomed and/or translated under operator control. In order to achieve the capabilities required to generate simulated dynamic sensor imagery, significant upgrading and new circuitry was required. A detailed block diagram of the PIS is shown in Figure 17. Each subsystem will be discussed as to its functional purpose, significant parameters, and changes in its configuration to optimize system performance.

The PIS now provides a highly versatile image generation capability for sensor system simulation. It affords the user interactive, dynamic control

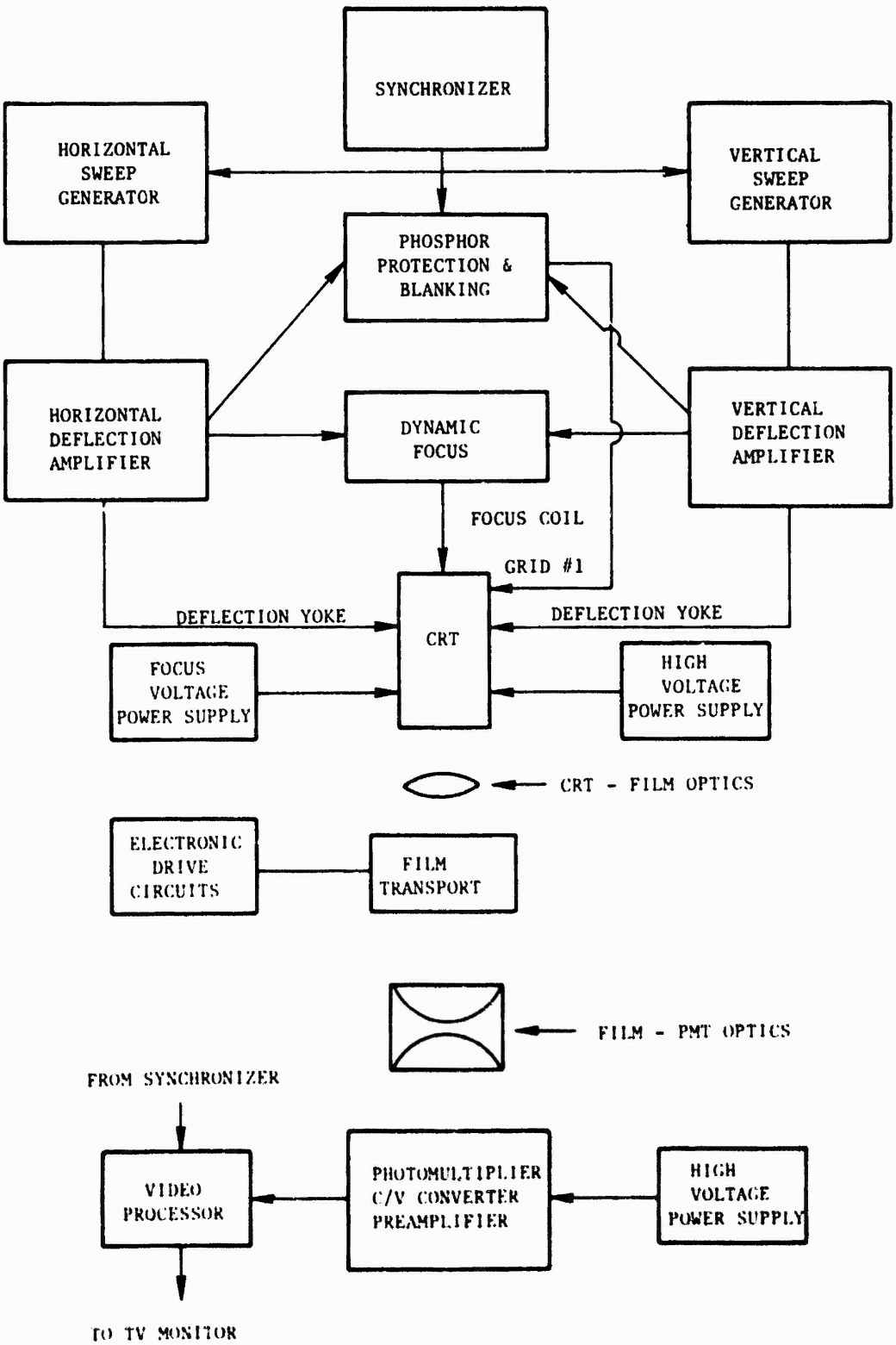

Figure 17. Block Diagram of Programmable Image Scanner

of displayed scene perspective over a wide range of sensor and aircraft characteristics. Areas of application include sensor comparisons, image metrics studies, system sensitivity investigation (weather, flight profiles, countermeasures, etc.), enhancement technique development, and mission/test planning.

Cathode Ray Tube Assembly

The CRT assembly (see Figure 18) includes a precision CRT, a magnetic deflection yoke, dynamic and static focus coils, high voltage and focus voltage power supplies, and the necessary mounting and support hardware. All of these items were carefully selected and integrated to result in the smallest possible spot of light on the tube face. The CRT was changed from a 5-inch to a 10-inch diameter tube to meet the need for larger rasters at the film plane. The CRT selected was a Thomas Electronics 10M 99P47. This tube has a specified spot size of 0.009 inch with a beam current of 50 microamperes. The persistence of its No. 47 phosphor is specified to have a decay time of 10 percent brightness of 0.08 microsecond. This rapid decay is required if high frequency video response is to be obtained. The magnetic deflection yoke and focus coils selected for use with this tube were purchased from Syntronic Instruments, Inc. and were custom made for this application. The new high voltage and focus voltage power supplies were purchased from Bertan Associates, Inc. and are rated at 25,000 volts, 300 microamperes and 1500 volts, 10 milliamperes, respectively.

Synchronizer

The synchronizer generates all timing signals required to control the system's sweep, blanking, and video processor control circuits. In addition, it generates synchronizing signals, in the format of EIA RS-170, for use with any standard video monitor.

This circuit uses a 31.5 kHz crystal oscillator as a timing reference. The square wave output of this oscillator is used to drive transistor-transistor logic (TTL) integrated circuit counters and control logic to generate the timing signals. No changes were made in this subsystem.

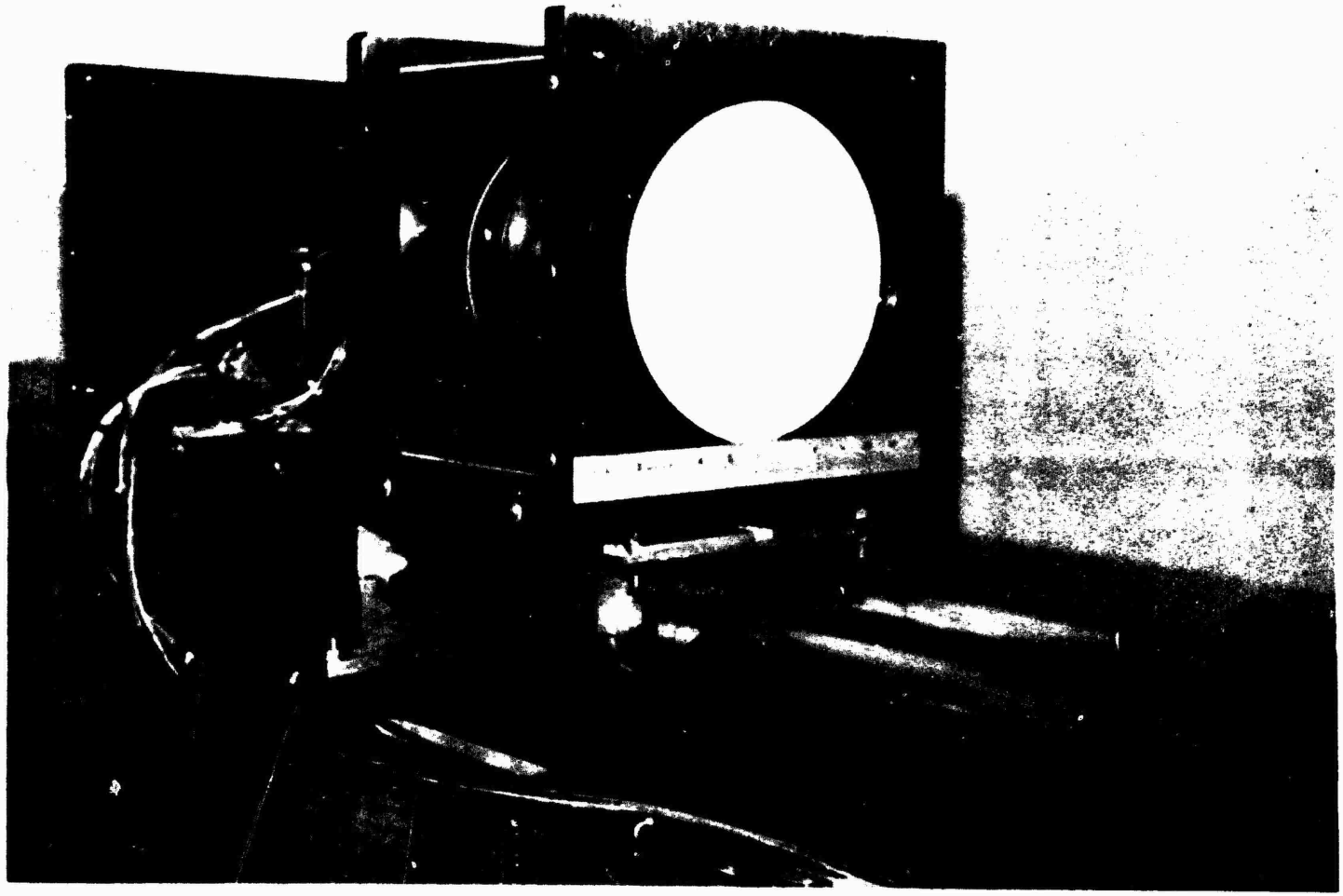

Figure 18. CRT Assembly

Sweep Generator Circuits

The horizontal and vertical sweep generator circuits form the ramp and modified-ramp voltage signals which ultimately are used to drive the electronic beam of the CRT in the manner appropriate to the desired raster "footprint" **(Appendices)**. The voltage used to scan horizontally within the raster has a frequency of 15,750 Hz; the voltage used to scan vertically has a frequency of 60 Hz. The effects of these two voltages is to produce a raster having two fields, each containing 262.5 horizontal lines. The two fields are offset vertically by one-half a line pair in order to form a two-to-one interlaced picture. The sweep generator circuits used in the RPV simulation utilize both analog and digital circuitry and were designed specifically for each of the three simulated sensors. The KA-98 and the Teledyne-Brown TV RECON mode are unique in their coverage characteristics; the sweep circuits for the slewable TV can be used much more generally (e.g., FLIR, "smart" weapons).

Phosphor Protection and Blanking Circuits

The phosphor protect and blanking circuits apply a voltage between the control grid and cathode of the CRT of sufficient magnitude to turn off the electron beam. The phosphor used on the face of a precision CRT can be damaged by an excessive concentration of the electron beam current such as might occur if one or both of the beam deflection signals are lost. The phosphor protect circuit continually samples both the horizontal and vertical deflection currents and immediately cuts off the electron beam if either signal amplitude decreases below 200 millivolts peak-to-peak. The blanking circuit is controlled by voltages derived from the synchronizer circuit. This blanking signal is used to ensure that the electron beam is cut off during the time interval used for vertical and horizontal retrace.

No changes to these circuits were required.

Dynamic Focus

The electro-optics of a precision CRT are such that minimum spot size cannot be maintained over the total face of the tube without some form of corrective influence. The most effective means for maintaining proper spot size is to drive the dynamic focus coil with a current which varies as the sum of the squares of the horizontal and vertical deflection currents. Such a circuit is utilized in the image scanner.

No changes were required for this simulation.

Video Amplifier Circuits

The video amplifier circuits include a current-to-voltage circuit, a preamplifier, and an amplifier/processor.

As the name implies, the current-to-voltage converter accepts the varying one milliampere signal from the PMT and converts it to a varying voltage of approximately 15 millivolts peak-to-peak. This signal is fed to the preamplifier where it is amplified by 20 dB and then to the amplifier/processor where it is further amplified under the control of an automatic gain control (AGC) circuit. In addition to AGC, the signal is as processed by a white limiting circuit. When a pseudo-horizon is required, as in the NAV mode for the Teledyne-Brown TV system, appropriate digital switching circuits are utilized.

All of these circuits were designed specifically to meet the needs of the simulation effort. They permit the PIS to exploit both low contrast and wide dynamic range photography in simulating sensor-generated imagery. These circuits can be modified to simulate jamming, atmospheric, and data link characteristics.

Photomultiplier Subsystem

The PMT was a flat-end-window type photocathode on which the light from the CRT is focused by the condenser lens. The output of the PMT is an ac current with peak-to-peak variations of approximately one milliampere. The tube is housed in a special mounting which also contains the resistive voltage divider chain needed to properly bias it, and a magnetic/electrostatic shield to reduce the effects of external electromagnetic noise.

All components of the subsystem, including the PMT power supply, were upgraded in order to increase the overall sensitivity of the PIS. The PMT selected was an EMI Gen Com Inc. No. 9558B, 10 dynode tube with an S-11 spectral response and an average sensitivity of 165 microamperes per lumen. Risetime for this tube is 10 nanoseconds. The new power supply was a Bertan Associates, Inc., Model 602-15N having a maximum output voltage of 1500 volts at 10 milliamperes.

Deflection Amplifiers

The vertical and horizontal deflection amplifiers are identical. Each is a dc coupled, push-pull current amplifier capable of converting ±5 volts input signals to currents of ±6.0 amperes. The large-signal frequency response of these amplifiers is approximately 500 kHz.

These circuits were not modified for this simulation.

Optical Subsystem

The optical subsystem has three major components: (1) the CRT-film optics, (2) the film-PMT optics, and (3) the optical table.

The CRT-film optics are used to focus the CRT raster at the film plane. For this simulation new high resolution, large-aperture lenses with focal lengths of 210, 102, and 58mm were procured. Manually adjustable mounts and lens positioners were fabricated. A motor driven, digitally controlled,

automatic lens changer (see Figure 19) was designed, fabricated and installed in the PIS. This changer facilitates the rapid switching between two lens of different focal lengths, thereby permitting the simulation of rapid changes in slant range as encountered in the Teledyne-Brown sensor.

The film-PMT optics are used to converge the light that has passed through the film into a relatively small beam that is then directed to the photosensitive window of the PMT. A new 40.6 cm diameter, 53.3 cm focal length condenser lens (see Figure 20) was procured and installed in the PIS using a specially designed lens mount.

The optical table is the support framework on which all mechanical and optical components are mounted. The table was extended in length and equipped with a more rigid mounting structure to permit installation of the new larger, heavier subsystems.

Film Transport Subsystem

The film transport subsystem is made up of: (1) The film transport, and (2) the electronic drive circuit (see Figure 21).

The film transport positions the film in the focal plane and supports it as it is moved through (the image of) the CRT raster. The required support is obtained by use of a glass platen designed to permit the film to be moved from the supply reel to the take-up reel. The speed at which the film moves is controlled by a Superior Electric Co. SlO-Syn stepping motor, Model M062-FC03.

The speed of the stepping motor is controlled by the electronic drive circuit which furnishes properly synchronized digital signals to the motor. The motor's speed can be varied from zero to 240 rpm, which equates to a maximum film velocity of 25 centimeters per second. Included in the digital control circuits are counters with appropriate visual readouts to permit the accurate and repeatable control of film motion.

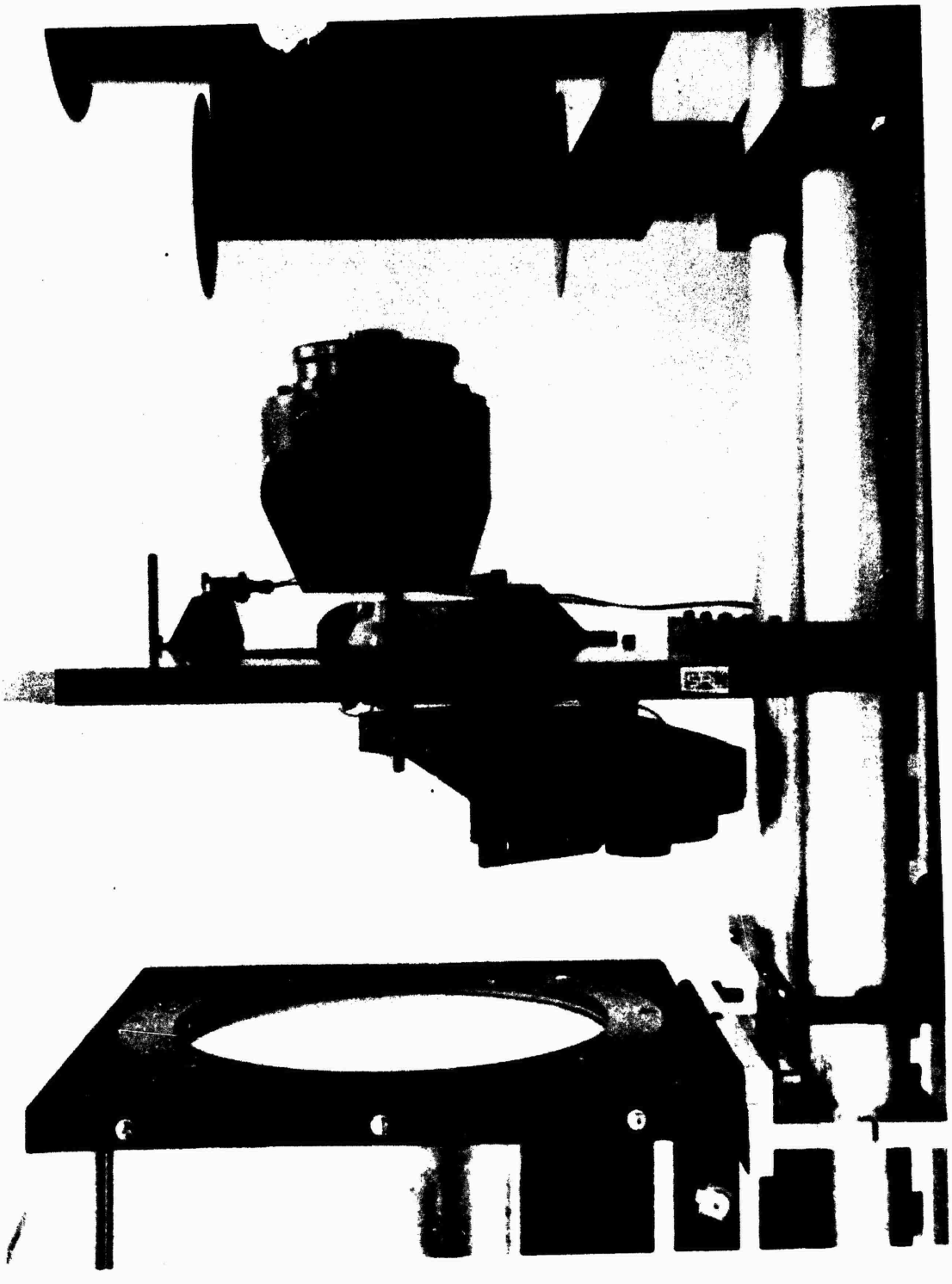

Figure 19. Automatic Lens Changer

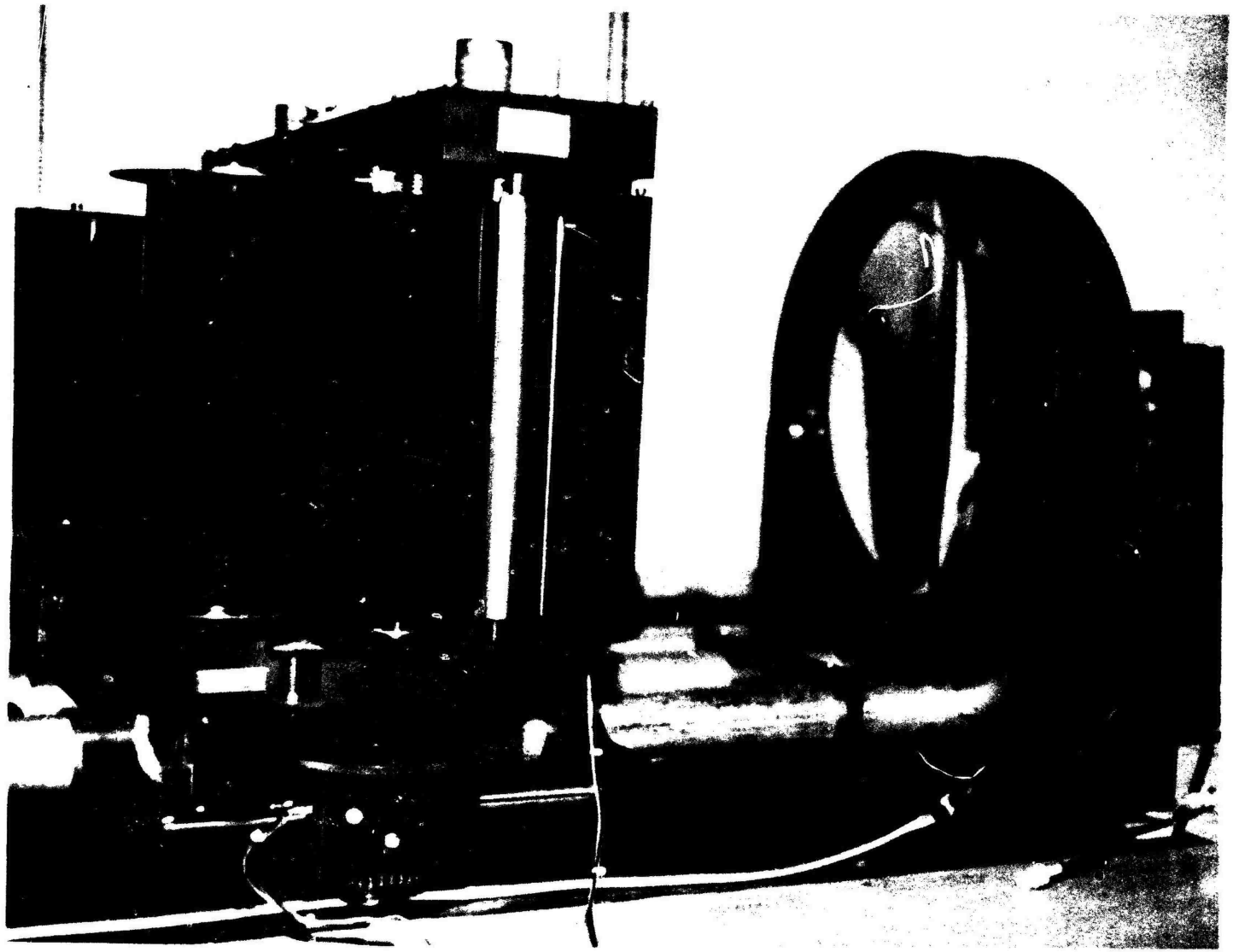

Figure 20. Focal Length Condenser Lens

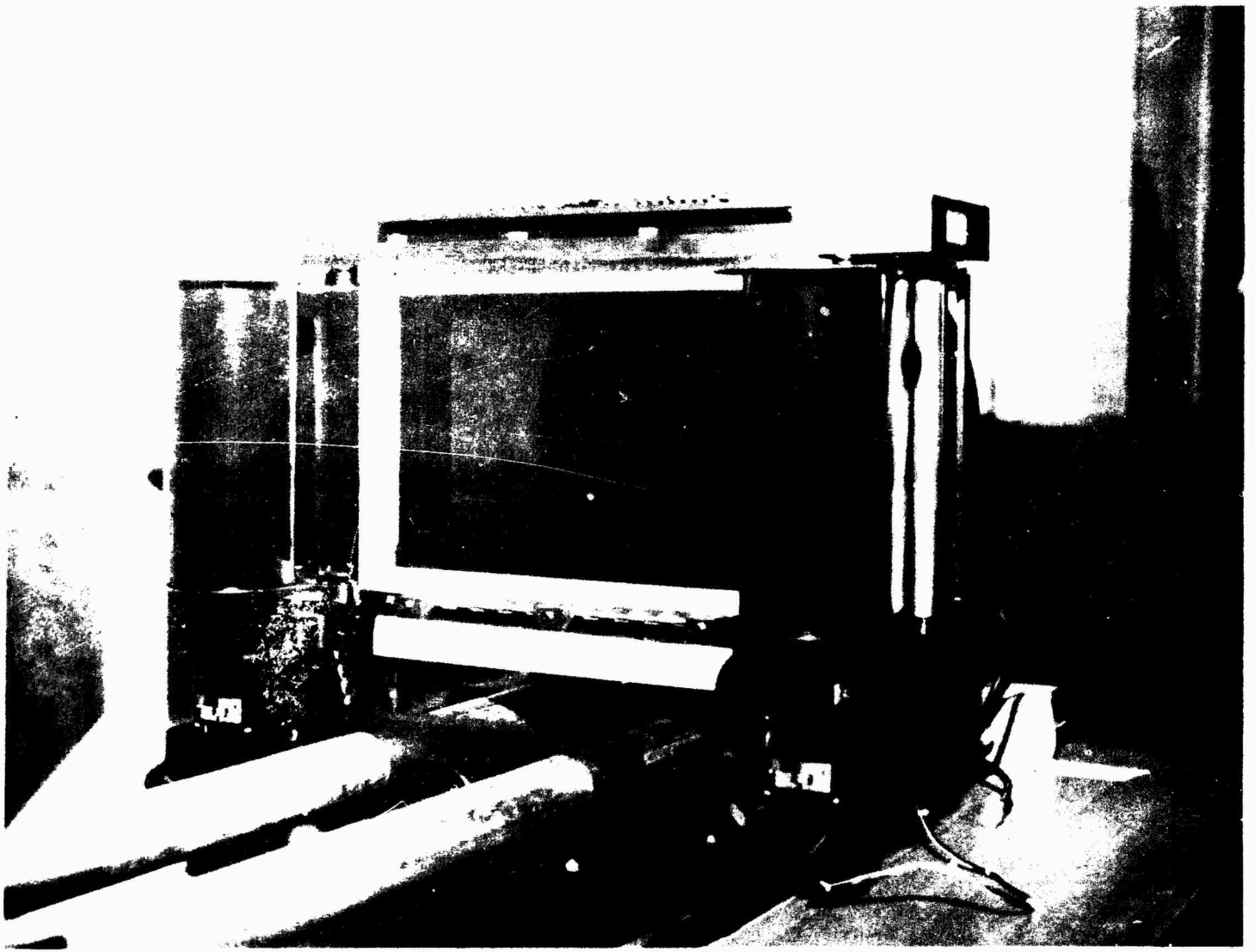

Figure 21. Film Transport Subsystem

The film transport was designed and fabricated specifically for use in this simulation. It is capable of use with film having 9-1/2 inch, 5 inch, and 70mm formats. In addition, single frames of any format up to 9 × 12 inches may be scanned.

Section 5
TARGET ACQUISITION EXPERIMENTS

OVERVIEW

During the planning of the NRT/RT reconnaissance RPV simulation experiments, several assumptions were made. These assumptions were based on the operation of the sensor system. The face validity of the simulation, or the degree to which the simulation corresponds to reality, was carefully considered on the basis of both hardware and procedures. Flight profiles (Table 6) were chosen to be representative of the BGM-34C vehicle. The sensors were modeled in terms of their respective geometric characteristics (Table 7). Thus, emphasis was placed on providing target displays which were accurate representations of sensor capabilities in terms of image scale, perspective, and motion.

The mission parameters were used to define the simulation scenarios. The RPV system relies on low altitude (500 feet) and high subsonic airspeed for survivability. Higher altitude "pop-up" may be employed to enhance area coverage. The RPV executes a preprogrammed set of course changes to achieve overflight of the planned target locations. Thus, the inherent navigation accuracy (±150 feet, typical error, to ±500 feet, worst case error) impacts strongly on mission success. The detection/recognition of the prebriefed targets is performed in real time, essentially as a confirmation of imagery acquisition. More detailed interpretation is a near real time function, using recording and playback capabilities (including stop motion).

These parameters, together with the sensor characteristics, determined the requirements for sensor simulation. Table 7 summarizes the sensor-specific portion of the simulations. The KA-98 is a scanned receiver-type line scanner. The collection aperture is scanned across the line of flight while the forward motion of the platform creates the second dimension of ground coverage. The scan is nonrectilinearized and a scale compression occurs off the nadir line. The imagery is scan converted for display on a video monitor. The type slewable TV was selected to offer a forward looking, narrow FOV alternative

TABLE 6. TARGET ACQUISITION SCENARIO

Parameter	Value(s)
Altitude	500 and 1,000 feet (AGL)
Airspeed*	350 knots (IAS)
Navigation Accuracy	±500 feet (maximum error) ±150 feet (typical error)
Targets	Prebriefed (collateral material, maps, prior coverage)
Acquisition	Sensor on prior to overflight to correct navigation (if necessary) and to confirm target
Detection/Recognition	Real Time
Interpretation	(Near) Real Time (imagery recording and playback)

*350 knots specified as representative; increased airspeed would degrade sensor performance across all systems.

TABLE 7. SENSOR SIMULATION

Parameter	Value		
	KA-98	Slewable TV	Teledyne-Brown
FOV (target acquisition)	136°	10°	32°
Azimuth	0°	0°	0°
Depression	90°	8°	8°
Scan Pattern	Line Scan	Raster	Raster
Display	4 × 3 Moving Map	3 × 4 TV	3 × 4 TV
FOV (interpretation)	136°	Zoom (target fills display)	26.6°

to the Teledyne-Brown NAV mode. Similarly, it assumed a target tracker and zoom optics to offer a forward looking alternative to the Teledyne-Brown RECON mode. The Teledyne-Brown TV camera uses a preset, wide FOV, focal length at fixed depression angle for target acquisition or navigation update (NAV). Prior to target overflight, a scanning mirror is interposed in the optical path, achieving a 90 degree depression angle, and a longer preset focal length is called. The mirror is driven through a preset azimuthal angle at 3.75 Hz. In combination with gated video at 30 frames per second, a sequence of indexed frames across the line of flight results.

The BGM-34C system was assumed, on the basis of system specifications, to be capable of maintaining a high degree of navigation accuracy. Thus, targets were presented relatively close to the RPV ground track. Since the KA-98 and Teledyne-Brown sensors have essentially deterministic FOV's (fixed or preplanned NAV mode), the slewable sensor was modeled to provide an alternative to the Teledyne-Brown NAV mode. The near, cross track edge of its footprint is about 400 feet wide thus ensuring that target locations would never pass laterally out of its FOV and, therefore, obviating any need for sensor azimuthal slewing. On the other hand, it was assumed to have a continuous zoom capability and a focal length of 60mm (versus 20mm for the Teledyne-Brown NAV mode).

The sensor imaging geometries and RPV flight profiles were analyzed to determine the appropriate ground footprint shapes and dimensions. From this, imagery requirements (scale and lateral coverage) were determined. The AMRL stimulus imagery library was screened and alternative sources of imagery (AFAL, DMA, DIA, and RADC) were contacted. Strip photography, satisfying the simulation requirements, was obtained from AFAL/WE.

Targets were selected from the available strip photography to correspond to tactically significant activities on the assumption that the imagery exploitation task differs only slightly, if at all, between detecting and interpreting a civilian complex and its military counterpart (e.g., a vehicle park). A similar assumption was made regarding the interpretation phase of the task. Naive subjects were used but the EEI checklists to be satisfied consisted of judging the shape, counting specific objects, determining the

presence or absence of familiar target elements (e.g., automobiles), and naming the activity at the target location in general terms (e.g., a cemetery might be described as a park with roads running through it). Similarly, the briefing aids (map and vertical photography) served to indicate both the flight path and the terrain/features which preceded each target. The simulations themselves were accomplished on an individual target basis corresponding to the Frag Orders that would be combined into an RPV sortie.

The face validity of the experiments was judged to be sufficient for the purpose of comparing operator performance with different sensors although only a part task simulation was employed and no attempt was made to duplicate the actual crew station. This assumption was validated by the participation of experienced operators during the pilot studies used to develop experimental procedure and the briefing and demonstration of the PIS to sensor design engineers for the KA-98 and Teledyne-Brown sensors.

Experimental Design

A two-factor, repeated measures experimental design (see Winer, 1962) was used. The two independent variables of interest were sensor type and altitude (AGL). Three levels of sensor type were used (see Table 8). Level I was a laser line scan sensor (KA-98) which is downward looking only, has a fixed effective focal length, and has its information displayed in a nonrectilinearized image in a moving map format. Level II was a slewable TV sensor which creates its perspective by changing the azimuth and elevation of camera pointing and changes scale by using zoom optics (as well as by changing slant range). Level III was an overflight TV sensor (Teledyne-Brown Engineering) which had a forward looking capability (for target acquisition/navigation) and a downward looking capabiltiy for reconnaissance, had a fixed effective focal length, and offered a forward oblique perspective in the navigation mode and a combination of vertical and nonderotated side oblique geometry in the reconnaissance mode. These three levels of sensors represent different approaches to solving the problem of acquiring exploitable imagery while also preserving sufficient lateral coverage to compensate for small navigational errors. Each also presents a characteristics display to the operator. (Table 7 presents the salient specifications for these three sensors).

TABLE 8. EXPERIMENTAL DESIGN

Sensor Type	B_1 (500 feet)	B_2 (1,000 feet)
A_1 Laser Line Scan	Group I	Group I
A_2 Slewable TV	Group II	Group II
A_3 Overflight TV	Group III	Group III

Two levels of altitude were used. Level I was 500 feet and Level II was 1,000 feet. These two levels were selected because the mission application for the reconnaissance RPV is defined at low altitude. The 500 foot altitude corresponds to the minimum threat environment, and the 1,000 foot altitude represents an upper limit that could be used if additional forward or lateral ground coverage were required.

Dependent Variables

Dependent variables used to determine the effect of the two variables of interest on operator performance were

1. Percent of Targets Detected: This is computed percentage score. It represents the probability that a prebriefed target will be correctly detected in real time. Thus, "false alarms" were equated with missed targets, and repeated misses were counted only once.

2. Time on Display to Detection: This measure represents the time it takes for an operator to respond to the presence of a target on the display from the time that the target first enters the sensor FOV.

3. Ground Range at Detection: This is the ground distance between the sensor/vehicle nadir point and the target at the instant of detection. For the KA-98 sensor, 3298 feet was added to each observation. This avoided negative ground ranges (i.e., the RPV having already passed the target before the subject detected it) while maintaining the

correct ordering of the observations. This correction also transformed the greatest negative ground range observation to zero feet.

4. Slant Range to Target Detection: This is the actual distance from the sensor to the target. The slant range values used in the analyses of the KA-98 were set equal to the altitude, while slant ranges for the other sensors were determined on the basis of the actual performance observed in the experiments.

5. Image Scale at Detection: Image scale, a dimensionless value, is the ratio of a dimension on the display to its true ground extent. It is a function of sensor FOV, slant range, and display size.

6. Accuracy of Interpretation: This dependent measure was based on the ratio of the number of correct responses to the total number of required responses.

7. Interpreter Confidence: The qualitative degree of certainty with which subjects responded to the interpretation questions was used as a dependent measure. Each question element was accompanied by a seven point scale of subject certainty. A response of one indicated absolute uncertainty, and a response of seven reflected absolute certainty.

Apparatus

Equipment used in this experiment consisted of (1) the upgraded PIS, (2) a 14 inch TV monitor, (3) an Hitachi disk recorder and TV monitor, (4) a video tape recorder, (5) briefing and navigational aids, and (6) miscellaneous and accessory equipment.

The PIS was used to generate imagery simulating each of the sensors from medium altitude strip photograph. Within the imagery generated, a total of ten target complexes were selected. The imagery was then recorded on video

tape in order to facilitate data collection. Each tape contained ten target pass runs and ten target information-extraction runs. Five of the target pass and target information-extraction runs simulated the 500 foot altitude, and five simulated the 1,000 foot altitude. Also on the tape was imagery simulating the 500 and 1,000 foot altitude perspective. This was used to familiarize the subjects with the imagery to be viewed.

The 14 inch TV monitor served as the subject's display upon which he viewed the simulated imagery. The Hitachi disk recorder and monitor served as the experimenter's station. An overlay grid was placed on the face of the monitor and was used by the experimenter to score detection performance. The tape recorder served as the vehicle for presenting the simulated imagery to the subject and experimenter.

Subjects

Eighteen subjects were used. All were paid volunteers from a local university and all had normal or corrected vision of 20/20. The subjects were randomly divided into three groups of six subjects each with each group differing in terms of the sensor which they were exposed to. Thus, Group I used the laser line scan sensor; Group II used the slewable TV sensor; and Group III used the overflight TV sensor.

Task and Procedure

The task used in this study consisted of two phases--a detection phase and an information-extraction phase. During the detection phase, subjects "flew" several missions against known, prebriefed targets. As soon as they detected a target, subjects depressed a handheld pushbutton. This action activated the field-freeze disk at the experimenter's station and allowed him to score performance. Immediately following the detection phase, subjects were required to extract as much information as they could about the target by filling in preprepared questionnaires (EEI checklist). During this phase they were allowed to view the target on a frame-by-frame basis utilizing the framing mode of the video tape recorder.

During this study, the following procedures were adhered to. Prior to a data run, each subject was given a 10-15 minute briefing which consisted of a detailed explanation of the purpose of the study and the tasks to be performed by him. Particular attention was placed on the way he was to respond and in the operation of the framing mode for the video tape recorder.

After answering any questions that they might have, the subjects were shown two familiarization missions depicting a 500 foot and 1,000 foot altitude scenario. During the showing of these tapes, subjects were instructed to familiarize themselves with the way various objects, structures, etc. appeared.

After again ascertaining whether subjects had any questions, each subject was given ten trials. During each trial they performed the two tasks described previously. During all data runs, subjects were seated approximately 28 to 32 inches from the display under ambient room illumination (see Figure 22).

Results

To determine the impact of sensor type and altitude upon operator performance, a conventional statistical analysis (i.e., analysis of variance or ANOVA) was used. The ANOVA allows one to evaluate the effects of one or more variables on performance. This evaluation is based on the probability associated with obtaining results as extreme as those actually obtained on the basis of pure chance. The particular ANOVA used was a two-factor, repeated measures design as described in Winer (1962). Selection of this design was based on the control that this kind of design provides over individual differences between experimental units. Prior to the actual analysis, tests for homogeneity of variance and transformation of the raw data (when necessary) to ensure normality were carried out. As pointed out by Kirk (1969, p. 64), "in order to test hypotheses concerning population means the homogeneity assumptions of analysis of variance must be tenable."

Whenever significant effects occurred between sensors, Scheffe's S test was applied to determine which means differed significantly from the other. This test was not applied to the altitude means since only two levels of

Figure 22. Experimenter and Subject Stations

altitude were used. If any interactions (sensors × altitude) proved significant, the method of orthogonal comparisons was applied to subdivide the treatment sum of squares and test the components in order to identify local interactions of significance. Snedecor & Cochran (1967, p. 348) point out that "the F-test of the AB interaction sum of squares as a whole is not a good guide as to whether interactions can be ignored."

An additional test, a one-way ANOVA on sensors (at the 500 foot AGL), was performed to investigate possible differences in performance at the preferred operational flight regime.

The results of the ANOVA's performed on the various dependent variables employed are presented in Table 9. The ANOVA's indicate (based on achieving statistical significance at $p < .05$ level) that sensor type significantly influenced performance as measured by time on display until detection, ground range at detection, slant range at detection, and image scale at detection. Altitude significantly influenced performance on ground range at detection, slant range at detection, and image scale at detection. Significant sensor-by-altitude interactions were obtained for probability of target detection, time on display until detection, ground range at detection, and image scale at detection. The summary tables (Tables 10 through 14) for all of the ANOVA's from which statistically significant findings were obtained are presented below.

The means and standard deviations for each treatment condition (i.e., broken out for each sensor type and altitude condition) for each performance measure are presented and plotted in Figures 23 through 29. Figures 23 through 27 depict performance on the detection task, while Figures 28 and 29 depict performance on the information-extraction (interpretation) task. Inspection of Figure 23 indicates that detection performance with the KA-98 sensor was better (95 vs 73 percent) than the other two sensors, though not significantly so, as indicated by the ANOVA (Table 10). The significant sensor × altitude interaction is derived from the reversal in trend between the slewable and Teledyne-Brown sensors.

TABLE 9. SUMMARY OF RESULTS

Dependent Measure	Significant* Finding(s)
Percent of Targets Detected	Sensor × Altitude Interaction
Time on Display Until Detection	Sensors
	Sensor × Altitude Interaction
Ground Range at Detection	Sensors
	Altitude
	Sensor × Altitude Interaction
Slant Range at Detection	Sensors
	Altitude
(Displayed) Image Scale at Detection	Sensors
	Altitude
	Sensor × Altitude Interaction
Accuracy of Interpretation	(None)
Interpreter Confidence	(None)

*In a statistical sense

TABLE 10. ANOVA SUMMARY: PERCENT OF TARGETS DETECTED

Source	S.S.	d.f.	M.S.	F
Between Subjects	1.2589	17		
Sensor	0.3819	2	0.1910	3.265
Subjects within groups	0.877	15	0.0585	
Within Subjects	0.380	18		
Altitude	0.0009	1	0.0009	<1.0
Sensor × Altitude	0.1691	2	0.0846	6.043*
Altitude × Subjects Within Groups	0.21	15	0.014	

*p<.05

TABLE 11. ANOVA SUMMARY: TIME ON DISPLAY UNTIL DETECTION (TRANSFORMED DATA)

Source	S.S.	d.f.	M.S.	F
Between Subjects	5.321	17	0.313	
Sensor	4.865	2	2.4325	80.*
Subjects Within Groups	0.456	15	0.0304	
Within Subjects	0.163	18		
Altitude	0.007	1	0.007	1.0
Sensor × Altitude	0.051	2	0.026	3.71*
Altitude × Subjects Within Groups	0.105	15	0.007	

*p<.05

TABLE 12. ANOVA SUMMARY: GROUND RANGE AT DETECTION

Source	S.S.	d.f.	M.S.	F
Between Subjects	6.179×10^8	17		
Sensor	5.036×10^8	2	2.52×10^8	33*
Subjects Within Groups	1.143×10^8	15	7620411	
Within Subjects	1.204×10^8	18		
Altitude	46644347	1	46655347	15.73*
Sensor × Altitude	29314006	2	14657003	4.94*
Altitude × Subjects Within Groups	44465779	15	2964385	

*p<.05

TABLE 13. ANOVA SUMMARY: SLANT RANGE AT DETECTION

Source	S.S.	d.f.	M.S.	F
Between Subjects	435390496	17		
Sensor	324084064	2	162042032	22.*
Subjects Within Groups	111306432	15	7420429	
Within Subjects	121106083	18		
Altitude	59046418	1	59046418	20.6*
Sensor × Altitude	18122883	2	9561442	3.3
Altitude × Subjects Within Groups	42938782	15	2862452	

*p<.05

TABLE 14. ANOVA SUMMARY: IMAGE SCALE AT DETECTION

Source	S.S.	d.f.	M.S.	F
Between Subjects	103211159	17		
Sensor	75460236	2	3773018	20.*
Subjects Within Groups	27750923	15	1850062	
Within Subjects	22411949	18		
Altitude	8147219	1	8147219	13.*
Sensor × Altitude	5202821	2	2600911	4.3*
Altitude × Subjects Within Groups	9062909	15	604194	

*p<.05

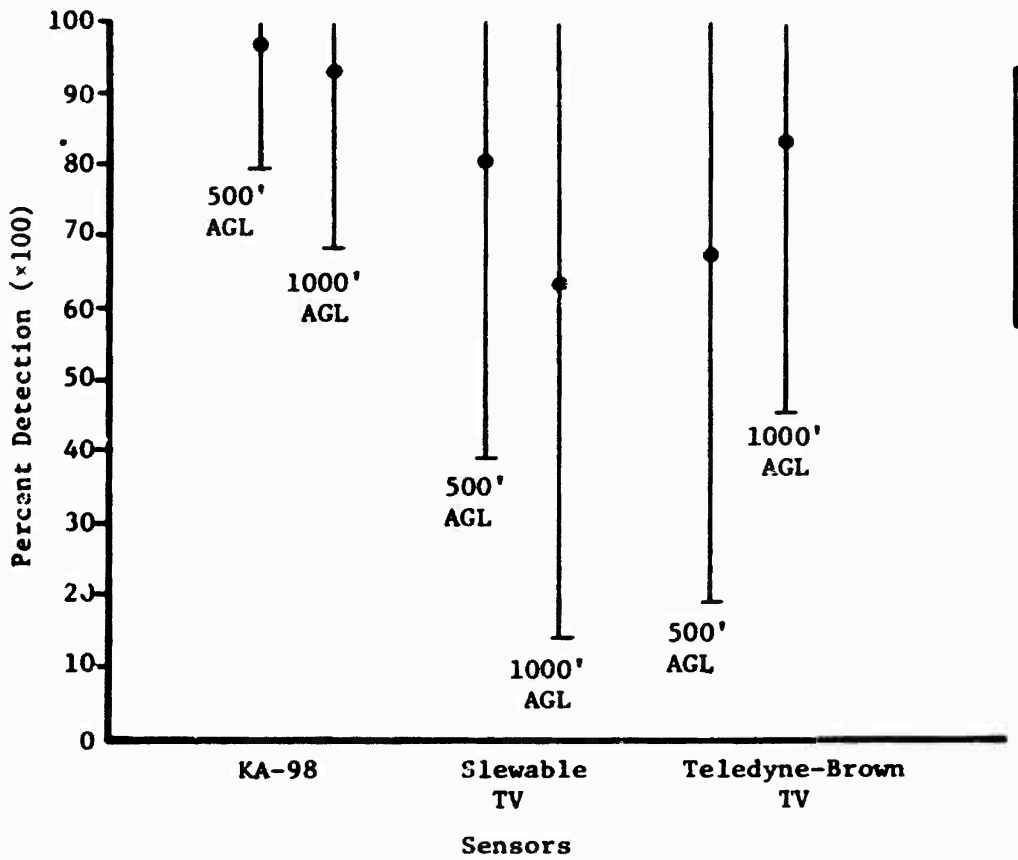

			ALTITUDE	
			500'	1000'
SENSORS	KA-98	$\bar{X}$	97	93
		S	18	25
	Slewable TV	$\bar{X}$	80	63
		S	41	49
	Teledyne-Brown TV	$\bar{X}$	67	83
		S	48	38

Key: Mean ± 1 Standard Deviation

Figure 23. Percent of Targets Detected

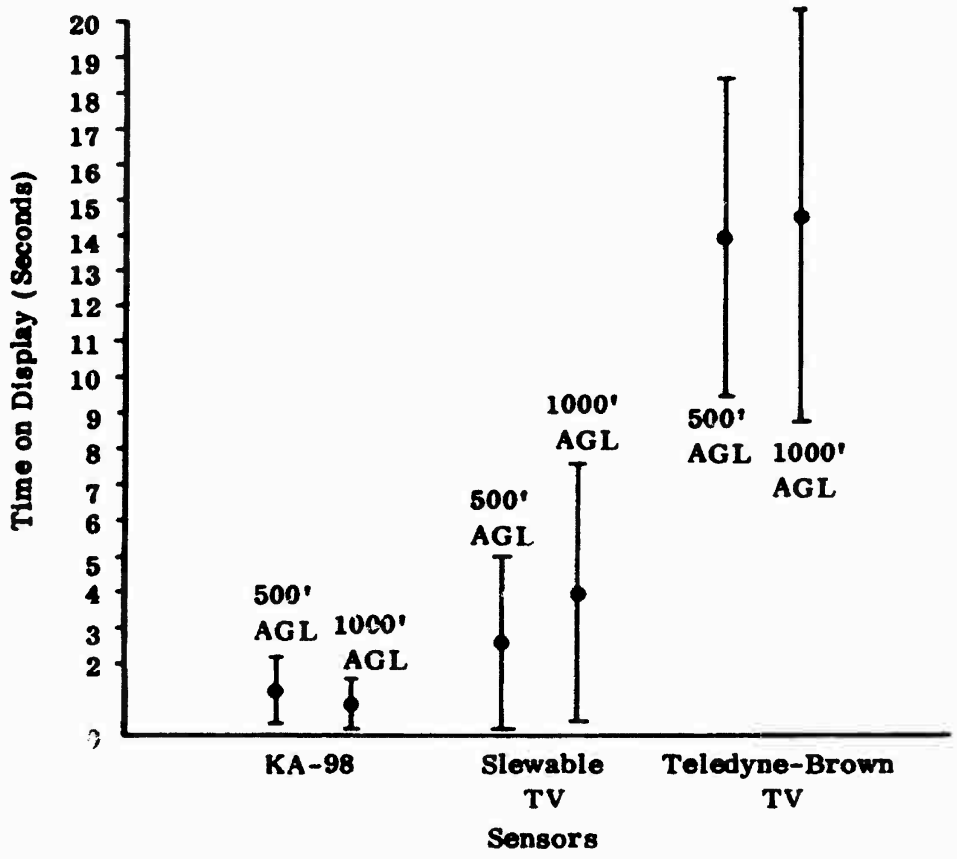

SENSORS			ALTITUDE 500'	ALTITUDE 1000'
	KA-98	$\bar{X}$	1.26	.85
		S	.91	.70
	Slewable TV	$\bar{X}$	2.56	4.00
		S	2.40	3.62
	Teledyne-Brown TV	$\bar{X}$	14.00	14.58
		S	4.51	5.78

Figure 24. Time on Display Until Detection

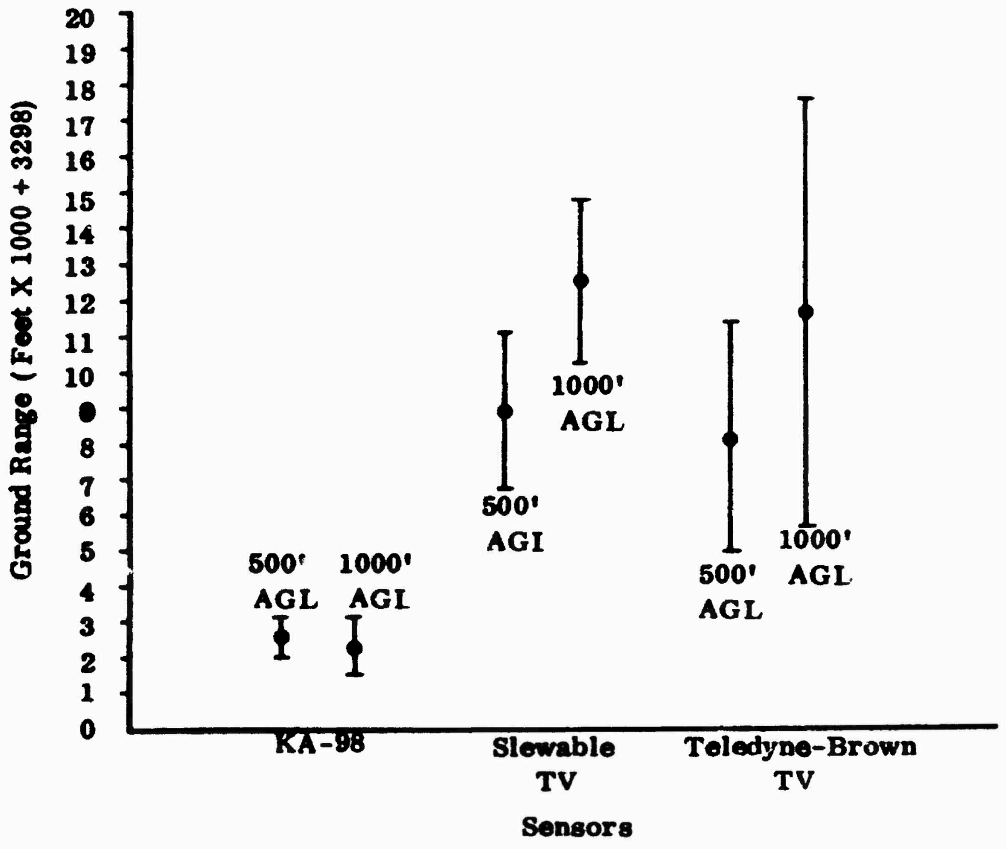

SENSORS			ALTITUDE 500'	ALTITUDE 1000'
	KA-98	$\bar{X}$	2558	2283
		S	536	823
	Slewable TV	$\bar{X}$	8899	12469
		S	2242	2312
	Teledyne-Brown TV	$\bar{X}$	8210	11746
		S	3170	6053

Figure 25. Ground Range at Detection

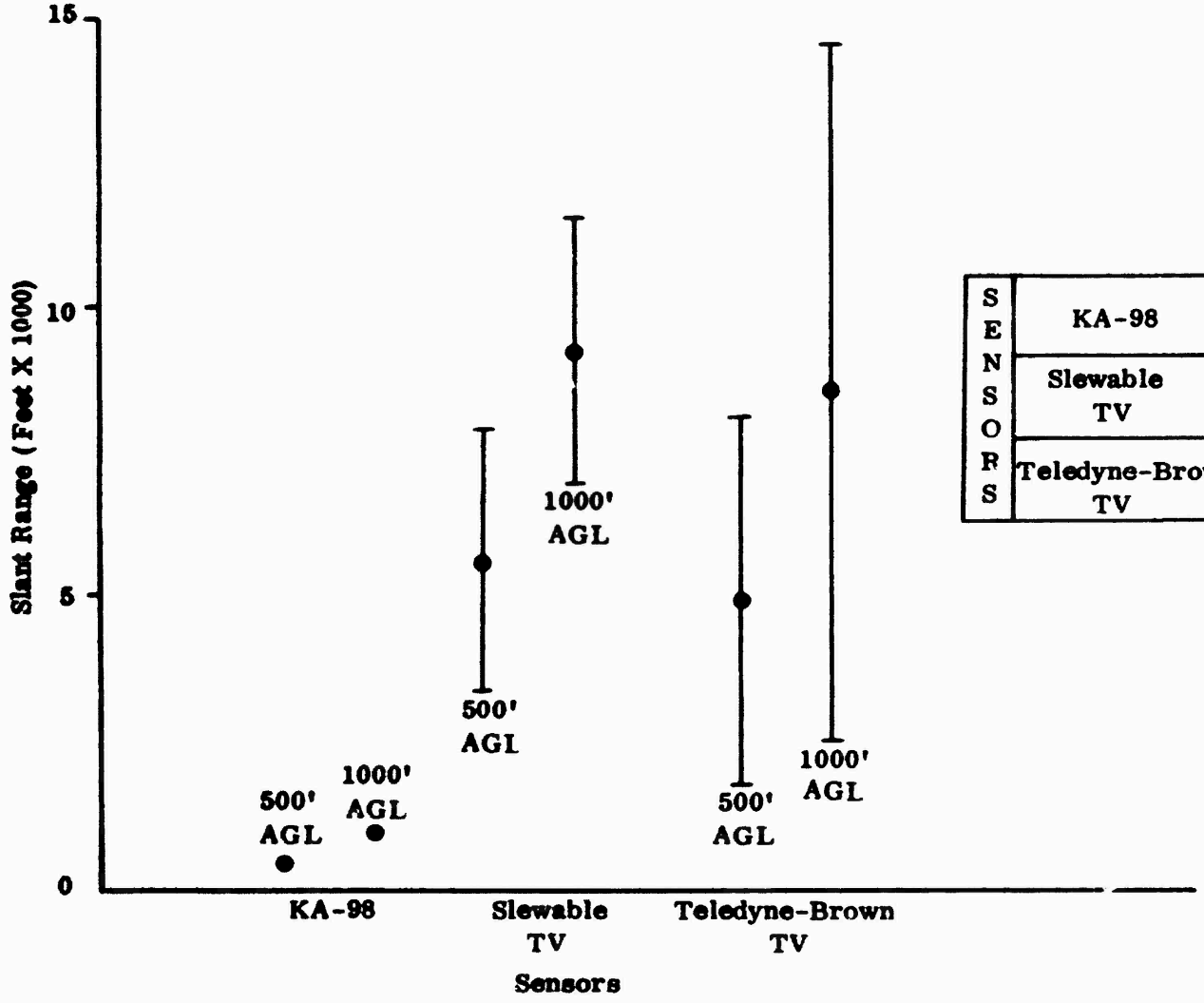

SENSORS			ALTITUDE 500'	ALTITUDE 1000'
	KA-98	$\bar{X}$	500	1000
		S	--	--
	Slewable TV	$\bar{X}$	5625	9229
		S	2252	2296
	Teledyne-Brown TV	$\bar{X}$	4959	8538
		S	3149	5998

Figure 26. Slant Range at Detection

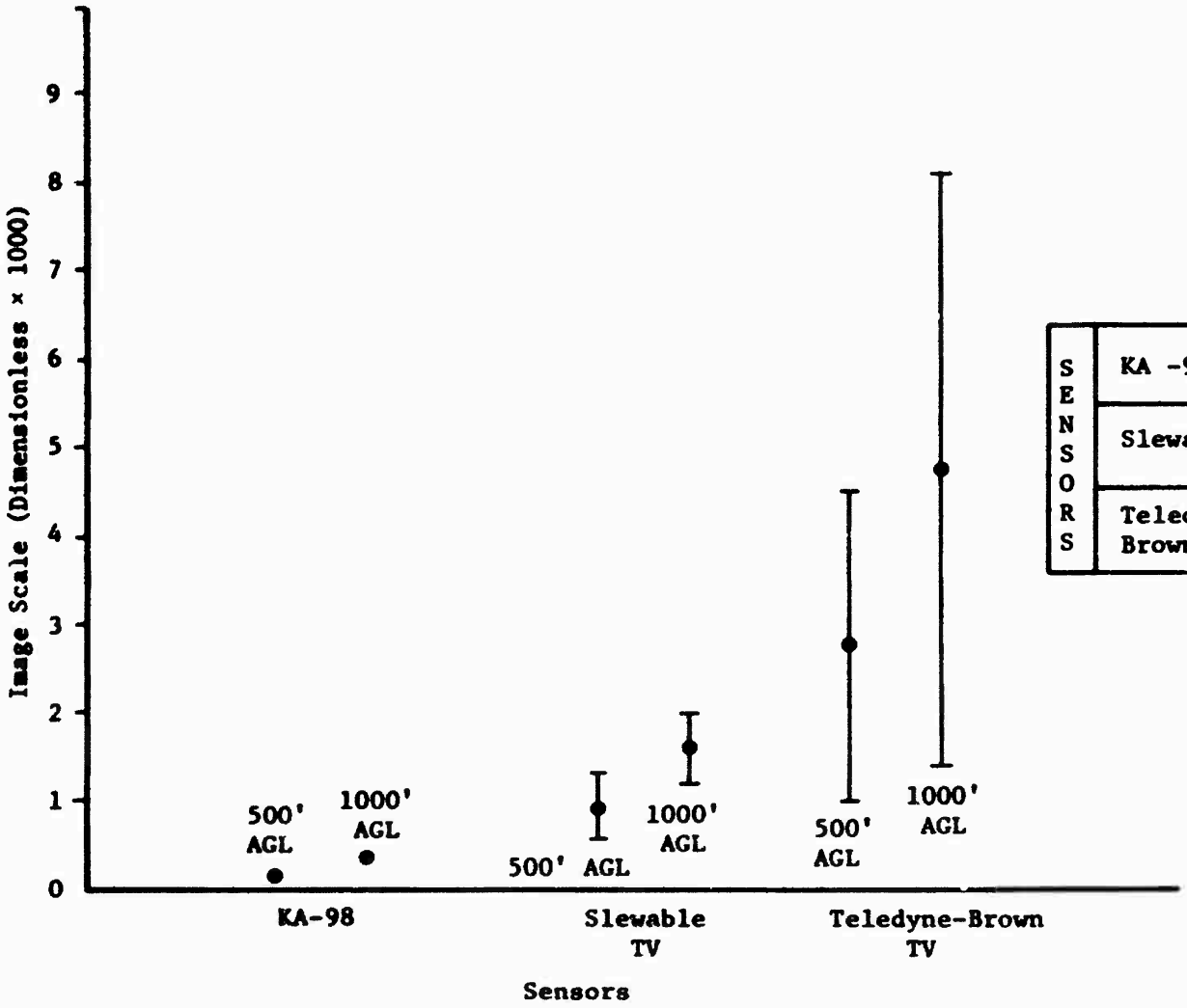

SENSORS			ALTITUDE 500'	ALTITUDE 1000'
	KA -98	$\bar{X}$	223	446
		S	--	--
	Slewable TV	$\bar{X}$	984	1615
		S	394	402
	Teledyne-Brown TV	$\bar{X}$	2772	4773
		S	1760	3353

Figure 27. Image Scale at Detection

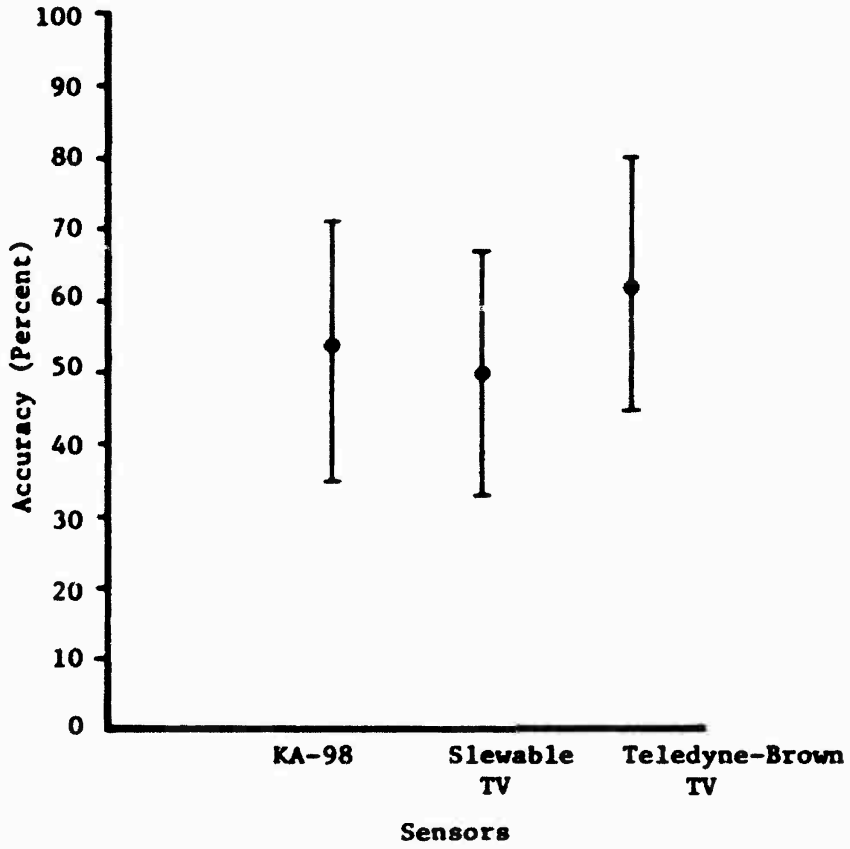

SENSORS			
	KA-98	$\bar{X}$ S	53.3 18.2
	Slewable TV	$\bar{X}$ S	50.0 16.8
	Teledyne-Brown TV	$\bar{X}$ S	62.4 17.7

(Pooled Across Altitude)

Figure 28. Accuracy of Interpretation

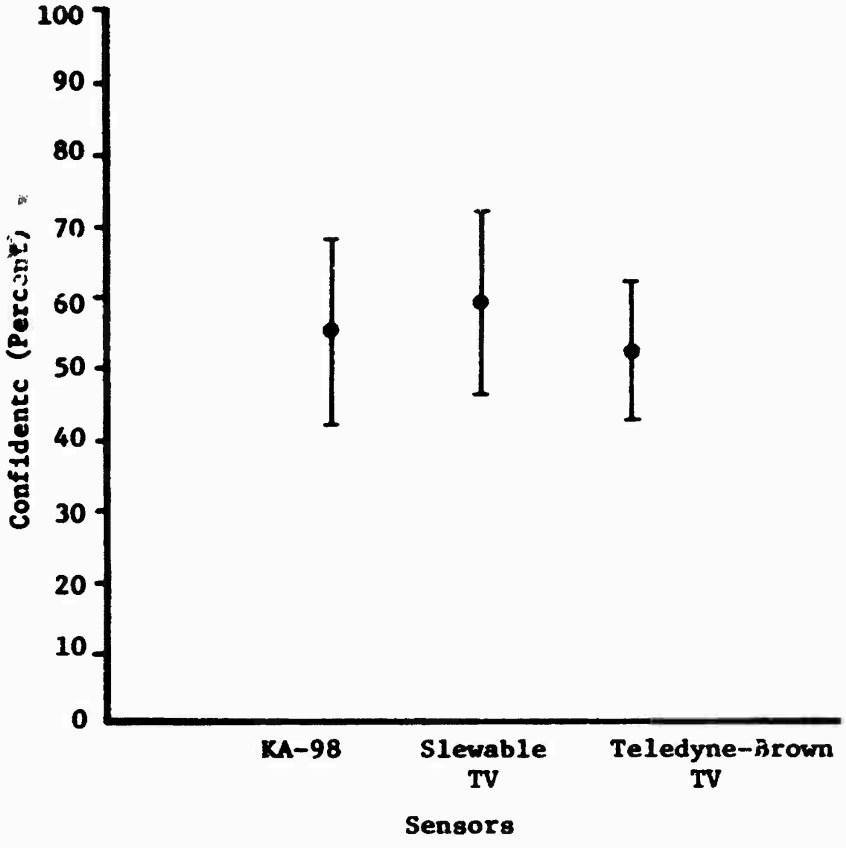

SENSORS			
	KA-98	$\bar{X}$ S	55.0 13.0
	Slewable TV	$\bar{X}$ S	59.3 12.9
	Teledyne-Brown TV	$\bar{X}$ S	51.7 9.1

(Pooled Across Altitude)

Figure 29. Confidence in Interpretations

Figure 24 shows performance for time on display until detection. Immediately apparent is the difference in speed with which subjects were able to detect targets as a function of sensor type. Collapsed over altitude, the data shows that the KA-98 yielded detection times that were at least three and 18 times faster than that for the slewable and Teledyne-Brown sensors, respectively. Additionally, detection performance for the slewable sensor was four times faster than the Teledyne-Brown sensor. These findings are in keeping with the significant findings of the ANOVA (Table 11). The significant sensor × altitude interaction is derived from the reversal in trend between the KA-98 and slewable TV sensors.

Figure 25 shows performance as measured by ground range at detection i.e., the ground distance between the sensor/vehicle nadir point and the target at the instant of detection. This measure is a critical consideration in terms of survivability, threat avoidance, and target coverage. It should be noted that the KA-98 could only acquire ground coverage, laterally, by actually overflying the center of the swath. This necessitated correcting the ground range data (based on target detection performance) by adding 3,298 feet to each observation. This correction avoided any negative ground ranges while maintaining correct ordering of the observations.

As indicated by the plots, subjects were able to detect targets at a longer distance using either the slewable or Teledyne-Brown sensors as compared with the KA-98. For the 500 foot altitude, this distance was three times greater; at the 1,000 foot altitude, it was five times greater. These findings are in keeping with the significant findings of the ANOVA (Table 12). The significant sensor × altitude interaction was due to the reversal in trend between the KA-98 and the slewable TV sensors.

Figure 26 shows performance as measured by slant range to target at detection, i.e., the actual distance from the sensor to the target. The slant range values used in the analyses of the KA-98 were set equal to the

altitude. This was done because the KA-98 will acquire swath width coverage equal to the typical navigation error (±150 feet) within 34 degrees of its FOV at 500 feet AGL. The actual slant range is equal to 500 feet at the center of each scan and is equal to 523 feet at ±17 degrees. Since this difference is small, the actual altitude was used. Slant ranges for the other sensors were determined on the basis of the actual performances observed.

The plots in Figure 26 show that subjects detected the targets sooner (at a longer slant range) with the slewable and Teledyne-Brown sensors as compared with the KA-98. Additionally, performance was better at the higher altitude as compared with the lower altitude. At the lower altitude, the slewable and Teledyne-Brown sensors were five times better than the KA-98, while at the higher altitude they were nine times better. Again, these findings reflect the significant findings of the ANOVA (Table 13).

Figure 27 shows performance as determined by image scale at detection, i.e., the ratio of a dimension on the display to its true ground extent. The observed data for slant range were transformed to produce appropriate values of horizontal image scale. For the KA-98, only a portion of the total FOV (the central 34 degrees) was considered since this was required to encompass the typical navigation error. In addition, the data was scaled to properly reflect the aspect ratio of the moving map display. It should be noted that since these were the scale factors actually required for target detection, the following analyses offer opportunities for predictive modeling.

The plots in Figure 27 indicate that performance with the KA-98 was better than with the slewable or Teledyne-Brown sensors and that the slewable was better than the Teledyne-Brown. Performance with the KA-98 was approximately four times better than the slewable and 13 times better than the Teledyne-Brown. The slewable was three times better than the Teledyne-Brown. These differences held for both altitudes, even though performance at the 500 foot altitude was approximately two times better than at the 1,000 foot altitude. These findings reflect the significant findings of the ANOVA (Table 14).

Figures 28 and 29 depict subject performance on the information-extraction (interpretation) task. Figure 28 shows performance as measured by accuracy of interpretation, i.e., the ratio of the number of correct responses to the total number of required responses. The image truth used in scoring this task was provided by a trained and experienced imagery interpreter utilizing the film directly on a variable illumination light table equipped with a Bausch & Lomb Zoom 24C binocular viewing head. As indicated by the plots, performance with all three sensors was essentially equivalent, with the best score being 6.24 (Teledyne-Brown) and the worst score being 5.00 (slewable). Performance with the KA-98 was 5.33. These findings were, of course, not significant.

Figure 29 shows performance as measured by confidence, i.e., the qualitative degree of certainty with which subjects responded to each question on the questionnaire. The slewable TV sensor elicited the greatest confidence score (4.15) while that for the KA-98 and Teledyne-Brown were essentially the same, 3.85 and 3.62 respectively. Again, no significant differences were found.

Discussion

To this point in the reporting of the target acquisition experiment, emphasis has been on the two factors, repeated measures design. In order to achieve an operationally relevant appreciation of the findings, the results of the post hoc analyses, already identified, must be considered as well. In the following discussion, the significant findings reported above are further studied in order to more specifically identify the underlying differences between the sensor systems and to form the bases for statements which reflect these differences with regard to their impact on sensor system capabilities and limitations.

The sensor × altitude interaction was significant with respect to the percent of targets detected. Specifically, the slewable TV × Teledyne-Brown TV × altitude interaction was significant. The narrow FOV slewable TV afforded the operator a 19 percent higher target acquisition rate at 500 feet AGL while the wide FOV Teledyne-Brown TV provided a 32 percent higher target

acquisiton at 1,000 feet AGL. Thus it appears that, for a forward looking sensor at the lower altitude, a narrower FOV provides the more desirable capability for target detection.

Both sensors and the sensor × altitude interaction were significant with respect to time on display until target detection. With regard to sensors, the significance arose from the difference between the Teledyne-Brown TV and the other two sensors (which were not different from each other). The average detection time required for the Teledyne-Brown TV was 550 percent longer than the average of the other two sensors. This appears to impact adversely on the application of the wide FOV NAV mode to multiple targets. With regard to the sensor × altitude interaction, the significant comparison was the KA-98 × slewable TV × altitude interaction. Detection time was 103 percent longer with the slewable TV at 500 feet AGL but 371 percent longer with the KA-98 at 1,000 feet AGL. Thus, the line scan sensor supports a more rapid detection process at the lower altitude.

In analyzing the ground range at detection dependent measure, all three variables (sensors, altitude, and sensor × altitude interaction) were significant. With regard to sensors, the KA-98 was different from the other two sensors (which were not different from each other). The KA-98 was 327 percent closer to the target at detection than was the average downtrack distance for the other sensors. This is not surprising since the line scanner must overfly the target in order to acquire imagery of it, while the other sensors employ forward looking capabilities. With regard to altitude, the average position for all three sensors was 35 percent closer to the targets at 500 feet than at 1,000 feet AGL. The sensor × altitude interaction achieved significance because of the comparison of the KA-98 with the other two sensors. The line scanner was 12 percent closer to the target at 1,000 feet AGL (than at 500 feet) while the other sensors were 42 percent closer to the target at 500 feet AGL (than at 1,000 feet). If proximity to the target, as measured in ground distance, is of operational import (for example, if the operator must modify the RPV flight program based on a target's presence at a location), then the forward looking sensors place the RPV closest to the target at the lower altitude.

Both sensors and altitude were significant for slant range at detection. With regard to sensors, the KA-98 was different from the other two sensors (which were not different from each other). Targets were 845 percent closer to the line scan equipped RPV than to the forward looking systems. Again, it should be noted that the KA-98 is a downward looking line scanner. With regard to altitude, targets were detected at 70 percent closer range at 500 feet than at 1,000 feet AGL.

All three factors (sensors, altitude, and sensor × altitude interaction) were significant for the image scale at detection dependent measure. Sensors produced a significant effect because the Teledyne-Brown TV was different from the other two sensors (which were not different from each other). Targets imaged by the Teledyne-Brown camera were 362 percent smaller at detection than was true for the remaining sensors. This is typical for a wide FOV, forward looking sensor and impacts on observer performance in that a target must subtend a minimum angular dimension, corresponding to dynamic foveal vision, in order to be detectable to the human. The difference in performance elicited by altitude was that targets, at detection, were displayed at 139 percent smaller size at 1000 feet than at 500 feet AGL. Again this impacts on the displayed target size required by the observer. The sensor × altitude interaction was generated by the interaction of the Teledyne-Brown TV with each of the other sensors (Teledyne-Brown TV × Slewable TV × Altitude and Teledyne-Brown TV × KA-98 × altitude). The impact is in terms of the rate at which targets get smaller on the display as altitude increased. Target scale became smaller 318 percent faster for the Teledyne-Brown TV than for the slewable TV and 897 percent faster than for the KA-98 as the altitude changed from 500 to 1,000 feet AGL.

Section 6

COMPARISON OF SENSOR PERFORMANCE

ANALYSIS

The approach followed in developing the comparison of the candidate sensors is discussed in detail in Kepner and Tregoe (1965). These authors term the approach "decision analysis" and define its result as follows: "A systematic decision is the product of a great many small judgements, organized and summarized." They further refine "decision analysis" into a logical sequence of phases:

1. Identifying performance criteria against which to evaluate alternative choices

2. Prioritizing these criteria to establish their relative importance in defining a "best" alternative

3. Identifying the set of alternative sensors within which to perform the selection (KA-98, Teledyne-Brown TV camera, and a type slewable TV camera)

4. Evaluating the alternatives against the performance criteria to make a choice

The criteria set used in the comparison of sensors was developed in the context of the BGM-34C operational mission. Program office documentation was reviewed to establish the pertinent mission requirements. These requirements were later reevaluated to reflect operator (SAC and TAC) experience and concept of system operation. These requirements were then used to generate a set of performance criteria capable of describing requirement satisfaction in quantitative terms. The criteria covered five basic areas of system capabilities: survival, exploitation, resources, mission growth, and reporting. An initial criteria set consisting of approximately thirty proposed performance measures was presented to the RPV SPO for discussion, review, and prioritization at a working group on 25 March 1976. As a result of this meeting, five specific

criteria were determined to impose mandatory, or GO/NO GO, capabilities on the system. Unless a candidate sensor could satisfy every one of these five performance objectives, it could not be considered for use in the BGM-34C system. The mandatory criteria are:

1. A sensor must provide a target acquisition capability commensurate with the navigation accuracy of the BGM-34C system. Since the maximum expected navigation error of the system is expected to be ±500 feet, the sensor must provide a swath width or cross line of flight coverage of at least this dimension.

2. The sensor must be capable of supporting the exploitation (or imagery interpretation) requirements of the BGM-34C mission. The EEI's to be answered by this system range from the identification of a tactical vehicle through the interpretation of target complexes.

3. The bandwidth of the sensor imagery must be compatible with the data links between the RPV and the DC-130 and between the DC-130 and the RRF.

4. The sensor mode of operation must allow for recording (up to twenty minutes) of imagery onboard both the RPV and the DC-130 director aircraft.

5. The sensor mode of operation must permit the playback of imagery for near real time interpretation onboard the DC-130 or at the RRF.

All three candidate sensors have sufficient FOV to achieve the required swath width at the 500 foot AGL altitude. All sensors provide imagery which is real time or near real time exploitable. Transmission bandwidth is presumed to be sufficient for all three sensors and the imagery can be recorded for subsequent playback or retransmission. Thus, the three candidate sensors were judged to be capable of satisfying the mandatory performance objectives. The remaining elements in the performance criteria set were assigned weighting factors to reflect their individual impact on the satisfaction of the BGM-34C mission.

The list of weighted performance criteria was reduced during the development of the review of sensor systems requirements, the analyses of each of the candidate sensors, and on the basis of the man-in-the-loop operator performance studies. Examples of the elimination process follow. Peripheral reconnaissance capability was deleted as a criterion as inconsistent with the concept of system operation; the BGM-34C is a tactical acquisition system achieving its operational survivability by high airspeed and low altitude. The criterion for minimum holidays in target coverage was deleted because all three sensors obviate the possibility of missing a target (within the worst case navigation offset); the KA-98 by its wide (136 degrees) lateral FOV and V/H range, the Teledyne-Brown camera by its NAV mode for target acquisition and the overlapping "step frame" sequence of its RECON mode, and the slewable TV by a tracker and operator control of FOV in zooming. Image orientation was deleted because the interpretation phase of the experiments determined no statistically significant difference in performance between the three sensors; although the Teledyne-Brown RECON imagery was simulated to produce the appropriate image rotation off ground track. The final criteria set and the respective weighting factor are presented in Table 15. The first seven of these critera formed the dependent measures used in the operator performance studies. The remaining five criteria are used as the performance measures in the following analyses.

Ground Spot Size

This parameter is the ground dimension of the sensor instantaneous FOV. It is one of the critical determinants of the transfer of spatial information to the operator. Considering the three sensors at 500 feet AGL and ±500 feet navigation error in an interpretation-oriented task, the slewable TV achieves the smallest ground spot size (approximately 0.16 feet at 80 degrees depression angle and an FOV of 6.5 degrees). The dynamic ground spot size for the KA-98 is about twice this value, and that of the Teledyne-Brown camera (RECON mode, vertical and intermediate footprints) is twice again as large.

TABLE 15. NRT/RT SENSOR PERFORMANCE CRITERIA

Criterion	Weighting Factor
Percent of Targets Detected	10
Time on Display to Detection	4
Ground Range at Detection	2
Slant Range at Detection	2
Image Scale at Detection	5
Accuracy of Interpretation	10
Interpreter Confidence	8
Ground Spot Size (Resolution)	5
Raster Lines on Target (Display)	5
Total Time on Target	4
Standoff Capability (Mission Growth)	2
Night Upgradeable	10

Raster Lines on Target

This is another parameter which describes the amount of information made available to the operator. It is referenced to the display itself. Considering the same conditions above and a target with a 30 foot downtrack dimension, the slewable TV would display it with about 250 raster lines (on a 525 line monitor), the Teledyne-Brown sensor would use about 45 lines (same monitor), and the KA-98 would use only about 7 lines (1025 line monitor).

Total Time on Display

The total time that a single target is displayed to the operator (real time) will, of course, influence both target acquisiton and real time interpretation. It is a function of both the sensor downtrack FOV and the RPV

groundspeed. Assuming the above scenario and a velocity of 350 knots, it takes about 5.5 seconds for a target to traverse the display of KA-98 imagery. This assumes a 4:3 aspect of the monitor (i.e., the long dimension of the monitor corresponding to the downtrack direction). The Teledyne-Brown camera is also deterministic for total time on display. The NAV mode uses a wide FOV (32 degrees) but can be varied somewhat in depression angle. Assuming a 10 degree depression angle, a target will traverse the display in about 23 seconds if a "usable" image of the target can be obtained at 2 degrees below the horizon. If a more conservative "usable" image is appropriate, perhaps at 4 degrees below horizon, then the time reduces to about 12 seconds. The slewable TV under consideration is equipped with a tracker and is capable of depression angles at least to nadir.

Standoff Capability

Should survivability become emphasized, mission planning could well require the BGM-34C to stand off from a defended target during imagery acquisition. The KA-98 is an overflight sensor. The NAV mode of the Teledyne-Brown camera would permit target imagery acquisition in a forward looking geometry. The slewable TV by definition would afford both forward and sidelooking flyby imagery acquisition.

Night Upgradeable

This is another area of system/mission growth. The TAC Concept of Operations emphasizes night reconnaissance. The KA-98 has a night mode operation using an active laser illuminator scanned in registration with the collection aperture. The slewable TV is considered to be replaceable with a passive FLIR sensor. The Teledyne-Brown camera (based on conversations with system engineer) can be upgraded to day/night by the use of an active illuminator as an ancillary subsystem.

The final step in the "decision analysis" process is that of performing the evaluation of the three candidate sensor systems against the set of performance criteria. Table 16 presents a summary of this evaluation. The

TABLE 16. COMPARISON OF CANDIDATE SENSORS

Performance Criterion	W	KA-98		Slewable TV		Teledyne-Brown TV	
		S	WXS	S	WXS	S	WXS
Percent of Targets Detected*	10	10	100	8	80	7	70
Time on Display (Detection)*	4	10	40	5	20	1	4
Ground Range at Detection*	2	4	8	10	20	10	20
Slant Range at Detection *	2	1	2	10	20	9	18
Image Scale at Detection *	5	10	50	2	10	1	5
Accuracy of Interpretation	10	9	90	8	80	10	100
Interpreter Confidence	8	9	72	10	80	9	72
Ground Spot Size	5	5	25	10	50	3	15
Raster Lines on Target (Display)	5	0[1]	0	10[2]	50	2[2]	10
Total Time on Display	4	4	16	10	40	8[3]	32
Standoff Capability (see Text)	2	0	0	10	20	4[3]	8
Night Upgradeable	10	10	100	8[4]	80	6[5]	60
TOTALS			503		550		414

W Weight

S Score

* Significant in 1-way ANOVA

1 1025 line monitor

2 525 line monitor

3 NAV Mode

4 Assumes FLIR presents no technical risk

5 Assumes Illuminator presents no technical risk

scores accorded each sensor are shown in the column marked "S" in Table 16. All scores are relative to 500 feet AGL; i.e., only the 500 feet AGL data was used in this comparison since this is the preferred operational altitude for the BGM-34C vehicle. For the first seven criteria, the raw data means were scaled such that the "best" (in an operational sense) performing sensor received a score of 10 and the other sensors were ranked against it (Tables 17 through 23 present the analyses). The criteria developed above were also scored in this manner.

Given the weighting factors shown in Table 15 and assuming an "ideal" sensor (i.e., one that would achieve the optimal 10 score on each criteria), a total weighted score of 670 would be earned by this sensor. The ideal sensor can then serve as the norm against which all other sensors can be compared. In this case, the sensors are the KA-98, the slewable TV and the Teledyne-Brown. Using this approach, the slewable TV sensor achieved 82 percent of the ideal sensor score (550 of 670); the KA-98 achieved 75 percent (503 of 670); and the Teledyne-Brown 62 percent (414 of 670).

The first eleven criteria are scored on the basis of either empiric results or deterministic sensor characteristics. Scoring of the twelfth performance measure, potential for night upgrading, relied on judgements regarding the achievement of a night capability and the technical risk inherent in each case.

Although the conclusion that the slewable TV sensor represents the best selection for use in the BGM-34C system is based on both the analytic and experimental results, this finding is heavily influenced by the assumptions under which these studies were performed. Of critical significance is the assumption of a highly accurate navigation system. Because of this, the target always appeared within the sensor FOV and no action was required to update the navigation system or to perform a true search for the target. The navigation accuracy may be too optimistic and may not reflect the system capability under operational constraints (e.g., EW). The authors strongly feel that reduced accuracy and the concomitant impact on system performance should also be considered in carrying out the sensor selection process.

TABLE 17. PERCENT DETECTION: ONE-WAY ANOVA AT 500 FEET AGL

Source	S.S.	d.f.	M.S.	F
Between Sensors	.272	2	.136	4.25*
Error	.486	15	.032	
TOTAL	.758	17		

* $p < .05$

TABLE 18. TIME ON DISPLAY: ONE-WAY ANOVA AT 500 FEET AGL

Source	S.S.	d.f.	M.S.	F
Between Sensors	2.33891	2	1.17	75.*
Error	.23422	15	.0156	
TOTAL	2.57313	17		

* $p < .05$

TABLE 19. GROUND RANGE: ONE-WAY ANOVA AT 500 FEET AGL

Source	S.S.	d.f.	M.S.	F
Between Sensors	145252903	2	72626452	20.*
Error	53165807	15	3544387	
TOTAL	198418710	17		

* $p < .05$

TABLE 20. SLANT RANGE: ONE-WAY ANOVA AT 500 FEET AGL

Source	S.S.	d.f.	M.S.	F
Between Sensors	93167086	2	46583543	13.*
Error	52481887	15	3498792	
TOTAL	145648972	17		

* $p < .05$

TABLE 21. IMAGE SCALE: ONE-WAY ANOVA AT 500 FEET AGL

Source	S.S.	d.f.	M.S.	F
Between Sensors	20548454	2	10274227	20.*
Error	7771225	15	518082	
TOTAL	28319679	17		

* $p < .05$

TABLE 22. ACCURACY: ONE-WAY ANOVA AT COMBINED ALTITUDE

Source	S.S.	d.f.	M.S.	F
Between Sensors	.0041754	2	.0020877	2.89
Error	.0108500	15	.0007233	
TOTAL	.0150224	17		

TABLE 23. CONFIDENCE: ONE-WAY ANOVA AT COMBINED ALTITUDE

Source	S.S.	d.f.	M.S.	F
Between Sensors	.8582	2	.4291	1.71
Error	3.7577	15	.2505	
TOTAL	4.6159			

CONCLUSIONS

Overall Performance

Based on the total weighted scores (Table 16), the slewable TV sensor represents the best performing choice for application to the NRT/RT reconnaissance RPV mission.

Optimum Sensor

Based on the criteria set used and the associated weighting factors, none of the candidate sensors included in the performance comparison represents a near-ideal approach to satisfying the system mission requirements. The highest weighted score achieved represents only 82 percent of the possible score. (Note that scores were relative only for the three sensors considered.)

Night Reconnaissance

Of the sensors considered, only the KA-98 now represents a night reconnaissance capability. In considering this area of mission growth (required in the TAC Concept of Operations), the slewable sensor was assumed to be directly upgradeable to a FLIR (e.g., AN/APQ-9) and the Teledyne-Brown TV was assumed to be combined with an active illuminator. If these assumptions are valid, spectral characteristics and enemy defenses must be investigated.

Target Detection

The interaction between sensor type and altitude, found significant in the percent detection analysis, raises an interesting question regarding ARCO performance. The authors suggest that this interaction may arise from two different strategies, identification of the target itself or recognition of where the target should be based on surrounding features. The successful use of either approach seems to depend upon image scale and sensor FOV. It is suggested that ARCO training can improve performance if a combination of these strategies is emphasized.

Operational Profiles

The analyses of percent detection, time on display until detection, and image scale at detection, suggest that careful study be given to the RPV airspeed. Although only the operational airspeed was simulated, higher speeds (or higher V/E ratios) may be necessitated by survival considerations. Performance degradation may be expected if they are implemented.

Section 7

PLAN FOR FUTURE INVESTIGATIONS

Based on the analytic studies, the results and analyses derived through the operator performance assessment studies, program management and operational briefings, and/or interaction with the RPV SPO itself, the following program for continued research and simulation is proposed. This proposed program, currently being reviewed on the RPV SPO, recommends the following research action items for further investigations.

1. Investigate Impact of Navigation Errors

   Basis: Assumptive navigation accuracy optimistic

   Approach: Utilize navigation error (± one mile) as independent variable. Use NAV mode to correct/minimize error.

2. Investigate Impact of Reduced Visibility on Sensor Performance

   Basis: Assumptive target contrast optimistic

   Approach: Review target signature and visibility literature. Develop video processing circuits. Replicate target detection and slant range at detection measures.

3. Investigate Utility of Tracking Sensor

   Basis: Requirement for both target acquisition and image interpretation.

   Approach: Simulate target offsets from ground track of slewable sensor. Provide operator interactive target tracker (edge, contrast, correlation, etc.). Replicate target detection, slant range at detection, and interpretation measures.

4. Perform Experiments to Optimize Flight Test Studies

   Basis: Requirements for BGM-34C Flight Test Planning

   Approach: Employ simulation facility to select targets and profiles, identify sensitive parameters, and determine parameter values and ranges for use in flight tests. Extend the findings of the flight tests on a post hoc basis by simulating additional conditions, parameters and values.

5. High Face Validity Study of the Teledyne-Brown Camera

   Basis: Current utilization of sensor, score in sensor comparison (Table 16)

   Approach: Extend the simulation to include planned upgrading of this sensor, multiple targets, continuous scenarios (30 minute duration).

6. Investigate Impact of NRT/RT Reconnaissance on Reconnaissance Reporting Facility (RRF).

   Basis: Briefing on RRF by RADC

   Approach: Develop detailed function/flow model using AMRL Systems Analysis of Integrated Networks of Tasks (SAINT) with both Quick Strike and RPV data linked to RRF.

7. Investigate Airborne Monitoring Station Work Load

   Basis: Briefing received from SAC operators

   Approach: Develop function/flow SAINT model based on task analysis. Use SAINT to identify probable limitations to ARCO performance. Design operator performance simulation to validate.

8. Upgrade Simulation Capability to Include Image Enhancement

   Basis: Current use of contrast enhancer

   Approach: Survey available equipment. Select video enhancer and add to PIS video chain. Design target detection/ interpretation experiment to compare.

9. Simulation of Night Imaging Sensors

   Basis: TAC Concept of Operations

   Approach: Simulate KA-98 night mode, AAD-5 line scan infrared, operational LLL TV, and operational FLIR. Utilize the same experimental design as this study to maintain direct comparisons.

10. Survivability Study

    Basis: Probable ground-to-air defenses (TAC 85 Studies)

    Approach: Investigate target detection/identification against prebriefed and heavily defended targets.

11. Investigate Sensor × Altitude Interactions

Basis: Significant sensor × altitude interaction as measured by percent of targets detected

Approach: Use trained subjects (possibly pilots, navigators, or image interpreters) to study apparent trade-offs between target size on display and sensor FOV.

12. Investigate Impact of Jamming of Imagery Transmission

Basis: Probable EW Environment (TAC 85 Studies)

Approach: Use of noise generation in imagery simulation.

13. Reconnaissance Performance Effectiveness Study

Basis: Need for "specialist" to perform interpretation (briefing by SAC ARCO)

14. Special Problem Investigations

Basis: TAC 85 studies, briefings by RADC

Approach: Simulate system capabilities against special targets such as camouflage netting, high threat, or large area complexes.

15. Incorporate Effects of RPV Dynamics

Basis: Validation of simulation in flight test

Approach: Analyze vehicle flight test data to obtain pitch, roll, yaw and respective rates to obtain statistical distributions. Create analog or digital circuits to return PIS footprints based on distributions.

16. Investigation of Operator Aids

Basis: TAC 85, Concept of Operations

Approach: Study and simulate use of edge sharpening, false color, target cueing, etc. as operator aids in detection and interpretation.

17. Target Location Studies

Basis: Reporting Requirements, RRF Concept of Operations

Approach: Simulate and evaluate sensor capabilities for providing navigation updates and for exploiting targets of opportunities.

APPENDIX A

KA-98 LASER CAMERA SYSTEM

1.0 INTRODUCTION

The KA-98 sensor system is an airborne, laser line-scanning system developed by Perkin-Elmer for producing day or night imagery of tactical targets and terrain. Only the day mode will be evaluated in this report.

The 6514th Test Squadron at Hill Air Force Base, Utah, conducted a flight demonstration program of a KA-98 sensor under the auspices of the RPV Special Project Office (ASD/YRS). A BGM-34B RPV equipped with a Wide Band Data Link (WBDL) was employed as the test vehicle. A series of four captive flights followed by a single free flight were flown. The video signal generated by the KA-98 sensor was data linked (via the WBDL) and displayed on a ground console located within the Mission Control Center (MCC). Wide band video recorders were used both onboard the vehicle and at the ground station to record the video signal for replay and evaluation. The demonstration program was deemed to have met its objectives. *

2.0 SYSTEM DESCRIPTION

The KA-98 laser camera utilizes a high speed scanner, a solid state silicon avalanche detector for sensing visible/near IR radiation, and a cooled laser for providing operation at night. The energy from the laser is transmitted to the ground, and subsequent ground reflections are collected on the detector, whose amplified signal is available for recording, data linking, and/or near real time monitoring.

The line scan generated video signal is alternately input per frame to two scan converters. The converters are then read sequentially in normal TV format and displayed on a high resolution (1029 line) monitor. Although a moving map display was not provided in the control aircraft for inflight target screening, this analysis assumed such a display is available.

---

* KA-98/RPV Demonstration Test Program, Perkin-Elmer Report No. 12761, December 1975.

As with all line scan sensors, the KA-98 laser camera must be roll stabilized for proper operation. A reference sync pulse is generated at the start of each scan relative to the frame of the vehicle. Variations in RPV roll add or subtract from the relative angular relationship between a fixed ground object and the reference sync pulse contained in the video chain.

The available system characteristics are presented in Table A-1.

3.0 PERFORMANCE

3.1 Operational Envelope

The maximum velocity/altitude (V_g/H) ratio for which the KA-98 will provide satisfactory performance is two radians per second. For the minimum operational RPV velocity of 350 knots, the minimum allowable altitude is 295 feet; for the maximum operational RPV velocity of 500 knots, the minimum allowable altitude is 422 feet (see Figure A-1). The maximum day altitude is essentially unlimited (passive mode), but the night maximum altitude is restricted to 1,200 feet (active mode).

3.2 Ground Coverage

The KA-98 camera's crosstrack (horizontal) FOV is 136 degrees. It was stated previously that a conventional 4:3 aspect ratio monitor will be rotated 90 degrees for use by the interpreter. Thus, the alongtrack ground coverage will correspond to an alongtrack FOV of 136 × 4/3 = 181 degrees. Ground coverage is shown in Figure A-2 for altitudes of 500 and 1,000 feet.

The crosstrack coverage (S_L) can be found by

$$S_L = 2\ H\ \tan(\theta_h/2) \quad \text{feet} \tag{A-1}$$

where

TABLE A-1. KA-98 LASER CAMERA SYSTEM CHARACTERISTICS

KA-98 Camera	
Type	line scan
Altitude Range	400-1200 ft AGL
V/H Max	2 rad/sec
Focal Length	10 in.
FOV	136 deg crosstrack
Ground Coverage	5000 ft across track at 1000 ft AGL
Day Resolution	0.6 mrad
Night Resolution	0.75 mrad
Number of Channels	1
Instantaneous FOV of Receiver (Night Mode)	32 mrad across track; 5 mrad along track
Roll Compensation	up to ±10 deg
Video Bandwidth	3.3 MHz
Laser Type	GaAs (850 nm)
Laser Power Output	0.6 W typical
Laser Cooling	liquid nitrogen (1 liter)
Transmit Beam Divergence	0.75 mrad (night resolution)
Transmit Aperture	0.3 in. across track; 4 in. along track
Receiver Spectral Bandwidth	827 to 1200 nm (50% pts)
Receiving Detector	silicon avalanche photodetector
Scanner	four-sided polygon
Mirror Speed	24,000 rpm (1600 scans/sec)
Start-up Time	6 min
Dimensions	18.5 × 16 × 11.9 in. (nominal)
Weight	camera = 88 lbs; shock absorbers = 2 lbs
Recording	video tape
Ground-Based Display Module	
Type of Display	one display unit, two storage tubes, one video recorder/playback unit
Picture Processing Time	from 0.7 to 7.0 sec/image
Storage Time	up to 12 min

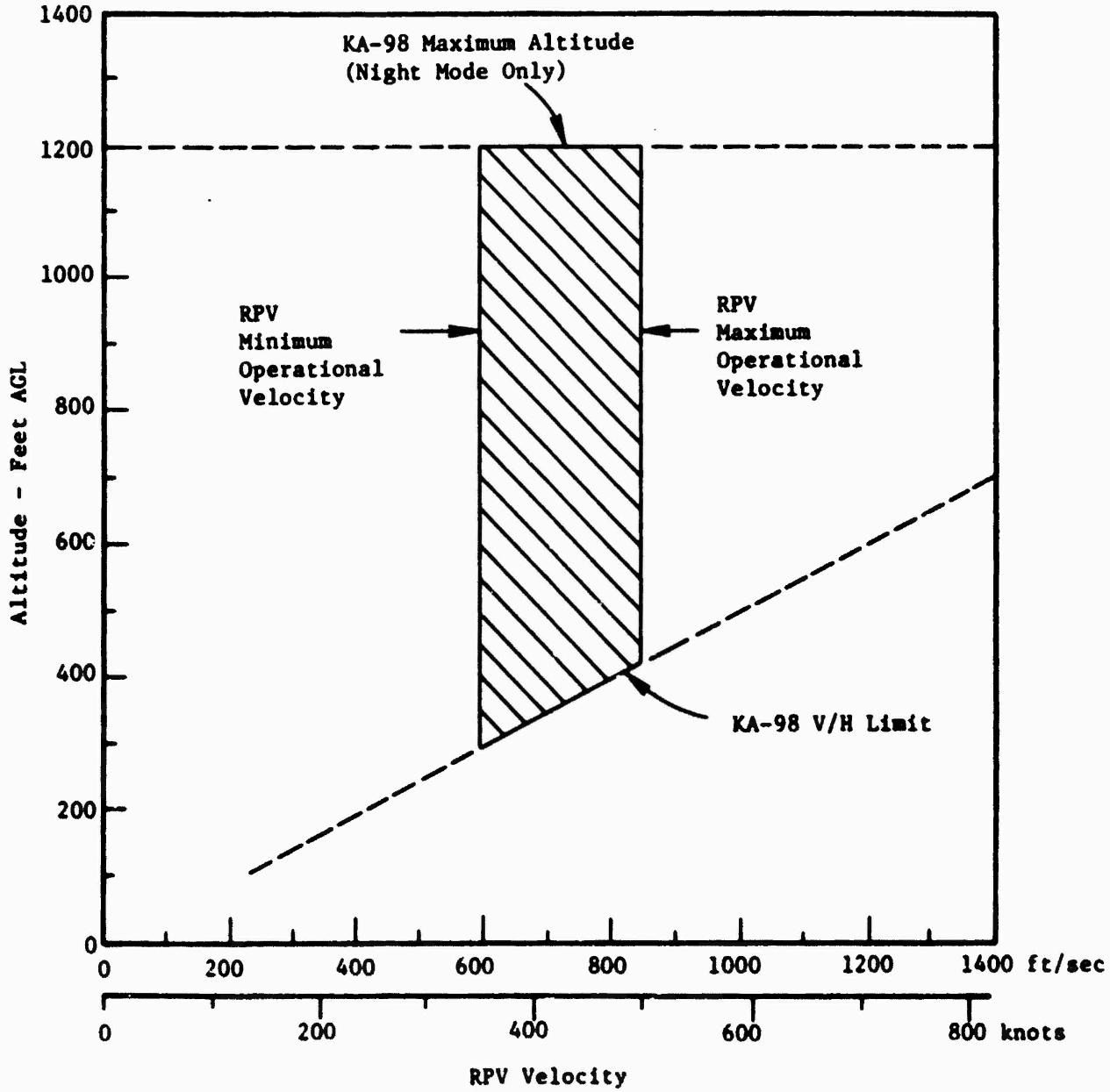

Figure A-1. Operational Envelope for KA-98 Laser Camera System - Day Mode

Sensor = KA-98 Laser Camera
Crab Angle = 0 deg

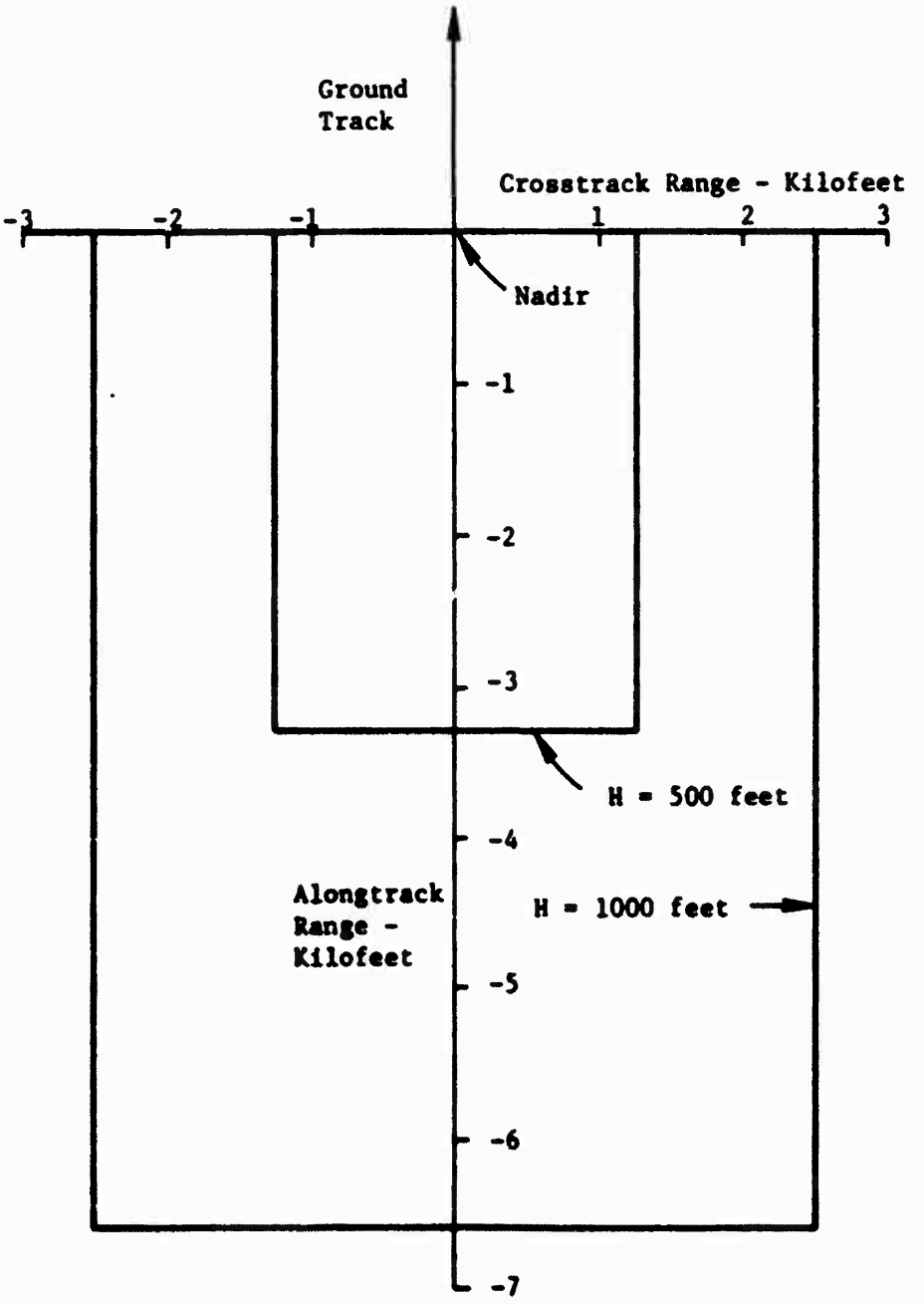

Figure A-2. Ground Coverage for KA-98 Laser Camera

θ_h = horizontal field of view (136 degrees)

H = altitude (feet)

Crosstrack coverage as a function of altitude is plotted in Figure A-3.

With reference to the figure, note that at an altitude of 500 feet the crosstrack coverage is 2,475 feet. Therefore, the displayed alongtrack coverage is 3,300 feet. Note in Figure A-3, and subsequent figures, that altitudes represented by the dotted lines (below 295 feet) cannot be flown unless the RPV ground velocity is correspondingly reduced below 350 knots, because of the velocity/altitude ratio limitation.

3.3 Scale

Scale for any point within the field of view (SC) can be found by

$$SC = \frac{F \cos \psi}{H} \quad \text{ratio} \tag{A-2}$$

where

F = focal length of optics (feet)

ψ = scan angle from vertical (degrees)

H = altitude (feet)

The effective focal length of the lens installed with the KA-98 receiver is ten inches. Scale as a function of altitude is presented in Figure A-4 for several scan angles.

3.4 Dynamic Resolution

3.4.1 Video Bandwidth

The geometrical angular resolution for the KA-98 sensor is quoted as 0.6 mrad. Not only must the proper video bandwidth be provided, but the detector must exhibit the required time constant in order for this angular

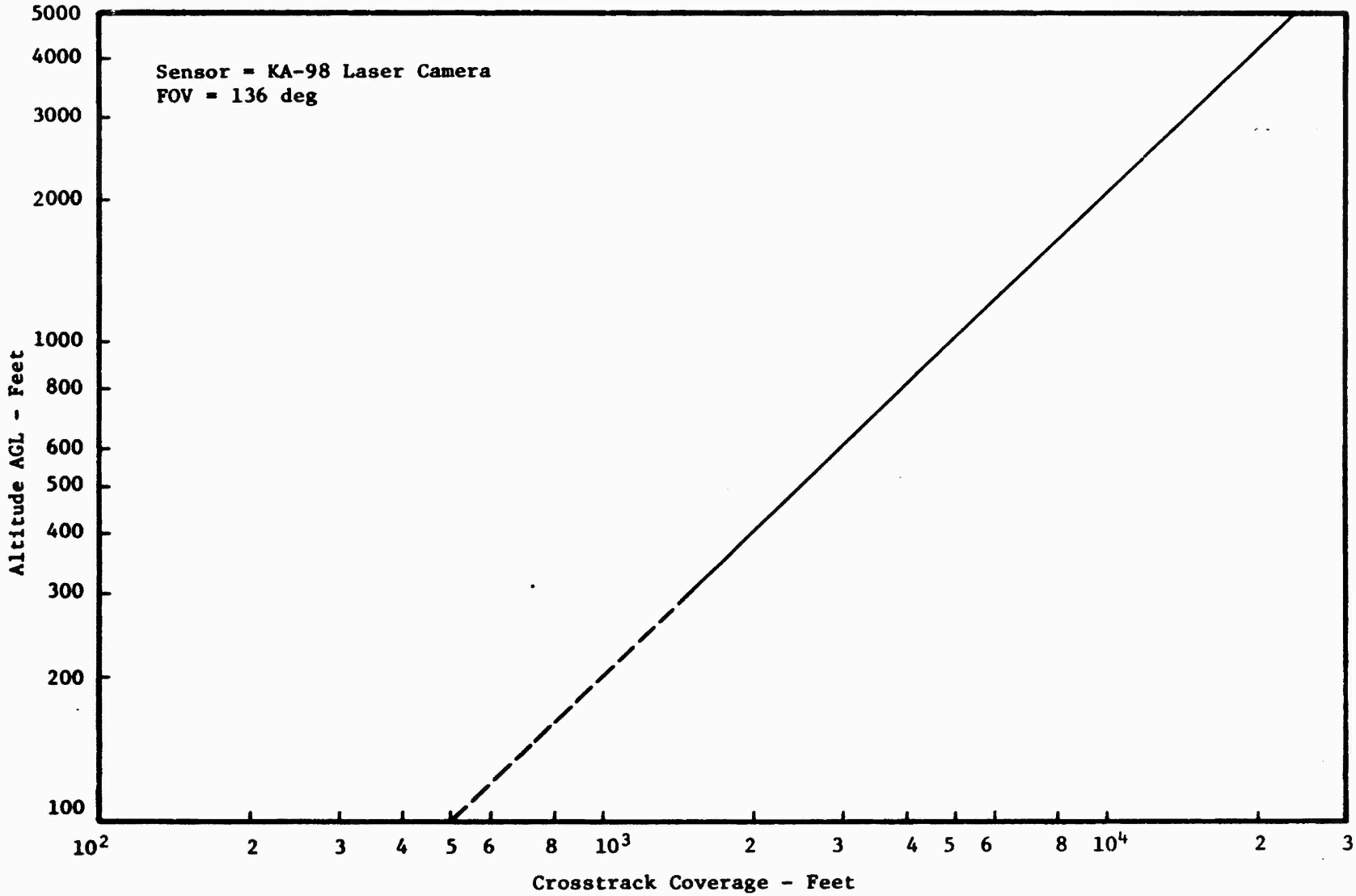

Figure A-3. Crosstrack Coverage for KA-98 Laser Camera

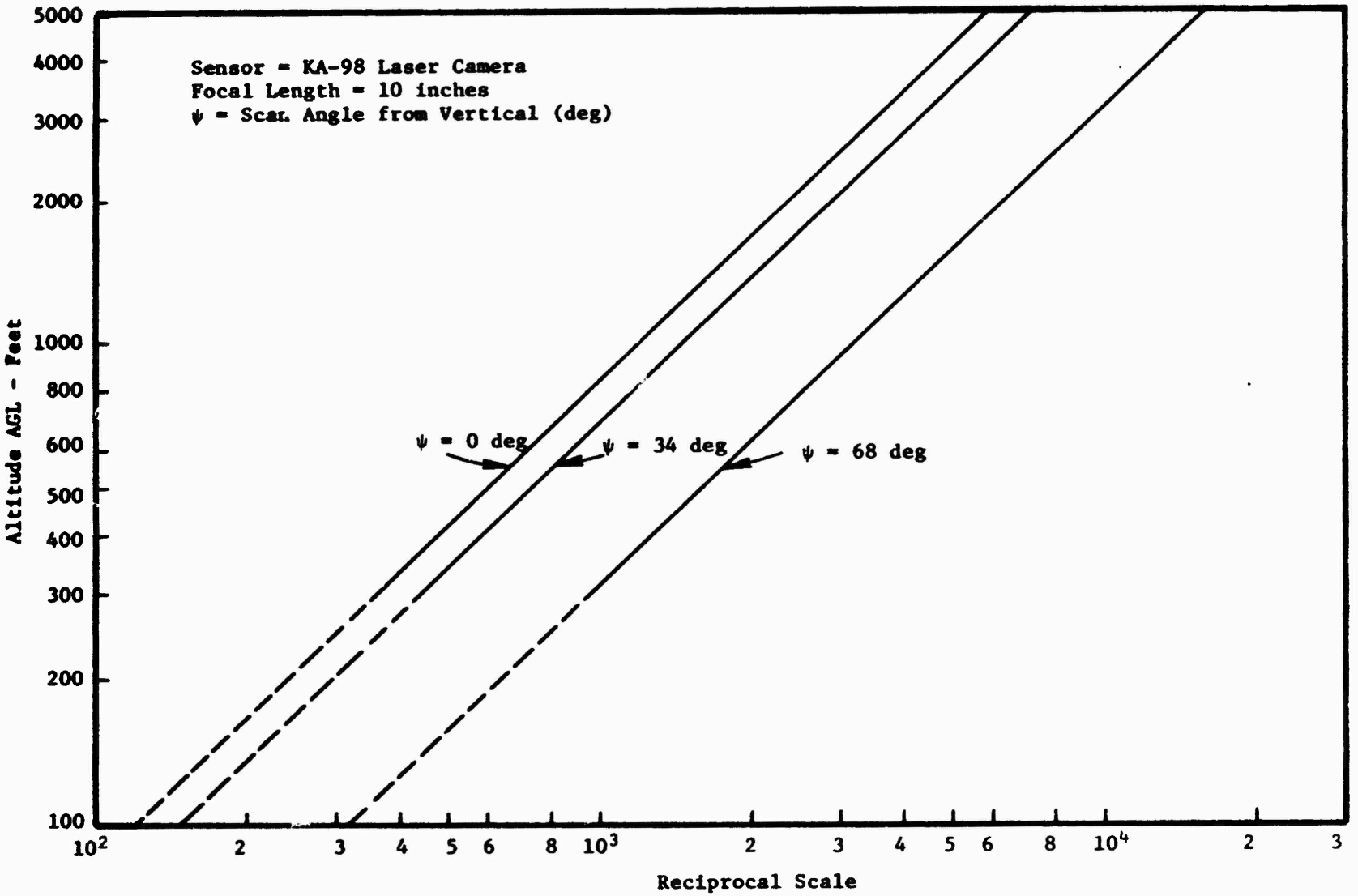

Figure A-4. Scale for KA-98 Laser Camera

resolution to be realized in the direction of the scanning mirror. The required video bandwidth (BW) can be found by

$$BW = \frac{k\ N\Omega\ \theta_h}{60\ \alpha\ E} \quad Hz \tag{A-3}$$

where

k = constant-one cycle represents two picture elements (0.5)

N = number of mirror faces on scanner (4)

Ω = mirror velocity (24,000 rpm)

θ_h = horizontal field of view (2.37 rad)

α = day angular resolution (0.6 mrad = 0.0006 rad)

E = scanner efficiency (unity assumed)

When the above equation is evaluated, the minimum video bandwidth can be found to be 3.16 Mhz. The actual system bandwidth is quoted as 3.3 MHz. Since the silicon avalanche photodiode detector provides satisfactory performance up to a bandwidth of 50 MHz, the 0.6 mrad geometrical resolution will be maintained.

3.4.2 Ground Spot Size

Ground spot size is found by

$$s = \frac{\alpha H}{\cos\psi} \quad feet \tag{A-4}$$

where

s = ground spot size (feet)

α = angular resolution (0.6 mrad day)

ψ = angular from vertical (0 to 68 deg)

Ground spot size as a function of altitude and several angles from vertical is shown in Figure A-5. Ground spot size at night was not plotted since night operation is currently not being evaluated. This is the geometrical spot size and does not take into account degrading factors such as uncompensated forward motion, RPV angular motion, or atmospheric attenuation.

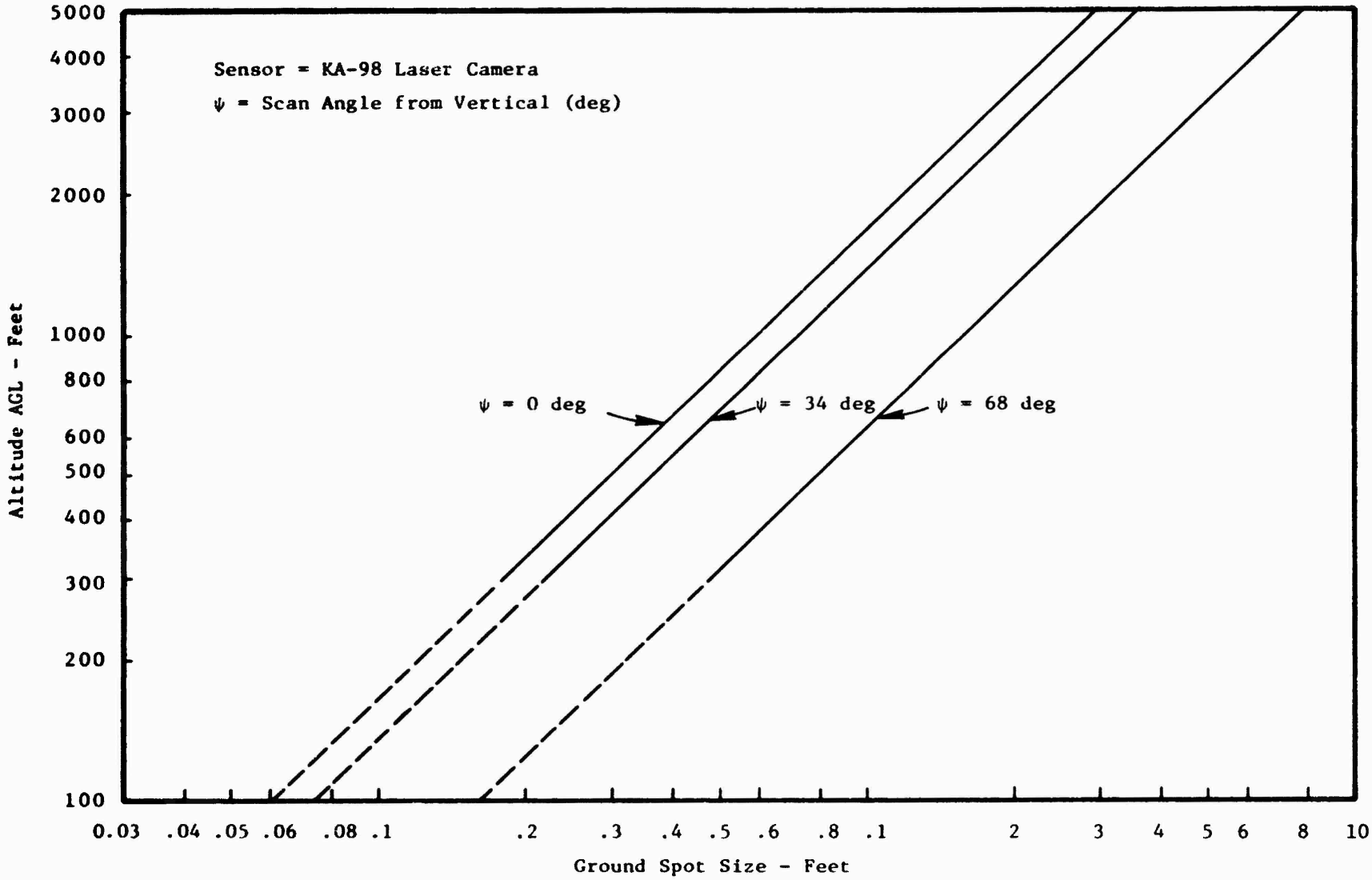

Figure A-5. Ground Spot Size for KA-98 Laser Camera

3.5 Time on Display

Target time on display (Td) can be found by

$$Td = \frac{2\ H\ \tan(\theta_h/2)}{V_g} \left(\frac{4}{3}\right) \quad \text{seconds} \qquad \text{(A-5)}$$

where

θ_h = horizontal FOV (136 degrees)
V_g = ground velocity of the RPV (feet/second)

Target time on the display as a function of altitude is presented in Figure A-6 for RPV velocities of 350 and 500 knots. Note that at an altitude of 500 feet the time on display is 5.58 seconds at 350 knots, and 3.91 seconds at 500 knots. Therefore, because the sensor generates imagery in a line scan fashion (rather than raster scan), the RPV must fly for 5.58 seconds at 350 knots and 3.91 seconds at 500 knots to fill the display with usable imagery every time a new heading is selected.

3.6 Eye/Display Relationships

It is assumed that a conventional 4:3 aspect ratio CRT-type display is employed. The display is placed in front of the interpreter so that the long dimension is vertical. The width of the active area is 12 inches and the height is 16 inches. Thus, since the horizontal dimension displays the ground footprint of the 136 degree lateral FOV, the vertical dimension displays the ground coverage that would be provided by a 168 × 4/3 = 191 degree FOV. A 1029 line raster is employed; the raster lines are displayed vertically.

3.6.1 Size of Displayed Image

Width of the displayed image (I) is found by

$$I = \frac{S\ T\ \cos\psi}{H\ \theta_h} \quad \text{inches} \qquad \text{(A-6)}$$

where

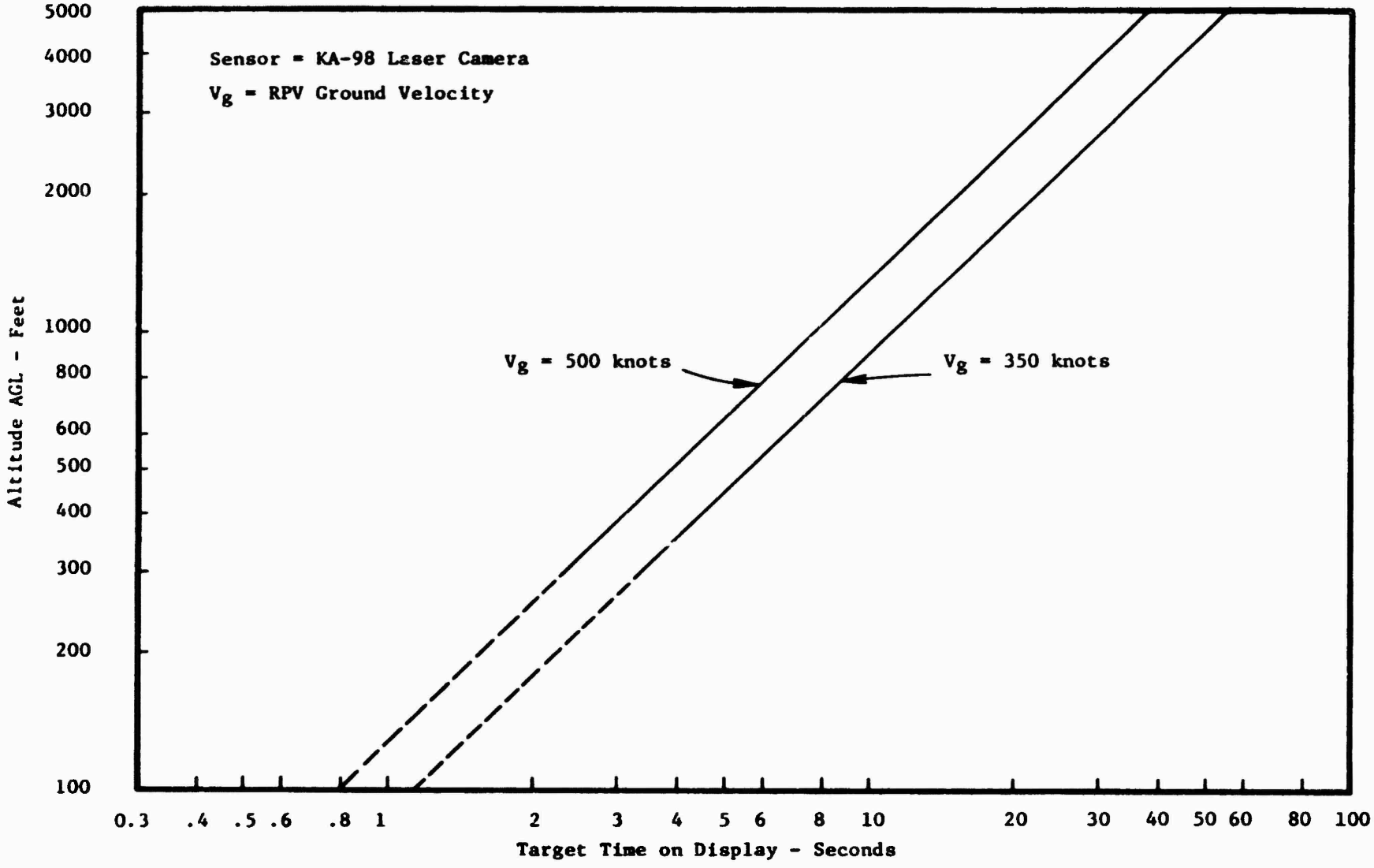

Figure A-6. Target Time on Display for KA-98 Laser Camera

S = width of active area of display (inches)

T = target horizontal dimension normal to slant range (feet)

θ_h = sensor horizontal field of view (radians)

H = altitude AGL (feet)

ψ = scan angle from vertical (degrees)

Width of the displayed target image as a function of altitude is presented in Figure A-7 for scan angles of ψ = 0, 34, and 68 degrees. A display width of S = 12 inches, a target projected horizontal dimension of T = 30 feet, and an FOV of θ_h = 136 degrees were assumed.

3.6.2 Raster Lines Across Image

The number of scan lines across the image (N_I) can be found by

$$N_I = \frac{T\ L_A \cos\psi}{H\ \theta_h}$$

$$= \frac{I\ L_A}{S} \qquad \text{(A-7)}$$

where

I = width of displayed image (inches)

S = width of display (inches)

L_A = number of active lines in raster (dimensionless)

The lateral FOV is 136 degrees, and the day angular resolution is 0.6 mrad (0.034 degree). Therefore, there are 4,000 resolution elements projected across flight path. The 1029 line raster, which provides 950 active lines, is the highest that can presently be realistically utilized. As a consequence, the KA-98 sensor is display limited.

The number of raster lines across the displayed image as a function of altitude, and for the same image width values previously calculated, are shown in Figure A-8. Based on data presented in Section 2 of this report, the value attained from an altitude of 500 feet are too low to permit satisfactory target acquisition and interpretation. Since higher raster line numbers cannot be

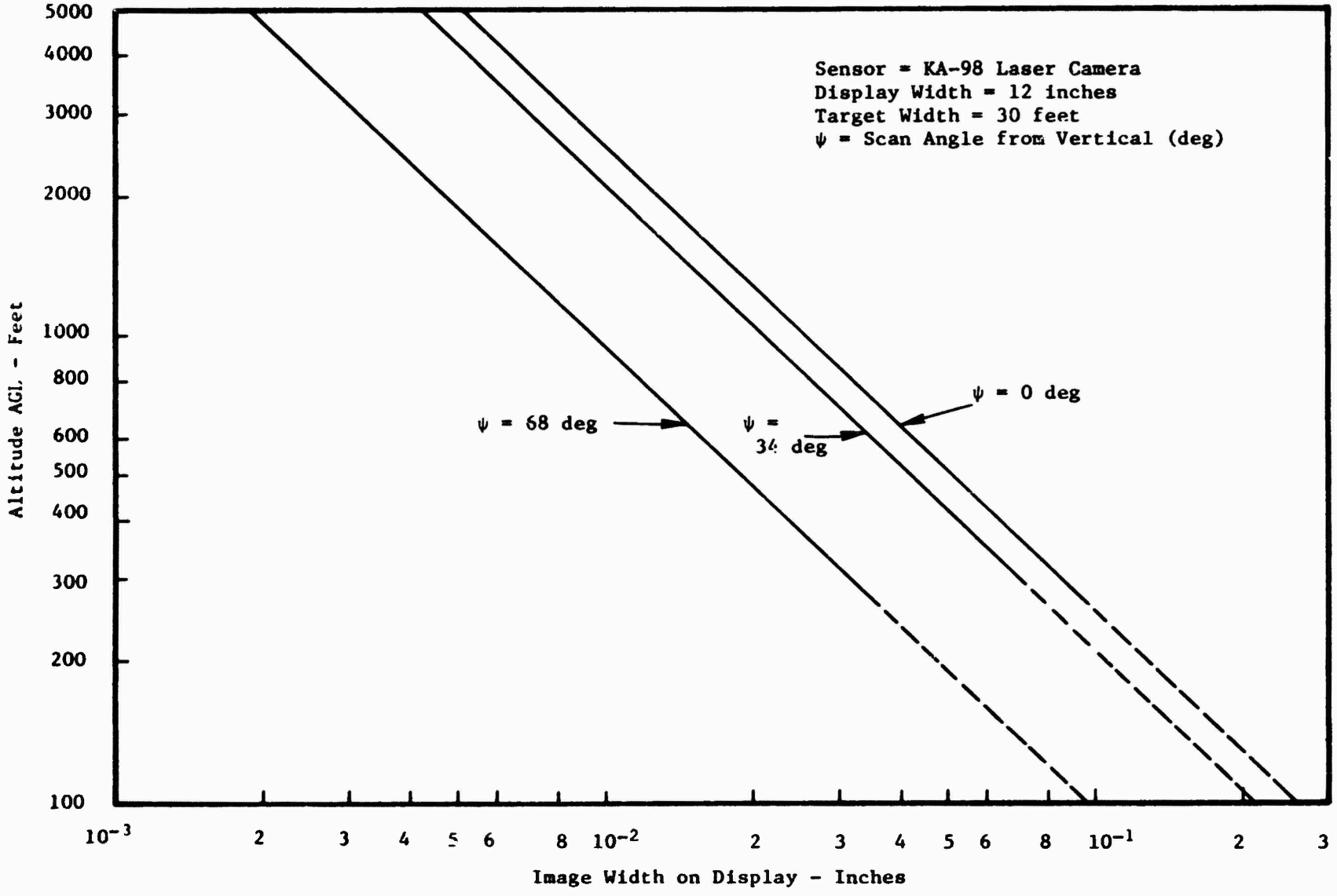

Figure A-7. Image Width on Display for KA-98 Laser Camera

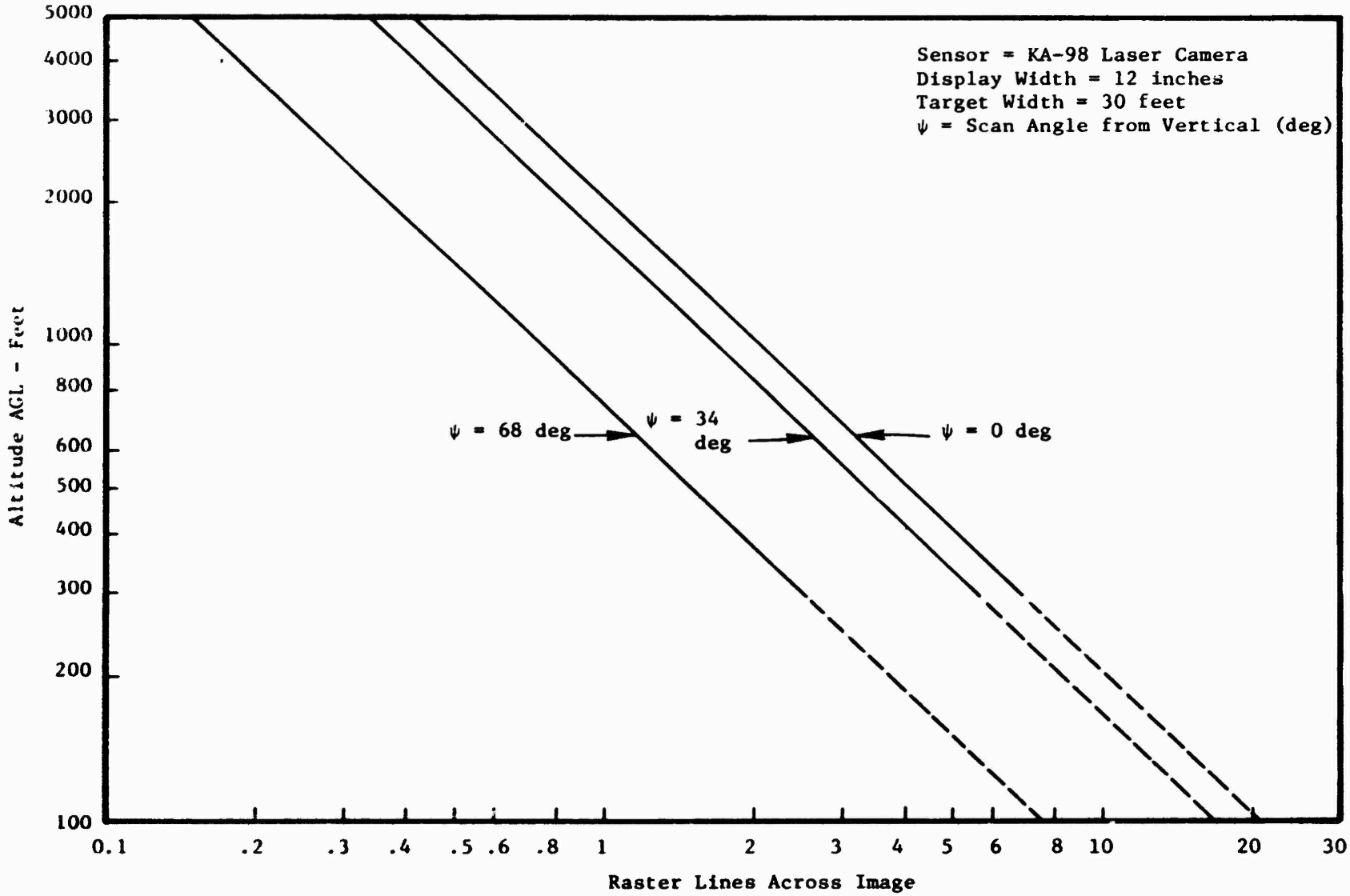

Figure A-8. Number of Raster Lines Across Image for KA-98 Laser Camera

utilized realistically, it is suggested that just one-fourth of the total FOV (34 degrees) be displayed on the monitor(s).

3.6.3 Angle Projected by Displayed Image

The angle subtended to the eye (γ) by image width (I) can be found by

$$\gamma = 2 \tan^{-1} \frac{S\ T}{2\ R\ Y\ \theta_h} \qquad \text{(A-8)}$$

$$\sim \frac{ST}{RY\theta_h}$$

or $$\gamma \sim \frac{I}{Y} \quad \text{radians}$$

where

Y = display to eye distance (inches)

I = height of displayed image (inches)

The angle projected to the eye by the displayed image as a function of altitude is presented in Figure A-9. The angles indicated are for an assumed eye/display distance of 28 inches, and the same image width values previously calculated.

Note from the figure that, even at the nadir, the projected angle is only about six arc minutes. The data in Section 2 of this report indicate that this value is insufficient for proper target identification and interpretation by the operator (the sensor is eye/display limited). As with the insufficient number of raster lines across the image condition, this problem could also be alleviated by displaying only a portion of the total FOV and using more displays.

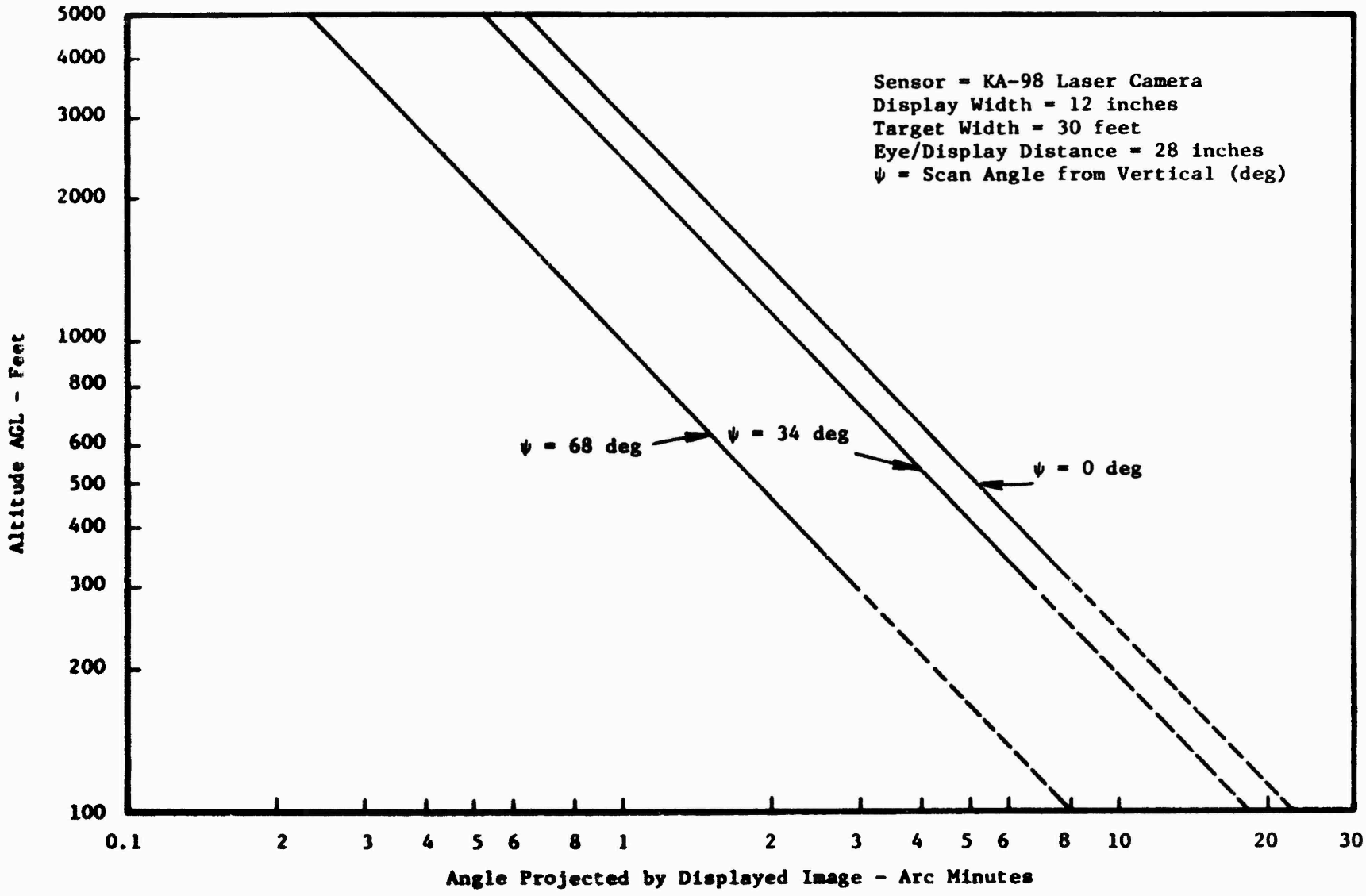

Figure A-9. Angle Projected to Eye by Image for KA-98 Laser Camera

APPENDIX B

SLEWABLE TELEVISION SYSTEM

1.0 INTRODUCTION

This appendix presents the evaluation of a slewable TV system which consists of a 525 line television camera equipped with remotely controlled zoom optics and installed in a two-axis remotely positioned gimbal system. Zoom optics with a range of 15 to 150mm are employed and provide an FOV from 4.4 to 42 degrees. The depression angle gimbal limits are zero to 90 degrees; the azimuth angle gimbal limits are ±60 degrees. Since a derotation device is not provided, the footprint will rotate with a 1:1 correspondence to the azimuth angle.

2.0 OPERATIONAL CONCEPT

A slewable television system offers several operational advantages over a TV system wherein the ability to remotely position the optical axis is limited to a few degrees of elevation.

On the negative side, the desired gimbal angles might be difficult to implement due to volume restrictions in the RPV nose section. In addition, the Microwave Command Guidance System (MCGS) would require a larger bandwidth to permit the Airborne Remote Control Operator (ARCO) to track a target that induced large gimbal rates. Several of the more significant advantages are discussed below.

2.1 Navigation Mode

2.1.1 NAV Update

An advantage of the slewable television system accrues from the fact that landmarks located at relatively large offset distances from the ground track can be employed to accurately update the navigation system. The ARCO will use his slewstick to cause the TV's optical axis to track the checkpoint; RPV position relative to the checkpoint can then be calculated by the NAV

computer from knowledge of RPV present position, heading, altitude and attitude, and the gimbal angles.

2.1.2 Target Acquisition

2.1.2.1 Prebriefed Target Mission

In the NAV mode, a footprint must be generated with sufficient lateral (crosstrack) coverage to assure that a prebriefed target will appear within the sensor FOV. Thus, the required lateral coverage is a function of the uncertainties in the presumed location of the prebriefed target and the accuracy of the RPV navigation system. For a given fixed-mounted sensor, the only way to increase the ground coverage of the NAV footprint is to decrease the optical focal length. This action decreases the scale and increases the ground spot size. Thus, the operator's proficiency in the tasks of target detection and recognition will become degraded.

If the TV camera is equipped with a remotely activated zoom lens and a remotely positioned two-axis gimbal system, the ARCO can use a longer focal length lens to acquire targets that are expected to be imbedded in their background. The necessary lateral coverage is achieved by slewing the optical axis back and forth across the ground track. At higher velocity/altitude ratios, however, there will be a trade-off between improved image quality versus the ability to provide contiguous ground coverage (along with sufficient time on display) to permit interpretation by the operator. Thus, the utility of employing an accurate navigation system to minimize the required slew angle is indicated.

2.1.2.2 Interdiction Mission

The slewable TV would be extremely useful for performing the tasks of navigation and target acquisition. The RPV could be programmed to fly straight legs between designated vertices, yet the ARCO and RO could monitor meandering lines of communication (e.g., rivers, canals, roads, railroads) with long focal length optics.

2.2 Reconnaissance Mode

2.2.1 Prebriefed Target Mission

When a nonslewable TV system is used, there is a 10-15 second transition period between the NAV and RECON modes; the target of interest is between the available footprints during this interval. Because of both alongtrack and crosstrack navigation errors, a series of frames must be recorded which include both side oblique footprints and forward overlap. Thus, an additional time interval will elapse before the frame containing the target can be identified during the playback mode. This time lag between target acquisition and target interpretation to extract EEI's could not be tolerated in a high density target area.

When a slewable TV sensor is utilized, the transition from the NAV to RECON mode is smooth since the RO merely continues to evaluate the target for EEI's during the 10-15 second closing interval. Because the target is being tracked, there is no target time on display problem, and degrading image motions are minimized. The imagery would be recorded to permit continuing near real time interpretation should the real time tracking interval (from acquisition to nadir) be insufficient to permit complete assessment of the EEI's.

Since there is no need to reacquire the target during flyover with the slewable configuration, a long focal length lens (with small footprint) can be employed. The longer focal length will enhance the RO's ability to extract the required EEI's since both the scale and ground spot size will be improved.

As target range decreases, the gimbal angular rates will increase to a value that is defined by the RPV velocity/altitude ratio and the target offset distance. If an automatic tracking device is not employed, the high tracking rates could exceed the RO's ability to accurately track the target. This, in turn, could cause the RO to select a shorter focal length (wider FOV) to assure that he could maintain the target within the FOV.

2.2.2 Interdiction Mission

The ability to identify and locate mobile and fleeting targets in real time, as compared to near real time, minimizes the time lag between acquisition by the RPV and reacquisition by a strike vehicle. This reduces the area that must be searched by the strike vehicle, which will yield a higher probability of reacquisition with less sophisticated sensors. The RPV would locate the target by use of data derived from the RPV navigation and flight control system, including heading, attitude, altitude and present position along with the LOS gimbal angles. Accurate target location requires the use of a precision RPV navigation system.

2.3 Other Considerations

2.3.1 Cueing Aids

More sophisticated future reconnaissance systems might employ cueing aids to localize areas which have a high probability of containing a target of interest. The operator can then perform a detailed analysis by tracking the cued coordinates by use of a gimbaled sensor that is equipped with long focal length optics.

Three different techniques can be used to generate the cues: (1) navigation, (2) multisensor, and (3) correlation. For navigation cueing, the coordinates of known or suspected targets are stored in the navigation computer. When the computer determines that the target coordinates are within the operational range of the sensor, the operator is alerted by some type of visual (and possibly aural) cue. If desired, a computer can be employed to automatically direct the optical axis of the sensor to the cued coordinates.

Multisensor cues are derived from ancillary sensors operating in conjunction with the sensor providing the primary imagery. These sensors need not be image forming but must exhibit some level of directional capability. Examples of this type of sensor are: (1) radar with MTI, (2) FLIR designed for hot spot detection, (3) ELINT, (4) COMINT, (5) ignition detection, and (6) interrogated ground based activity sensors.

A variety of correlation devices have been developed. They can be designed to recognize either a specific area or classes of targets. The specific area correlator requires storage in computer memory of imagery collected on a previous mission. For automatic target detection (screening), the pertinent target signature characteristics are stored in computer memory.

2.3.2 Automatic Target Tracking

Closed loop video trackers can be employed for tracking a target, or suspected target. These systems can track a target much more accurately than can the human operator. This is particularly true during periods of high stress, such as when large gimbal rates are required and/or when the air vehicle is experiencing extreme turbulence. Several variations of video trackers have evolved (edge, centroid, correlation) but all require some minimum contrast differential for proper operation.

2.3.3 Scene Rotation

Scene rotation is defined as rotation of the sensor LOS (and therefore the displayed scene) nonisomorphically with the "out-of-the-window" horizon when the air vehicle is flying straight and level (Figure B-1). Target detection, recognition, and tracking using CRT displays may be degraded if the sensor gimbals do not maintain a stable LOS to the target. In addition, a TV displayed scene that rolls nonisomorphically with what would be seen out of the aircraft window can cause physiological disturbances such as motion sickness and disorientation effects associated with a conflict between visual and proprioceptive cues.

Several techniques have been employed to "derote" the image, such as optical rotation, sensor rotation, or the use of a third gimbal. All of these methods require additional weight, volume, and primary power which might be difficult to realize in the RPV nose section.

Three-dimensional gimbal systems (with the gimbal systems providing three sets of orthogonal pivot points) exhibit the most flexibility, since

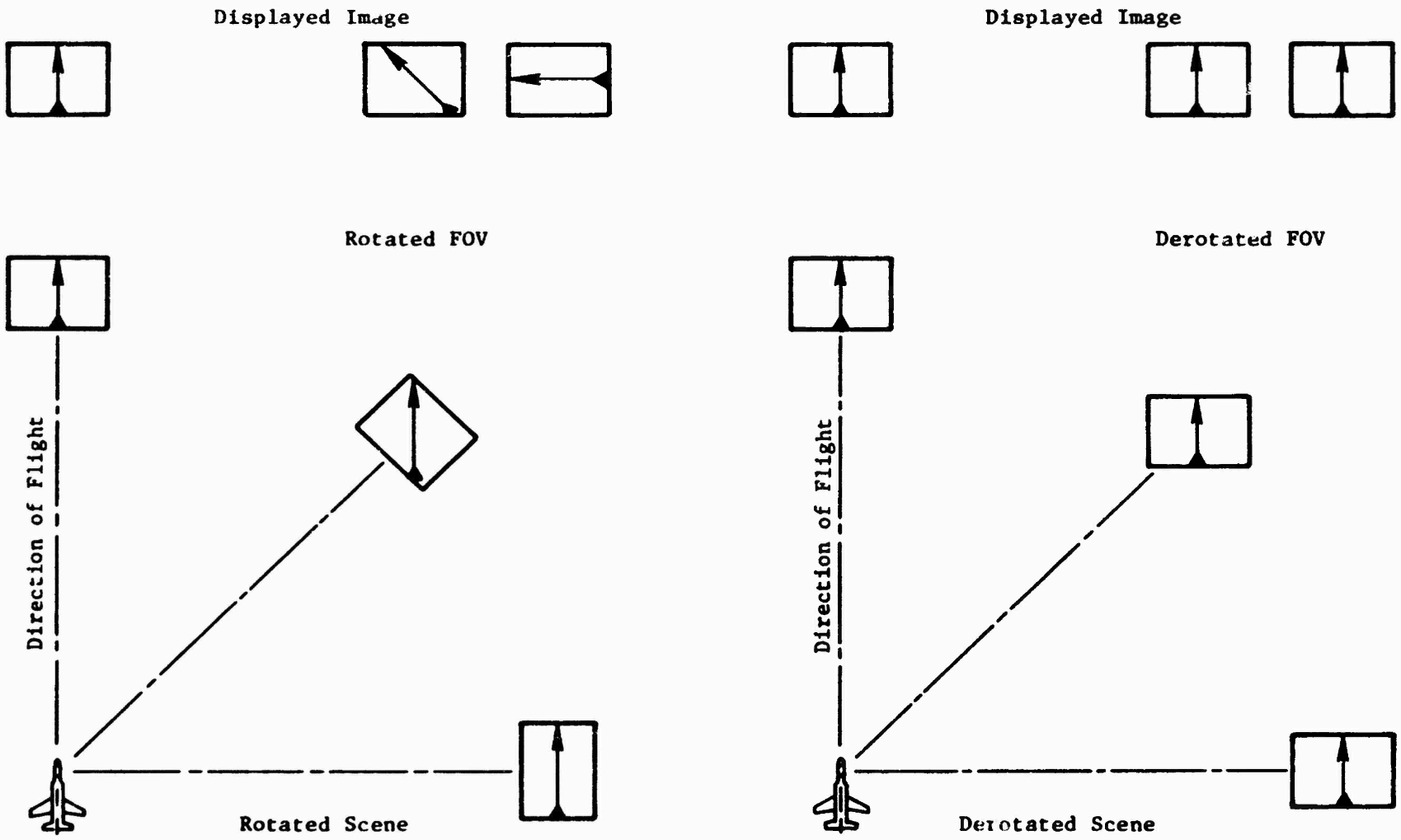

Figure B-1. Effects of Scene Rotation on the Displayed Imagery

they usually permit hemispherical coverage, freedom from gimbal ambiguity and lockup, and the ability to produce a display isomorphic with the real world. However, this capability results in a variety of penalties associated with requirements for weight, volume, complexity, reliability, and maintainability. Therefore, some installations use two-order systems which are less costly while affording minimum tracking ability.

Two-order systems are typically lighter, smaller, and more reliable and maintainable; hence, they are ideal for such applications as RPV's and for pod-mounting on attack aircraft. As noted previously, a two-order gimbal system will produce scene anomalies on the display which can reduce operator performance.

3.0 SYSTEM DESCRIPTION

The assumed TV system characteristics are identical to those presented in Appendix C except that continuously variable 10:1 zoom type optics and two-axis remotely directed gimbals are employed. All support systems installed in the RPV are identical and will not be discussed further. Characteristics of the 525 line TV camera are presented in Table B-1.

TABLE B-1. SLEWABLE TELEVISION SYSTEM CHARACTERISTICS

TV Camera	
Tube Type	gated SIT vidicon
Line Rate	525 lines/frame
Frame Rate	30 frames/sec
Interlace	2:1
Aspect Ratio	1:1
Image Size	11.4 × 11.4 mm
Exposure Control	automatic 100 μsec to 33 msec
Optics	
Type	motorized zoom
Focal Length Range	15-150 mm
FOV Range	4.4 × 4.4 to 42 × 42 deg
Gimbals	
Quantity	2-axis
Order	azimuth/elevation
Azimuth Limits	±60 deg
Depression Limits	0 to 90 deg

4.0 PERFORMANCE

4.1 Ground Coverage

The optical axis can be remotely slewed from 0 to 90 degrees in elevation, and ±60 degrees in azimuth. The FOV is remotely zoomed from 15 to 150 mm. The field of view corresponding to a given focal length can be found by

$$\theta = 2 \tan^{-1} \left(\frac{W}{2F}\right) \quad \text{mm} \tag{B-1}$$

where

W = raster dimensions of the vidicon photocathode (mm)

F = effective optical focal length (mm)

θ = sensor FOV (degrees)

Since W = 11.4 × 11.4 mm, the corresponding FOV range is 4.4 × 4.4 to 42 × 42 degrees. Alongtrack ground coverage for these extreme FOV's is plotted in Figure B-2 for a depression angle of 16 degrees. Since the wide FOV extends above the horizon, ground coverage was plotted out to a depression angle of 2 degrees.

The lateral coverage of the near and far sides of the footprint for the above stated conditions is shown in Figures B-3a and B-3b. The geometrical relationships are presented in Figure B-4 and Table B-2.

4.2 Scale

Scale for the optical axis (SC_A), the near edge of the field of view (SC_B), and far edge of the field of view (SC_C), can be found by

$$SC_A = \frac{F \sin\beta}{H} \quad \text{ratio} \tag{B-2}$$

$$SC_B = \frac{F \sin(\beta+\theta_V/2)}{H} \quad \text{ratio} \tag{B-3}$$

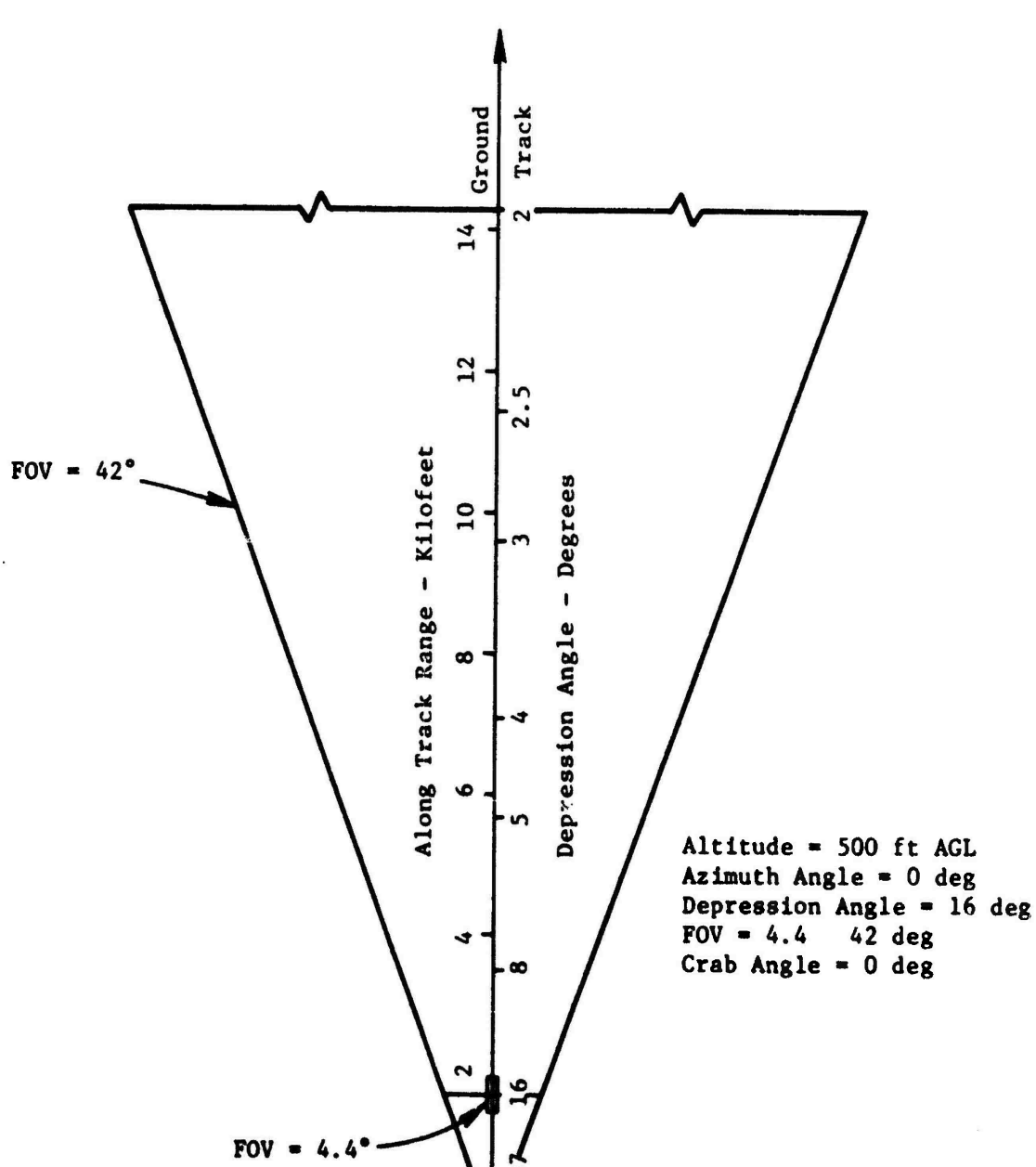

Figure B-2. Ground Coverage for Slewable TV Camera

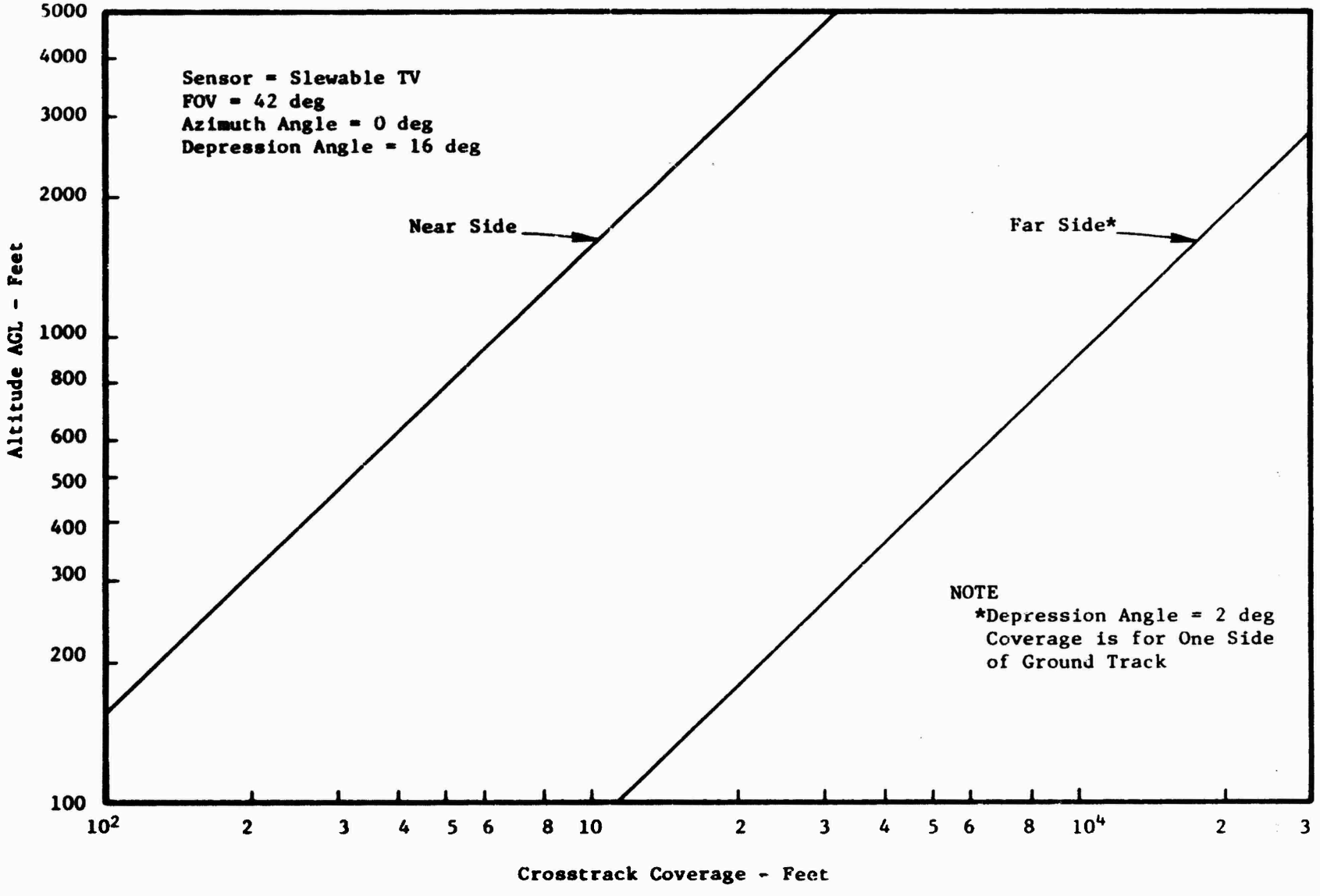

Figure B-3a. Crosstrack Coverage for Slewable TV Camera (FOV = 42 deg)

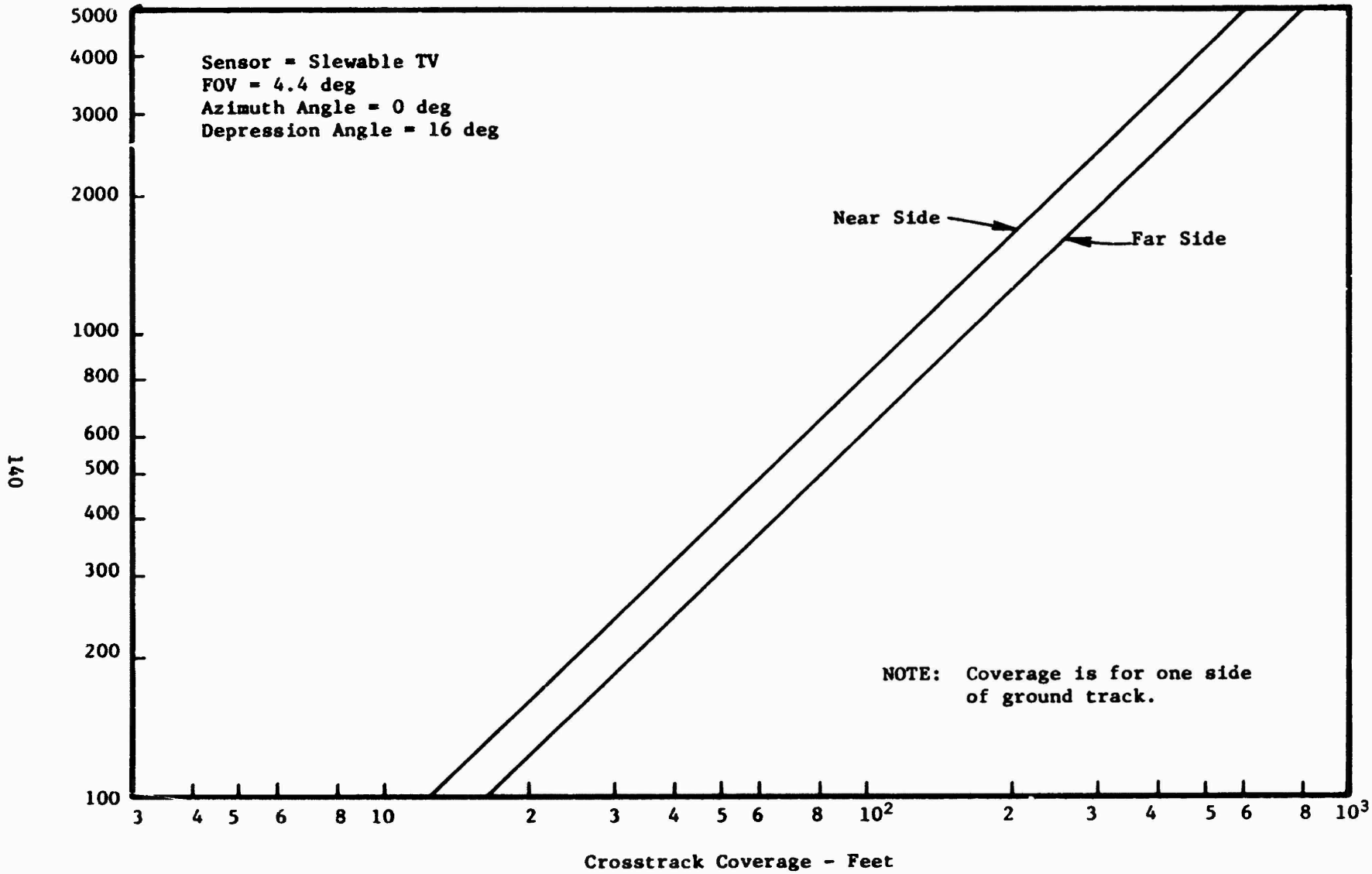

Figure B-3b. Crosstrack Coverage for Slewable TV Camera (FOV = 4.4 deg)

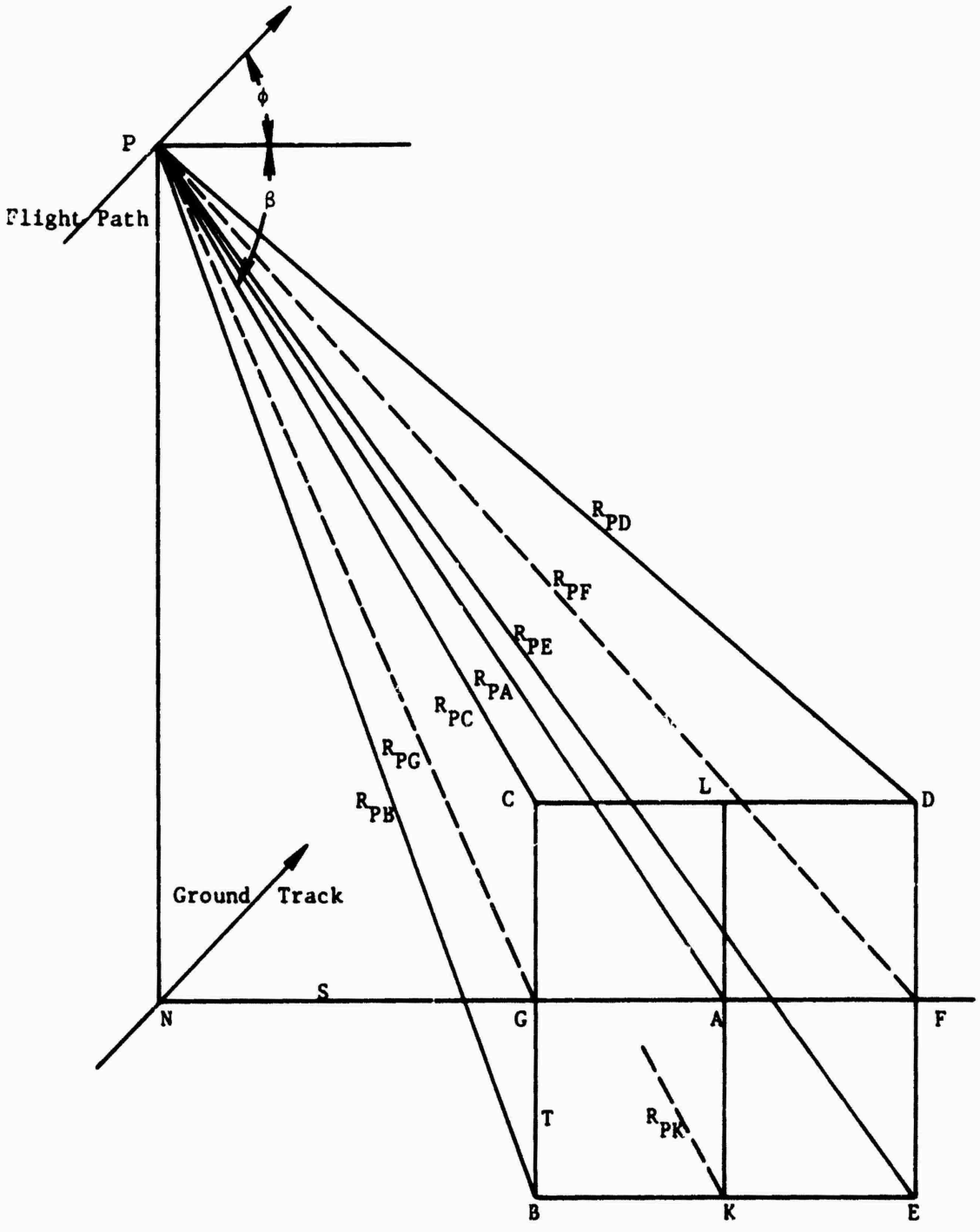

Figure B-4. Viewing Geometry for Slewable TV Camera

TABLE B-2. GEOMETRICAL RELATIONSHIPS FOR SLEWABLE TV CAMERA

Slant Range (R)

$R_{PA} = H/\sin\beta$

$R_{PG} = H/\sin(\beta+\theta_v/2)$

$R_{PF} = H/\sin(\beta-\theta_v/2)$

H = altitude
θ_v = vertical FOV
θ_h = horizontal FOV
β = depression angle
ϕ = azimuth angle

$R_{PK}, R_{PL} = R_{PA}/\cos(\theta_h/2) = H/\sin\beta\cos(\theta_h/2)$

$R_{PB}, R_{PC} = R_{PG}/\cos(\theta_h/2) = H/\sin(\beta+\theta_v/2)\cos(\theta_h/2)$

$R_{PD}, R_{PE} = R_{PF}/\cos(\theta_h/2) = H/\sin(\beta-\theta_v/2)\cos(\theta_h/2)$

Crosstrack Range (T)

$T_{LK} = 2R_{PA}\tan(\theta_h/2) = 2H\tan(\theta_h/2)/\sin\beta$

$T_{CB} = 2R_{PG}\tan(\theta_h/2) = 2H\tan(\theta_h/2)/\sin(\beta+\theta_v/2)$

$T_{DE} = 2R_{PF}\tan(\theta_h/2) = 2H\tan(\theta_h/2)\sin(\beta-\theta_v/2)$

Alongtrack Range (S)

$S_{NA} = H/\tan\beta$

$S_{NG} = H/\tan(\beta+\theta_v/2)$

$S_{NF} = H/\tan(\beta-\theta_v/2)$

$S_{NF} - S_{NG} = H[\cot(\beta-\theta_v/2)-\cot(\beta+\theta_v/2)]$

Point B

$$X = \frac{H\{\sin\phi+\cos\phi[\tan(\theta/2)/\cos(\beta+\theta/2)]\}}{\tan(\beta-\theta/2)}$$

$$Y = \frac{H\{\cos\phi-\sin\phi[\tan(\theta/2)/\cos(\beta+\theta/2)]\}}{\tan(\beta+\theta/2)}$$

Point C

$$X = \frac{H\{\sin\phi-\cos\phi[\tan(\theta/2)/\cos(\beta+\theta/2)]\}}{\tan(\beta+\theta/2)}$$

$$Y = \frac{H\{\cos\phi+\sin\phi[\tan(\theta/2)/\cos(\beta+\theta/2)]\}}{\tan(\beta+\theta/2)}$$

Point D

$$X = \frac{H\{\sin\phi - \cos\phi[\tan(\theta/2)/\cos(\beta-\theta/2)]\}}{\tan(\beta-\theta/2)}$$

$$Y = \frac{H\{\cos\phi + \sin\phi[\tan(\theta/2)/\cos(\beta-\theta/2)]\}}{\tan(\beta-\theta/2)}$$

Point E

$$X = \frac{H\{\sin\phi + \cos\phi[\tan(\theta/2)/\cos(\beta-\theta/2)]\}}{\tan(\beta-\theta/2)}$$

$$Y = \frac{H\{\cos\phi - \sin\phi[\tan(\theta/2)/\cos(\beta-\theta/2)]\}}{\tan(\beta-\theta/2)}$$

$$SC_C = \frac{F \sin(\beta-\theta_V/2)}{H} \quad \text{ratio} \tag{B-4}$$

where

F = effective focal length (feet)

H = altitude AGL (feet)

θ_V = sensor vertical FOV (degrees)

The scale to any point in the FOV can be found by

$$SC = \frac{F \sin(\beta \pm \theta_{VT}) \cos\theta_{hT}}{H} \quad \text{ratio} \tag{B-5}$$

where θ_{VT} and θ_{hT} are the vertical and horizontal angles of interest with respect to the optical axis. The scale at the optical axis for the minimum and maximum FOV's is presented in Figure B-5.

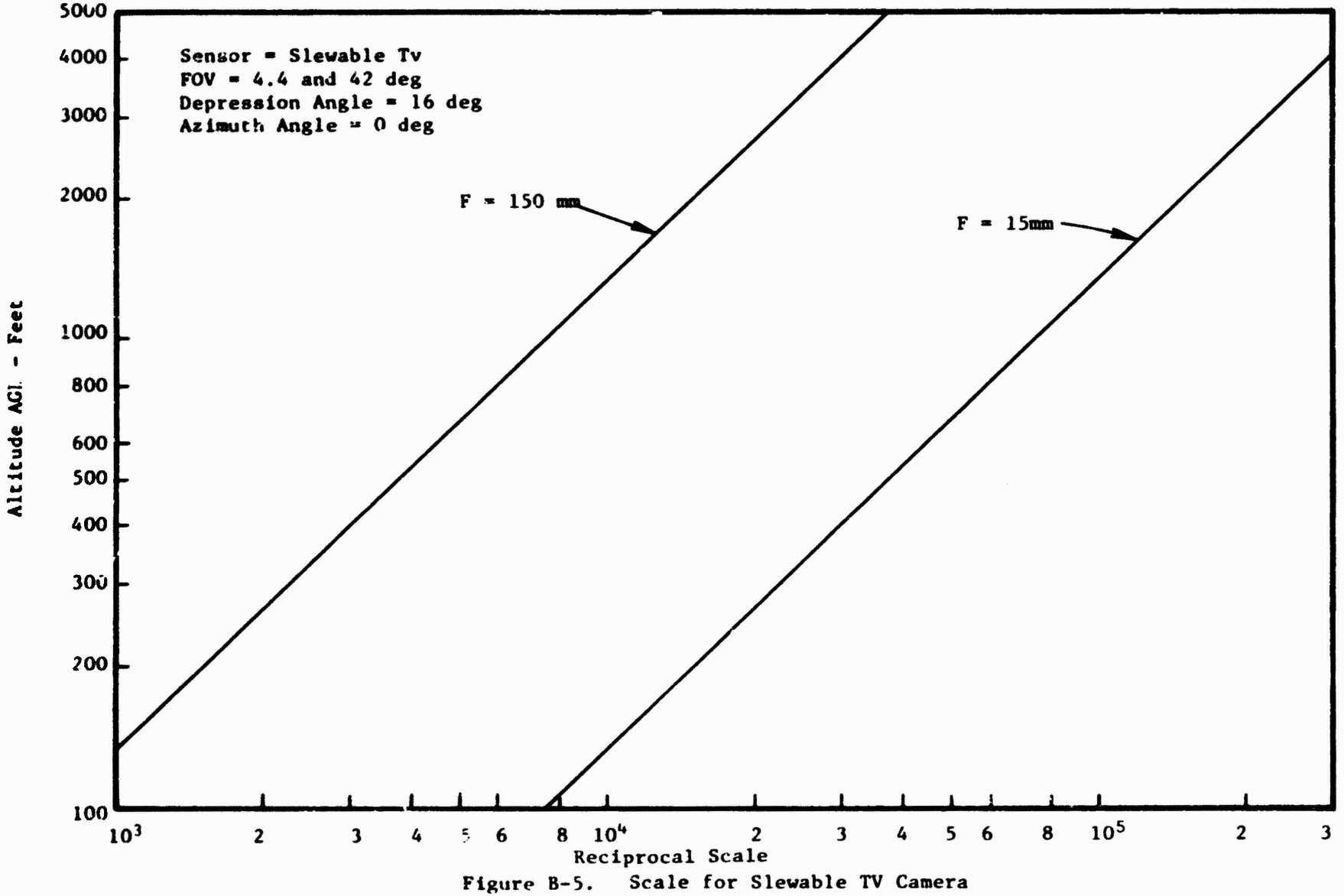

Figure B-5. Scale for Slewable TV Camera

4.3 Dynamic Resolution

The angular resolving power of a television system can be defined by

$$\alpha_D = [\alpha_S^2 + \alpha_O^2 + \alpha_I^2 + \alpha_T^2]^{0.5} \quad \text{radians} \tag{B-6}$$

where

α_D = system dynamic angular resolution

α_S = static angular resolution of the TV camera

α_O = limiting angular resolution of the optics

α_I = limiting angular resolution due to image motion

α_T = limiting angular resolution due to optical atmospheric turbulence

As discussed in Appendix C, Section 4.3.4, the effects of optical atmospheric turbulence are insignificant for this application and will be be considered further.

4.3.1 Television Camera

4.3.1.1 Vertical Resolution

The limiting resolution of a 525 line television camera (N_t) is determined primarily by the number of active lines multiplied by the Kell factor (N_t = 344 vertical TV lines).

The angular resolution (α_S) can be found by

$$\alpha_S = \frac{\theta_V}{N_t} \quad \text{radians} \tag{B-7}$$

The vertical FOV can be remotely zoomed between the limits of 4.4 to 42 degrees. For θ_V = 4.4 degrees, α_S = 0.22 mrad; for θ_V = 42 degrees, α_S = 2.13 mrad.

4.3.1.2 Horizontal Resolution

The bandwidth (BW) required to produce a given horizontal resolution (N_h) at the optimum SNR can be found by

$$BW = N_h \cdot f \cdot L \cdot A \cdot K \cdot \frac{1-B_v}{1-B_h} \quad Hz \qquad (B-8)$$

where

N_h = horizontal resolution (defined in terms of TV lines/picture height)

f = frame rate (frames/sec = 30)

L = line number (scan lines/frame = 525)

A = aspect ratio (width/height = 4/3)

K = constant (one cycle represents two picture elements = 0.5)

B_v = vertical blanking (ratio = 0.78)

B_h = horizontal blanking (ratio = 0.173)

A bandwidth of 6.1 MHz is required to produce a horizontal resolution equal to the vertical resolution.

4.3.2 Optics

The diffraction limit, expressed in terms of angular resolution (α_0), is found by

$$\alpha_0 = \frac{1.22\lambda}{D} \quad \text{radians} \qquad (B-9)$$

where

α_0 = diffraction limited resolution (radians)

λ = wavelength of white light (5.6×10^{-4} mm)

D = diameter of optics (mm)

The effective diameter of the optics is defined to be 54 mm (f/no. = 2.8) so that α_0 = 13 μrad. Since the expense of employing essentially diffraction limited optics with a 525 line television system usually is not warranted, we will assume a limiting resolution of α_0 = 13/0.8 = 16 μrad.

4.3.3 Image Motion

Relative motion during the exposure interval degrades the system resolution. Relative motion is induced primarily by the forward motion of the RPV, and by perturbations of the RPV about its orthogonal axes. The limiting angular resolution due to the uncompensated image motion (α_I) is expressed by

$$\alpha_I = [\alpha_F^2 + \alpha_A^2]^{0.5} \quad \text{radians} \qquad \text{(B-10)}$$

where

α_F = limiting angular resolution due to forward motion of the air vehicle (radians)

α_A = limiting angular resolution due to changes in RPV attitude (radians)

Since no data is currently available concerning RPV dynamics, the effects of vehicle induced angular velocities were assumed to be zero for this analysis ($\alpha_A = 0$).

Limiting angular resolution as a function of uncompensated image motion is found by

$$\alpha_F = \Omega T \, E_f \quad \text{radians} \qquad \text{(B-11)}$$

where

T = exposure interval (seconds)

E_f = image motion compensation (IMC) error (ratio)

An automatic light control (ALC) device adjusts the exposure interval between the limits of 100 μsec to 33 msec, as a function of the ambient illumination. Exposure intervals of 100 and 1000 μsec were assumed for this analysis. Since no IMC techniques are employed, E_f is unity.

The angular velocity (Ω) resulting from the forward motion of the RPV can be defined by

$$\Omega = \frac{V_g \sin\beta}{H} \text{ r/s} \qquad \text{(B-12)}$$

where

β = depression angle (degrees)

V_g = ground velocity of RPV (ft/sec)

H = altitude AGL (feet)

Angular velocity will be a factor only during the NAV mode since the target will be tracked, either manually or automatically, after it has been acquired. As a consequence, there will be no forward motion component at the optical axis, and only a small uncompensated amount at the extremes of the small FOV normally employed during this mode. If we assume two typical NAV mode depression angle extremes of 5 and 20 degrees, V_g = 500 knots, and H = 500 feet AGL, then Ω_5 = 0.147 radians/second and Ω_{20} = 0.577 radians/second.

The limiting angular resolution can now be found by use of Eq. (B-11).

	Exposure Interval	
Depression Angle	T = 100 μsec	T = 1000 μsec
β 5 deg	14.7 μrad	147 μrad
β = 20 deg	57.7 μrad	577 μrad

4.3.4 System Angular Resolution

The limiting dynamic angular resolution (α_D) for the maximum and minimum FOV's, depression angles of 5 and 20 degrees, and exposure times of 100 and 1000 μsec, were caluclated by use of Eq. (B-6) and presented in Table B-3.

Analysis of the data presented in Table B-3 for the NAV mode indicates that the angular resolution associated with the wide FOV is relatively insensitive to both depression angle and exposure interval. The narrow FOV is not affected by shutter speed at the small depression angle, but degrades at the larger exposure interval when the depression angle is increased.

TABLE B-3. DYNAMIC ANGULAR RESOLUTION FOR SLEWABLE TV CAMERA

Depression Angle		Exposure Interval	
		T = 100 μsec	T = 1000 μsec
FOV = 4.4 deg	5 deg	0.22	0.26
	20 deg	0.23	0.62
FOV = 42 deg	5 deg	2.13	2.14
	20 deg	2.13	2.21

All values are in milliradians

The poor angular resolution exhibited by the wide FOV is directly related to the degradation in resolution as the FOV is increased. Thus, the desirability of selecting the smallest FOV in the NAV mode consistent with contiguous ground coverage is indicated.

At depression angles greater than about 20 degrees, the operator will have selected the tracking mode, and the degrading effects of angular motion will be minimized. If the target is tracked manually, rather than by means of a video tracker, the operator will induce small angular deviations. In addition, if a two-axis gimbal system is employed instead of a three-axis system, vehicle perturbations will result in roll components about the optical axis.

4.4 Ground Spot Size

Ground spot size is difficult to pictorialize due to the large number of FOV, azimuth angle, and depression angle combinations available to the operator of a slewable TV system. Ground spot size as a function of altitude is presented in Figures B-6a and B-6b for typical NAV mode depression angle extremes of 5 and 20 degrees. Ground spot size for typical extreme RECON depression angles of 40 and 80 degrees are shown in Figure B-7. As stated previously, the effects of air vehicle perturbations have not been included because of the unavailability of RPV dynamics data.

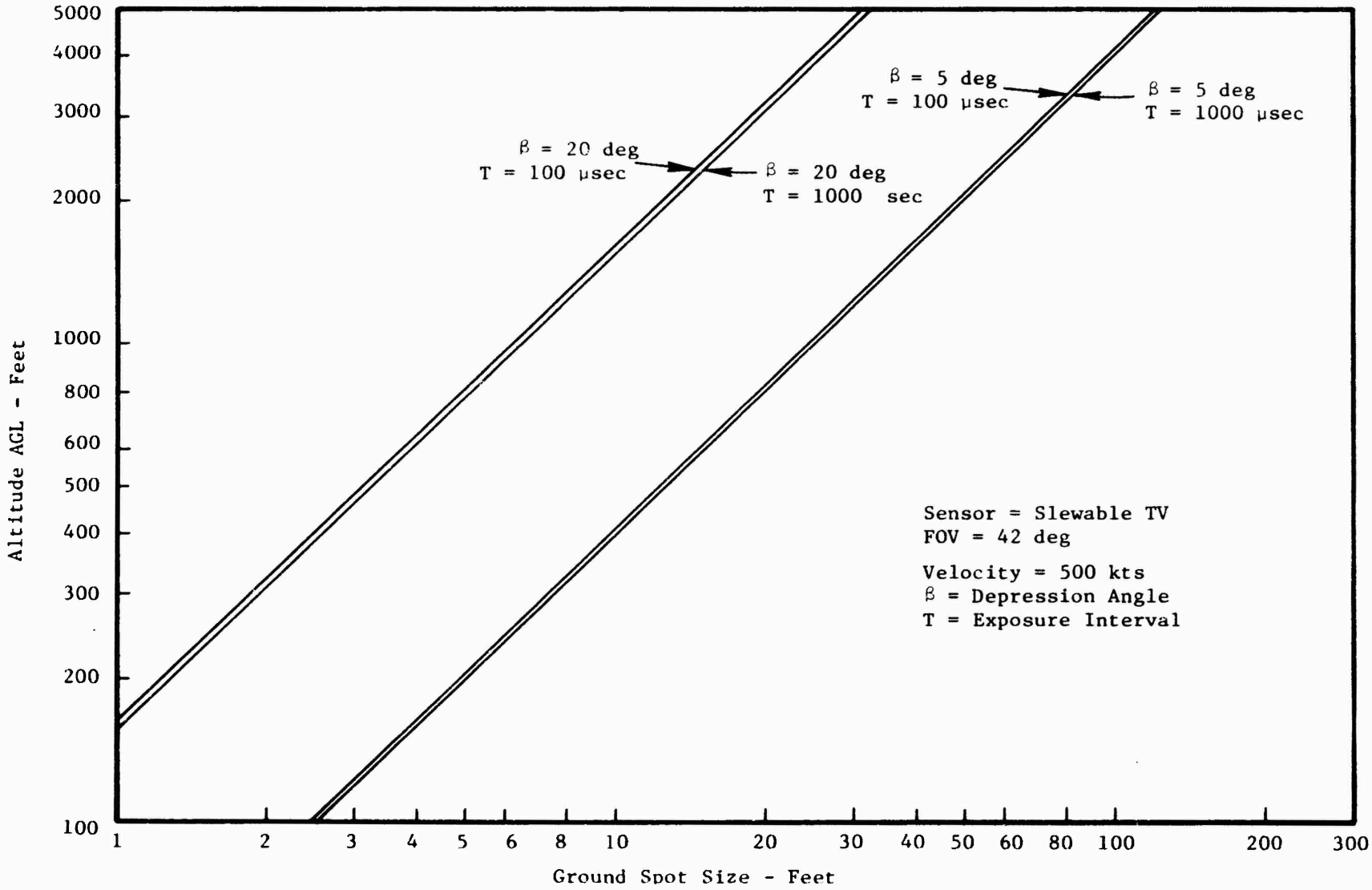

Figure B-6a. Ground Spot Size for Slewable TV Camera - NAV Mode (FOV = 45 deg)

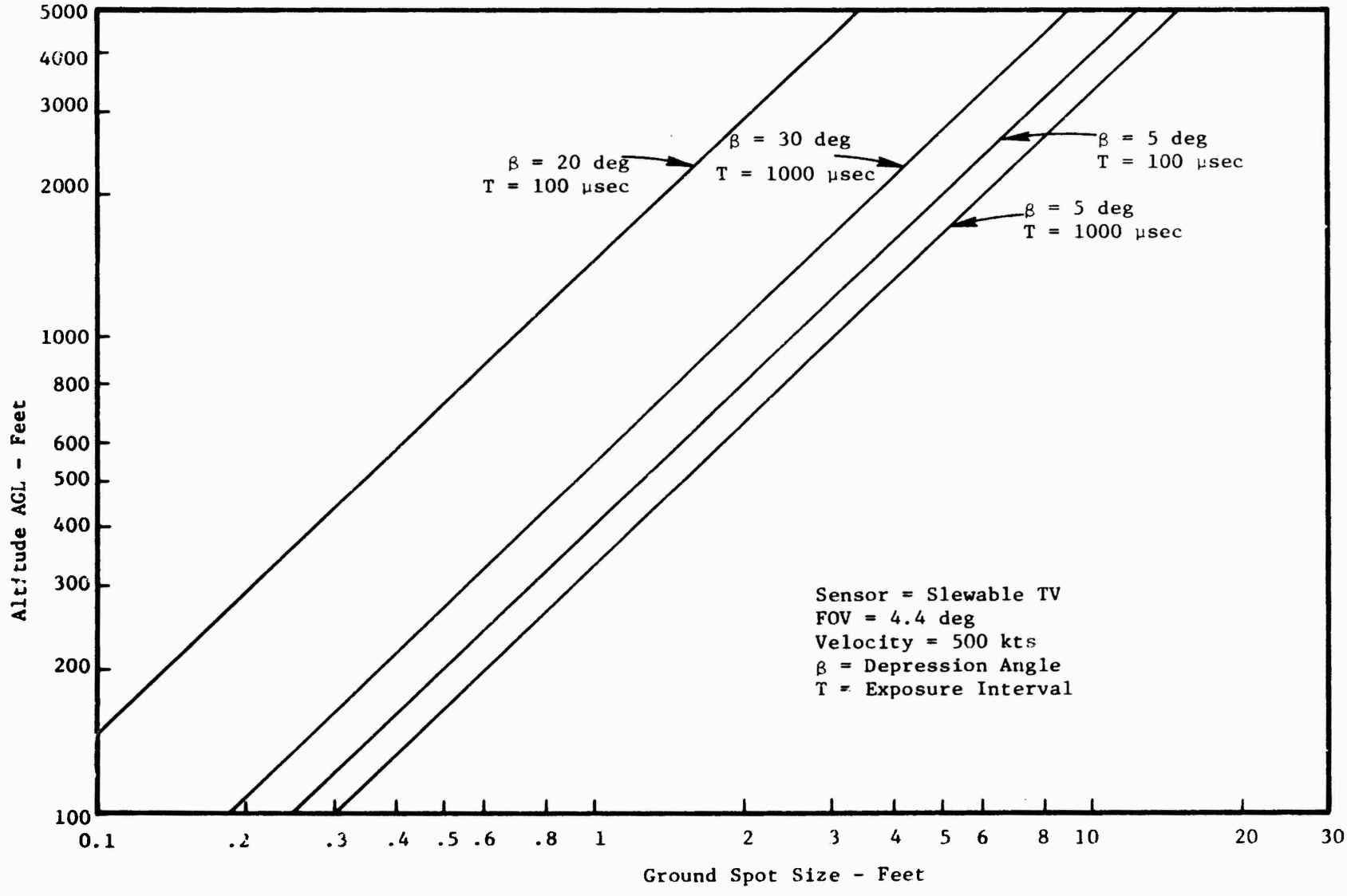

Figure B-6b. Ground Spot Size for Slewable TV Camera - NAV Mode (FOV = 4.4 deg)

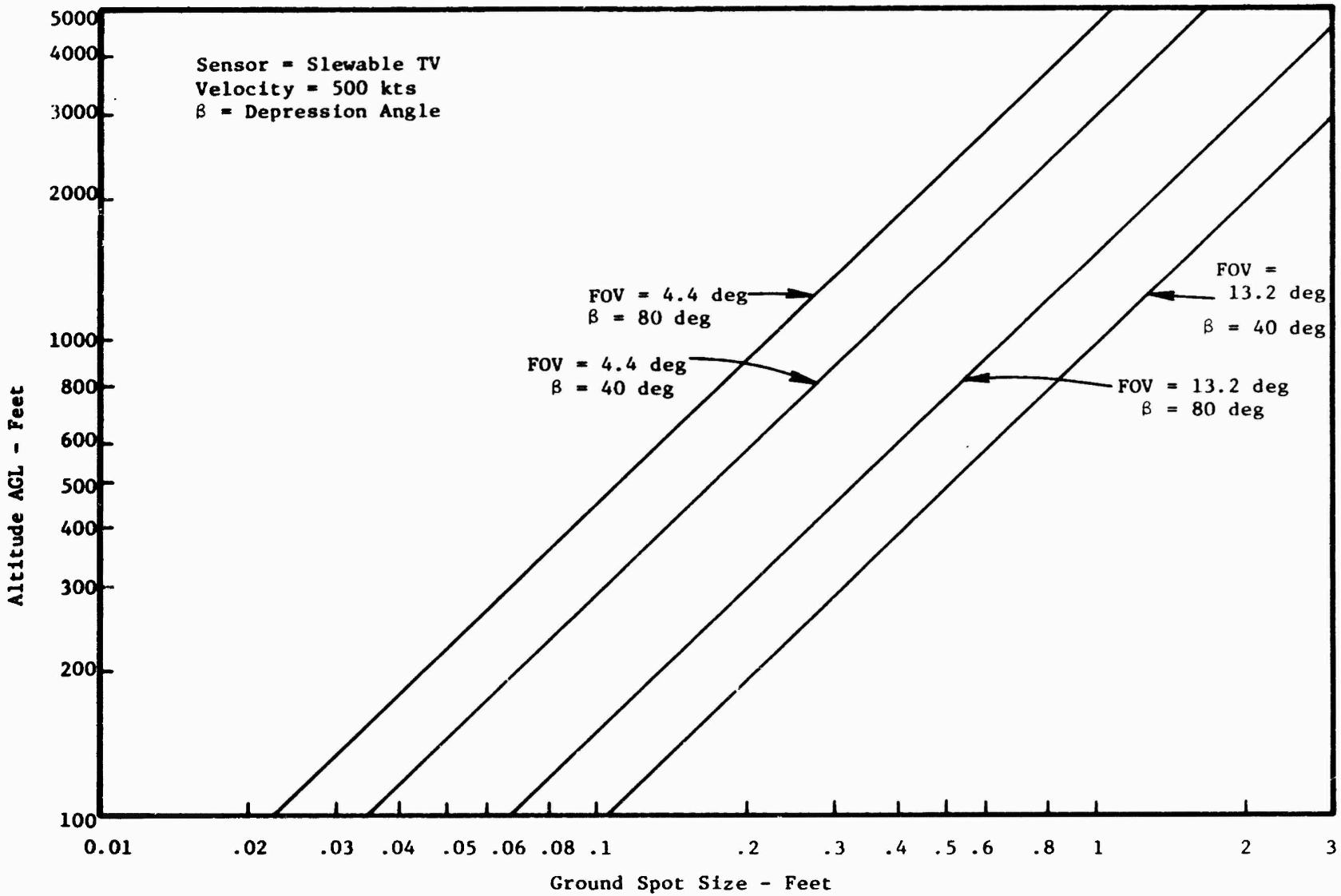

Figure B-7. Ground Spot Size for Slewable TV Camera - RECON Mode

4.4.1 NAV Mode

The ground spot size requirements defined in Sec 2 (this report) for the task of target recognition indicates that a ground spot size of from 0.75 to 3 feet is required. Figure B-6a indicates that satisfactory performance would be provided with the widest FOV (42 deg) at an altitude of 500 feet and a depression angle of 30 degrees. Performance would not be acceptable at a more realistic depression angle of 20 degrees (or less). Decreasing the FOV would produce the desired ground spot size.

Figure B-6b shows the ground spot size that would be realized by use of the narrowest FOV (4.4 deg). This figure is presented for reference only since, even with an accurate navigation system, experience has shown that FOV's this small are not suitable for either the navigation or the target acquisition function.

4.4.2 RECON Mode

The ground spot size requirements which permit target identification and assessment were defined in Section 2 to be 0.2 to 1 foot. With reference to Figure B-7, note that the satisfactory spot size can be realized from an altitude of 500 feet for FOV's from minimum (4.4 degrees) to about 20 degrees.

4.5 Eye/Display Relationships

4.5.1 Size of Displayed Image

Height of the displayed image (I) is found by

$$I = \frac{S\xi}{\theta_V} \quad \text{inches} \tag{B-13}$$

where

S = height of active area of display (inches)

ξ = angular subtense of target's height projected toward TV sensor (degrees)

θ_V = sensor vertical FOV (degrees)

but

$$\xi = 2 \tan^{-1} (T/2R)$$

$$\sim T/R \quad \text{ratio} \tag{B-14}$$

where

T = target vertical dimension normal to TV optical axis (feet)

R = slant range of optical axis (feet)

and

$$R = \frac{H}{\sin\beta} \quad \text{feet} \tag{B-15}$$

where β = depression angle (degrees)

so that

$$I = \frac{S\ T \sin\beta}{H\ \theta_V} \quad \text{inches} \tag{B-16}$$

Height of the target's displayed image as a function of altitude is presented in Figures B-8a and B-8b for the maximum and minimum FOV's. A display height of S = 12 inches, a target projected vertical dimension of T = 30 feet, and depression angles of β = 5, 20, 40, and 80 degrees were assumed.

4.5.2 Raster Lines Across Image

The number of scan lines across the image (N_I) can be found by

$$N_I = \frac{T\ L_A \sin\beta}{H\ \theta_V}$$

$$= \frac{I\ L_A}{S} \tag{B-17}$$

where L_A = number of active scan lines in raster

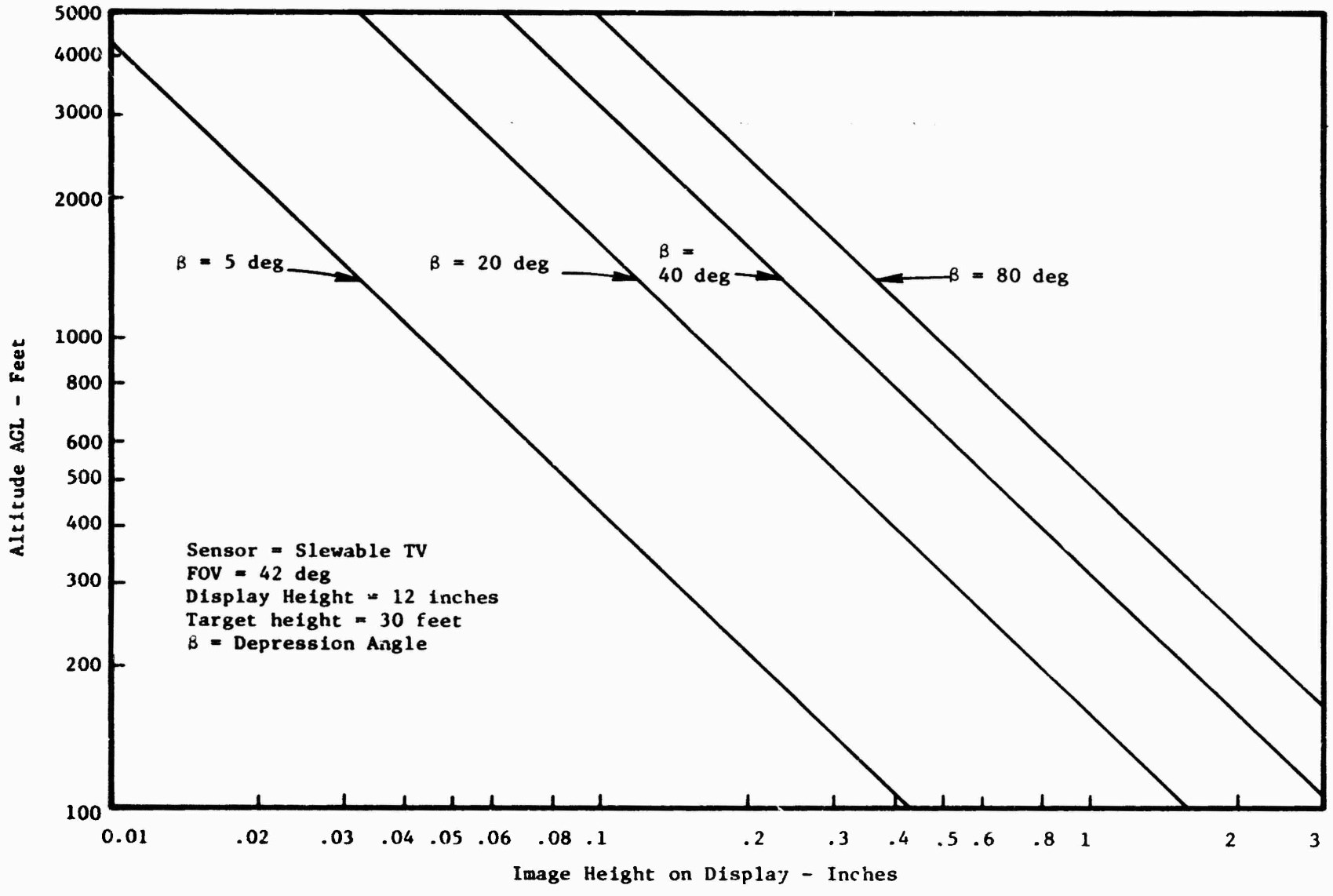

Figure B-8a. Image Height on Display for Slewable TV Camera (FOV = 42 deg)

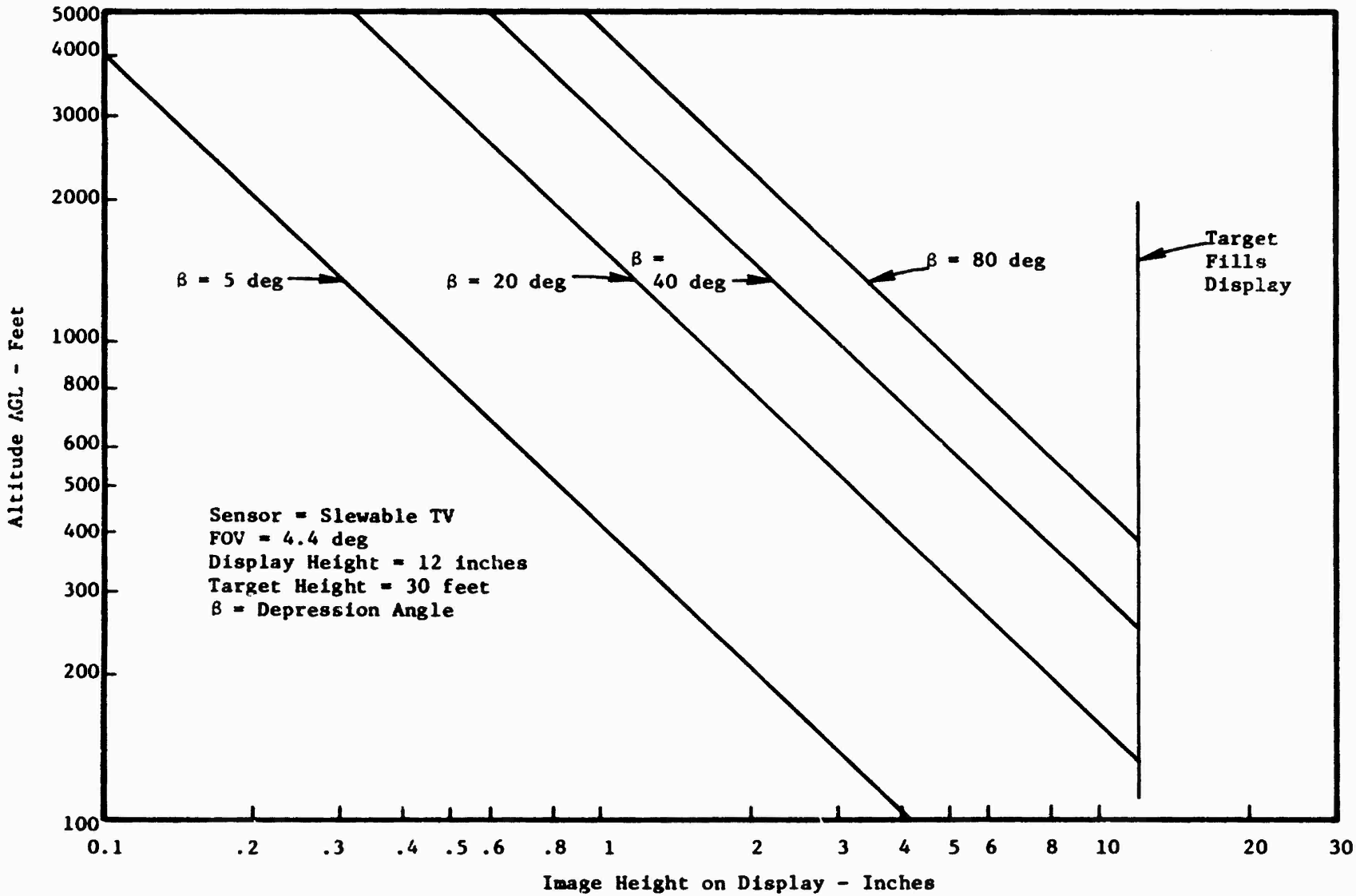

Figure B-8b. Image Height on Display for Slewable TV Camera (FOV = 4.4 deg)

For a 525 line raster, $L_A = 487$. The display height was assumed to be S = 12 inches.

The number of raster lines across the displayed image as a function of altitude is shown in Figures B-9a and B-9b for the maximum and minimum FOV's, and for four depression angles.

4.5.3 Angle Projected by Displayed Image

The data in Sec 2 (this report) indicate that an image interpreter's ability to identify targets is a function of the angle subtended to the eye by the displayed image. The angle subtended to the eye (γ) by the image height (I) can be found by

$$\gamma = 2 \tan^{-1} \frac{S\ T}{2\ R\ Y\ \theta_V}$$

$$\sim \frac{S\ T}{R\ Y\ \theta_V}$$

or

$$\gamma = \frac{I}{Y} \quad \text{radians} \tag{B-18}$$

where

Y = display to eye distance (inches)

I = height of displayed image (inches)

The angle projected to the eye by the displayed image as a function of altitude is presented in Figures B-10a and B-10b for the maximum and minimum FOV's. The angles indicated are for an assumed eye/display distance of 28 inches, and the same image height values previously calculated. The data corresponds to targets located on the optical axes.

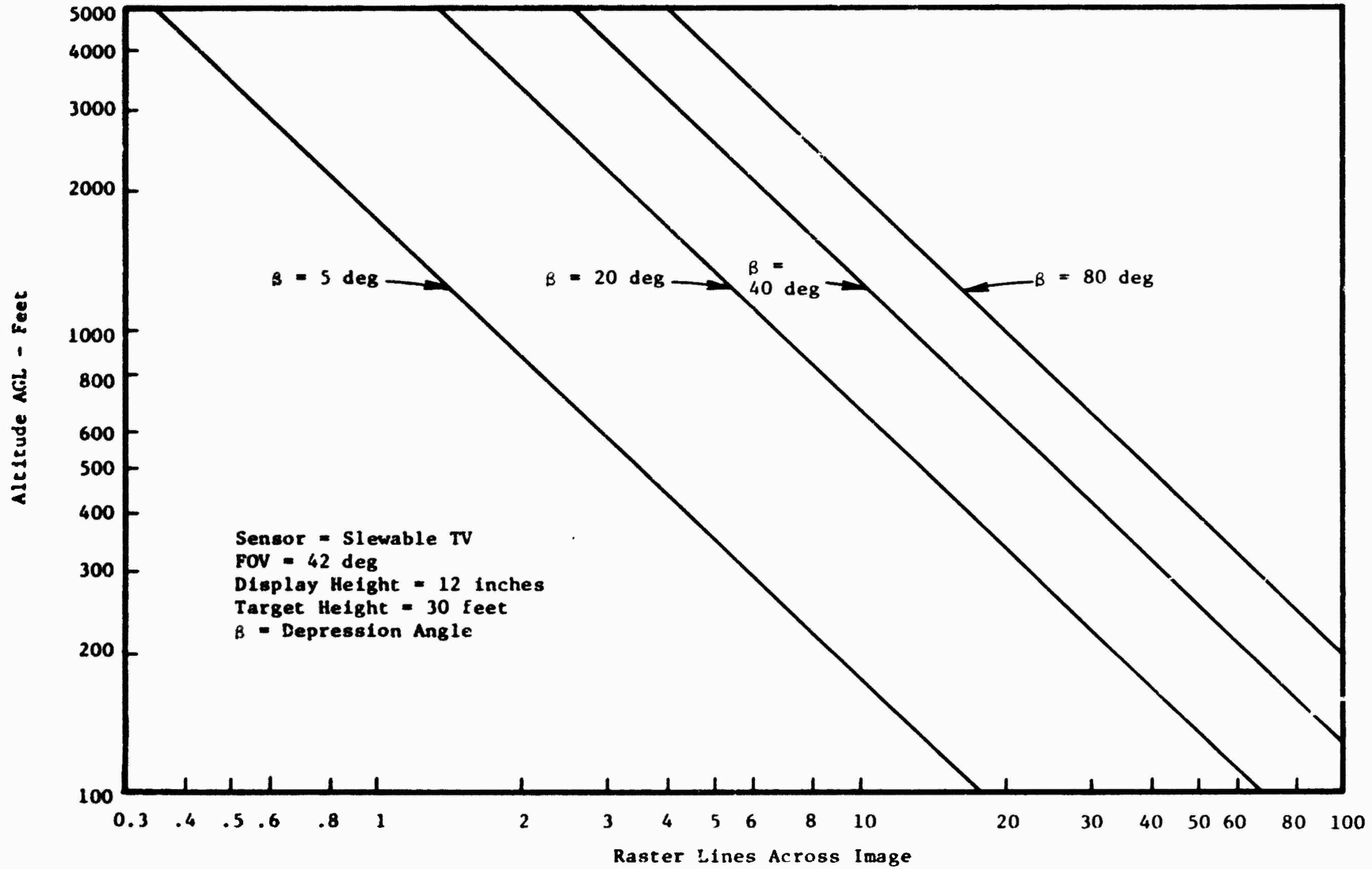

Figure B-9a. Number of Raster Lines Across Image for Slewable TV Camera (FOV = 42 deg)

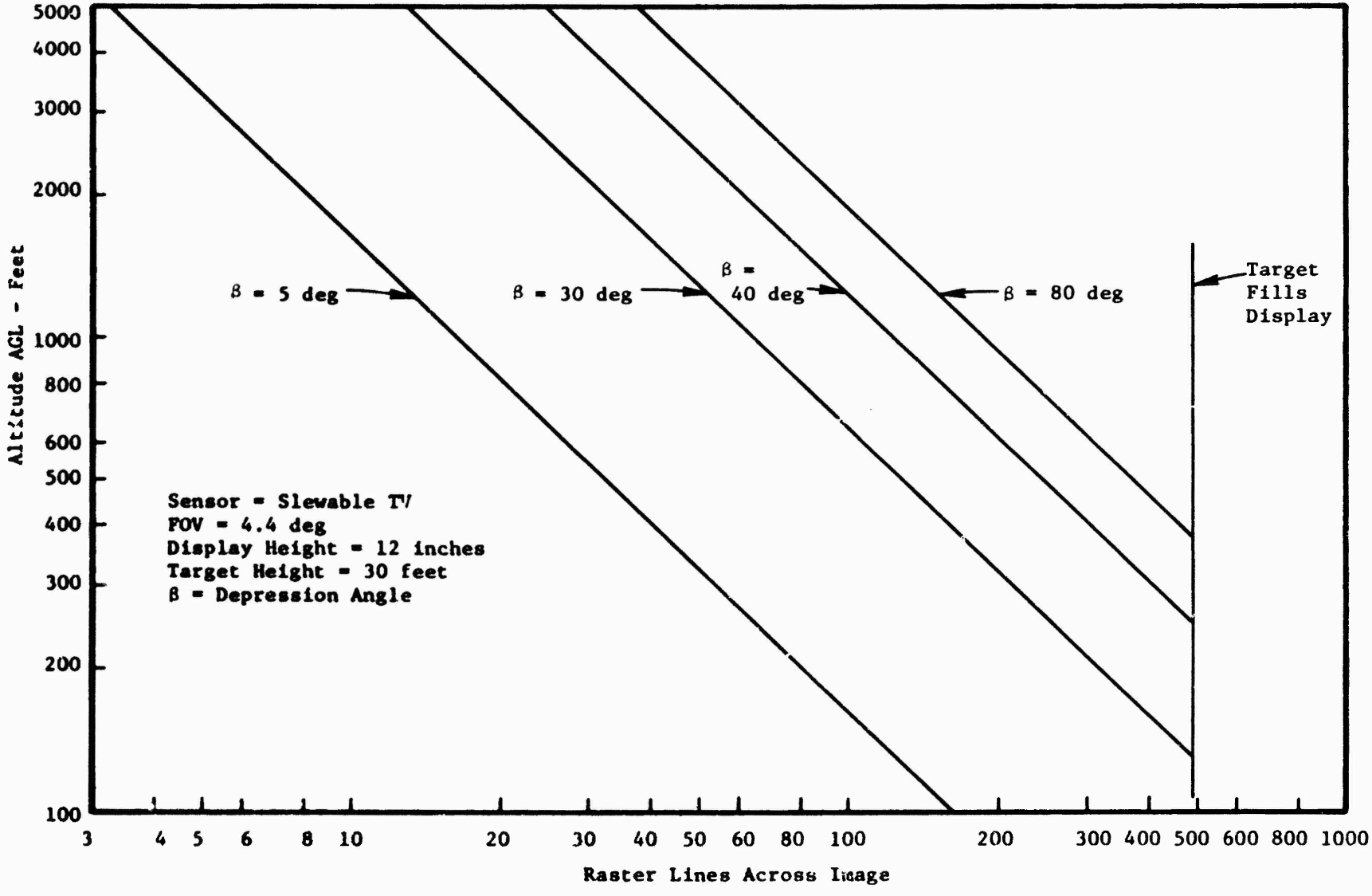

Figure B-9b. Number of Raster Lines Across Image for Slewable TV Camera (FOV = 4.4 deg)

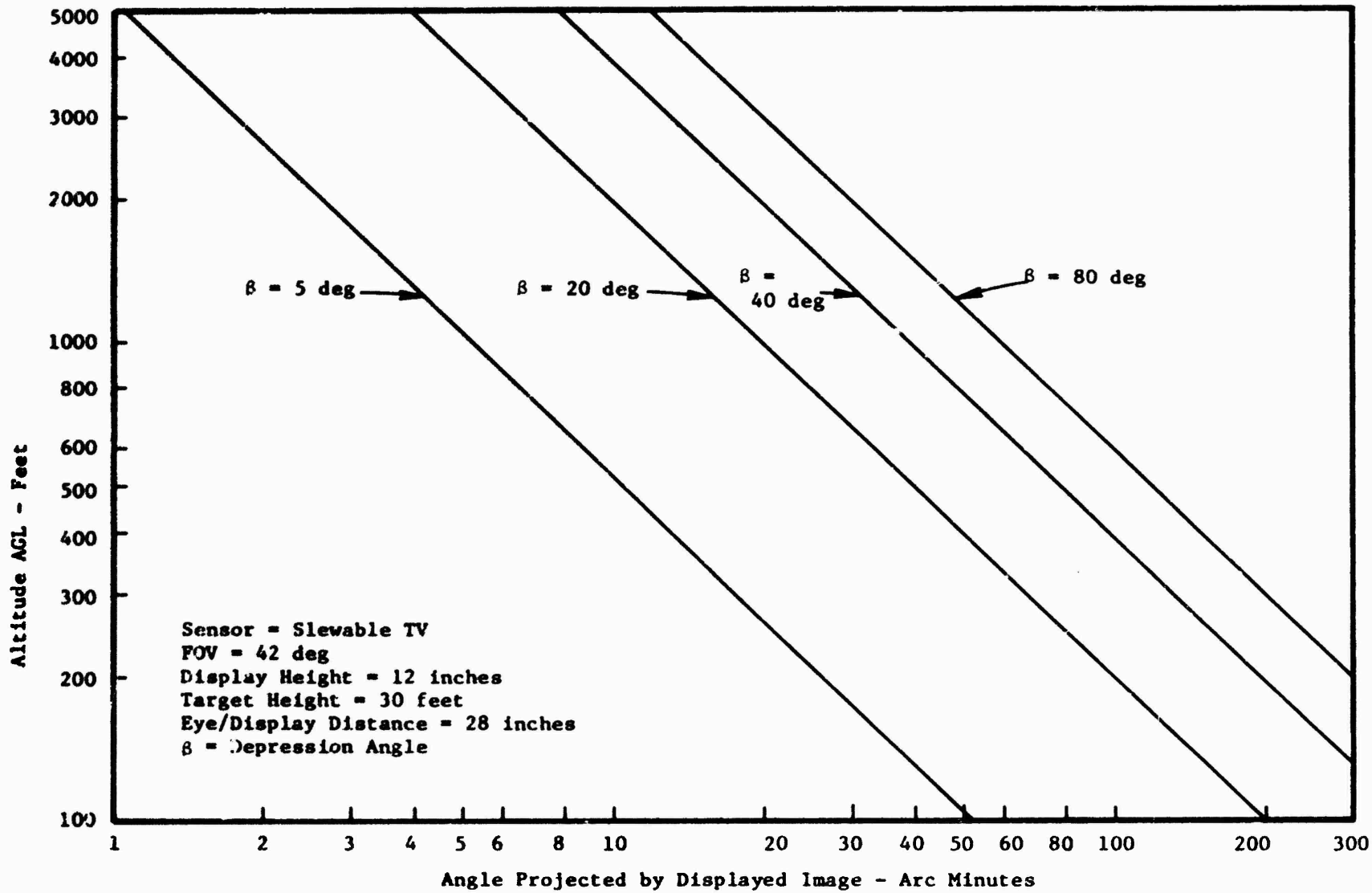

Figure B-10a. Angle Projected to Eye by Image for Slewable TV Camera (FOV = 42 deg)

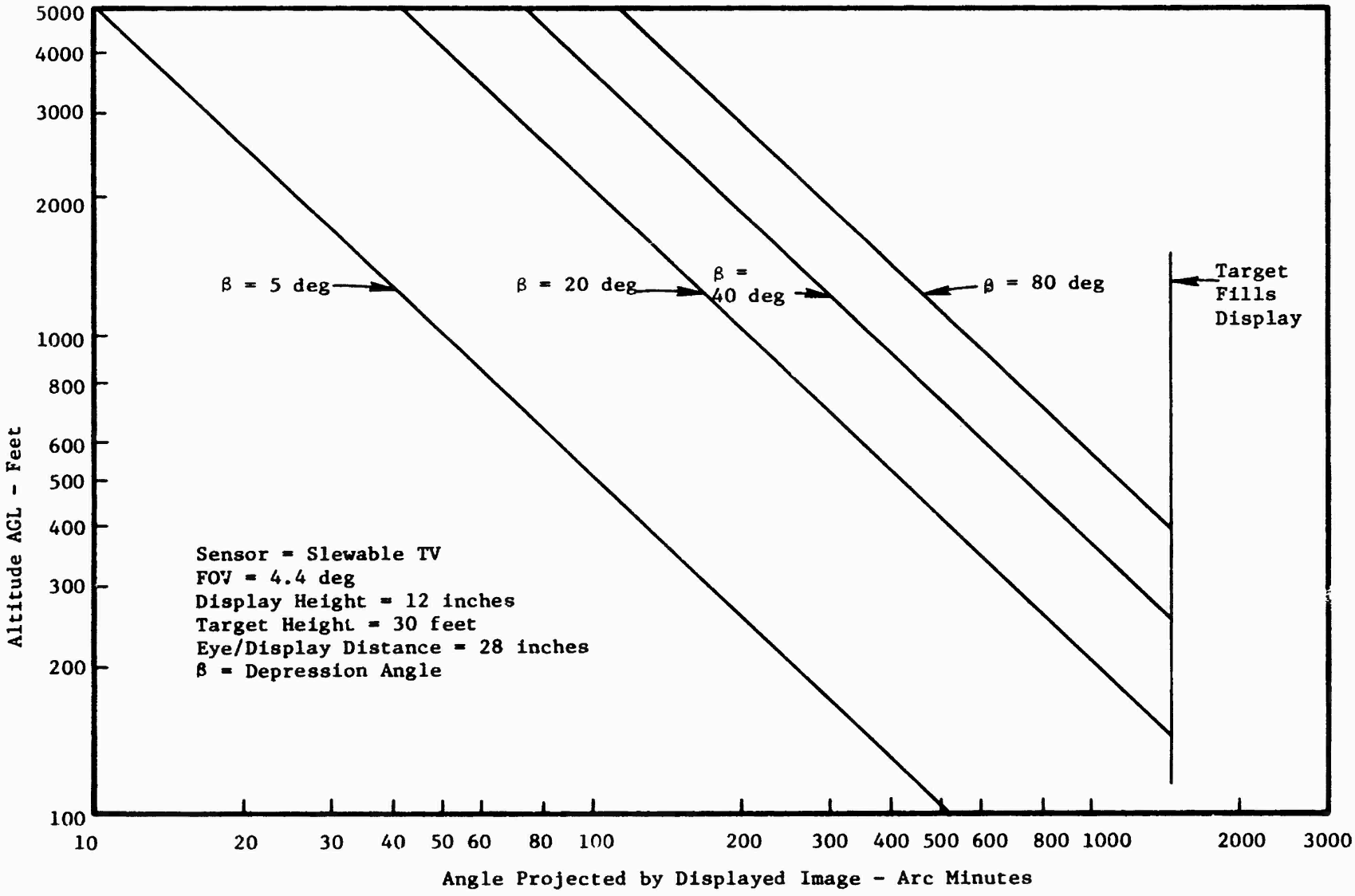

Figure B-10b. Angle Projected to Eye by Image for Slewable TV Camera (FOV = 4.4 deg)

APPENDIX C

TELEDYNE-BROWN TELEVISION SYSTEM

1.0 INTRODUCTION

The Teledyne-Brown (TB) television system is installed in the Improved AQM-34L(TV) Remotely Piloted Vehicle (RPV). The improved AQM-34L(TV) is a basic AQM-34L photographic reconnaissance vehicle modified to provide near real time reconnaissance capability at low altitudes via a microwave data link between the RPV and launch aircraft. The launch aircraft is also used as an airborne remote control station. All of the features of the basic AQM-34L, except the 523 doppler system have been retained; however, three new systems have been added. These systems are (1) TV camera with tilt actuator and nose cone, (2) camera interface unit, and (3) data link transmitter and antenna system.

2.0 OPERATIONAL CONCEPT

The Improved AQM-34L(TV) RPV is designed to provide the capability of remotely assisting in the RPV via a data link to selected targets; conducting low level TV reconnaissance of the targets, and relaying the information to an airborne Reconnaissance Officer (RO) for evaluation on a near real time basis while retaining the mission capabilities of the basic AQM-34L vehicle.

2.1 Television Modes

A single TV camera is employed which can be operated in either a navigational (NAV) or reconnaissance (RECON) mode by an Airborne Remote Control Officer (ARCO) aboard the launch aircraft. Remote command is transmitted via a microwave control guidance system (MCGS). The NAV mode is a forward looking mode, and the RECON mode is a downward looking mode utilizing an oscillating mirror system. The navigational TV, coupled with a "track on curser" flight control capability, enables the ARCO to fly the RPV

accurately over selected targets at altitudes from 500 to 3,000 feet above the terrain. While passing over the target, the reconnaissance mode is used to scan the terrain directly beneath the RPV along the flight path. During this mode of operation the Reconnaissance Officer in the DC-130 aircraft can record up to 40 seconds of TV imagery on disc recorders for instant playback evaluation.

2.1.1 Navigation Mode

This mode is used primarily to assist the ARCO in flying the RPV over a desired target. When in the NAV mode, a forward looking field of view is presented on TV monitors at the ARCO and RO stations. The RO identifies the target area on the TV monitor and directs the ARCO to fly over the target in order to assist in locating targets; a remotely controllable two-position zoom lens and camera tilt capability is provided.

Once the target is selected, the ARCO has the option of using a "track on curser" (TOC) flight control mode to fly the RPV accurately over the target. In this mode, the RPV will fly along a heading established by the position of a cursor (black vertical line on the TV monitor). The cursor can be remotely slewed by the ARCO at a maximum rate of 1.5 degrees per second to either edge of the TV display. When TOC is commanded a heading change up to ±15 degrees can be added to the programmed heading in the flight control system. The ARCO can return to programmed heading control at any time by issuing an MCGS restore command.

2.1.2 Reconnaissance Mode

This mode is used to provide a near real time reconnaissance capability while passing over targets at low altitudes. This is accomplished as follows: Several seconds prior to passing over a target, the ARCO remotely commands the TV camera to the RECON mode. At the same time, the RO starts one of two disc recorders which enables TV video data to be recorded for 20 seconds. At the end of this time, the RO has the option of recording video data on the second disc recorder to effectively provide up to 40 seconds of continuous

target coverage. Instant playback of the recorded video data, at selectable speeds varying from "still" to the normal 30 frames per second rate, is available to the RO for evaluation. A contrast enhancer may also be used by the RO to facilitate evaluation of low contrast targets.

3.0 SYSTEM DESCRIPTION

3.1 Television System

The data presented in this section has been extracted from the referenced documents. The Television System consists of a TV camera, Camera Control Unit (CCU), and Optical Assembly. All three units are mounted to a support structure which attaches to the forward bulkhead of the RPV. The camera system is mounted so that it can be pivoted in a vertical play by an actuator assembly. Windows are installed in the nose cone to permit viewing terrain ahead of and directly below the RPV. The pertinent characteristics of the Teledyne-Brown Television System are presented in Table C-1.

TABLE C-1. TELEDYNE-BROWN TELEVISION SYSTEM CHARACTERISTICS

TV Camera	
Tube type	gated SIT
Line Rate	525 lines/frame
Frame Rate	30 frames/second
Interlace	2:1
Aspect Ratio	1:1
Image Size	11.4 × 11.4 mm
Field of View	
Minimum	6.4 deg
Maximum	32 deg
Focal Length	20 - 100 mm
Mirror	
Cycle Rate	3.75 cycles/second
Maximum Scan Angle	±60 deg
Exposure Control	automatic 100 μsec to 33 msec
Stabilization	none

3.1.1 TV Camera

The TV camera operates at a 525 line rate, 30 frames per second with interlaced fields. A 1:1 aspect ratio is used (square format). The major features of the camera which enable it to be used as a reconnaissance sensor are the electronically gated Silicon Intensified Target (SIT) picture tube and the associated Automatic Light Control (ALC) system. This enables the camera to be operated in either a NAV or RECON mode at altitudes from 500 to 3,000 feet under dawn to dusk light conditions. Gating (exposure) of the SIT tube occurs once per field during the vertical blanking time in the NAV mode and once per frame in the RECON mode. Gating effectively freezes the TV image on the SIT tube for the duration of the frame/field scan time. The exposure time varies automatically from 100 μsec to 33 msec depending on light level. Short exposure times (100 μsec to one msec) are necessary in the RECON mode to minimize image smear when low altitude missions are flown.

3.1.2 Optical Assembly

The Optical Assembly consists of a zoom lens, mirror, filter, and associated drive motors mounted as a complete unit to the front of the TV camera.

1. Zoom Lens - The lens is a 20 to 100 mm focal length fast zoom lens with provisions for mounting haze filters as required. When the lens is used with the 11.4 by 11.4 mm image format of the SIT vidicon, the field of view can be varied from 6 by 6 degrees to 32 by 32 degrees. The focal lengths are preflight adjustable to permit selection of fields of view within these limits which are compatible with mission requirements.

   For the "zoom in" (narrow field of view) mode, the 100 mm focal length is recommended for all mission altitudes. For the "zoom out" (wide field of view) mode, the focal length is preadjusted for a focal length between 24 and 95 mm depending on the specific mission altitude to be flown. The wide field of view adjustment is

necessary to obtain the desired ground coverage (overlap) when the system is operated in the RECON mode.

Either field of view may be remotely selected in less than one second for both the NAV and RECON modes. However, use of the zoom feature in the RECON mode at altitudes less than 2,000 feet will produce gaps in the ground coverage. Also, if the RPV is flown at altitudes significantly lower or higher than that for which the focal length has been preset, then loss of resolution (target detectability) will occur.

2. Mirror Assembly - A remotely selectable two-position mirror is used to provide the NAV and RECON modes of operation. Positioning of the mirror is accomplished in less than one second to prevent possible loss of data when approaching a target. In the NAV mode, the mirror is rotated out of the field of view of the camera. This provides a forward looking view along the longitudinal axis of the camera. In the RECON mode, the mirror is positioned at a 45 degree angle with the line of sight of the camera. This directs the field of view downward at a 90 degree angle to the camera longitudinal axis. The mirror is then rotated back and forth at a rate of 3.75 Hz over the preadjustable scan angle. The scanning action allows the center line of the field of view (optical axis) to be scanned up to ±60 degrees either side of the line of flight. To provide proper ground coverage it is necessary to adjust focal length, scan rate, and scan angle for the mission altitude to be flown.

3. Tilt Actuator - The camera is attached through lever arms to an actuator assembly which provides the capability for tilting the entire camera assembly through depression angles from zero to 10 degrees with respect to the waterline of the RPV.

3.1.3 Camera Control Unit

All of the remote command and control functions that are associated with the various camera modes of operation are routed to and processed by the CCU. It also contains the adjustment controls for the optical assembly.

3.2 Camera Interface Unit

The CIU is mounted in the aft equipment compartment in place of the Doppler Converter Unit. The CIU provides all of the command and control interface functions for the TV camera system, Flight Control System, and MCGS which are peculiar to the Improved AQM-34L(TV) RPV. The various functions of the CIU can be divided into the following categories:

1. ON/OFF Commands
2. Track on Cursor
3. Program Update/Inhibit

3.2.1 ON/OFF Commands

TV ON/OFF
Curser ON/OFF
Zoom IN/OUT
NAV/RECON Mode
Tile UP/DOWN
Cursor LEFT/RIGHT

The cursor ON command enables circuits within the TV camera which add a specially generated signal to the normal TV video. At the TV monitor, this appears as a black vertical line. The position of the line is remotely controlled by the Cursor LEFT/RIGHT commands. Also, when Zoom IN or RECON mode is commanded, the cursor line is inhibited by logic circuits within the camera.

3.2.2 Track on Cursor

The CIU provides the ARCO with the capability of remotely flying the RPV in a "Track on Cursor" mode of operation. This mode requires the utilization of the cursor functions in conjunction with a TOC enable command. This mode can only be utilized in the NAV and Zoom OUT modes. Implementation is as follows: The ARCO commands cursor ON and then slews the cursor to the desired position (target). A signal is generated which represents a heading change that is proportional to the slew angle of the cursor. Cursor slew angles (heading changes) are preflight adjusted to correspond to a 26 degree field of view (±13 degree heading changes). When the cursor is positioned, the ARCO commands TOC which enables the cursor slew (heading change) signal to be summed with the actual RPV heading signal. The resultant signal is applied to the flight control system to effectively make the RPV track the cursor. Once the TOC is commanded, any subsequent slew commands will result in heading change signals to the flight control system. Thus, the ARCO effectively has a proportional flight control capability within the limits established. NOTE: Bank angle step commands will result if sufficient heading error signal exists prior to adding the TOC heading change signal. For this reason, the minimum heading error signal required to initiate a bank angle step command has been changed from 15 to 20 degrees, and the programmer should be programmed to provide a TOC restore ON and OFF after each programmed turn.

3.2.3 Program Update/Inhibit Functions

The CIU contains a pulse generator which supplies mileage pulses to the digital programmer to step the programmer through programmed events. The mileage pulses, which are two seconds long, are preflight adjusted to occur at a rate of one pulse every 4.67 to 7.35 seconds (350 to 550 knots) depending on the mission requirements. If during the mission it is determined that the programmed events are occurring late or early, the ARCO has the option of using the remote Program Update and Program Inhibit commands to update the programmer at certain preprogrammed events.

3.3 Airborne Receiving Station

The receiving station consists of: (1) a rack-mounted FM receiver; (2) a roll-on cart containing a 15 inch high resolution TV monitor, an IVC-800 tape recorder, two disc cassette recorders, two dc to ac power inverters, and contrast enhancer; (3) a 15 inch TV monitor and contrast enhancer rack mounted at the ARCO station, and (4) a diplexer coupled with waveguide to the two foot MCGS disk antenna. The disk antenna is used to receive the transmitted data link signal in addition to its normal MCGS function. The data link signal is then separated from the MCGS signals by a diplexer and demodulated by the FM receiver.

The receiver (modified by Univac to provide a 7 MHz bandwidth and de-emphasis) provides two video outputs. One output is applied to the tape recorder, contrast enhancer and TV monitor (at ARCO station). The tape recorder provides the capability of recording all TV data for the entire mission, and replayed for post mission analysis. The contrast enhancer and TV monitor are used by the ARCO during the NAV mode. The other output is applied to the two disc recorders, TV monitor, and contrast enhancer on the roll-on cart.

A reconnaissance officer (RO) uses the equipment on the roll-on cart to record and evaluate reconnaissance data on a near real-time basis. The RO observes the TV monitor in the NAV mode to assist the ARCO in locating targets. When the ARCO commands RECON (several seconds prior to passing over the target) the RO starts recording video data on one of the two disc recorders. As the disc approaches the end of the recording time (20 seconds) an indicator light illuminates. At this time the RO can start the second disc recorder to record an additional 20 seconds of data. The ARCO can then return the TV to the NAV mode. Program Inhibit may also be used at this time to make another pass over the target. Immediately after recording the data, the RO may replay the video on the TV monitor to evaluate the presence of threats. During playback, the recorder can be operated at various speeds from "still" to 30 frames per second. Most evaluation will be performed at frame rates of six per second or less.

4.0 PERFORMANCE

4.1 NAV Mode

4.1.1 Ground Coverage

In the NAV mode the optical axis is fixed at zero degrees azimuth angle but can be remotely positioned in elevation from zero to minus 10 degrees with respect to the waterline of the RPV. The wide and narrow fields of view are selected during the preflight procedures by setting the minimum and maximum focal lengths of the zoom lens. Either focal length can then be selected during flight. The focal length required for a given field of view can be found by

$$F = \frac{W}{2 \tan (\theta/2)} \quad \text{mm} \qquad \text{(C-1)}$$

where W = dimensions of raster on the SIT vidicon (mm)

F = effective optical focal length (mm)

θ = sensor FOV (degrees)

Since the focal length range of the zoom lens is 20 to 100 mm and W = 11.4 · 11.4 mm, the corresponding FOV range is 6.4 by 6.4 to 32 by 32 degrees. Ground coverages for these fields of view are plotted in Figures C-1a and C-1b for depression angles of 4 and 10 degrees and an altitude of 500 feet AGL. Because the wide FOV extends above the horizon in both cases, ground coverage was plotted to a depression angle of one degree.

The lateral coverage of the near and far sides of the footprint is shown in Figure C-2a and C-2b for the 6.4 and 32 degree fields of view. The geometrical relationships are presented in Figure C-3 and Table C-2.

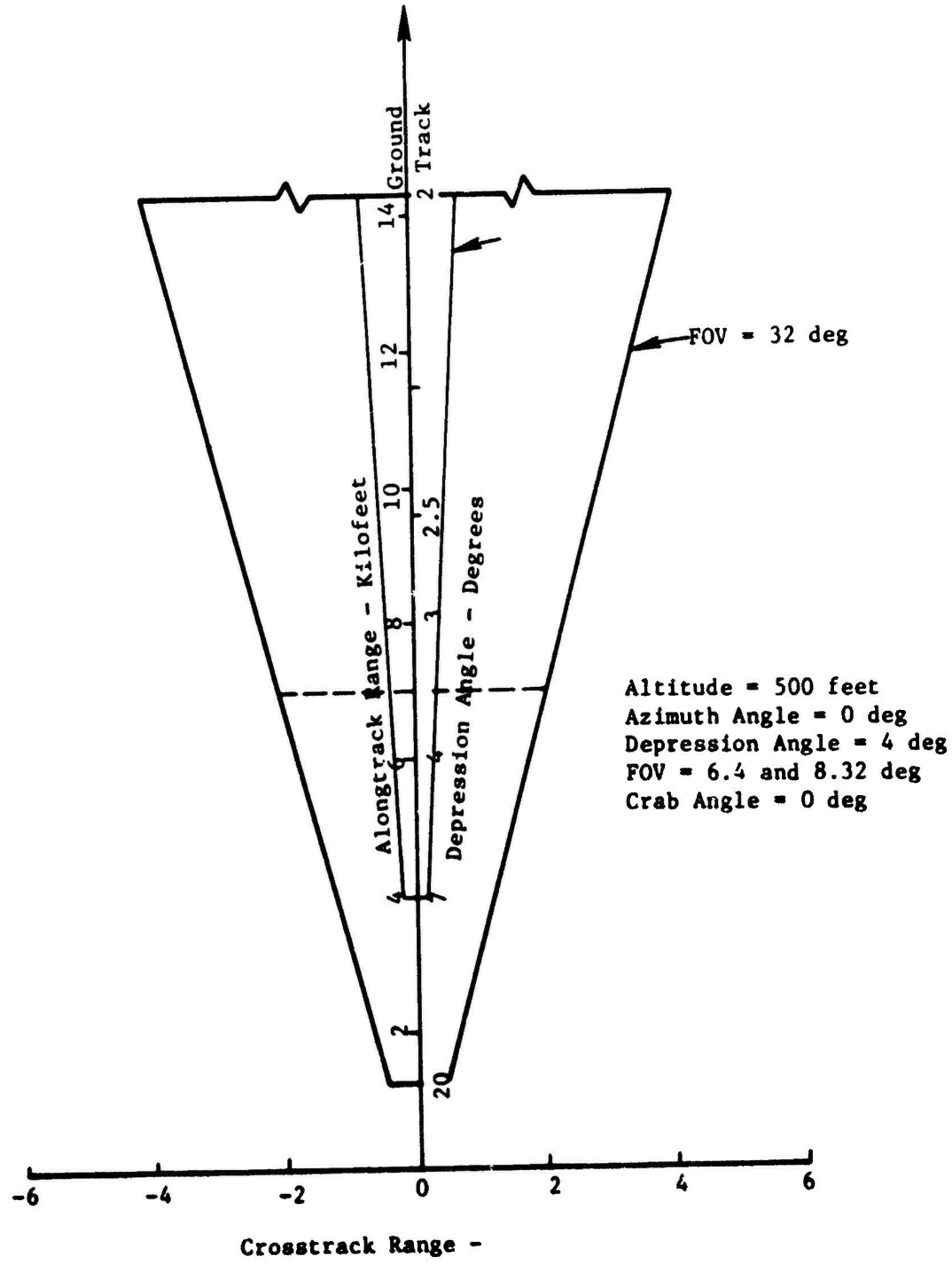

Figure C-1a. Ground Coverage for Teledyne-Brown TV Camera - NAV Mode (Depression Angle = 4 deg)

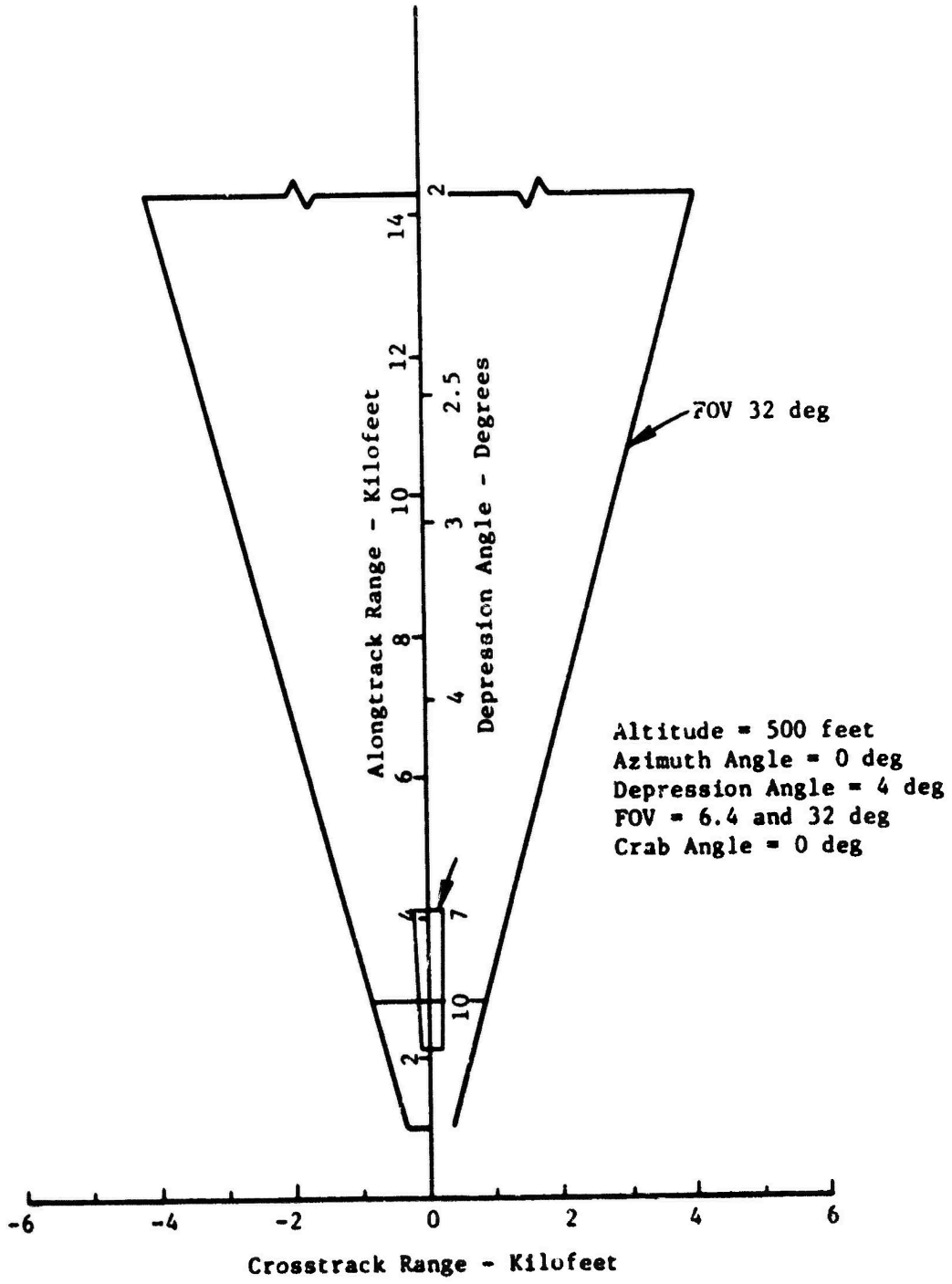

Figure C-1b. Ground Coverage for Teledyne-Brown TV Camera - NAV Mode (Depression Angle = 10 deg)

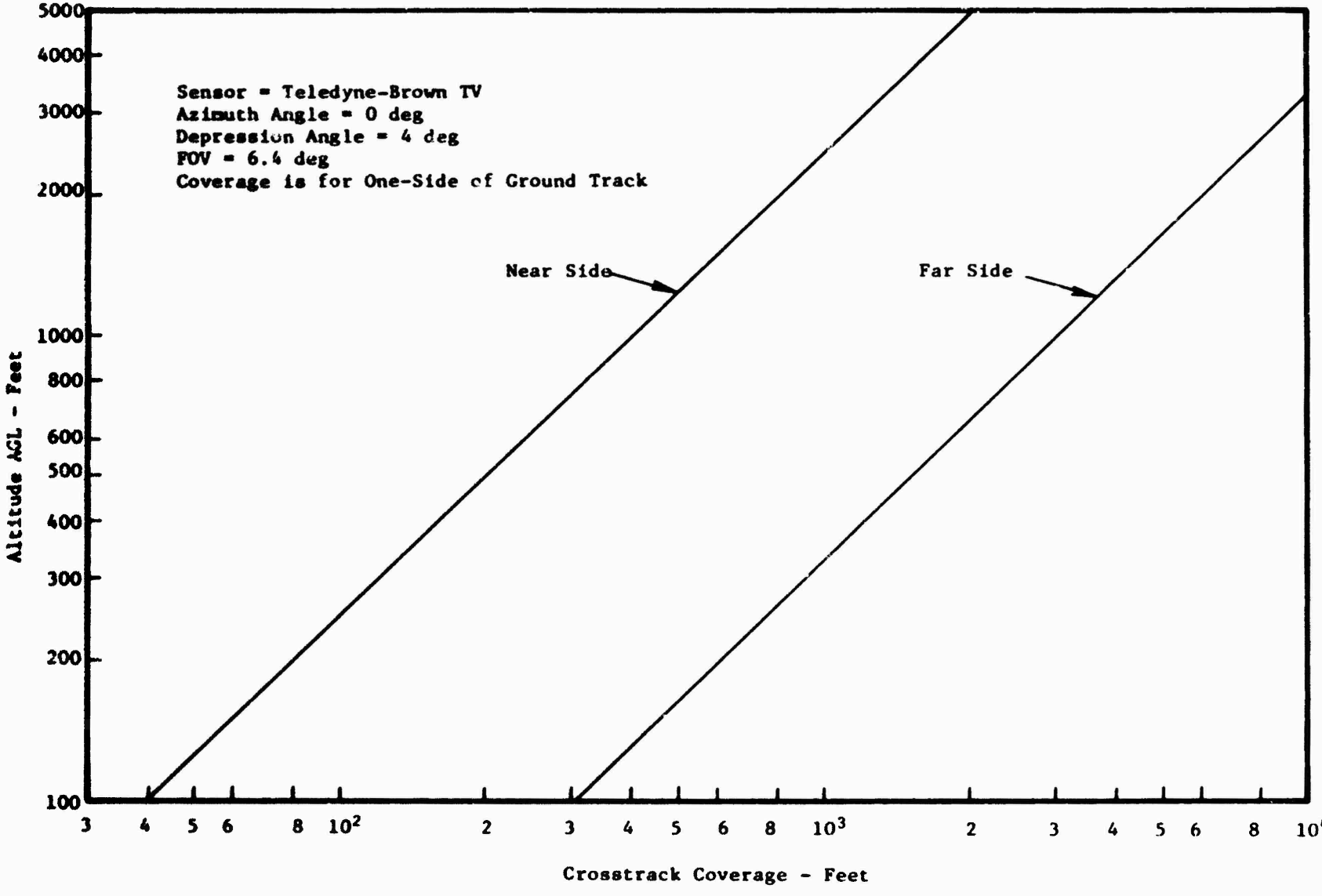

Figure C-2a. Crosstrack Coverage for Teledyne-Brown TV Camera - NAV Mode (FOV = 6.4 deg)

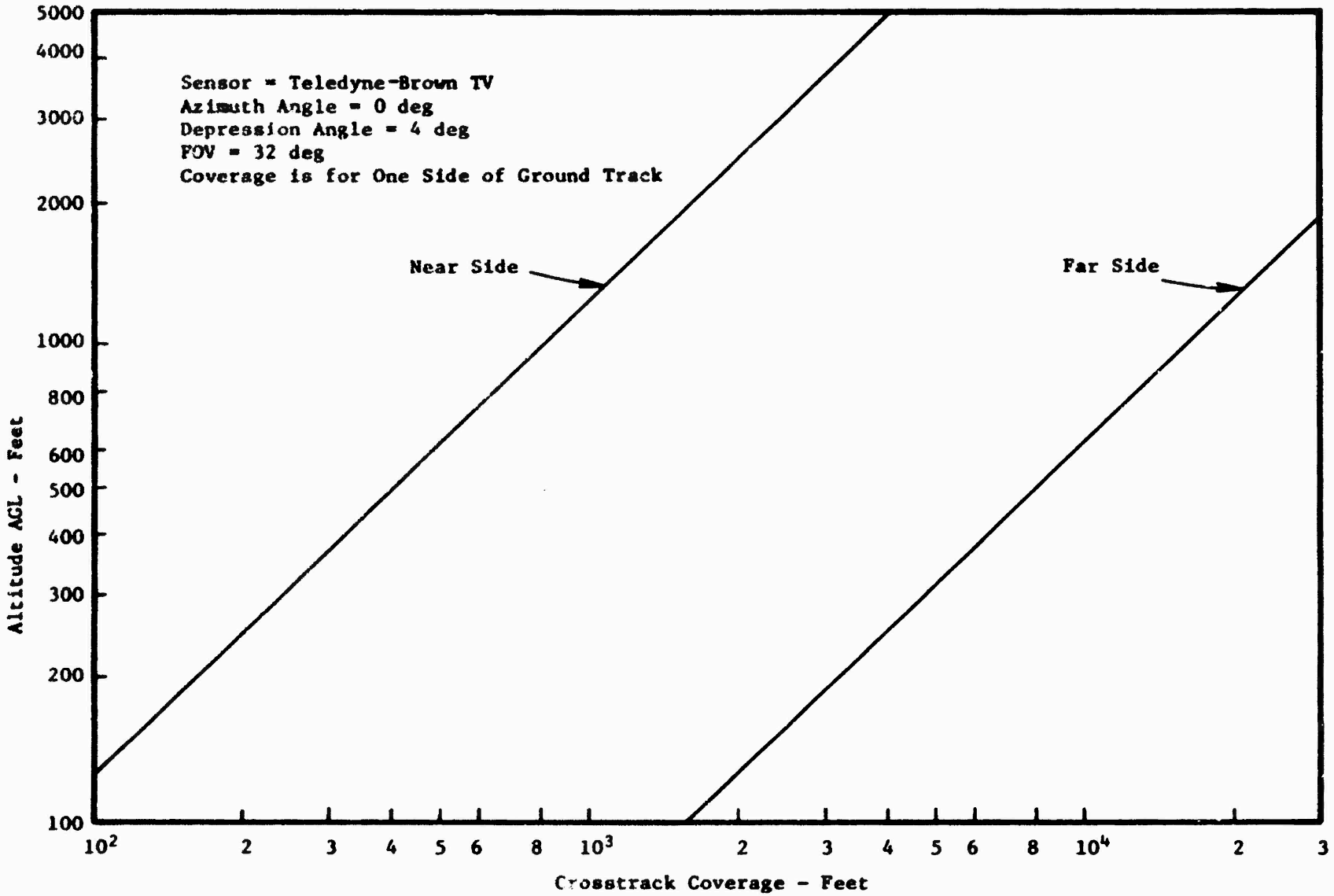

Figure C-2b. Crosstrack Coverage for Teledyne-Brown TV Camera - NAV Mode (FOV = 32 deg)

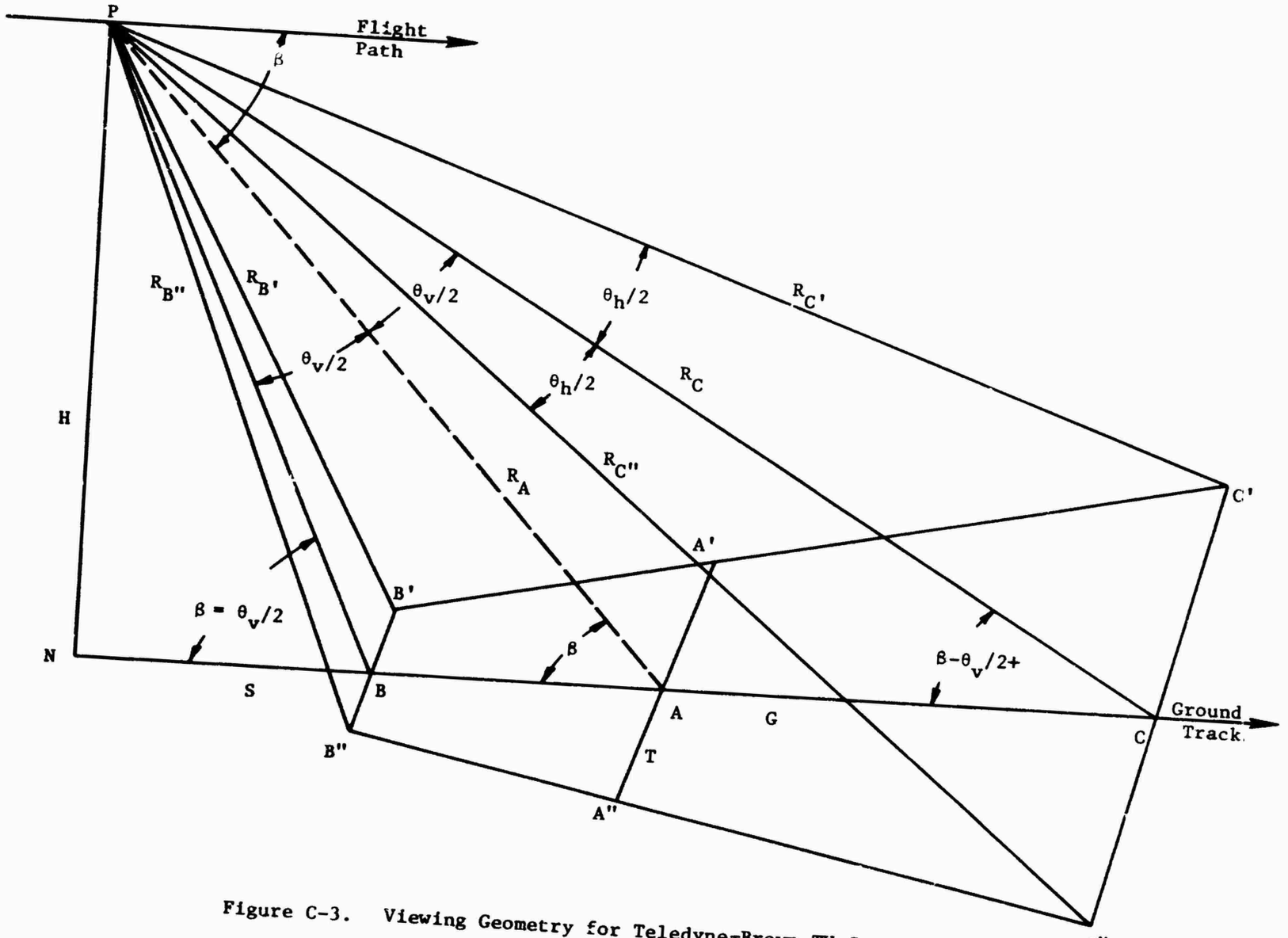

Figure C-3. Viewing Geometry for Teledyne-Brown TV Camera - NAV Mode

TABLE C-2. GEOMETRICAL RELATIONSHIPS FOR TELEDYNE-BROWN TV CAMERA - NAV MODE

Slant Range (R)

$R_A = H/\sin\beta$ (optical axis)

$R_B = H/\sin(\beta+\theta_v/2)$

$R_C = H/\sin(\beta-\theta_v/2)$

$R_{A'} = R_{A''} = H/\sin\beta\cos(\theta_h/2)$

$R_{B'} = R_{B''} = H/\sin(\beta+\theta_v/2)\cos(\theta_h/2)$

$R_{C'} = R_{C''} = H/\sin(\beta-\theta_v/2)\cos(\theta_h/2)$

H = altitude
β = depression angle
θ_v = horizontal FOV
θ_h = vertical FOV
θ_{vT}, θ_{hT} = angular deviations from the optical axis

Slant Range to Any Point in FOV

$$R = H/\sin(\beta\pm\theta_{vT})\cos\theta_{hT}$$

Alongtrack Range (S)

$S_{NB} = H/\tan(\beta+\theta_v/2)$

$S_{NA} = H/\tan\beta$

$S_{NC} = H/\tan(\beta-\theta_v/2)$

Alongtrack Range to Any Point in FOV

$$R = H/\tan(\beta\pm\theta_{vT})$$

Crosstrack Dimension of Footprint (T)

$$T_{B'B''} = \frac{2H\tan(\theta_h/2)}{\sin(\beta+\theta_v/2)}$$

$$T_{A'A''} = \frac{2H\tan(\theta_h/2)}{\sin\beta}$$

$$T_{C'C''} = \frac{2H\tan(\theta_h/2)}{\sin(\beta-\theta_v/2)}$$

TABLE C-2 (cont'd)

Crosstrack Dimension for Any Point in Format

$$T = \frac{2H \tan(\theta_h/2)}{\sin(\beta \pm \theta_{vT})}$$

Alongtrack Dimension of Footprint (G)

For offset distance $\leq T_{BB'}$ or $T_{BB''}$

$$G_B = \frac{H}{\tan(\beta-\theta_v/2)} - \frac{H}{\tan(\beta+\theta_v/2)} = H[\cot(\beta-\theta_v/2) - \cot(\beta+\theta_v/2)]$$

For offset distance $T_{BB'} \leq O_T \leq T_{CC'}$ or $T_{BB''} \leq O_T \leq T_{CC''}$

$$G_{BC} = h[\cot(\beta-\theta_v/2) - \cot(\beta+\theta_v/2)] \left[1 - \left\{\frac{O_T - T_{BB'}}{T_{CC''} - T_{BB'}}\right\}\right]$$

where $0 \leq \{\ \} \leq 1$

4.1.2 Scale

Scale for the optical axis (SC_A), the near edge of the FOV (SC_B), and the far edge of the FOV (SC_C) can be found by

$$SC_A = \frac{F \sin\beta}{H} \quad \text{ratio} \tag{C-2}$$

$$SC_B = \frac{F \sin(\beta+\theta_v/2)}{H} \quad \text{ratio} \tag{C-3}$$

$$SC_C = \frac{F \sin(\beta-\theta_v/2)}{H} \quad \text{ratio} \tag{C-4}$$

where

F = focal length (feet)

H = altitude AGL (feet)

β = elevation angle (degrees)

θ_v = sensor vertical FOV (degrees)

These functions are plotted in Figures C-4a and C-4b (refer to Figure C-3 and Table C-2).

The scale to any point in the field of view can be found by

$$SC = \frac{F \sin(\beta+\theta_{vT})\cos\theta_{hT}}{H} \quad \text{ratio} \tag{C-5}$$

where θ_{vT} and θ_{hT} are the vertical and horizontal angular deviations from the optical axis.

4.1.3 Target Time on Display

Target time on the display (T_d), in seconds, can be found by the expression

$$T_d = \frac{H}{V_g}\left[\cot(\beta-\theta_v/2) - \cot(\beta+\theta_v/2)\right]\left[1 - \left\{\frac{O_T - T_{B'B''}/2}{T_{C'C''}/2 - T_{B'B''}/2}\right\}\right] \tag{C-6}$$

where

$$T_{B'B''}/2 = \frac{H \tan(\theta_h/2)}{\sin(\beta+\theta_v/2)}$$

$$T_{C'C''}/2 = \frac{H \tan(\theta_h/2)}{\sin(\beta-\theta_v/2)}$$

$$0 \le \{\ \} \le 1$$

V_g = ground velocity of the RPV (feet/second)

Refer to Figure C-3 and Table C-2 for a definition of the symbols.

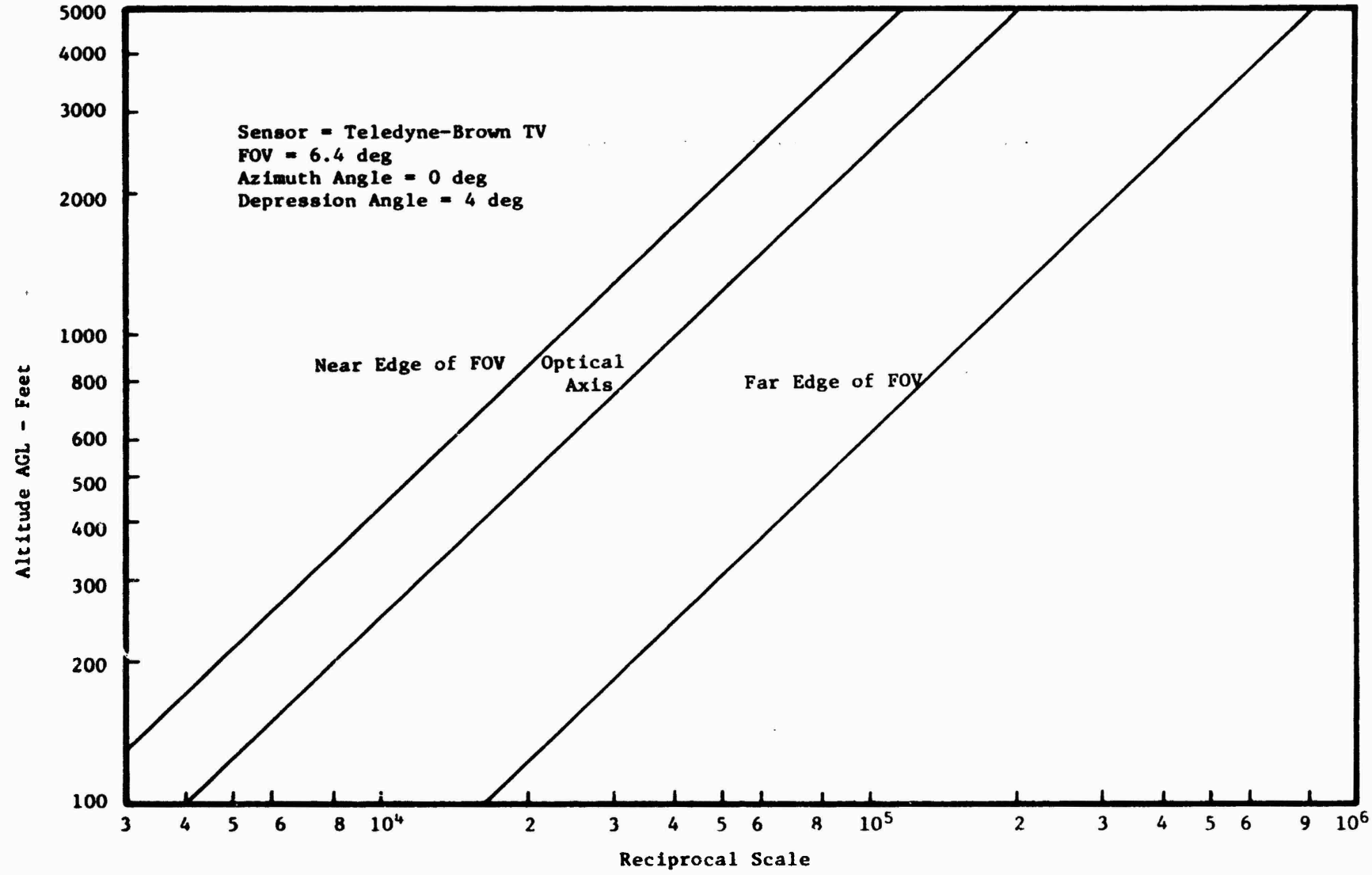

Figure C-4a. Scale for Teledyne-Brown TV Camera - NAV Mode (FOV = 6.4 deg)

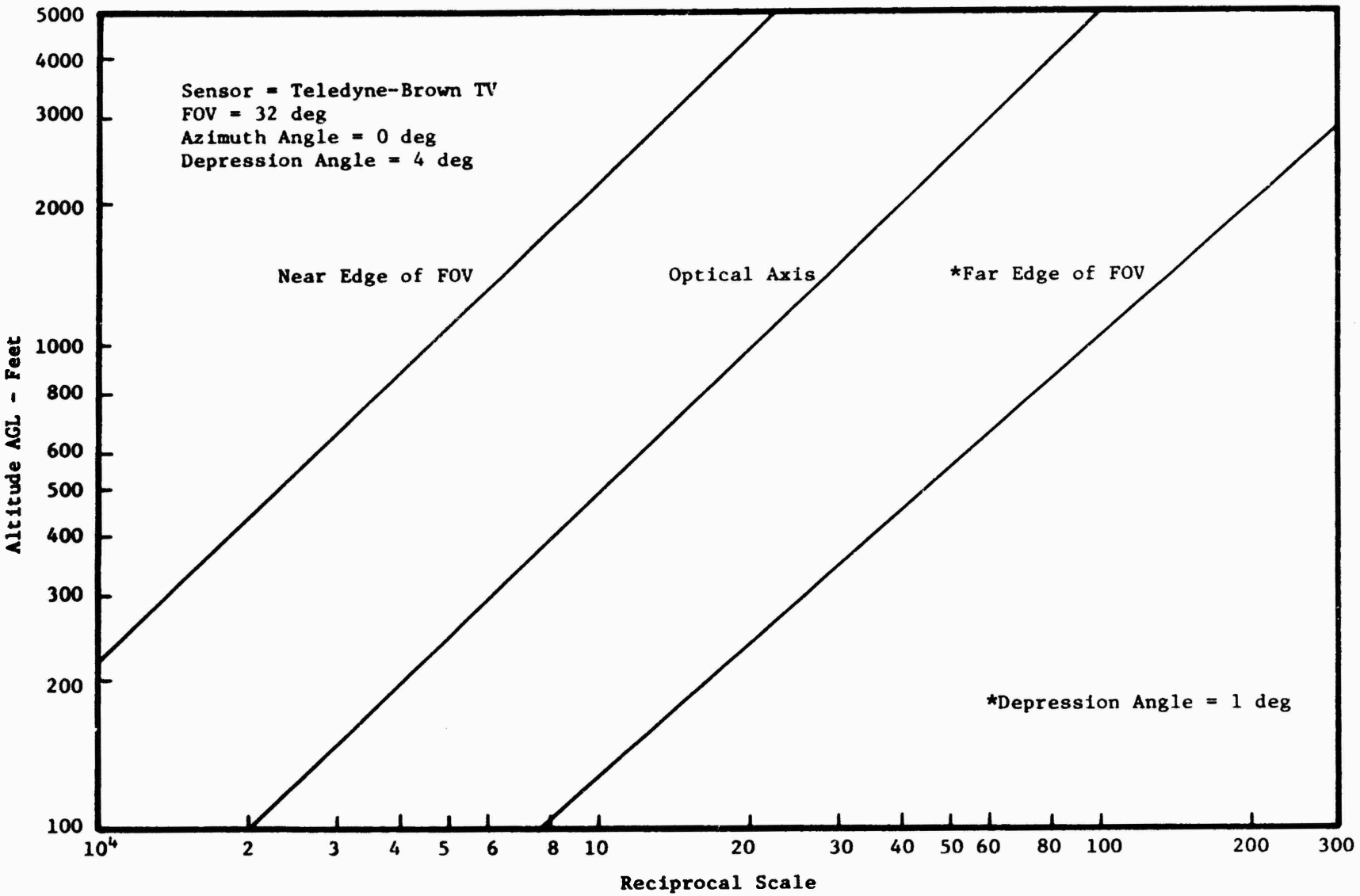

Figure C-4b. Scale for Teledyne-Brown TV Camera - NAV Mode (FOV = 32 deg)

When the target offset distance (O_T) is equal to, or less than, one-half the length of the near side of the footprint $T_{B'B''}$, the target will traverse the maximum footprint dimension. Time on display is then found by H/V times the value of the first set of brackets in Eq. (C-6). As the offset distance increases, the time on display decreases until it reaches zero at the point where $O_T = T_{C'C} = T_{CC''}$.

Target time on the display for the 6.4 and 32 degree fields of view is presented in Figures C-5a and C-5b for a ground velocity of 500 knots.

4.2 RECON Mode

4.2.1 Ground Coverage

The optical axis is scanned through nadir, normal to the ground track, by means of a mirror that is placed in the FOV when the RECON mode is selected. The scan angle is selected prior to flight within the limits of ±60 degrees with respect to nadir. The velocity of the mirror drive motor is then adjusted so that the mirror cycles at a rate of 3.75 Hz. Since the TV camera cycles at a rate of 30 frames per second, eight frames of imagery are collected per mirror cycle. The mirror and TV camera cycle asynchronously.

The gound coverage produced during two mirror cycles is plotted in Figure C-6 for a maximum scan angle of 90 degrees, an altitude of 500 feet, and a ground velocity of 500 knots. Note that the scanning mirror causes the footprints to rotate as a function of the scan angle. For convenience, the footprints will be referred to as "Nadir," "Intermediate" and "Extreme."

4.2.1.1 Nadir Footprint

4.2.1.1.1 Crosstrack Coverage

Since both the horizontal FOV (θ_h) and vertical FOV (θ_v) are identical, both the crosstrack (S_C) and alongtrack (S_A) dimensions are equal and can be found by

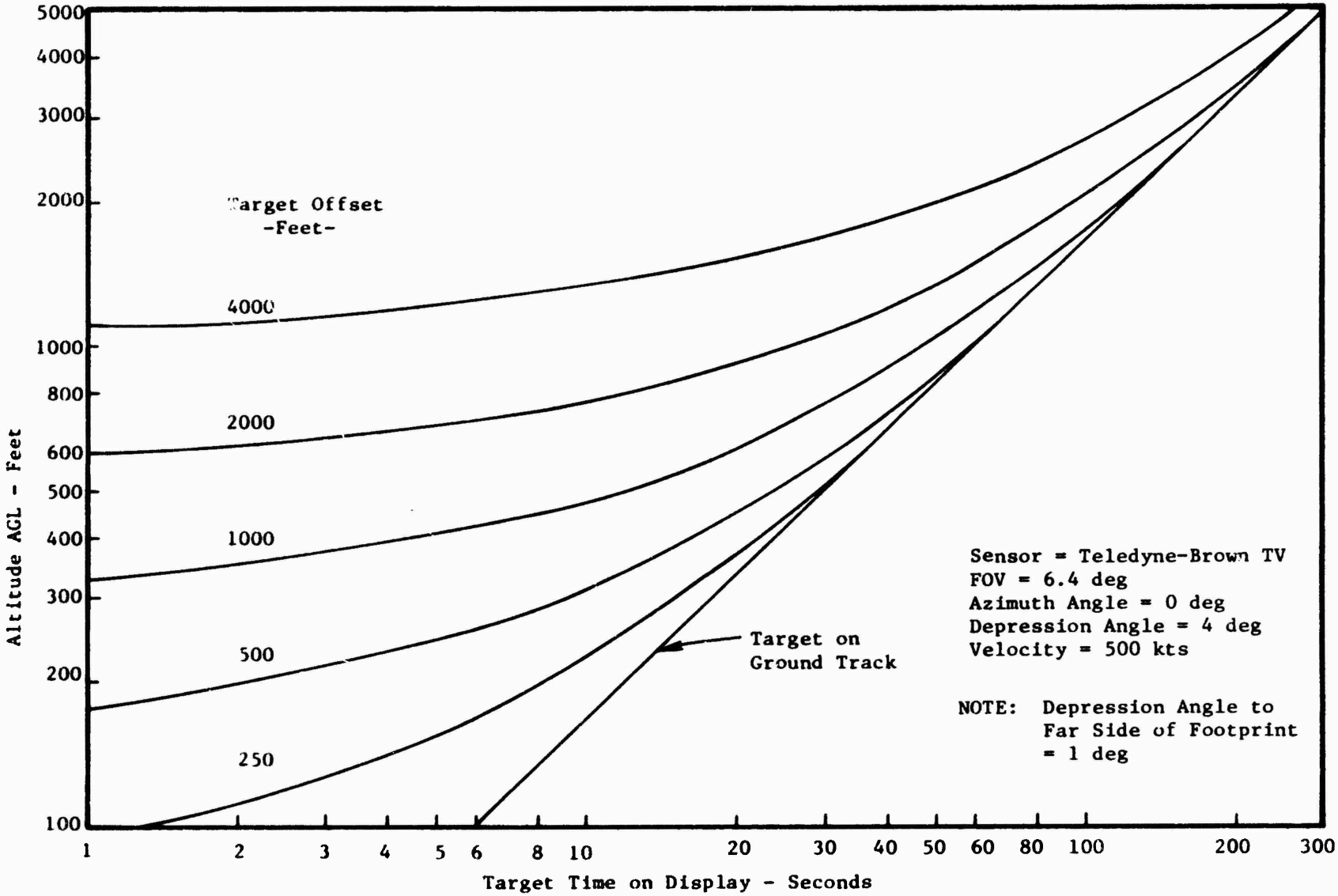

Figure C-5a. Target Time on Display for Teledyne-Brown TV Camera - NAV Mode (FOV = 6.4 deg)

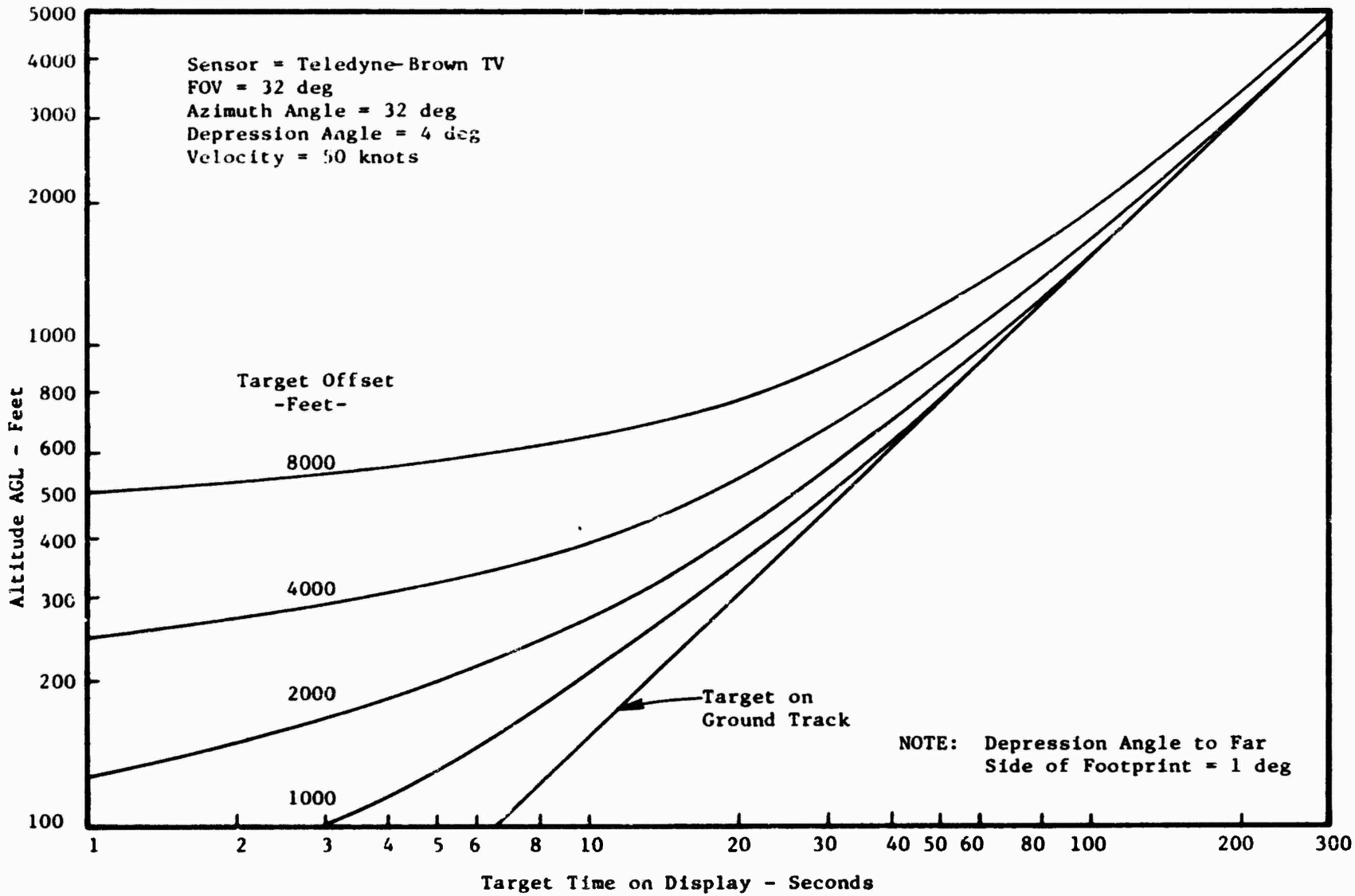

Figure C-5b. Target Time on Display for Teledyne-Brown TV Camera - NAV Mode (FOV = 32 deg)

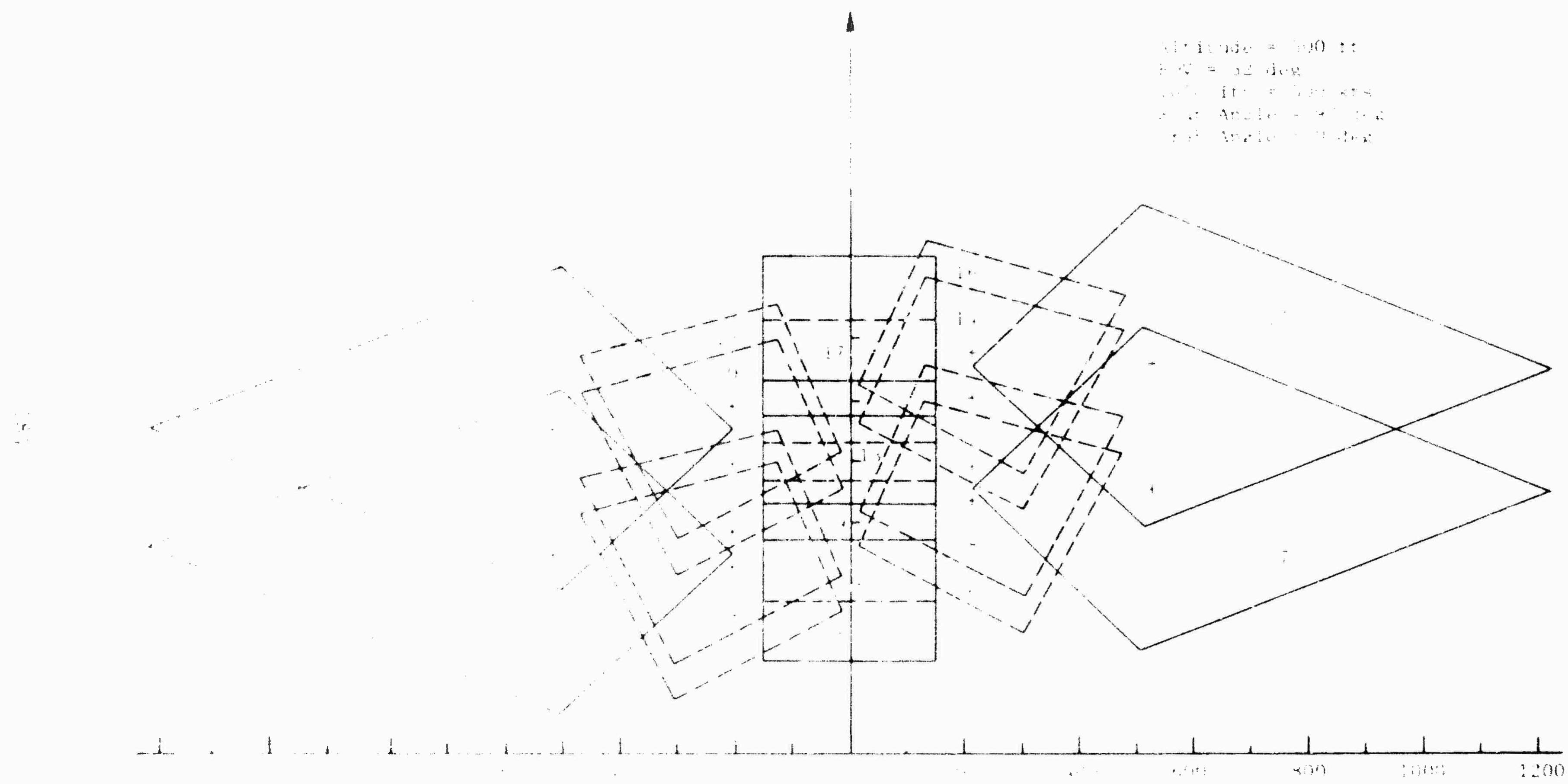

... Brown TV Camera – RECON Mode

$$S = 2H \tan(\theta/2) \quad \text{feet} \tag{C-7}$$

where H = altitude AGL (feet)

For the narrow field of view ($\theta_{h,v}$ = 6.4 deg), S_A and S_L are 56 feet at 500 feet altitude; for the wide FOV ($\theta_{h,v}$ = 32 deg), S_A and S_L are 287 feet at 500 feet altitude. These footprint dimensions are plotted as a function of altitude in Figure C-7.

4.2.1.1.2 Alongtrack Coverage

There are two discs available for recording; one disc provides a recording time of 20 seconds. The TV camera collects imagery at a rate of 30 frames per second so that 600 frames can be recorded per disc.

The alongtrack coverage can be found by

$$V_g T + 2H \tan(\theta_v/2) \quad \text{feet} \tag{C-8}$$

where

V_g = ground velocity (ft/sec)
T = recording time (seconds)

For a ground velocity of 500 knots and an altitude of 500 feet, the recorded ground coverage is 17,024 feet per disc for the 32 degree field of view. Since the Nadir footprint is collected only every fourth TV frame, just 150 Nadir footprints will be collected.

4.2.1.1.3 Forward Overlap

The focal length (F) required to produce a given overlap (OL) is related by

$$F = \frac{HW(1-OL)}{V_g CI} \quad \text{mm} \tag{C-9}$$

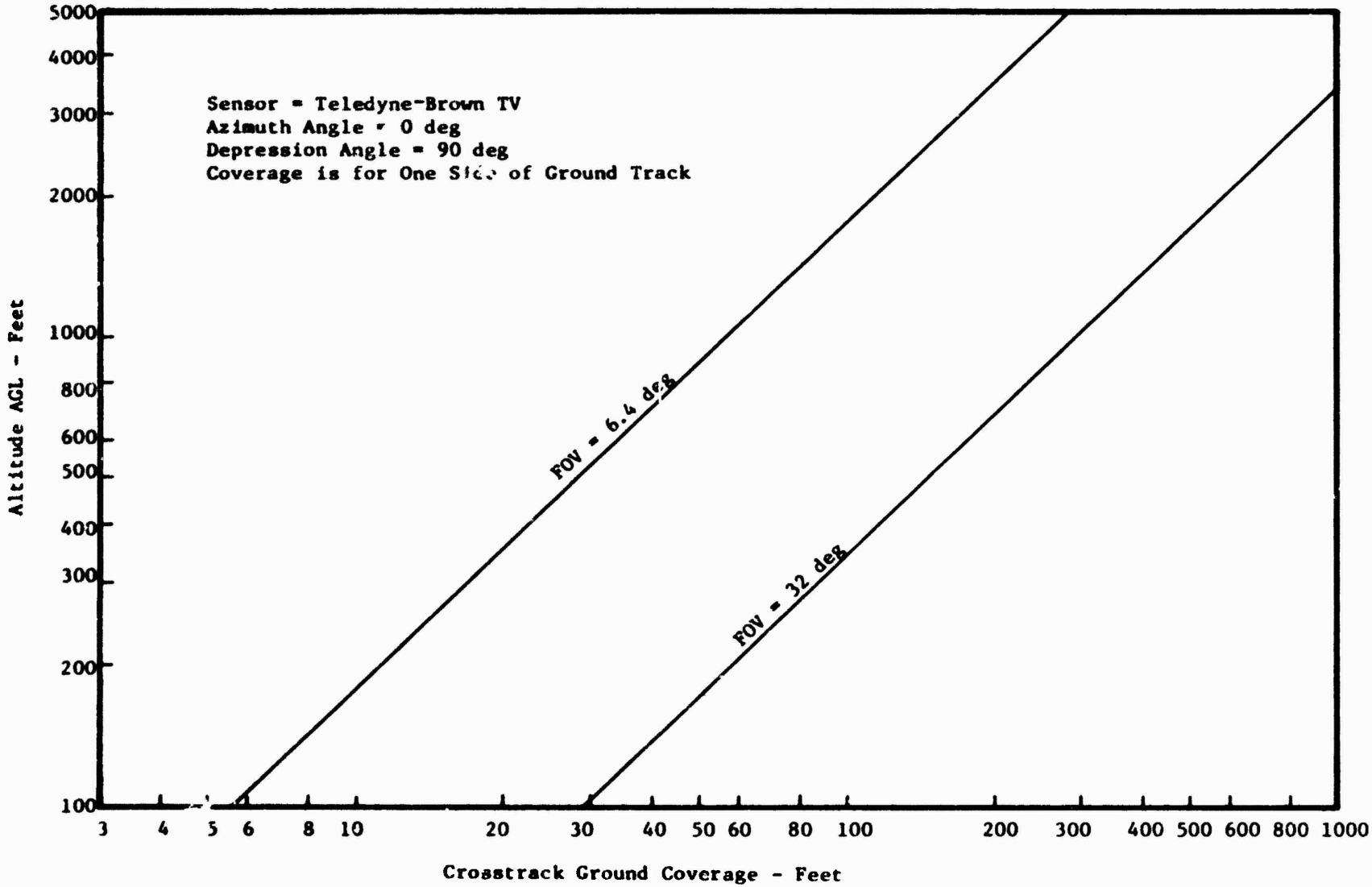

Figure C-7. Crosstrack Coverage for Teledyne-Brown TV Camera - RECON Mode (Nadir Footprint)

where

W = length of format in direction of flight (mm)

CI = cycle interval (sec)

As discussed previously, the Nadir footprint is exposed only every fourth TV camera frame. Since the cycle interval of the TV camera is 1/30 second, the cycle interval for the Nadir footprint is CI = 4/30 = 0.133 seconds. The focal length required to produce a given overlap as a function of altitude is presented in Figure C-8.

4.2.1.1.4 Scale

Scale (SC) for the nadir is defined as the ratio between the focal length (F) and the height above terrain (H)

$$SC = \frac{F}{H} \quad \text{ratio} \tag{C-10}$$

The vertical scale at an altitude of 500 feet varies from 1:1524 for the 100mm focal length to 1:7620 for the 20mm focal length. Vertical scale as a function of altitude is presented in Figure C-9. Scale to any point in the format (T) can be found by

$$SC = \frac{F}{H \cos[(\theta_h/T)^2 + (\theta_v/T)^2]^{0.5}} \quad \text{ratio} \tag{C-11}$$

4.2.1.2 Intermediate and Extreme Footprints

4.2.1.2.1 Orientation

The velocity of the scanning mirror is essentially linear and is adjusted as a function of the maximum scan angle to provide a cycle rate of 3.75 Hz. As stated previously, the 30 Hz cycle rate of the TV camera produces eight frames per mirror cycle. Thus, if we assume that the TV camera exposes a frame at nadir, the mirror cycle rate is exactly 3.75 Hz, and the maximum scan angle (each side of nadir) is 45 degrees, then one series of frames

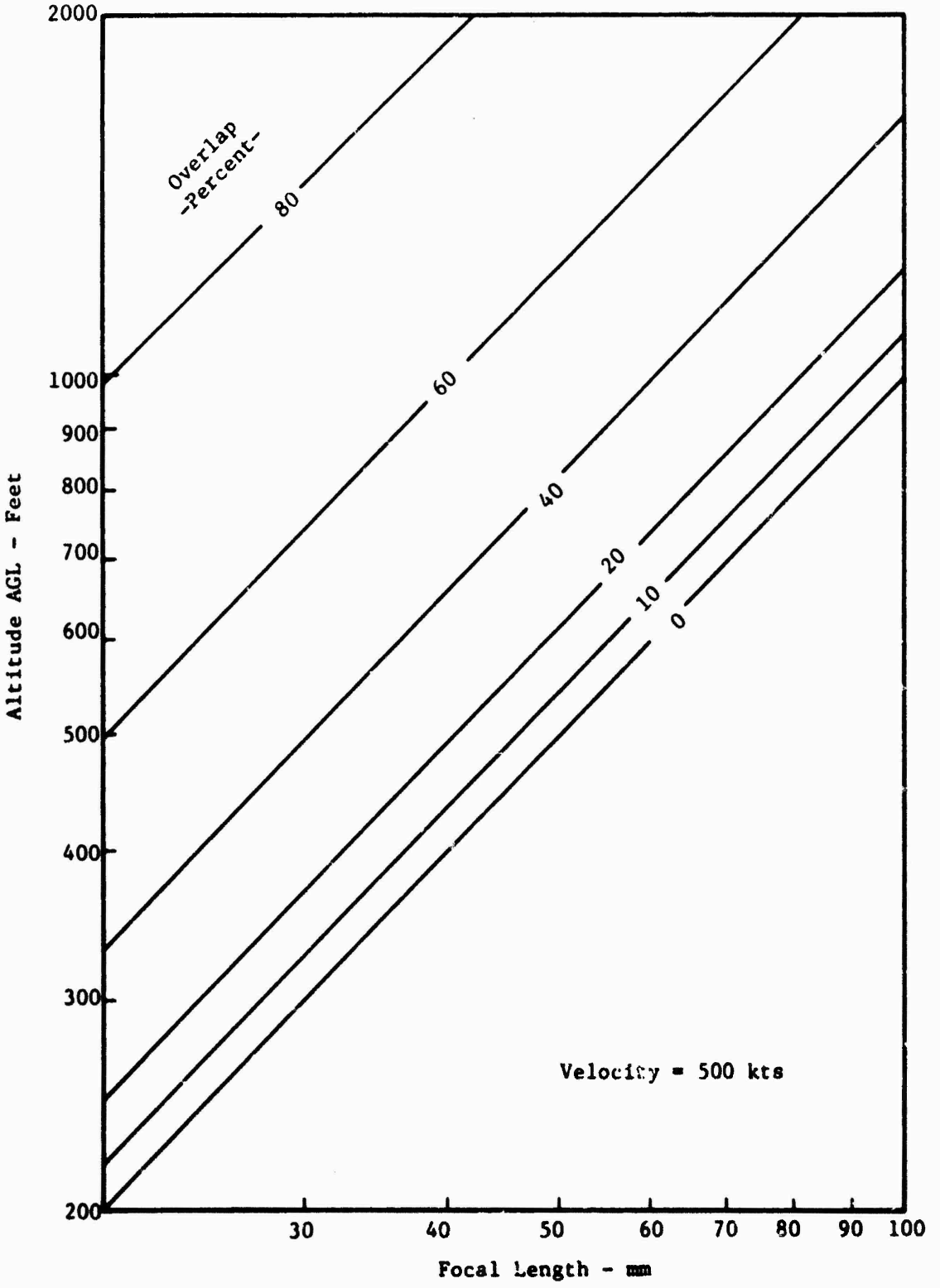

Figure C-8. Forward Overlap for Teledyne-Brown TV Camera - RECON Mode (Nadir Footprint)

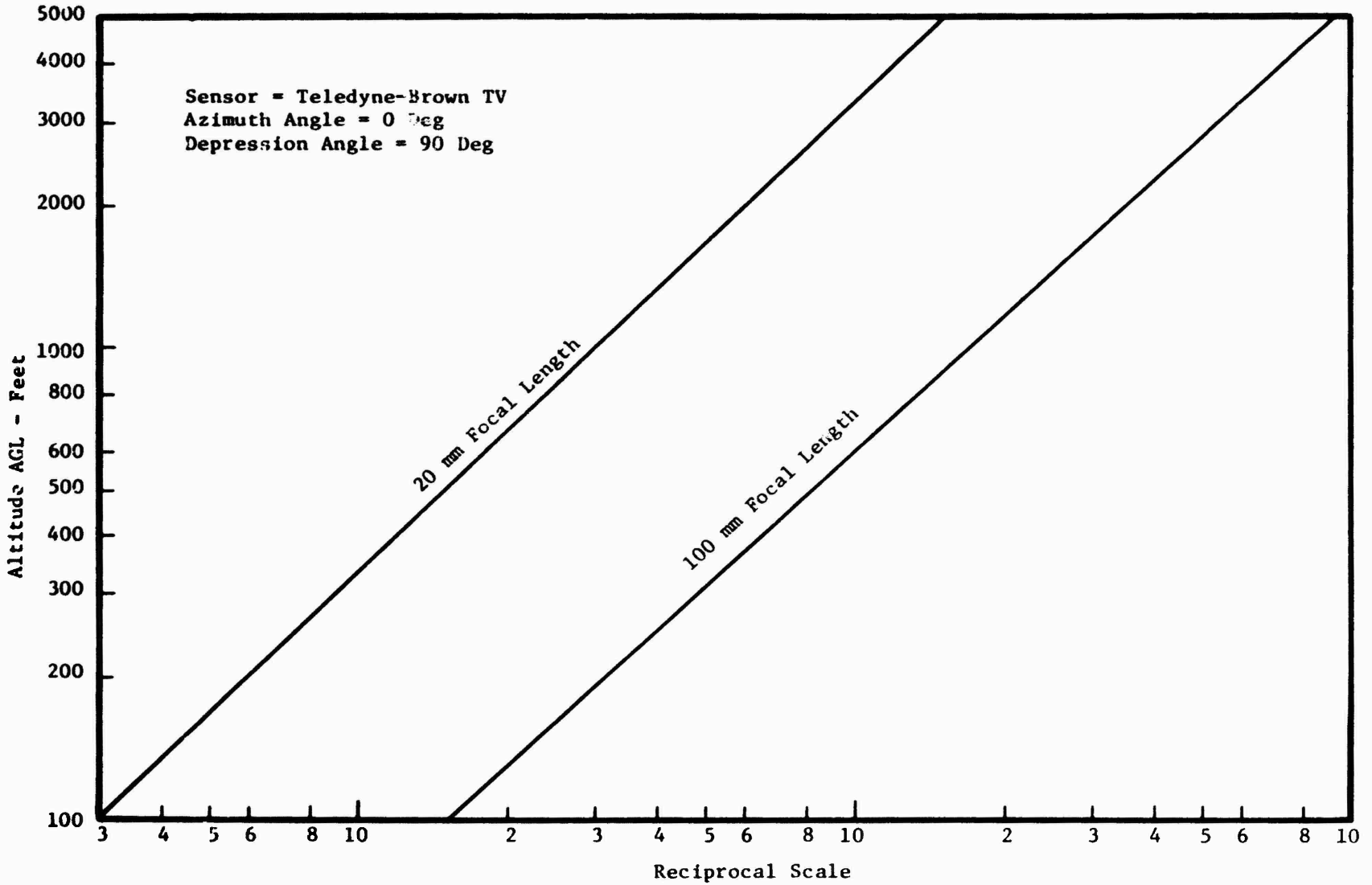

Figure C-9. Scale for Teledyne-Brown TV Camera - RECON Mode (Nadir Footprint)

will be collected at ψ_N = 0 degrees, a series will be collected at ψ_I = ±22.5 degrees, and a series will be collected at ψ_E = ±45 degrees.

The action of the scanning mirror is to rotate the footprint about the optical axis at an angle (γ) equal to the scan angle; therefore, $\gamma = \psi$. The geometrical relationships are presented in Figure C-10 and Table C-3.

4.2.1.2.2 Scale

Scale along the optical axis of the Intermediate and Extreme footprints can be found by (F sinβ)/H. Scale as a function of altitude is presented in Figure C-11 for a maximum scan angle of ψ = ±45 degrees.

4.3 Dynamic Resolution

The static TV resolution will be degraded by the optics, uncompensated image motion, and atmospheric turbulence. The modulation transfer function (MTF) is usually the analytic tool employed for specifying image quality. However, since sufficient data is not available, we will use the resolving power criteria for determining sensor performance. Angular resolving power of the TV system is defined, to a close approximation, by the sum of the individual limiting angular resolutions exhibited by all contributing elements in the system.

$$\alpha_D = [\alpha_S^2 + \alpha_O^2 + \alpha_I^2 + \alpha_T^2]^{0.5} \quad \text{radians} \qquad \text{(C-13)}$$

where

α_D = system dynamic angular resolution

α_S = static angular resolution of the TV camera

α_O = limiting angular resolution of the optics

α_I = limiting angular resolution due to image motion

α_T = limiting angular resolution due to optical atmospheric turbulence

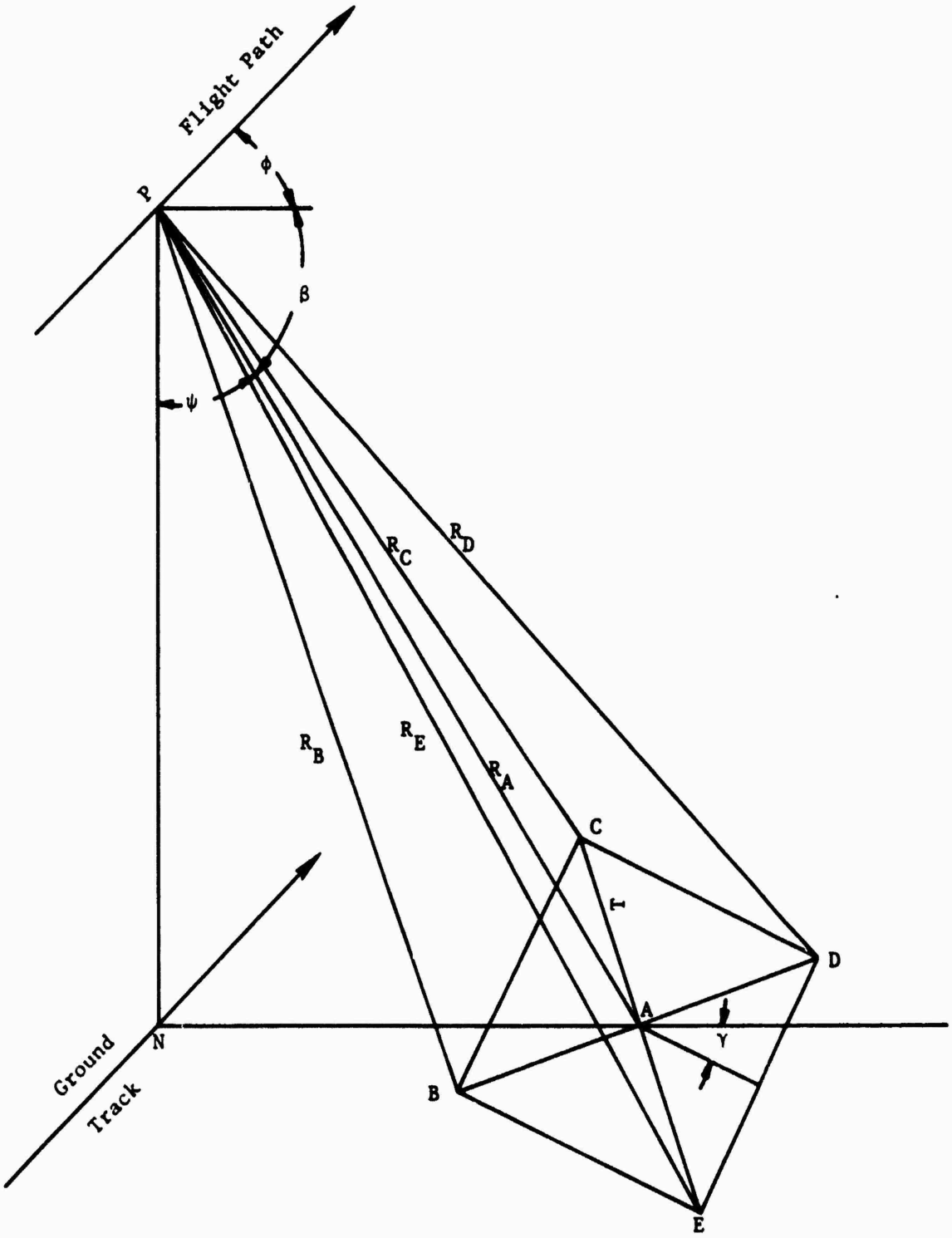

Figure C-10. Viewing Geometry for Teledyne-Brown TV Camera - RECON MODE (Intermediate and Extreme Footprints)

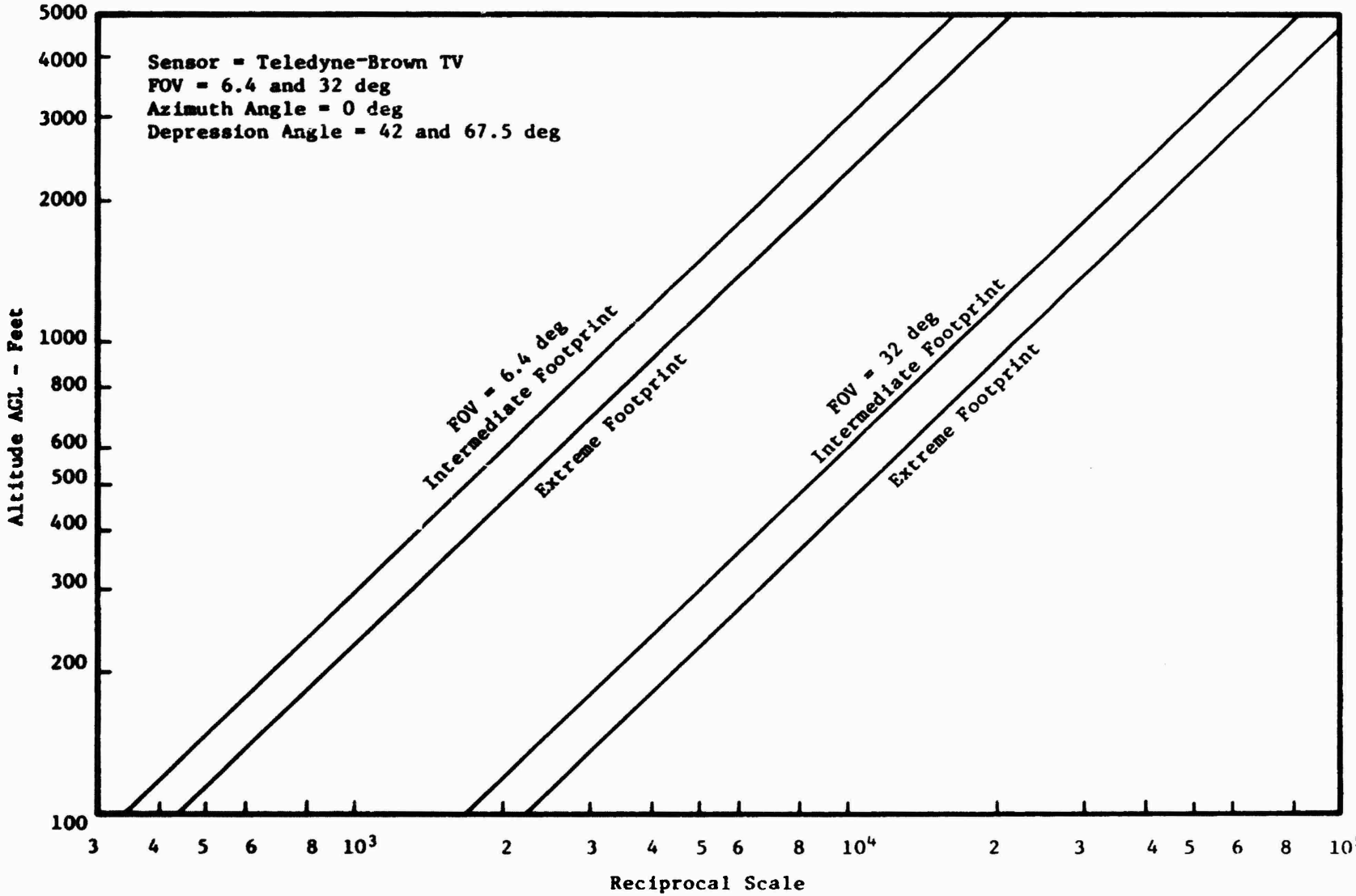

Figure C-11. Scale for Teledyne-Brown TV Camera - RECON Mode (Intermediate and Extreme Footprints)

TABLE C-3. GEOMETRICAL RELATIONSHIPS FOR TELEDYNE-BROWN TV CAMERA - RECON MODE

Slant Range (R)

$R_A = H/\sin\beta$ (optical axis)

$R_B = H/\sin[\beta-0.71\theta\cos(225-\gamma)]$

$R_C = H/\sin[\beta+0.71\theta\cos(315-\gamma)]$

$R_D = H/\sin[\beta-0.71\theta\cos(45-\gamma)]$

$R_E = H/\sin[\beta+0.71\theta\cos(135-\gamma)]$

H = altitude
ψ = scan angle
β = depression angle
γ = rotation angle
$\theta_h = \theta_v = \theta$ = horizontal and vertical sensor FOV

X, Y Coordinates

Point A $X = H/\tan\beta$

$Y = 0$

Point B $X = H/\tan[\beta-0.71\theta\cos(225-\gamma)]$

$$Y = \frac{H\tan[0.71\theta\cos(225+\gamma)]}{\sin[\beta-0.71\theta\cos(225-\gamma)]}$$

Point C $X = H/\tan[\beta+0.71\theta\cos(315-\gamma)]$

$$Y = \frac{H\tan[0.71\theta\cos(315+\gamma)]}{\sin[\beta+0.71\theta\cos(315-\gamma)]}$$

Point D $X = H/\tan[\beta-0.71\theta\cos(45-\gamma)]$

$$Y = \frac{H\tan[0.71\theta\cos(45+\gamma)]}{\sin[\beta-0.71\theta\cos(45-\gamma)]}$$

Point E $X = H/\tan[\beta+0.71\theta\cos(135-\gamma)]$

$$Y = \frac{H\tan[0.71\theta\cos(135+\gamma)]}{\sin[\beta+0.71\theta\cos(135-\gamma)]}$$

4.3.1 Television Camera

4.3.1.1 Vertical Resolution

The limiting resolution of the television camera is defined primarily by the 525 line raster, rather than by the performance of the silicon intensified target (SIT) vidicon. A 525 line raster contains just 487 active lines. This value must be multiplied by the Kell factor to determine the number of vertical resolution elements N_t = 487 (0.707) = 344 vertical TV lines. This value can be achieved only for high contrast targets.

The angular resolution (α_S) can be found by

$$\alpha_S = \frac{\theta_v}{N_t} \quad \text{radians} \tag{C-14}$$

The vertical field of view (θ_v) can be preflight selected between 6.4 and 32 degrees. For θ_v =6.4 degrees, α_S = 0.32 mrad; for θ_v = 32 degrees, α_S = 1.62 mrad.

4.3.1.2 Horizontal Resolution

Horizontal resolution is defined by the bandwidth of the video amplifier. The bandwidth (BW) required to produce a given horizontal resolution (N_h) at the optimum signal-to-noise ratio is given by

$$BW = N_h \cdot f \cdot L \cdot A \cdot K \cdot \frac{1 - B_v}{1 - B_h} \quad \text{Hz} \tag{C-15}$$

where

N_h = horizontal resolution (defined in terms of TV lines/picture height)

f = frame rate (frame/second = 30)

L = line number (scan lines/frame = 525)

A = aspect ratio (width/height = 1)

k = constant (one cycle represents two picture elements = 0.5)

B_v = vertical blanking (ratio = 0.078)

B_h = horizontal blanking (ratio = 0.173)

The bandwidth that will yield a horizontal resolution equal to the vertical resolution is 4.6 MHz (N_h = 525 in the equation).

4.3.2 Optics

The diffraction limit, expressed in terms of angular resolution, is found by

$$\alpha_0 = \frac{1.22\lambda}{D} \quad \text{radians} \tag{C-16}$$

where

λ = wavelength of white light (5.6×10^{-4} mm)

D = diameter of optics (mm)

The effective diameter of the optics is 35.7 mm (for F = 100mm) so that α_0 = 19 μrad.

The angular resolution associated with a 525 line television system does not warrant the expense of zoom optics which operate at the diffraction limit. Consequently, we will assume that the actual optics employed exhibit a limiting angular resolution of α_0 = 19/0.9 = 21 μrad. This corresponds to 238 ℓp/mm.

4.3.3 Image Motion

Relative motion between the image and object during the exposure interval degrades the system resolution. Relative motion normally occurs primarily because of forward motion of the air vehicle, and attitude (roll, pitch and heading) changes of the RPV. However, in this application the RECON Mode employs a scanning mirror which also produces an image motion component. The limiting angular resolution due to uncompensated image motion is expressed by

$$\alpha_I = [\alpha_F^2 + \alpha_A^2 + \alpha_M^2]^{0.5} \quad \text{radians} \tag{C-17}$$

where

α_F = limiting angular resolution due to forward motion of the air vehicle

α_A = limiting angular resolution due to changes in RPV attitude

α_M = limiting angular resolution due to the angular velocity of the scanning mirror

4.3.3.1 Forward Motion

The angular velocity (Ω) due to forward motion of the RPV can be defined by

$$\Omega = \frac{V_g \sin\beta}{H} \quad \text{rad/sec} \qquad \text{(C-17)}$$

where

V_g = ground velocity of RPV (ft/sec)

H = altitude AGL (feet)

β = depression angle (degrees)

4.3.3.1.1 NAV Mode

If we assume a depression angle of β = 4 degrees, a ground velocity of V_g = 500 knots, and an altitude of H = 500 feet, then Ω = 0.118 radians per second.

Limiting angular resolution as a function of image motion compensation error is found by

$$\alpha_{FD} = T\Omega E_f \quad \text{radians} \qquad \text{(C-18)}$$

where

T = exposure interval (seconds)

E_f = IMC error (ratio)

Since no image motion techniques are employed, E_f is unity. An automatic light control (ALC) device is used to adjust the exposure interval between the limits of 100 < T < 3300 μsec, depending upon the ambient illumination. According to the supplier, the minimum exposure interval of 100 μsec is not exceeded unless the ambient illumination falls below 50 fc. This corresponds to the illumination level available at Civil Twilight. We will assume that the operational day is further extended so that the exposure interval has increased to 1,000 μsec. Based upon these exposure values, the limiting angular resolution due to forward motion of the RPV for the NAV mode can be found (Eq. (C-18)) to be 11.8 μrad for T = 100 μsec and 118 μrad for T = 1,000 microseconds.

4.3.3.1.2 RECON Mode

The angular velocity resulting from the forward motion of the RPV can be found for the optical axis of the three RECON Mode footprints by use of Eq. (C-17).

Nadir (ω_N) = 1.69 rad/sec

Intermediate (Ω_I) = 1.56 rad/sec

Extreme (Ω_E) = 1.19 rad/sec

The corresponding limiting angular resolutions due to forward image motion can be calculated by means of Equation (C-18).

	T = 100 μsec	T = 1,000 μsec
Nadir (α_{FN})	0.169	1.69
Intermediate (α_{FI})	0.143	1.43
Extreme (α_{FE})	0.119	1.19

All values are in milliradians.

4.3.3.2 Mirror Velocity

The mirror angular velocity ($\dot{\psi}_m$) is adjusted prior to flight so that a constant cycle rate (CR) of 3.75 Hz is achieved for the selected maximum scan angle (ψ_E).

$$\dot{\psi}_m = 4\psi_E CR \quad \text{deg/sec} \qquad \text{(C-19)}$$

$$= 15\psi_E$$

where

ψ_E = maximum scan angle from vertical (deg)
CR = cycle rate of mirror (3.75 Hz)

By use of this equation, we can find the velocity of the Intermediate and Nadir footprints to be 675 deg/sec = 11.78 rad/sec. The velocity of the mirror at the time of exposure of the Extreme footprint is assumed to be zero; however, there is some mirror movement during the 30-40 msec turnaround time. When the shutter speeds are taken into account, the limiting angular resolutions due to the mirror angular velocity are

	T = 100 μsec	T = 1,000 μsec
Nadir (ι_{MN})	1.18	11.8
Intermediate (ι_{MI})	1.18	11.8
Extreme (ι_{ME})	0	0

All values are in milliradians.

4.3.3.3 Vehicle Perturbations

Angular rotations of the TV camera's optical axis due to perturbations of RPV attitude can seriously degrade the dynamic resolution of the TV system. These deviations can occur both because of the effects of atmospheric turbulence and because of deliberate changes in RPV attitude directed by the ARCO. Although stabilized mounts can be employed to minimize the effects of these angular motions, the Teledyne-Brown TV camera is not so equipped. Since no data concerning RPV dynamics is currently available, the effects of vehicle induced angular velocities were assumed to be zero for this analysis ($\iota_A = 0$).

4.3.3.4 Resolution Due to All Angular Motion

By use of Eq. (C-17), the angular resolution (α_I) resulting from the effects of forward motion and scanning mirror velocity can be calculated to be

Footprint	T = 100 μsec	T = 1,000 μsec
Forward	0.012	0.12
Nadir	1.19	11.9
Intermediate	1.19	11.9
Extreme	0.12	1.19

4.3.4 Optical Atmospheric Turbulence

The heterogeneous nature of the atmosphere alters the shape of an optical wavefront in a random manner. The results of investigations to measure the effects of atmospheric turbulence upon angular resolution vary considerably. A study and analysis of existing data by SRL for a recent Air Force program indicated that use of a nominal value of 9 μrad and worst case of 12 μrad would be realistic. These values are insignificant with respect to the angular resolution achievable by use of an unstabilized 525 line television system equipped with relatively short focal length optics, and, therefore, does not limit any of the sensors evaluated herein.

4.3.5 System Angular Resolution

The limiting dynamic angular resolution (α_D) for the maximum and minimum fields of view, and for exposure times of 100 and 1,000 μsec, was calculated by use of Eq. (C-13) and listed in Table C-4.

4.3.6 Remarks

Examination of the data presented in Table C-4 indicates that the angular resolution associated with the Forward footprint indicates that the angular resolution associated with the Forward footprint varies proportional to the field of view, almost independent of the exposure interval. Thus,

TABLE C-4. L'MITING DYNAMIC RESOLUTION

Footprint	T = 100 μsec	T = 1,000 μsec
FOV = 6.4 deg		
Forward	0.32	0.34
Nadir	1.23	11.9
Intermediate	1.23	11.9
Extreme	0.34	1.27
FOV = 32 deg		
Forward	1.62	1.62
Nadir	2.01	12.0
Intermediate	2.01	12.0
Extreme	1.62	2.01

All values are in milliradians.

performance is not significantly affected by the angular velocity produced by the forward motion of the vehicle. It should be restated that other vehicle perturbations were not considered during this analysis.

It can be seen from Table C-4 that exposure time is not a significant factor for the Extreme footprint when the widest field of view is selected. However, its effect becomes more pronounced as the field of view is decreased. This is the result of uncompensated image motion due to the forward velocity of the vehicle.

Again, with reference to Table C-4, note that the angular resolution of the Nadir and Intermediate footprints is dominated by exposure, although the field of view does have some effect. This is a direct result of the high angular velocities imparted by the scanning mirror during the time that the Nadir and Intermediate TV frames are exposed.

When the static angular resolution is compared to the dynamic angular resolution, it can be noted that the mirror angular velocity degrades the narrow FOV angular resolution by almost a factor of four even at the highest available shutter speed. At an exposure interval of 1,000 μsec, the static angular resolution is debased by a factor of 37 in the Nadir and Intermediate footprints. The static angular resolution exhibited by the 32 degree FOV is not significantly reduced by the scanning mirror at the highest shutter speed, but the angular resolution deteriorates by a factor of 7.4 at an exposure of 1,000 μsec.

4.4 Ground Spot Size

Ground spot size as a function of altitude, based upon the angular resolution depicted in Table C-4, is presented in Figures C-12a, C-12b, C-13a, and C-13b. The values shown are normal to the optical axes of the designated footprints.

Consider now the ground spot size requirements derived in Section 2 (Table 3 and Figure C-5) for the tasks of recognition and identification of typical tactical targets. It was found that most targets require a ground spot size of from 0.75 to 3 feet for recognition (NAV Mode), and from 0.2 to 1 foot for identification (RECON Mode).

4.4.1 NAV Mode/Targets of Opportunity

With reference to Figures C-12a, C-12b, C-13a, and C-13b, note that for a typical altitude of 500 feet AGL, the ground spot size provided by the forward footprint varies from about 2.5 feet for the smallest FOV to about 12 feet for the largest field of view. This is acceptable for navigation and affords some capability for acquiring targets of opportunity. The operator's ability to recognize vehicular sized tactical targets would be possible only by use of the smallest field of view. However, the extremely small crosstrack coverage associated with the 6.4 degree FOV would dictate the use of a very accurate navigation system to assure that the prebriefed target would appear within the field of view. Target acquisition would likely be difficult anyhow because insufficient cues would be available in the ground coverage for proper operator orientation.

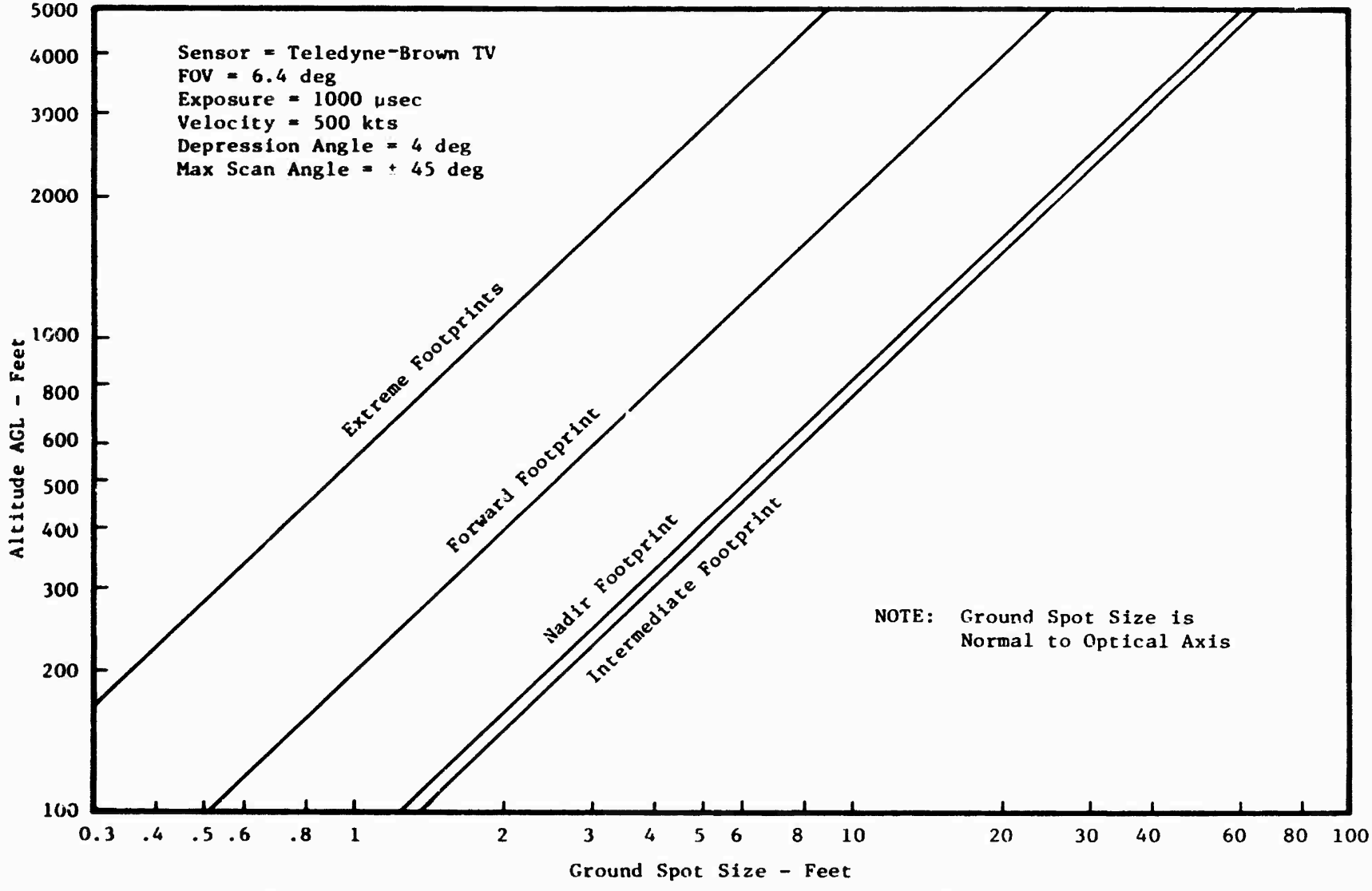

Figure C-12a. Ground Spot Size for Teledyne-Brown TV Camera (FOV = 6.4 deg, T = 1000 µsec)

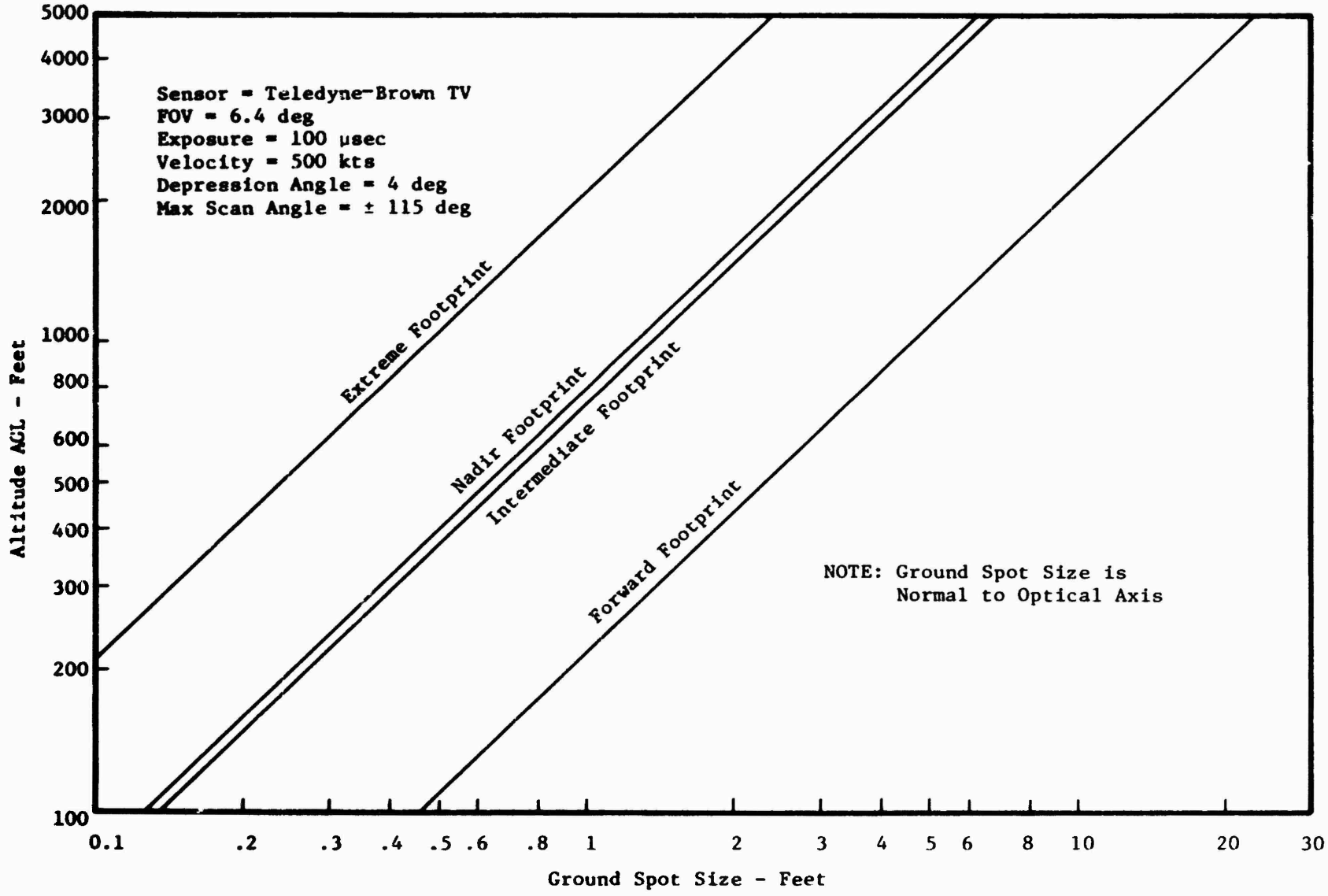

Figure C-12b. Ground Spot Size for Teledyne-Brown TV Camera (FOV = 6.4 deg, T = 100 µsec)

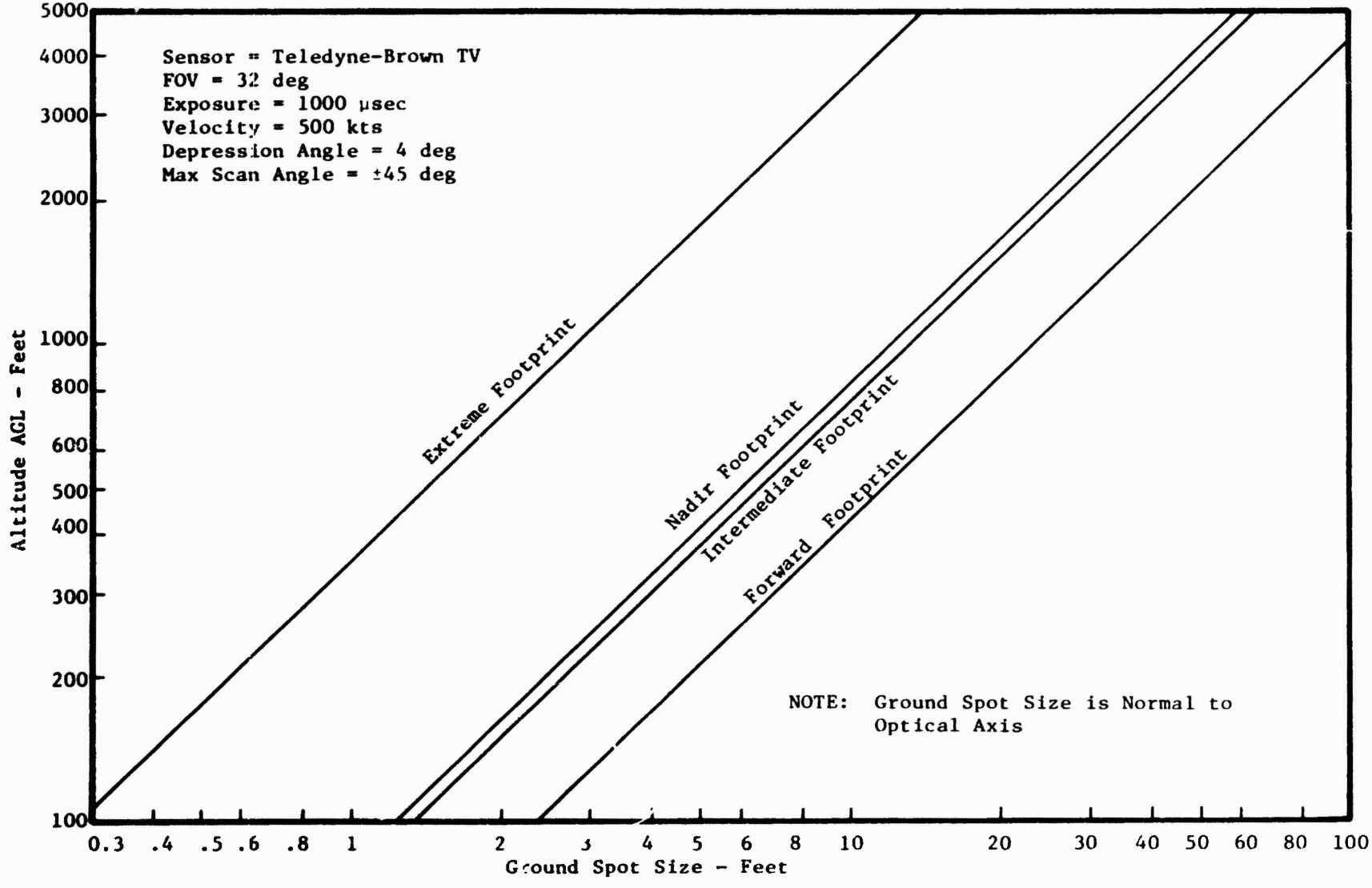

Figure C-13a. Ground Spot Size for Teledyne-Brown TV Camera (FOV = 32 deg, T = 1000 µsec)

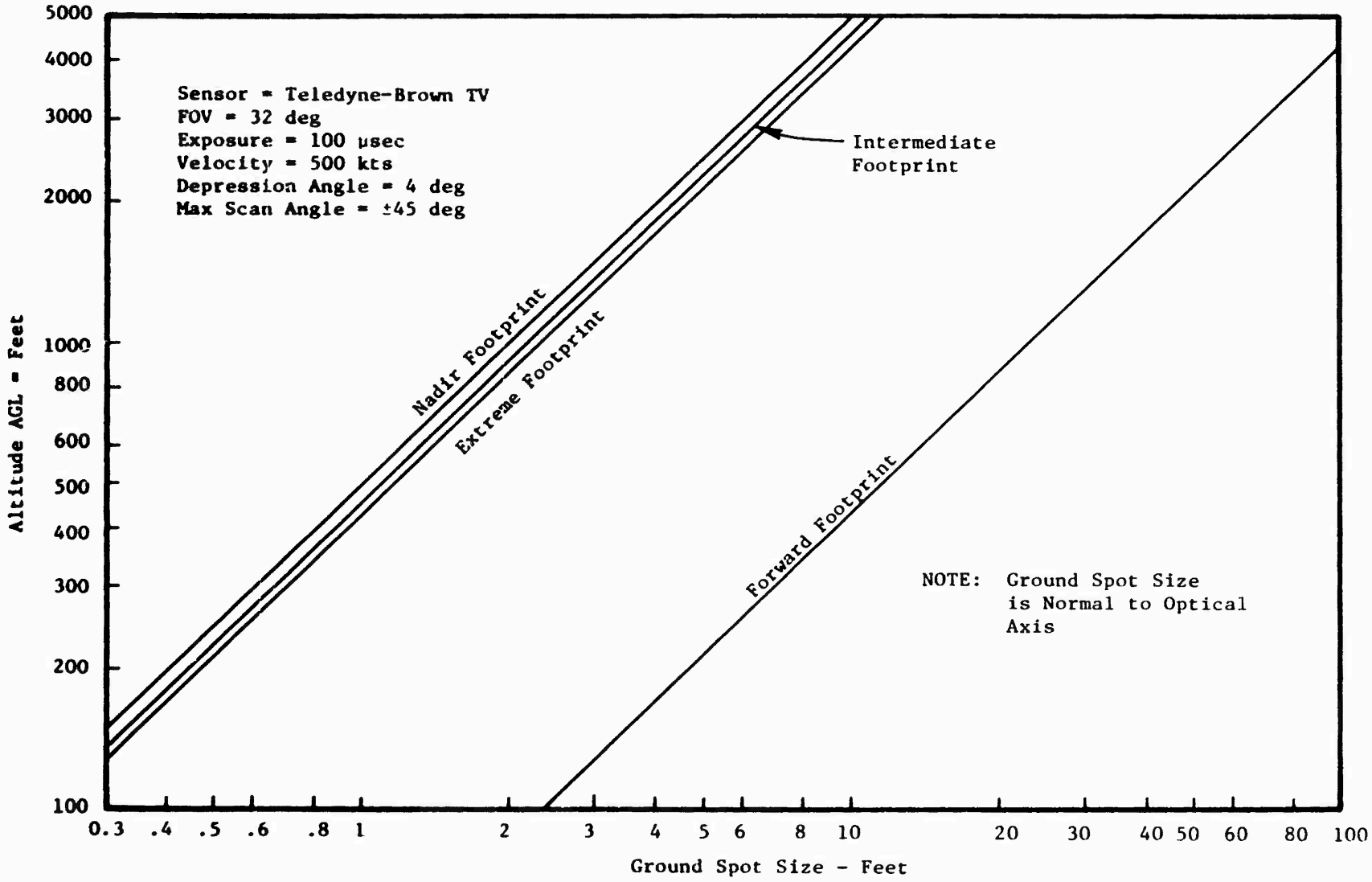

Figure C-13b. Ground Spot Size for Teledyne-Brown TV Camera (FOV = 32 deg, T = 100 µsec)

One possible solution for achieving the desired performance would be to increase the depression angle and select a compromise field of view. Ground spot size shown in the figures is based on a depression angle of 4 degrees. If a depression angle of -10 degrees could be physically realized, the slant range of the optical axes would be reduced to 0.4 of the 4 degree slant range. If the field of view is reduced to 16 degrees, the angular resolution would be improved to 0.5 of the values found for the 32 degree field of view. As a consequence, the 12 foot ground spot size shown in Figures C-13a and C-13b for an FOV of 32 degrees would be reduced to about 2.4 feet.

While the above stated FOV and depression angle would yield the required ground spot size with marginal crosstrack coverage, it might not be too desirable from an operational standpoint. This is a result of the fact that the horizon would no longer be within the field of view during level flight.

4.4.2 RECON Mode

Figures C-12a, C-12b, C-13a, and C-13b indicate that, for a typical operational altitude of 500 feet, only the Extreme footprint can provide the ground spot size specified in Sec 2 (this report) for identifying and evaluating most tactical targets. The figures show that Extreme footprint produces a satisfactory spot size only at faster shutter speeds and/or smaller fields of view. The Nadir and Intermediate footprint ground spot sizes are unsatisfactory even for the fastest shutter speeds. It is obvious that employing a higher line rate (such as 875) to improve ground spot size would not be beneficial as long as the scanning mirror concept was retained. It should be noted that this sensor was actually used successfully in Southeast Asia. Target type, RPV profile, and operator experience all combine with ground spot size in determining reconnaissance effectiveness.

4.5 Eye/Display Relationships

Investigators have found that, within limits, there is a relationship between the ability of the interpreter to identify targets and both the number of TV raster lines across the image and the angle projected by the displayed image. It should be noted that the number of scan lines across the

target is not the same as the number of resolution elements projected across the target. The number of resolution elements is always less due to degrading effects such as the Kell factor, angular motion, and contrast attenuation by the atmosphere.

4.5.1 Size of Displayed Image

Height of the displayed image (I) can be found by

$$I = \frac{S\xi}{\theta_V} \quad \text{inches} \tag{C-21}$$

where

S = height of active area of display (inches)

ξ = angular subtense of target's height projected toward TV sensor (degrees)

θ_V = sensor vertical field of view (degrees)

but

$$\xi = 2 \tan^{-1}(T/2R)$$

$$\sim T/R \text{ ratio} \tag{C-22}$$

where

T = target vertical dimension normal to TV optical axis (feet)

R = slant range of optical axis (feet)

so that

$$I = \frac{ST}{R\theta_V} \quad \text{inches} \tag{C-23}$$

Height of the target's displayed image as a function of altitude is presented in Figures C-14a and C-14b for the minimum and maximum fields of view of 6.4 and 34 degrees. A display height of S = 12 inches, and a target projected vertical dimension of T = 30 feet were assumed.

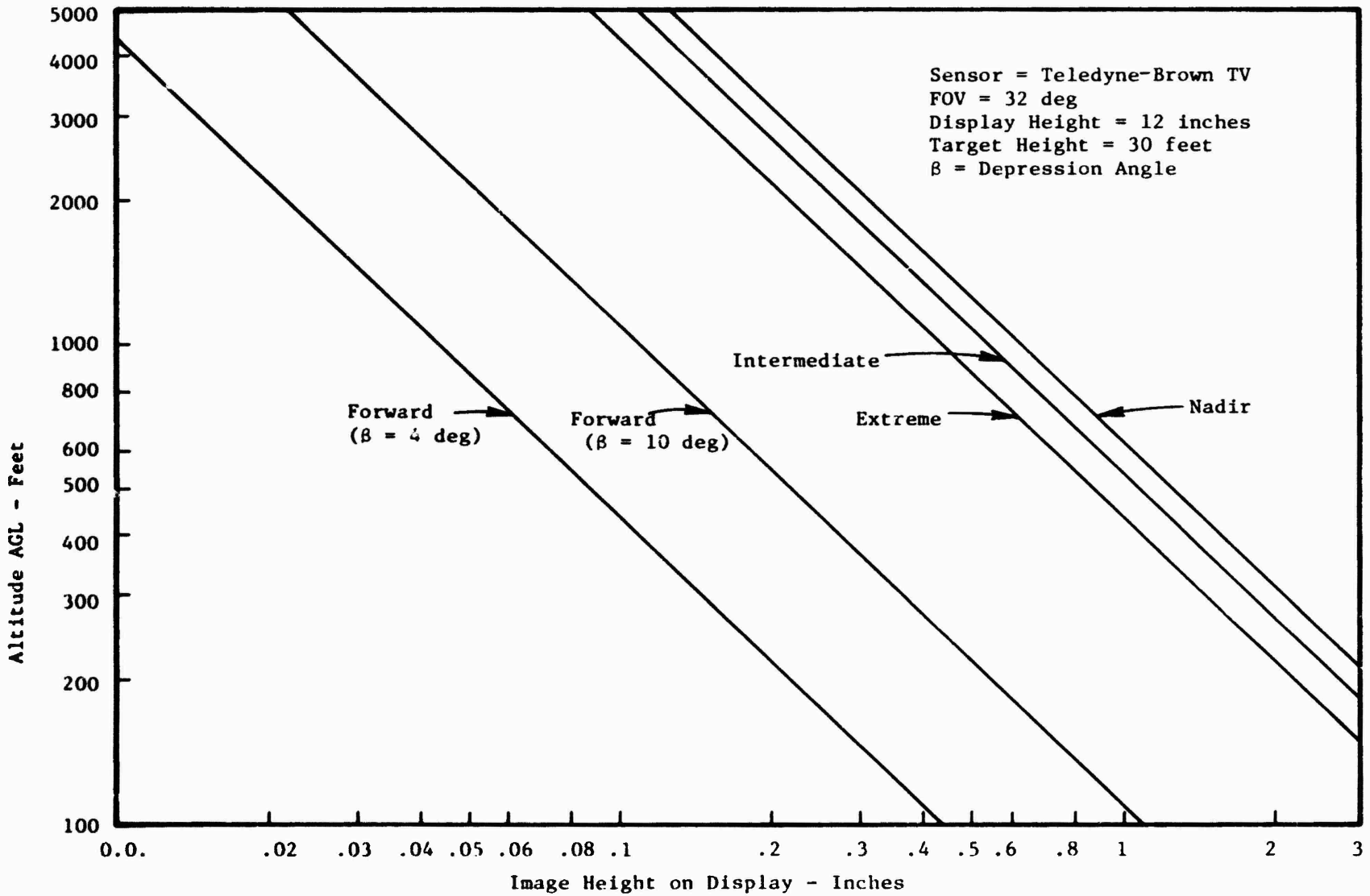

Figure C-14a. Image Height on Display for Teledyne-Brown TV Camera (FOV = 32 deg)

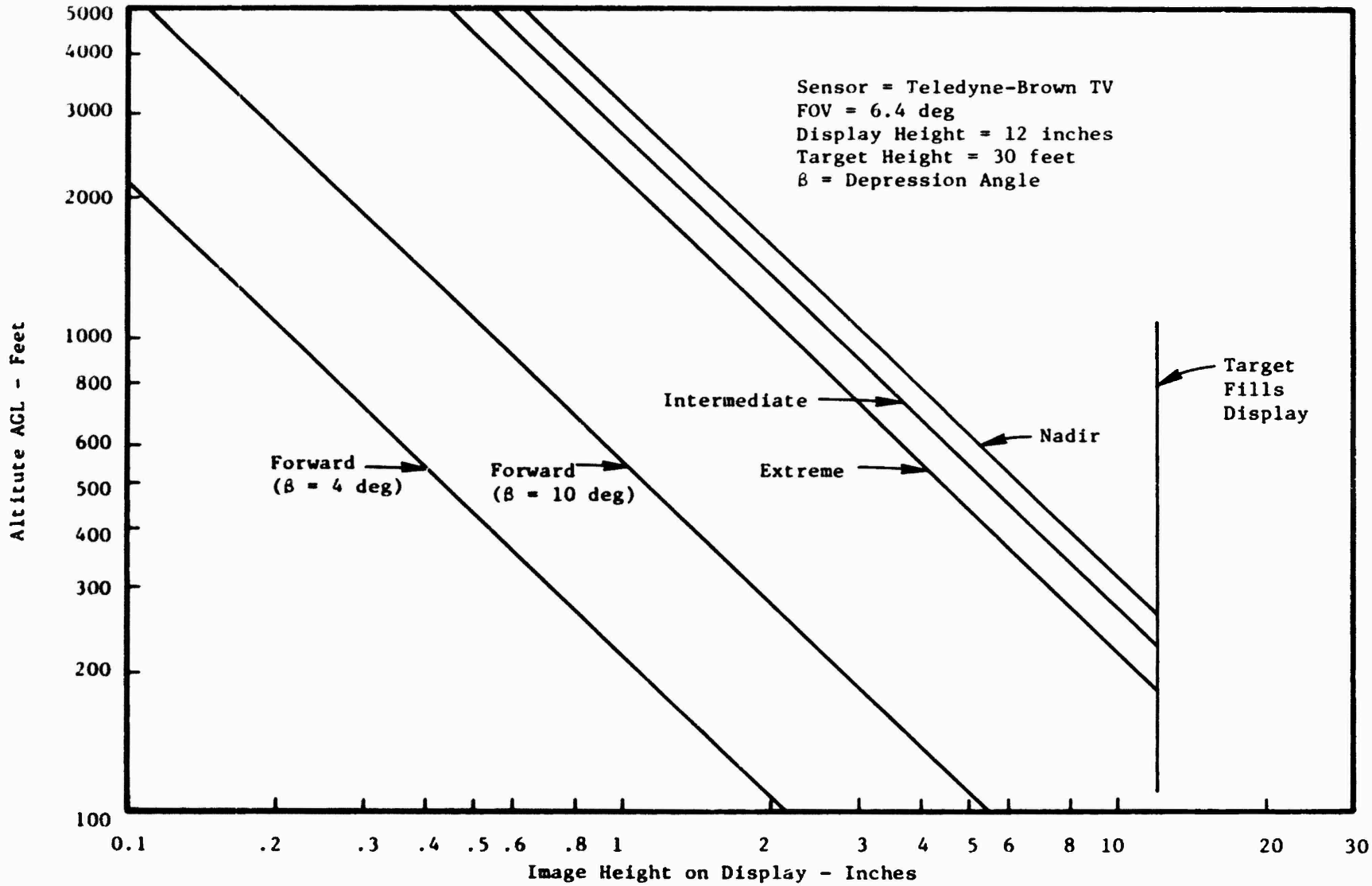

Figure C-14b. Image Height on Display for Teledyne-Brown TV Camera (FOV = 6.4 deg)

4.5.2 Raster Lines Across Image

Section 2 of this report shows that the image interpreter's performance is related to the number of raster (scan) lines across the image. The number of scan lines across the image (N_I) can be found by

$$N_I = \frac{TL_A}{R\theta_V} = \frac{IL_A}{S} \qquad \text{(C-24)}$$

where L_A = number of active scan lines in raster.

For a 525 line raster, L_A = 487. As stated previously, the display height (S) was assumed to be 12 inches.

The number of raster lines across the displayed image as a function of altitude is shown in Figures C-15a and C-15b for the maximum and minimum fields of view.

4.5.3 Angle Projected by Displayed Image

The data in Sec 2 (this report) indicate that an image interpreter's ability to identify targets is a function of the angle subtended to the eye by the displayed image. The angle subtended to the eye (γ) by the image height (I) can be calculated by

$$\gamma = 2 \tan^{-1} \left(\frac{ST}{2RY\theta_V}\right) \sim \frac{ST}{RY\theta_V} \qquad \text{(C-25)}$$

or

$$\gamma \sim \frac{I}{Y}$$

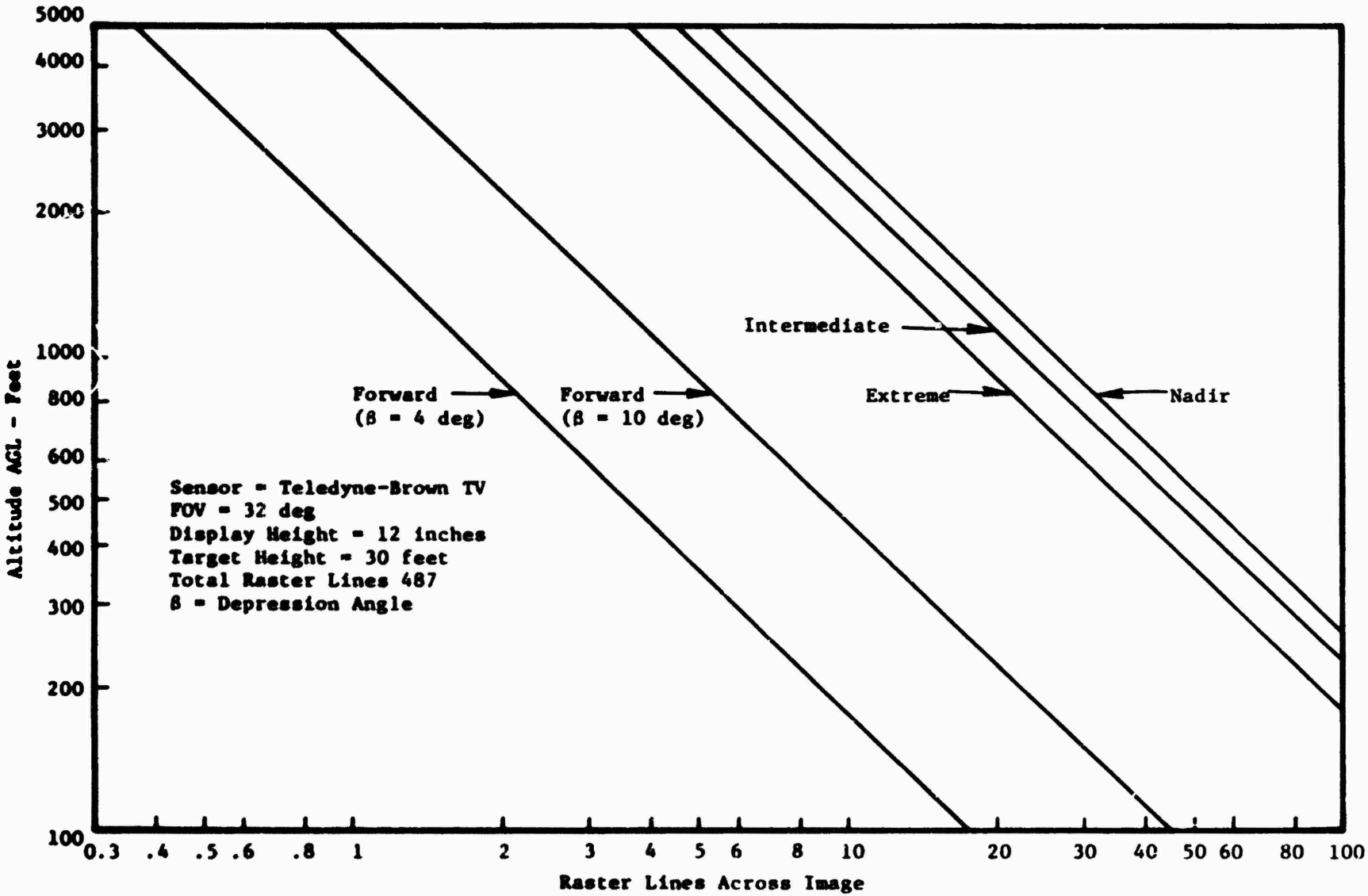

Figure C-15a. Number of Raster Lines Across Image for Teledyne-Brown TV Camera (FOV = 32 deg)

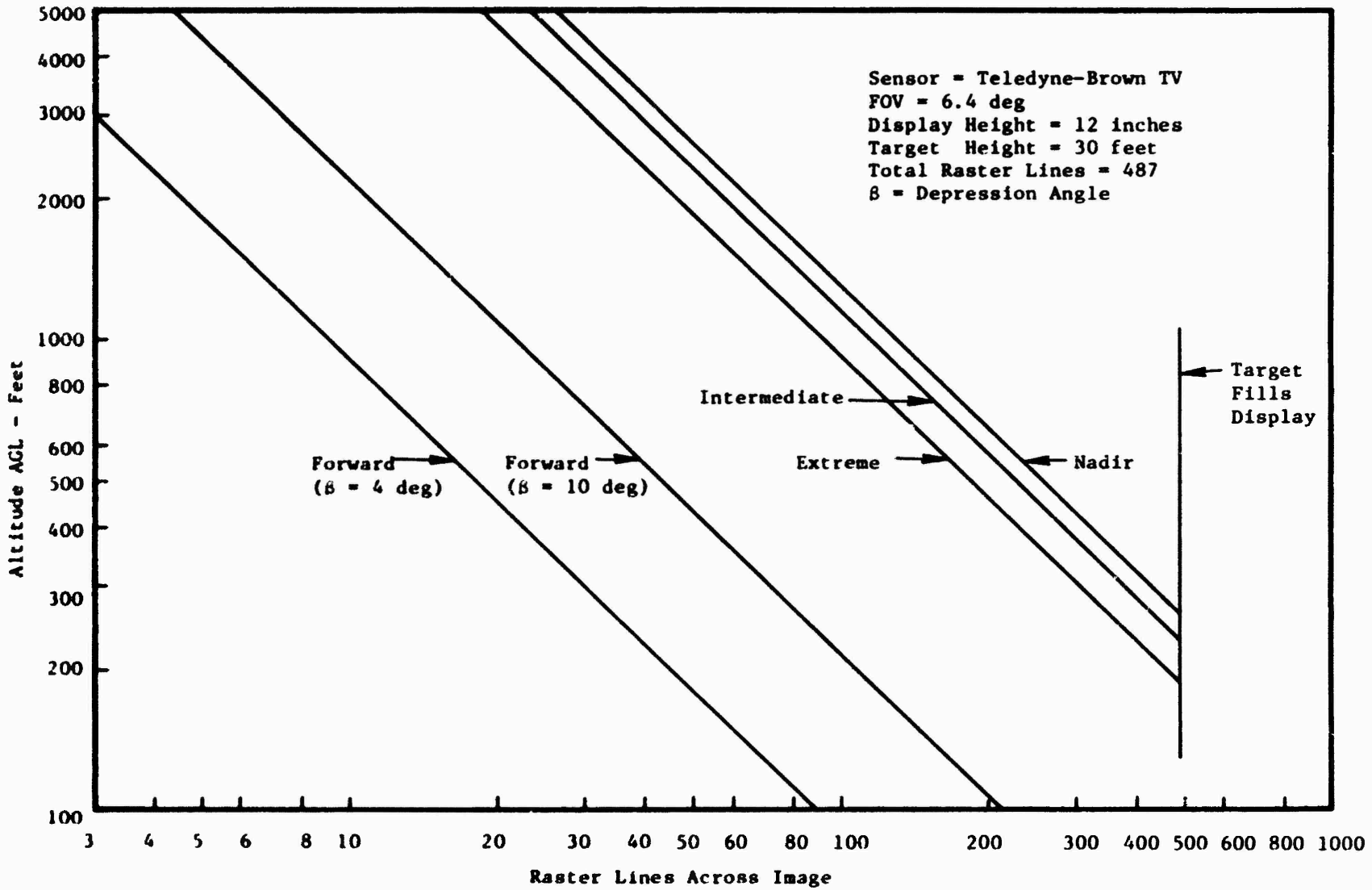

Figure C-15b. Number of Raster Lines Across Image for Teledyne-Brown TV Camera (FOV = 6.4 deg)

where

I = height of displayed image of target (inches)

Y = eye-to-display distance (inches)

The angle projected to the eye by the displayed image as a function of altitude is presented in Figures C-16a and C-16b for the maximum and minimum fields of view. The angles indicated are for an assumed eye/display distance of 28 inches, and the same image height values previously calculated. The data correspond to targets located at the optical axes of the four footprints.

4.6 Optical Defocusing

The optics can defocus in flight due to thermal gradients which cause a shift in the effective focal length. The optics will also be defocused when the altitude actually flown is different from the specific altitude for which the optics have been focused. We will consider only the effects of defocusing due to RPV flight trajectories at altitudes other than planned.

Figure C-17a shows the geometrical relationships that result when the flight altitude is below the predesignated altitude, and Figure C-17b describes the condition where the actual flight altitude is above the preset altitude of best focus. Note that the more general term of slant range is used rather than altitude since this value is required by all footprints other than the Nadir footprint.

The diameter of the blur circle (d_a) due to altitude defocusing can be found by

$$d_a = \frac{A(V-V_o)}{V_o} \quad \text{mm} \qquad \text{(C-27)}$$

where

A = lens aperture (mm)

V = lens to plane of best focus distance for actual range R (mm)

V_o = lens to focal plane distance for preset range R_o (mm)

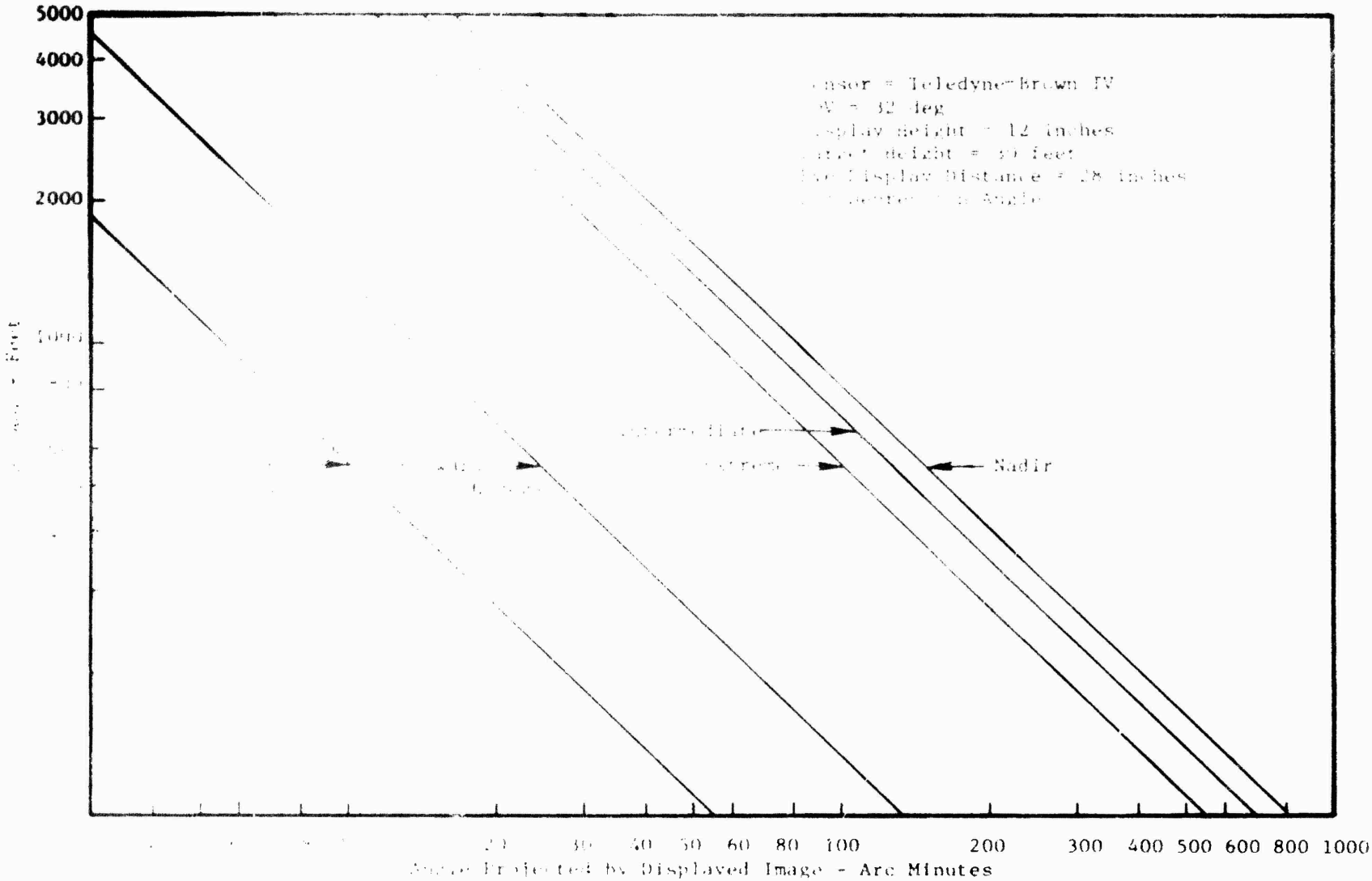

Angle Projected by Displayed Image - Arc Minutes

Angle Projected by Image for Teledyne-Brown TV Camera (FOV = 32 deg)

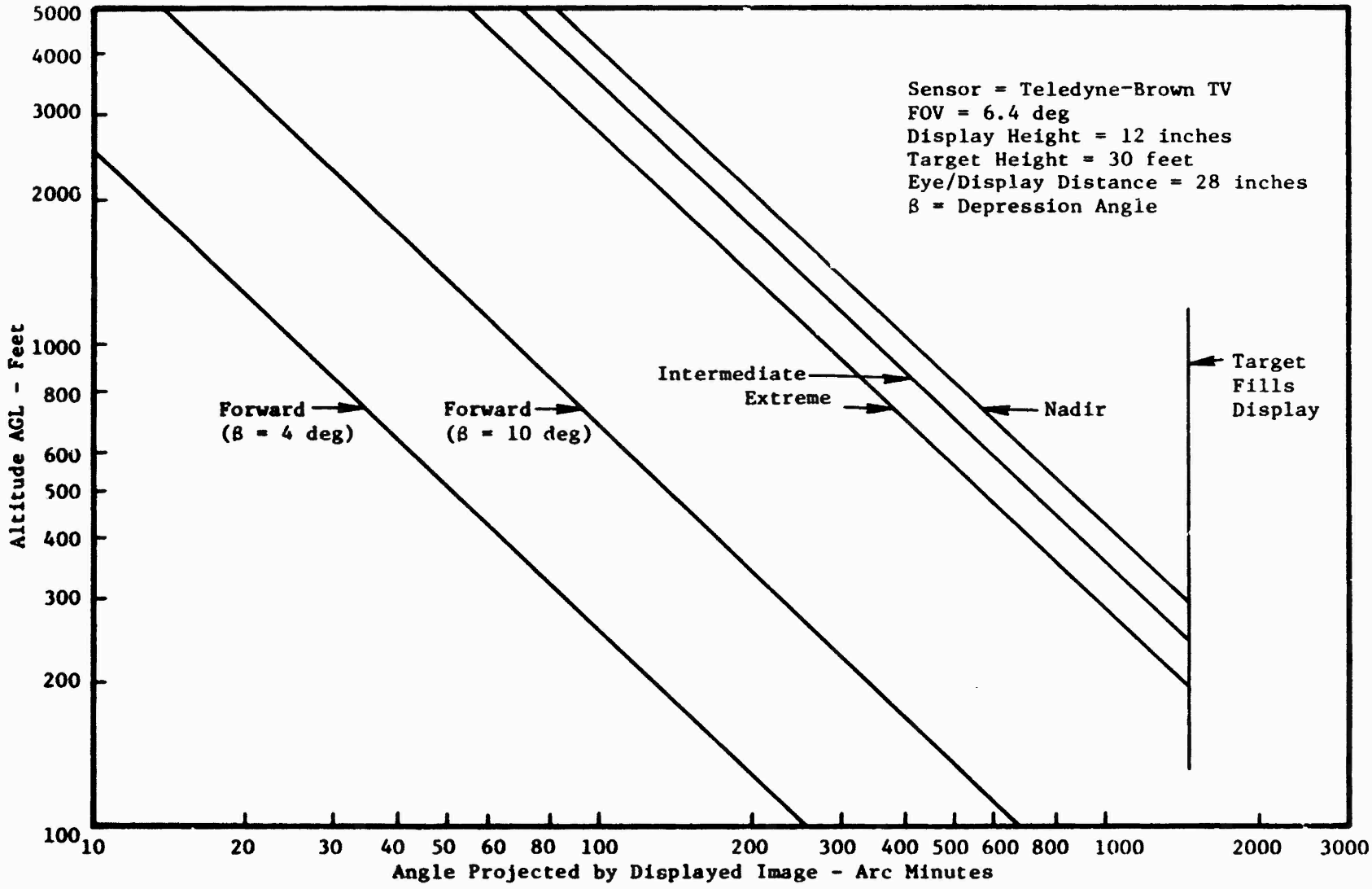

Figure C-16b. Angle Projected to Eye by Image for Teledyne-Brown TV Camera (FOV = 6.4 deg)

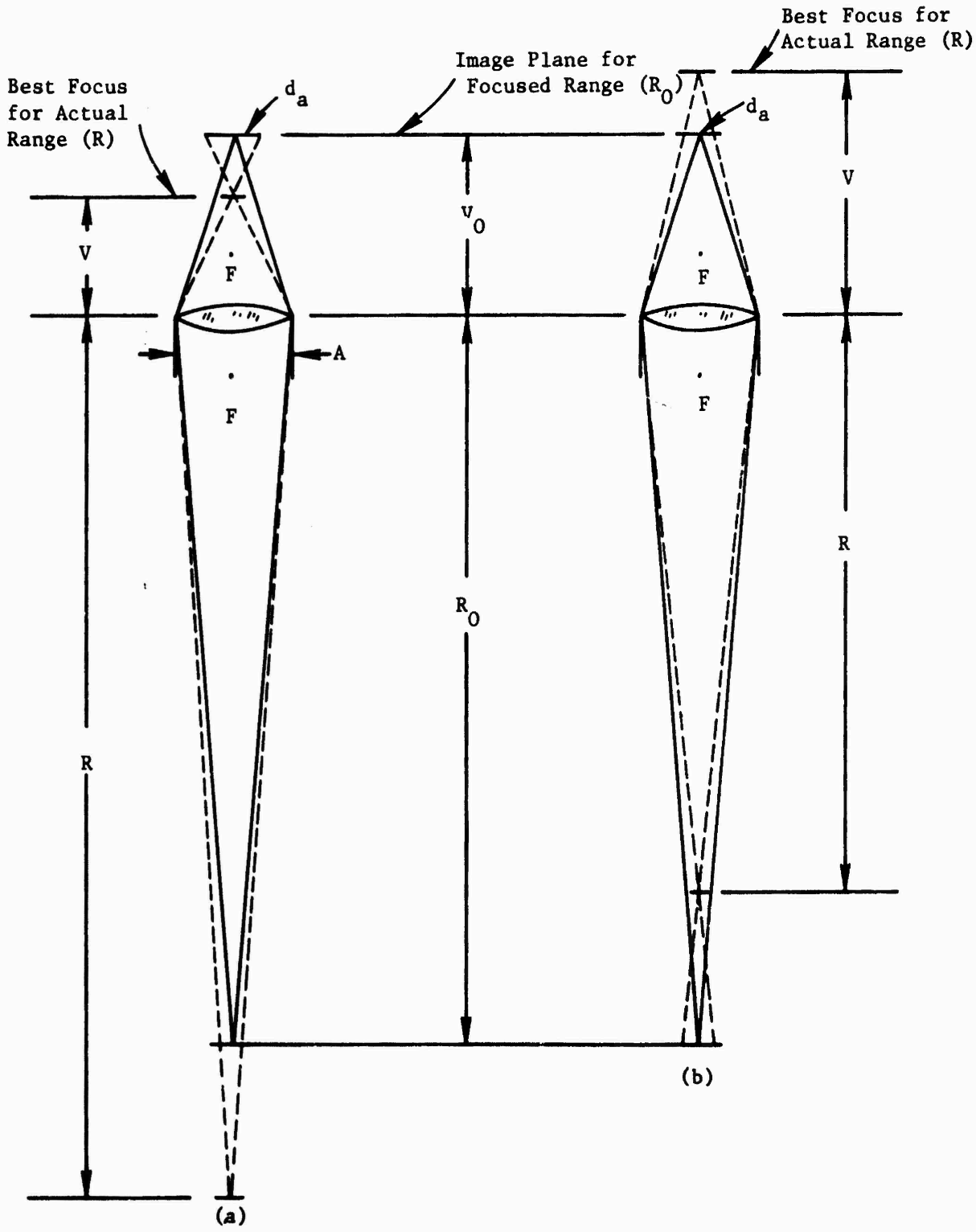

Figure C-17. Geometry for Optical Focus

From the image equation in Newtonian form

$$(V-F)\ (R-F) = F^2$$

Since $R - S \sim R$ we can obtain to a close approximation

$$V = \frac{F^2}{R} + F \quad \text{mm} \tag{C-28}$$

Similarly

$$V_o = \frac{F^2}{R_o} + F \quad \text{mm} \tag{C-29}$$

where F = focal length (mm)

Substituting in Eq. (C-27) gives

$$d_a = \frac{AF|R_o-R|}{RR_o} \quad \text{mm} \tag{C-30}$$

The relative aperture is f/2.8 throughout the focal length range of 20 to 100mm.

The effects of optical defocusing on the assumed optical resolution of 238 ℓp/mm is presented in Figure C-18. It can be seen that improper focus can seriously degrade the focal plane resolution when the 100mm focal length is selected.

The limiting resolution produced by the raster on the SIT vidicon target (R_L) is related by

$$R_L = \frac{N_t}{W} \quad \ell p/mm \tag{C-31}$$

where

N_t = number of vertical resolution elements (TV lines)

W = dimensions of raster height on SIT vidicon (mm)

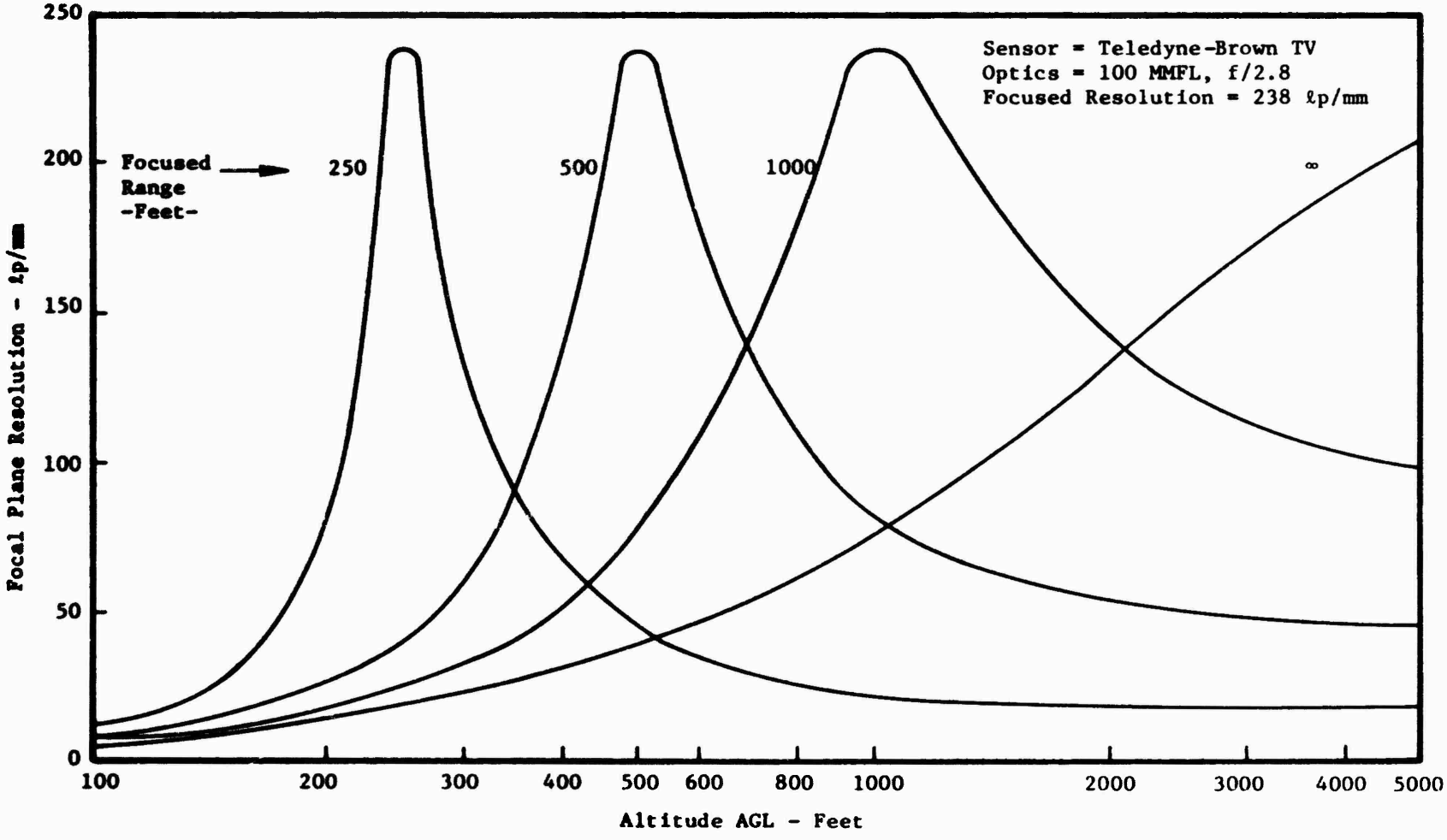

Figure C-18. Focal Plane Resolution for Several Focusing Conditions - Teledyne-Brown Optics

The values of N_t and W were defined previously as 344 TV lines and 11.4 mm, respectively; therefore, R_L = 15.1 ℓp/mm.

The effects of optical defocusing on system resolution are shown in Figure C-19. The curves indicate that system performance falls off rapidly at flight altitudes below the focused altitude, but is only minimally affected at flight altitudes above the focused altitude.

With reference to Table C-4, note that optical defocusing would not affect the system angular resolution calculated for the Nadir and Intermediate footprints. This is due to the fact that the resolution obtained during slant range defocusing is still more than an order of magnitude better than the resolution realized with the rotating mirror.

The system angular resolution of the Forward footprint would be degraded by optical defocusing only when a small field of view was selected--independent of shutter speed. The system angular resolution for the Extreme footprint would be significantly affected only when both a small FOV and a slow shutter speed were realized.

A potential problem exists in selecting an altitude which provides optimum focus slant ranges since the optical axis of the Forward and Extreme footprints define different slant ranges. For example, if the RPV were at an altitude of 500 feet AGL, the Forward footprint slant range would be 7,200 feet for a depression angle of six degrees. However, the Extreme footprint slant range would be only 710 feet for a scan angle of 45 degrees. With reference to Figure C-19, a good compromise would result if the optics were focused to a range of 1,000 feet.

Similar effects apply to the other sensors considered. The computations performed above require that the specific focal length and aperture be identified.

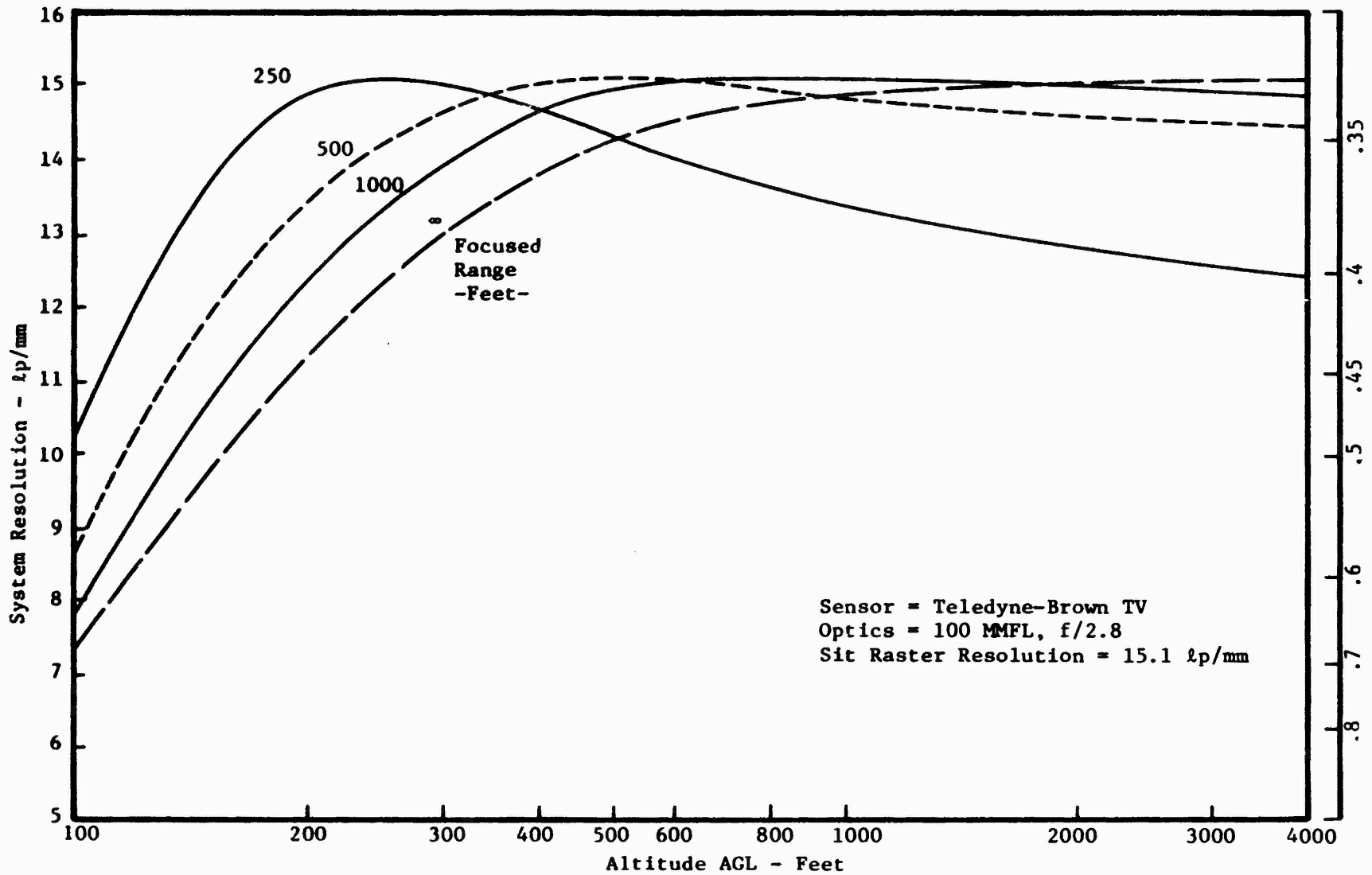

Figure C-19. System Resolution for Several Focusing Conditions - Teledyne-Brown TV

APPENDIX D

SIMULATION CONSIDERATIONS

1.0 KA-98 LASER CAMERA SYSTEM SIMULATION CONSIDERATIONS

1.1 Footprint on Ground

The line scan field of view is fixed at 136 degrees. The raster, which is generated by the forward velocity of the RPV, is displayed with a 3:4 aspect ratio. That is, the raster is oriented so that the long dimension is along the ground track.

Altitudes of 500 and 1,000 feet AGL will be simulated. Typical RPV ground velocities of 350 and 500 knots will also be simulated.

Figure D-1 depicts the ground footprint that corresponds to the above stated conditions. A summary of the assumptions employed are shown in Table D-1.

TABLE D-1. KA-98 LASER CAMERA SYSTEM ASSUMPTIONS

The following assumptions were made:

Altitude (H)	500 feet, 1,000 feet
Velocity (V_g)	350 knots, 500 knots
FOV (θ)	136 degrees
Aspect Ratio	3:4
Crosstrack Coverage (W_C)	2,475 ft for H = 500 ft
	4,950 ft for H = 1,000 ft
Alongtrack Coverage (L_A)	3,300 ft for H = 500 ft
	6,600 ft for H = 1,000 ft
FSS Useful Diameter (D)	4 in.
Transparency Format Width (W_F)	4.5 in.
Transparency Scale (SC)	1:18,000

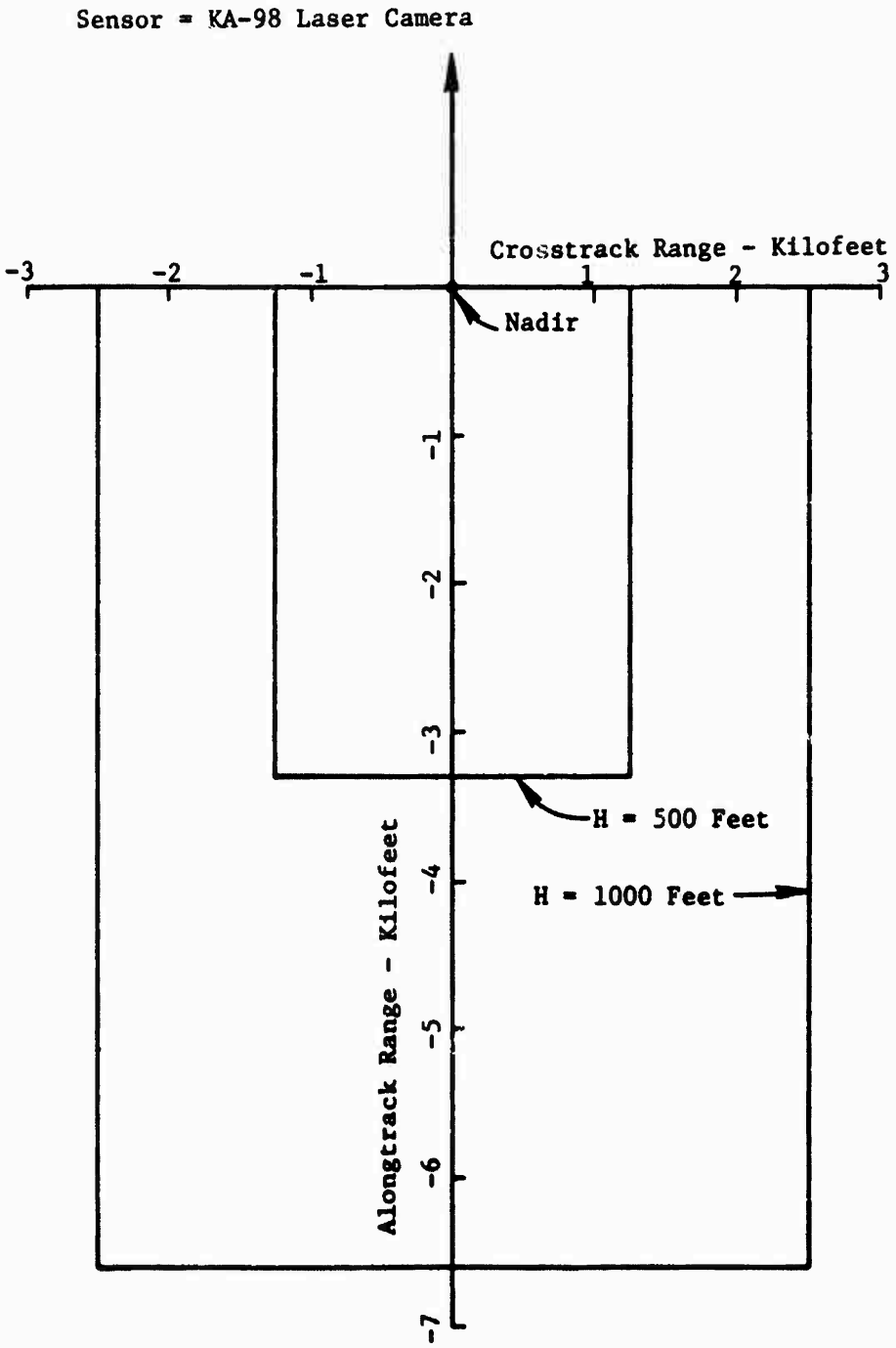

Figure D-1. Ground Coverage for KA-98 Laser Camera Simulation

1.2 Footprint on Transparency

The five inch positive transparency has a format width (W_F) of 4.5 inches, or 0.375 feet. The scale is 1:18,000; thus 6,750 feet of ground coverage is recorded across the transparency. This corresponds to 1,500 feet of ground coverage per inch.

Crosstrack ground coverage (W_C) of the KA-98 laser camera is 2,475 feet at H = 500 feet, and 4,950 feet at H = 1,000 feet. Therefore, the required footprint width on the transparency is W_T = 2,475/1,500 = 1.65 inches for H = 500 feet, and W_T = 3.30 inches for H = 1,000 feet.

The alongtrack ground coverage is L_A = (4/3)(2,475) = 3,300 feet at H = 500 feet, and 6,600 feet at H = 1,000 feet. Thus, the length of the footprint on the transparency is L_T = 3,300/1,500 = 2.2 inches for H = 500 feet, and L_T = 4.4 inches for H = 1,000 feet.

1.3 Raster on FSS

The useful diameter of the flying spot scanner (FSS) is 4 inches. Therefore, the H = 1,000 foot footprint on the positive transparency (3.2 × 4.26 inches) must be generated at a smaller scale (assume 0.707) by the FSS and then magnified optically (m = 1/0.707 = 1.414). The resulting FSS footprint is then 2.26 inches crosstrack and 3.01 inches alongtrack (Figure D-2).

For H = 500 feet, the 1.6 × 2.13 inch footprint on the transparency could be generated on the FSS with a one-to-one correspondence. However, from the standpoint of providing the best resolution (smallest FSS spot size at the transparency) and to minimize the effects of FSS phosphor grain, it is better to generate the largest FSS footprint possible and optically reduce it. Thus, the 2.26 × 3.01 inch FSS footprint generated for H = 1,000 feet will be optically reduced to the required H = 500 size transparency footprint of 1.6 × 2.13 inches (Figure D-3). The required optical magnification is m = 1.6/2.26 = 0.707.

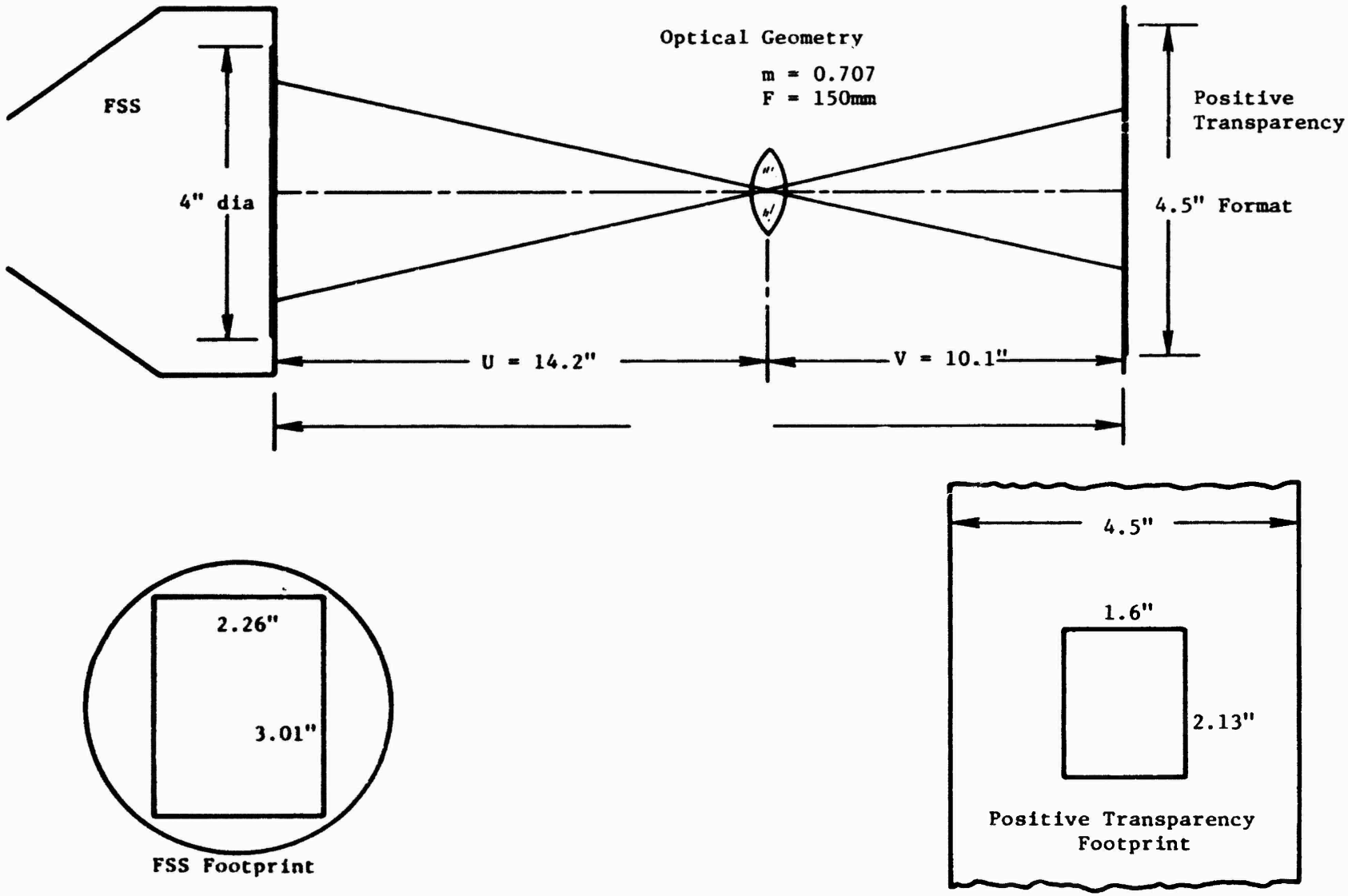

Figure D-2. Geometry for KA-98 Laser Camera Simulation (H = 500 feet)

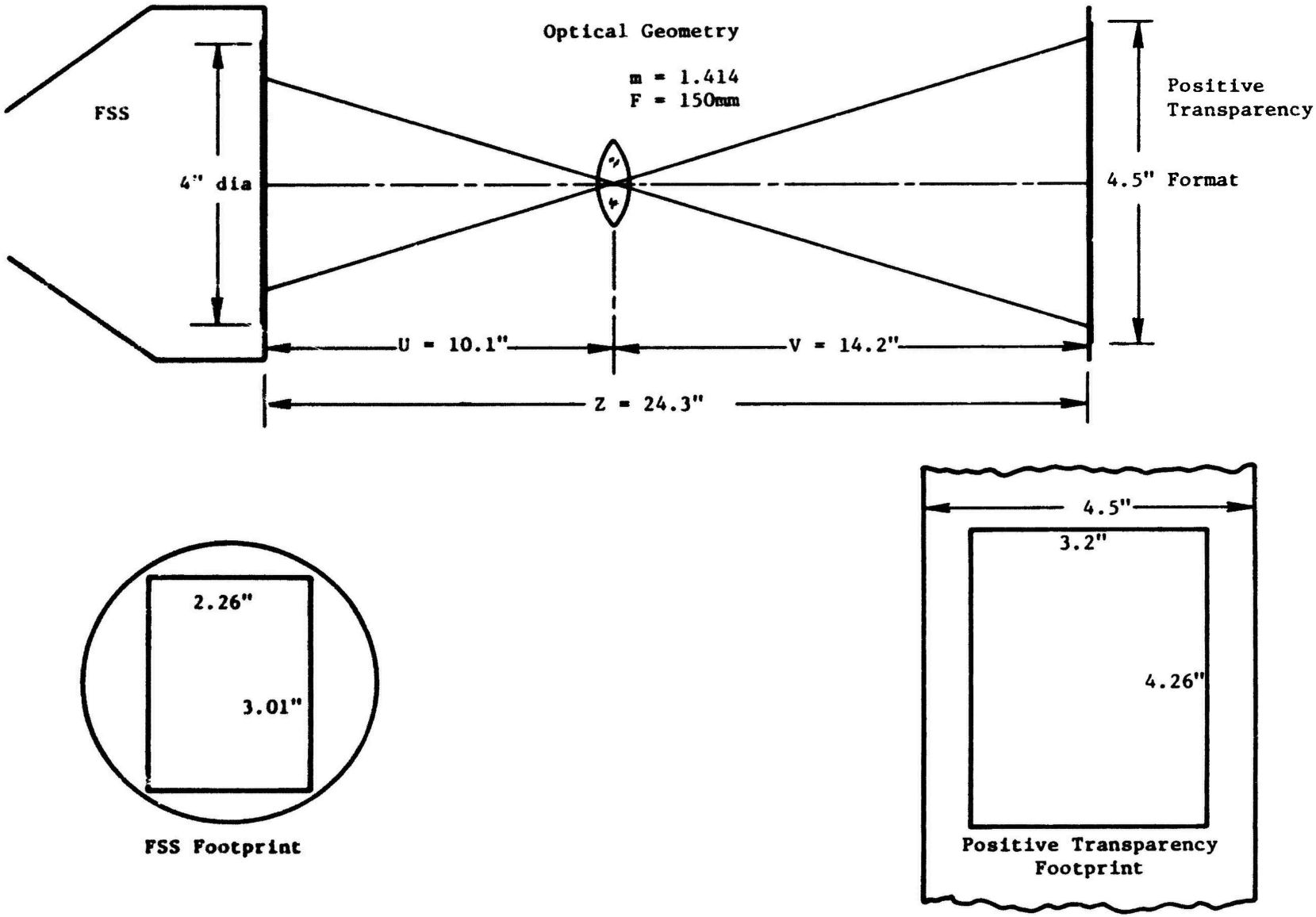

Figure D-3. Geometry for KA-98 Laser Camera (H = 1000 feet)

1.4 Optics

1.4.1 H = 1,000 feet

The existing 150 mm focal length (F) lens will be utilized to provide the magnification m = 1.414 required for H = 1,000 feet. The FSS phosphor to transparency emulsion distance (Z) can be found by (Figure D-2)

$$Z = \frac{F(m+1)^2}{m} \qquad \text{(D-1)}$$

$$= 24.3 \text{ inches}$$

Lens to FSS phosphor distance (U) is related by

$$U = \frac{F}{m} + F \qquad \text{(D-2)}$$

$$= 10.1 \text{ inches}$$

Lens to positive transparency emulsion distance (V) can be found by

$$V = Fm + F \qquad \text{(D-3)}$$

$$= 14.2 \text{ inches}$$

1.4.2 H = 500 feet

Since both the magnification (m) and the FSS to transparency distance (Z) were specified for H = 1,000 feet, we must find the required focal length. Because the magnifications for H = 500 and H = 1,000 feet are reciprocals, the focal lengths will be identical. This can be confirmed by solving Eq. (D-1) for F.

$$F = \frac{mZ}{(m+1)^2}$$

$$= 5.91 \text{ inches} = 150\text{mm}$$

The lens to FSS (U) and lens to transparency distance (V) will be transposed.

$$U = \frac{F}{m} + F$$

$$= 14.2 \text{ inches}$$

and

$$V = Fm + F$$

$$= 10.1 \text{ inches}$$

1.5 Time on Display

Time on display (T_d) can be found by

$$T_d = \frac{L_A}{V_g} \quad \text{seconds} \qquad \text{(D-4)}$$

The alongtrack dimension (L_A) is 3,300 feet at H = 500 feet and 6,600 feet at H = 1,000 feet. The ground velocity (V_g) will be simulated at 350 and 500 knots. By use of Eq. (4), we can find

	Altitude	
Ground Velocity	500 feet	1,000 feet
350 knots	5.6	11.2 sec
500 knots	3.9	7.8 sec

1.6 Transparency Velocity

Transparency velocity (V_t) can be found by dividing the RPV ground velocity (V_g) by the number of feet per inch recorded on the transparency (1,500). This gives 0.39 inches per second for V_g = 350 knots, and 0.56 inches per second for V_g = 500 knots. Transparency velocity is independent of the simulated altitude.

2.0 TELEDYNE-BROWN TELEVISION SYSTEM SIMULATION CONSIDERATIONS

2.1 NAV Mode

2.1.1 Footprint on Ground

The field of view can be preflight selected from 6.4 × 6.4 to 32 × 32 degrees. A field of view of 32 × 32 will be used for simulation.

The depression angle can be preflight selected between the angles of zero to 10 degrees. It was found during the flight test program that 20 to 25 percent of sky FOV was desirable. Therefore, a depression angle of 10 degrees will be used.

An altitude of 500 feet AGL provides a good trade-off between sensor performance and RPV survival and will be simulated. Typical RPV ground velocities of 350 and 500 knots will also be simulated.

Figure D-4 shows the ground footprint that corresponds to the above stated conditions. For convenience in implementing the simulator, maximum ground coverage is limited to a depression angle of two degrees. A summary of the assumptions employed are listed in Table D-2.

2.1.2 Footprint on Transparency

Scale of the positive transparency (SC) is 1:22,000 so that the nine inch format width (W_F) contains (22,000) (0.75 = 16,500 feet of ground coverage). This corresponds to 1,833 feet of ground coverage per inch.

The crosstrack ground coverage at the far side of the footprint is 8,600 feet. Therefore, the required far side footprint width on the transparency W_{TF} = 8,600/1,833 = 4.7 inches. The crosstrack coverage at the footprint is 700 feet so that W_{TN} = 0.38 inches (Figure D-5).

The alongtrack ground coverage is 13,500 feet. Therefore, the length of the footprint on the transparency is L_T = 13,500/1,833 = 7.4 inches.

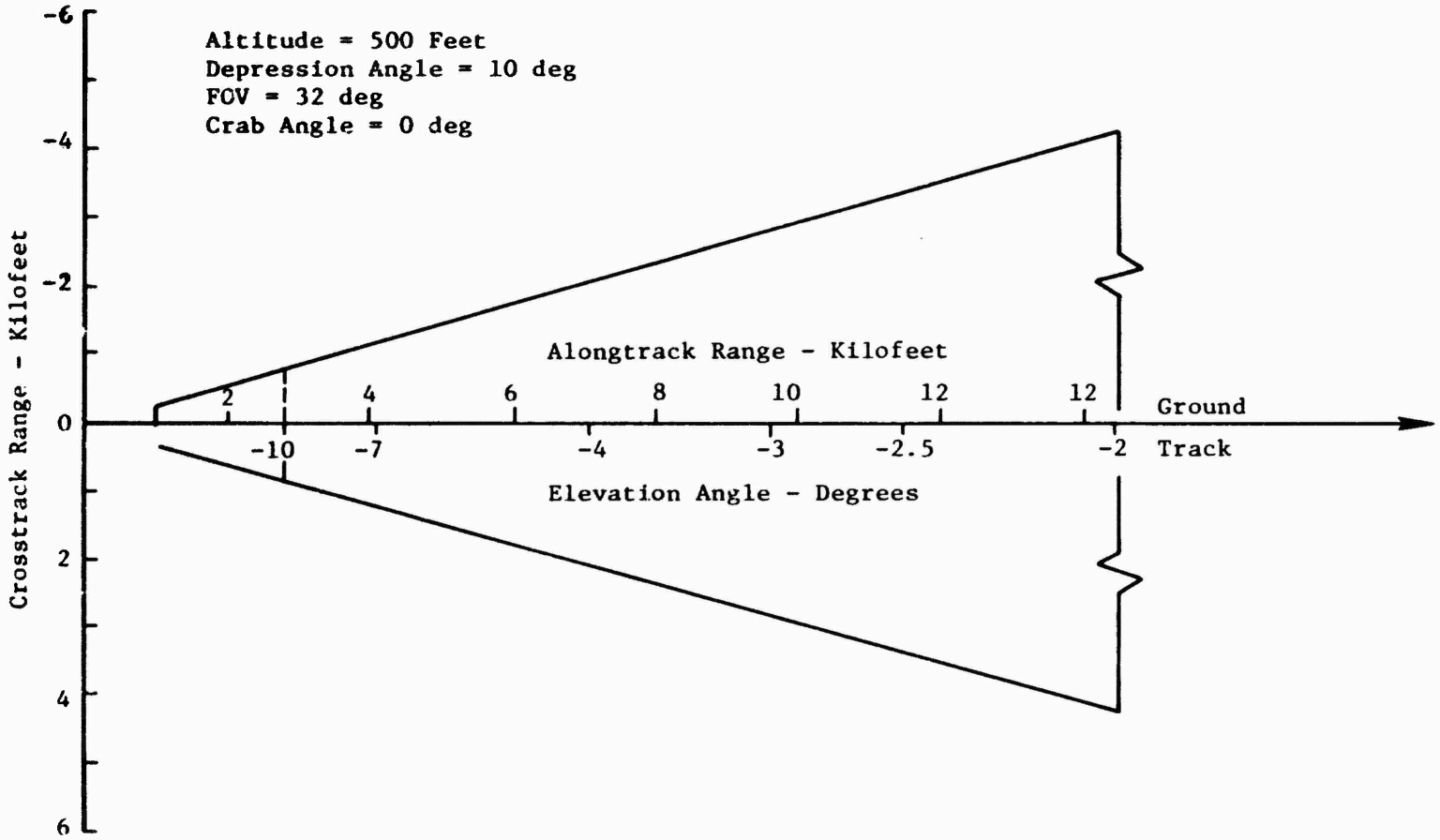

Figure D-4. Ground Coverage for Teledyne-Brown TV Camera Simulation - NAV Mode

TABLE D-2. TELEDYNE-BROWN TV SYSTEM ASSUMPTIONS - NAV MODE

The following assumptions were made:

Altitude (H)	500 feet
Velocity (V_g	350 knots, 500 knots
FOV (θ)	32 × 32 deg
Depression Angle (β)	10 deg
Max Ground Coverage*	2 deg depression angle

Footprint Dimensions

Ground range - near edge (S_N) = 1,000 ft
- optical axis (S_O) = 2,800 ft
- far edge (S_F) = 14,500 ft

Crosstrack - near side (W_N) = 700 ft
- far side (W_F) = 8,600 ft

Alongtrack (L_A) = $S_F - S_N$ = 13,500 ft

FSS Useful Diameter (D) 9 inches

Transparency Format Width (W_F) 1:22,000

*The displayed scene will be composed of 19 percent sky, 6 percent indistinct background, and 75 percent imagery.

2.1.3 Raster on FSS

The useful diameter (D) of the flying spot scanner (FSS) is nine inches. Therefore, the raster size required for the positive transparency can be generated by the FSS with a one-to-one correspondence. The FSS raster is shown in Figure D-5.

2.1.4 Optics

The FSS phosphor to transparency emulsion distance (Z) can be found by (Figure D-5)

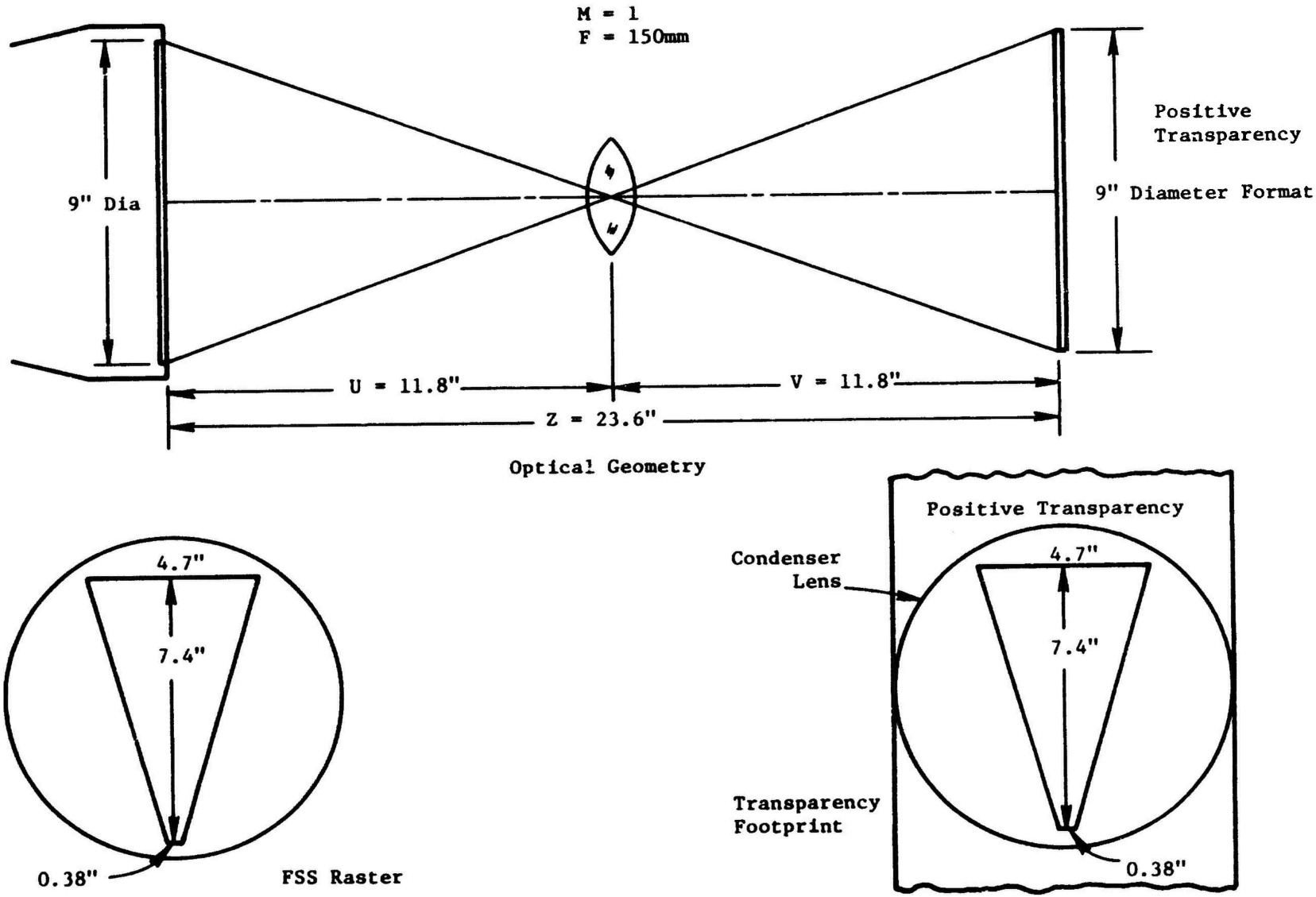

Figure D-5. Geometry for Teledyne-Brown TV Camera Simulation - NAV Mode

$$Z = \frac{F(m+1)^2}{m} \qquad \text{(D-5)}$$

$$= 23.62 \text{ inches}$$

Lens to FSS phosphor distance (U) is related by

$$U = \frac{F}{m} + F \qquad \text{(D-6)}$$

$$= 11.81 \text{ inches}$$

Lens to positive transparency emulsion distance (V) can be found by

$$V = Fm + F \qquad \text{(D-7)}$$

$$= 11.81 \text{ inches}$$

The required lens field angle (θ) is

$$\theta = 2 \tan^{-1} \left[\frac{(L_T^2 + W_{TF}^2)^{1/2}}{2V_g} \right] \quad \text{degrees}$$

$$= 2 \tan^{-1} \left[\frac{(7.4^2 + 5^2)^{1/2}}{2(11.81)} \right]$$

$$= 41.4 \text{ degrees}$$

2.1.5 Time on Display

For a target on or near the ground track, the time on display can be found by

$$T_d = \frac{L_A}{V_g} \quad \text{seconds} \qquad \text{(D-8)}$$

2.1.6 Transparency Velocity

Transparency velocity (V_t) can be found by dividing the ground velocity by the number of feet per inch recorded on the transparency (1833). This gives 0.322 inches per second for V_g = 350 knots, and 0.460 inches per second for V_g = 500 knots.

2.2 RECON Mode

2.2.1 Footprint on Ground

The field of view can be preflight selected between 6.4 × 6.4 to 32 × 32 degrees. The lateral scan angle can be preflight selected between zero and ±60 degrees. A field of view smaller than 32 degrees requires that a small scan angle also be selected to prevent holidays in the lateral coverage. An FOV of 26.6 degrees and a scan angle of ±44 degrees will be simulated.

The footprints rotate with a one-to-one correspondence to the scan angle. Therefore, the intermediate footprint is rotated 22 degrees, and the extreme footprint is rotated 44 degrees. The altitude and ground velocity must correspond to the values selected for the NAV mode, i.e., an altitude of 500 feet and a velocity of 500 knots.

Figure D-6 shows the ground footprint that corresponds to the above stated conditions. A summary of the assumptions employed are listed in Table D-3. The geometric relationships are presented in Table D-4 and Figure D-7.

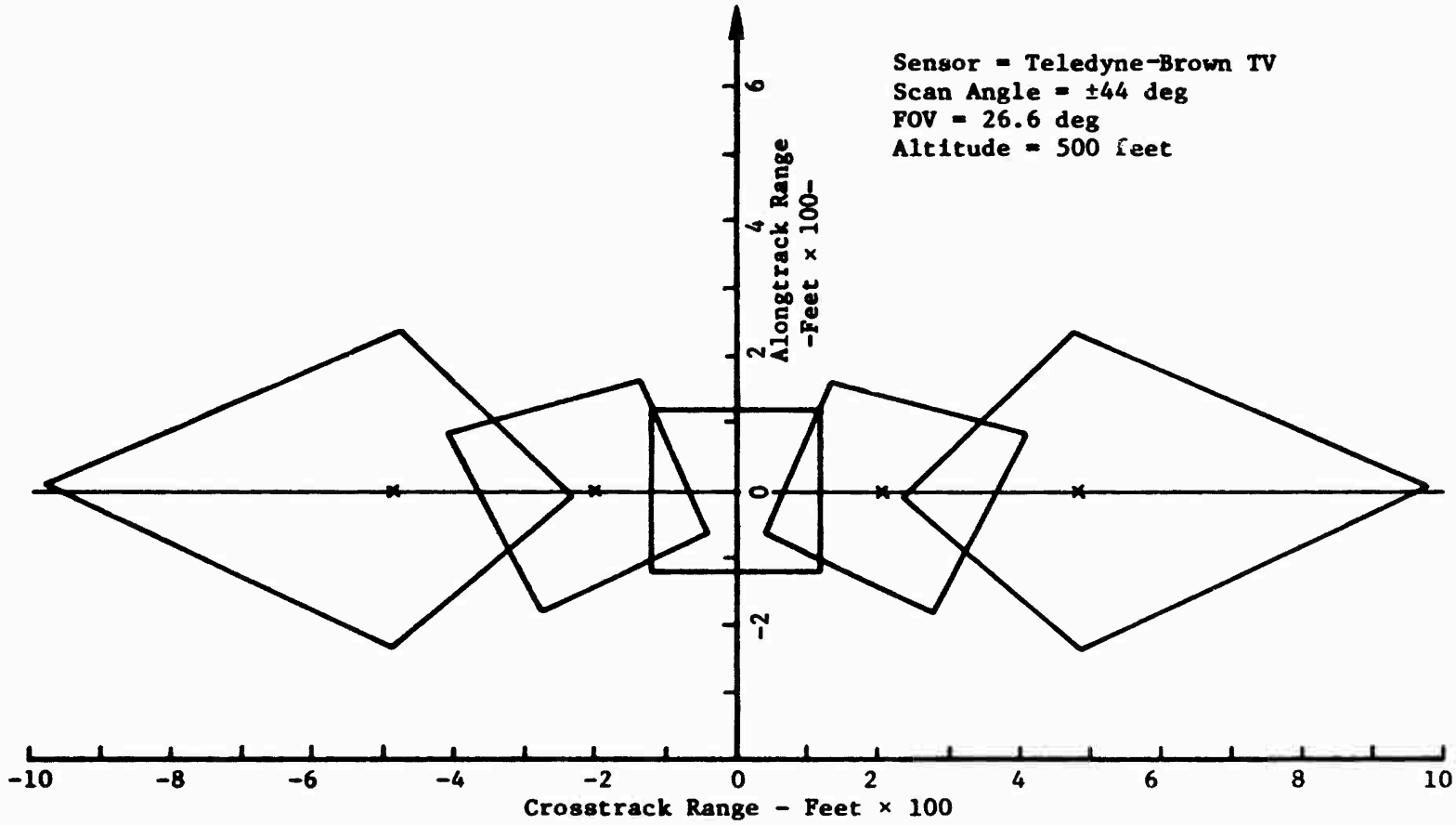

Figure D-6. Ground Coverage for Teledyne-Brown TV Camera Simulation - RECON Mode

TABLE D-3. TELEDYNE-BROWN TV SYSTEM ASSUMPTIONS - RECON MODE

The following assumptions were made:

Altitude (H)	500 feet
Velocity (V_g)	350 knots, 500 knots
FOV (θ)	26.6 × 26.6 deg
Depression Angle (β)	46 deg
Scan Angle (ψ)	±44 deg

Footprint Dimensions

Vertical Footprint

$S = 2H \tan\theta/2 = 236$ ft (118 ft each side of ground track)

Intermediate Footprint

Point A	X = 202 ft (optical axis)		
	Y = 0		
Point B	X = 40 ft	Point C	X = 132 ft
	Y = -63 ft		Y = 162 ft
Point D	X = 411 ft	Point E	X = 279 ft
	Y = 82 ft		Y = -180 ft

Extreme Footprint

Point A	X = 483 ft (optical axis)		
	Y = 0		
Point B	X = 235 ft	Point C	X = 478 ft
	Y = -3 ft		Y = 235 ft
Point D	X = 973 ft	Point E	X = 488 ft
	Y = 6 ft		Y = -238 ft

TABLE D-4. GEOMETRICAL RELATIONSHIPS FOR TELEDYNE-BROWN TV CAMERA - RECON MODE

Slant Range (R)

$R_A = H/\sin\beta$ (optical axis)

$R_B = H/\sin[\beta-0.71\theta\cos(225-\gamma)]$

$R_C = H/\sin[\beta+0.71\theta\cos(315-\gamma)]$

$R_D = H/\sin[\beta-0.71\theta\cos(45-\gamma)]$

$R_E = H/\sin[\beta+0.71\theta\cos(135-\gamma)]$

H = altitude
ψ = scan angle
β = depression angle
γ = rotation angle
$\theta_h = \theta_v = \theta$ = horizontal and vertical sensor FOV

X, Y Coordinates

Point A $X = H/\tan\beta$

$Y = 0$

Point B $X = H/\tan[\beta-0.71\theta\cos(225-\gamma)]$

$$Y = \frac{H \tan[0.71\theta\cos(225+\gamma)]}{\sin[\beta-0.71\theta\cos(225-\gamma)]}$$

Point C $X = H/\tan[\beta+0.71\theta\cos(315-\gamma)]$

$$Y = \frac{H \tan[0.71\theta\cos(315+\gamma)]}{\sin[\beta+0.71\theta\cos(315-\gamma)]}$$

Point D $X = H/\tan[\beta-0.71\theta\cos(45-\gamma)]$

$$Y = \frac{H \tan[0.71\theta\cos(45+\gamma)]}{\sin[\beta-0.71\theta\cos(45-\gamma)]}$$

Point E $X = H/\tan[\beta+0.71\theta\cos(135-\gamma)]$

$$Y = \frac{H \tan[0.71\theta\cos(135+\gamma)]}{\sin[\beta+0.71\theta\cos(135-\gamma)]}$$

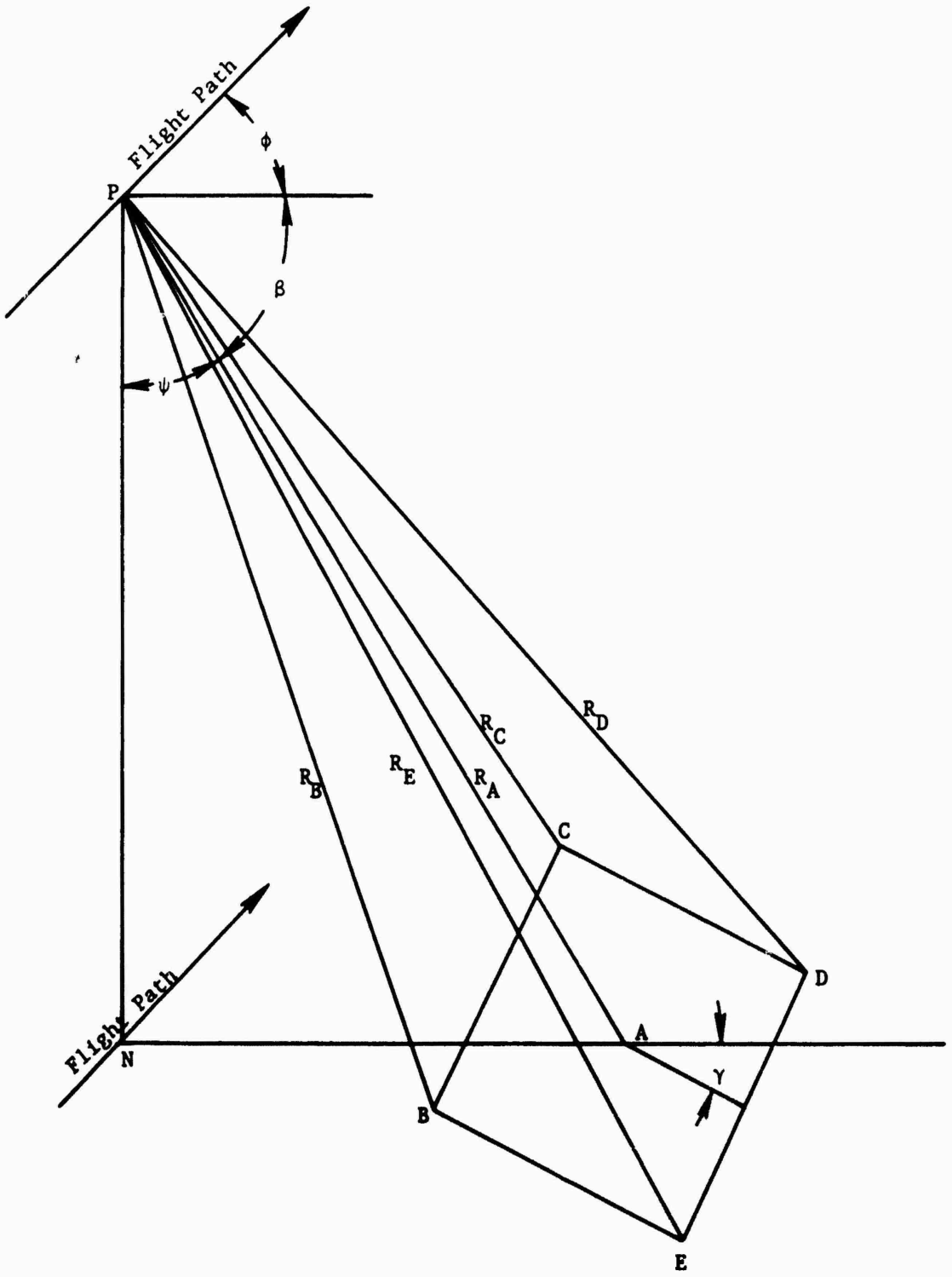

Figure D-7. Viewing Geometry for Teledyne-Brown TV Camera Simulation - RECON Mode

2.2.2 Footprint on Transparency

Scale of the positive transparency (SC) is 1:22,000. Thus, there are 1,833 feet of ground coverage per inch.

The sides of the nadir footprint were found to be 236 feet in length. Therefore, the length of the sides on the transparency can be found to be 236/1,833 = 0.13 inches. The position of the corner points relative to nadir of the intermediate and extreme footprints were found by dividing the values presented in Table D-3 by 1,833. The results are shown in Table D-5 and plotted in Figure D-8.

TABLE D-5. TRANSPARENCY FOOTPRINT DIMENSIONS FOR TELEDYNE-BROWN RECON MODE SIMULATION

Intermediate Footprint		Extreme Footprint	
Point A	X = 0.110	Point A	X = 0.264
	Y = 0		Y = 0
Point B	X = 0.022	Point B	X = 0.128
	Y = -0.034		Y = -0.002
Point C	X = 0.072	Point C	X = 0.261
	Y = 0.088		Y = 0.128
Point D	X = 0.224	Point D	X = 0.531
	Y = 0.045		Y = 0.003
Point E	X = 0.152	Point E	X = 0.226
	Y = -0.098		Y = -0.130

All dimensions are in inches. The sides of the vertical footprint are 0.064 inches from the nadir.

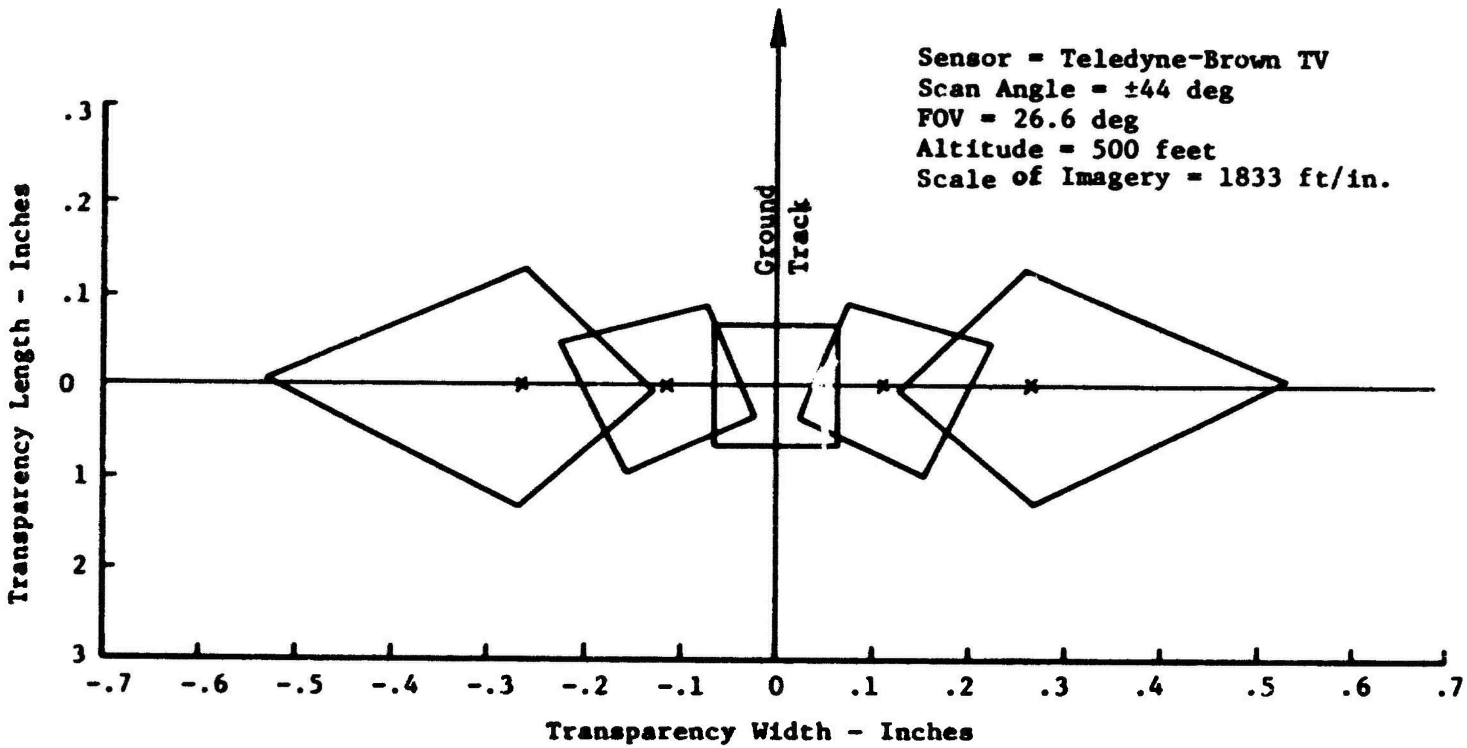

Figure D-8. Geometry for Teledyne-Brown TV Camera Footprints on Transparency - RECON Mode

2.2.3 Raster on FSS

The useful diameter of the FSS raster is nine inches. The extreme points of the footprint set on the transparency are 1.06 inches apart. Therefore, an optical magnification of 1.06/9 = 0.117 can be realized between the FSS raster and the transparency footprint.

The magnification that has been selected is m = 0.12 (see next paragraph). Thus, the FSS raster will be 1/0.12 = 8.33 times larger than the transparency footprint. The results are presented in Table D-6 and plotted in Figure D-9.

In order to take full advantage of the FSS size, the RECON footprint is generated on the FSS diameter. This position is not in the proper spatial relationship with respect to the NAV footprint. Consequently, the transparency will be rapidly advanced to the correct position during the NAV-to-RECON transition period.

TABLE D-6. FSS RASTER DIMENSIONS FOR TELEDYNE-BROWN RECON MODE SIMULATION

Intermediate Raster		Extreme Raster	
Point A	X = 0.916	Point A	X = 2.20
	Y = 0		Y = 0
Point B	X = 0.183	Point B	X = 1.07
	Y = -0.283		Y = -0.017
Point C	X = 0.600	Point C	X = 2.17
	Y = 0.733		Y = 1.07
Point D	X = 1.87	Point D	X = 4.42
	Y = 0.375		Y = 0.025
Point E	X = 1.27	Point E	X = 2.22
	Y = -0.816		Y = -1.09

All dimensions are in inches. The sides of the square vertical raster are 1.07 inches long.

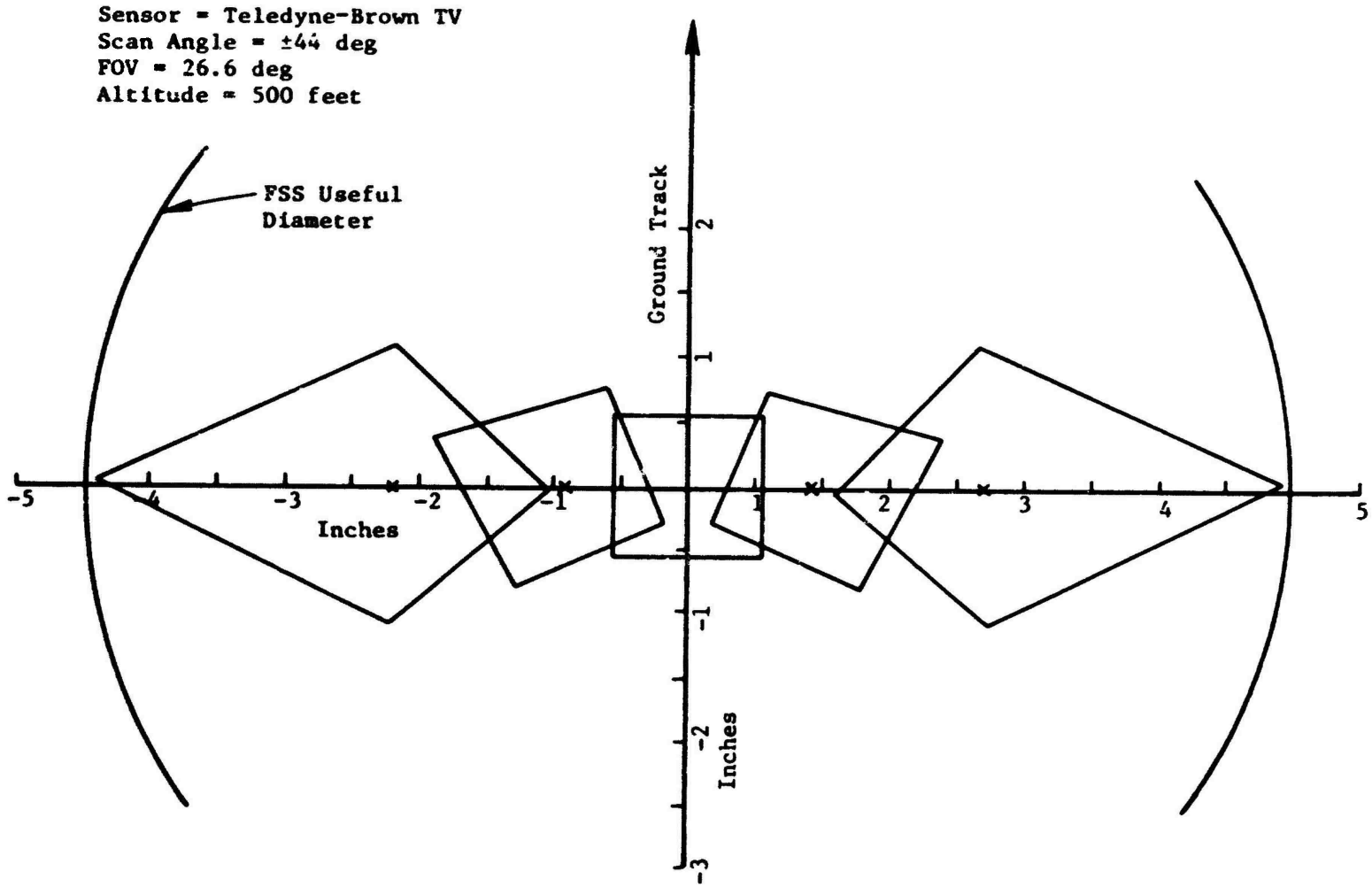

Figure D-9. Geometry for Teledyne-Brown TV Camera FSS Rasters - RECON Mode

2.2.4 Optics

The FSS phosphor to transparency emulsion distance required for the NAV mode is 23.62 inches (paragraph 2.1.4). This dimension must be maintained when the RECON mode is selected. Since we wish to employ a focal length for which lenses are in stock, available focal lengths were inserted in the following equation.

$$m = \frac{Z - 2F \pm (Z^2 - 4FZ)^{0.5}}{2F} \qquad \text{(D-9)}$$

It was found that a 58mm focal length lens will provide a magnification of 0.122 at the given FSS to transparency separation.

Lens to FSS phosphor distance (U) can be found by

$$U = \frac{F}{m} + F \qquad \text{(D-10)}$$

$$= 21.06 \text{ inches}$$

Lens to positive transparency emulsion distance (V) is related by

$$V = Fm + F \qquad \text{(D-11)}$$

$$= 2.56 \text{ inches}$$

See Figure D-10.

2.2.5 Transparency Velocity

Transparency velocity (V_t) is found by dividing the ground velocity by the number of feet recorded on the transparency, which is 1,833. This gives 0.322 inches per second for V_g = 350 knots, and 0.460 inches per second for V_g = 500 knots.

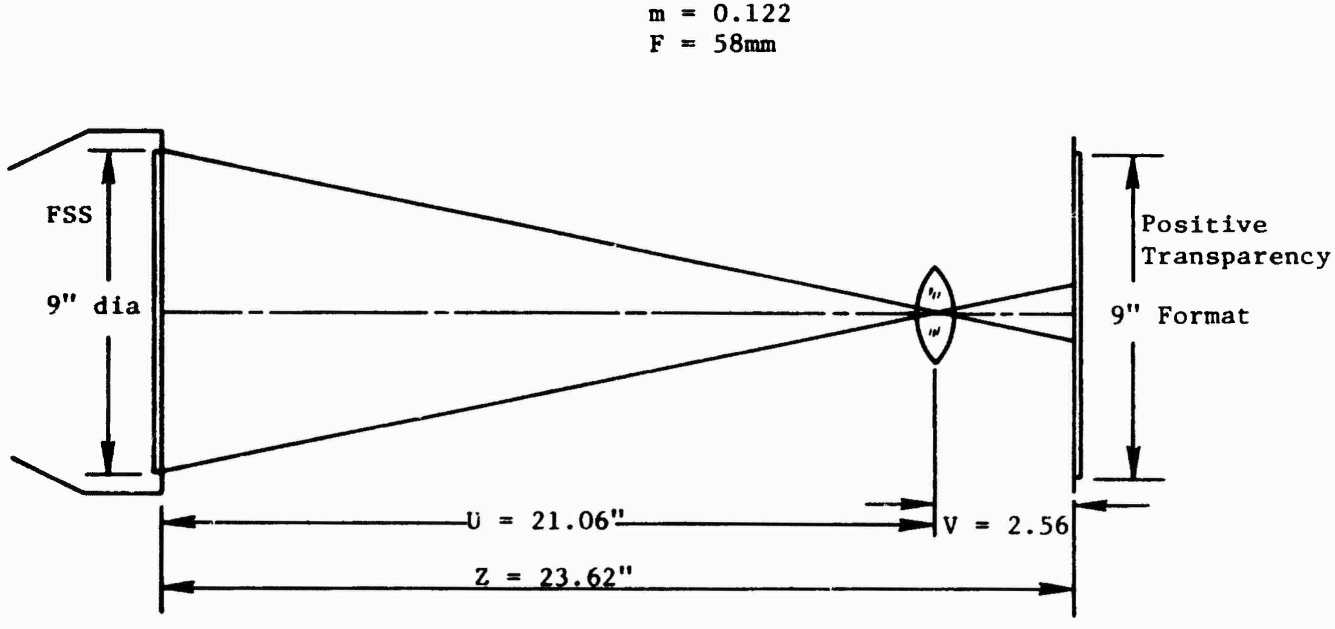

Figure D-10. Optical Geometry for Teledyne-Brown TV Camera - RECON Mode

3.0 SLEWABLE TELEVISION SYSTEM SIMULATION ASSUMPTIONS

3.1 Footprint on Ground

The field of view typically can be remotely zoomed over a 10:1 range. A 3:1 zoom range from 8 to 24 degrees will be simulated. Gimbal limits of ±32 degrees in azimuth and 6 to 18 degrees in depression will also be simulated.

A look at the ground coverage depicted in Figure D-11 shows that the stated gimbal limits will provide a good simulated mission capability. Note that depression angles greater than 18 degrees would not significantly increase the ground coverage. Hence, the additional time on display would be of limited value to the image interpreter. The ±32 degrees of azimuth gimbal freedom will permit targets offset from the ground track by as much as 1,000 feet to be tracked to the maximum depression angle of 18 degrees.

The ground coverage is limited to 3.2 degrees depression angle in order to minimize the large footprint size dynamic range generated by the real world TV system. However, the area immediately below the horizon will normally be of little use during actual missions so that its deletion will not materially affect simulation validity.

The footprint extremes that can result from operator manipulation of the optical zoom, and slewing of the azimuth and elevation gimbals, are presented in Figure D-11. A summary of the assumptions made for the simulation is shown in Table D-7. The equations and geometry for finding the pertinent dimensions, and positions of the corner points relative to nadir, of the ground footprint are provided in Table D-8 and Figure D-12.

3.2 Footprint on Transparency

Scale of the positive transparency (SC) is 1:22,000 so that 1,833 feet of ground coverage is contained in each lineal inch of the nine inch format transparency. The footprint extremes are shown in Figures D-13a and D-13b.

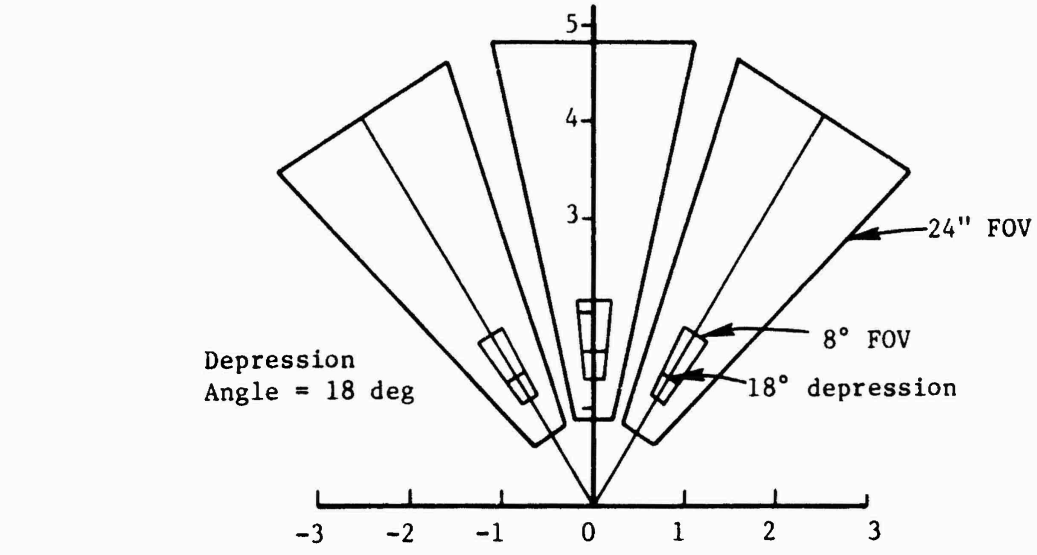

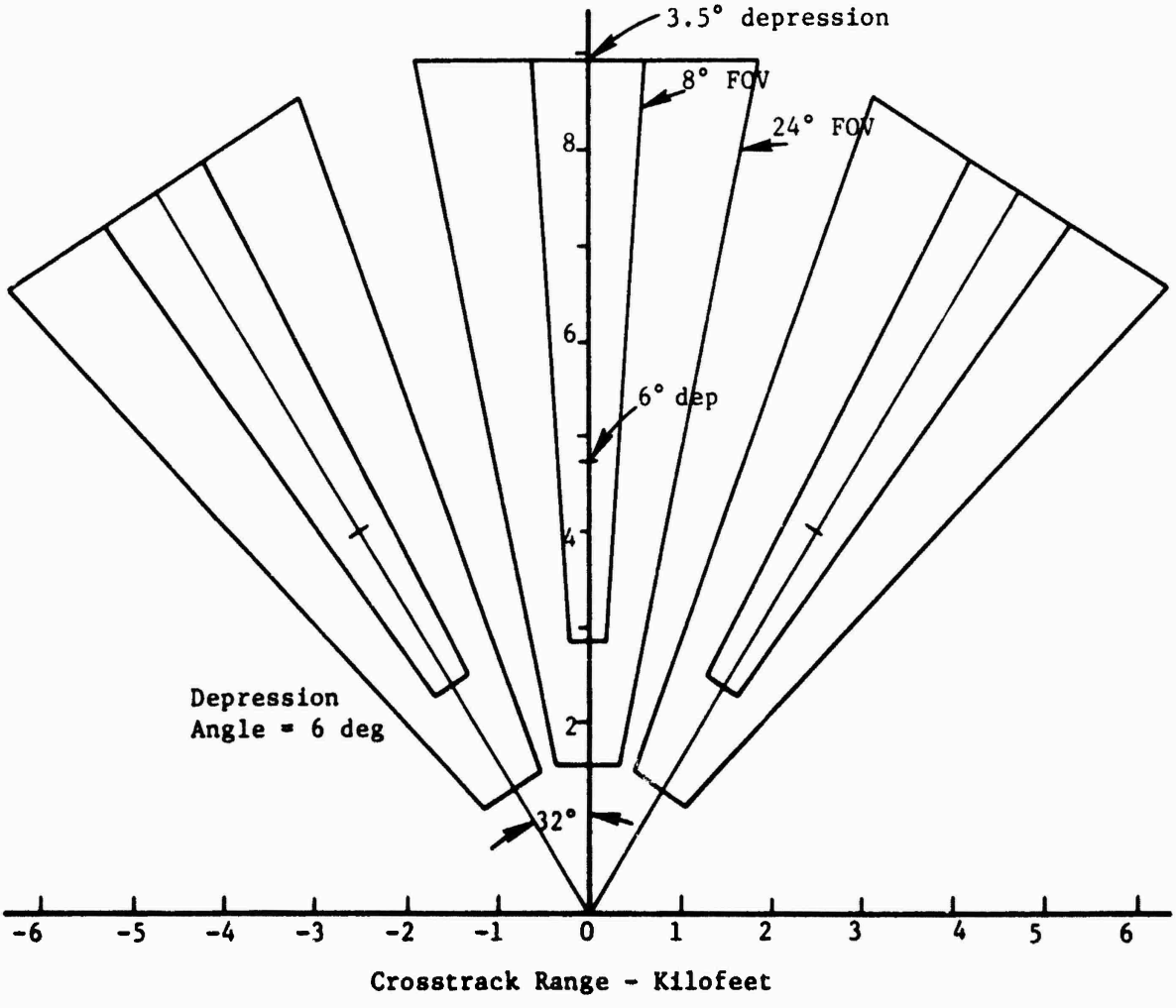

Figure D-11. Ground Coverage for Slewable TV Camera Simulation

TABLE D-7. SLEWABLE TV SYSTEM ASSUMPTIONS

The following assumptions were made:

Altitude (H)	500 feet
Velocity (V_g)	350 knots, 500 knots
Focal Length (F)	zoom 81.5mm to 26.8mm
FOV (θ)	8 × 8 to 24 × 24 deg
Depression Angle (β)	selectable 6 to 18 deg
Azimuth Angle (ϕ)	selectable ±32 deg
Maximum Ground Coverage*	3.2 deg depression angle

Footprint Dimensions (β = 6 deg)

FOV = 8 deg

Ground Range - near edge (S_N) = 2,840
- optical axis (S_O) = 4,762
- far edge (S_F) = 8,943

Crosstrack - near side (W_N) = 201
- optical axis (W_O) = 333
- far side (W_F) = 625

Alongtrack (L_A) = $S_F - S_N$ = 6,103

FOV = 24 deg

Ground Range - near edge (S_N) = 1,538
- optical axis (S_O) = 4,762
- far edge (S_F) = 8,943

Crosstrack - near side (W_N) = 345
- optical axis (W_O) = 1,014
- far side (W_F) = 1,907

Alongtrack (L_A) = $S_F - S_N$ = 7,405

Footprint Dimensions (β = 18 deg)

FOV = 8 deg

Ground Range - near edge (S_N) - 1,238
- optical axis (S_O) = 1,538
- far edge (S_F) = 2,008

TABLE D-7 (cont'd)

Crosstrack - near side (W_N) = 93

- optical axis (W_O) = 113

- far side (W_F) = 145

Alongtrack (L_A) = $S_F - S_N$ = 770

FOV = 24 deg

Ground Range - near edge (S_N) = 867

- optical axis (S_O) = 1,538

- far edge (S_F) = 4,762

Crosstrack - near side (W_N) = 213

- optical axis (W_O) = 344

- far side (W_F) = 1,014

Alongtrack (L_A) = $S_F - S_N$ = 3,895

*The displayed scene will be composed of 25 percent sky, 13 percent indistinct background, and 62 percent imagery (for FOV = 24 deg and depression angle = 6 deg).

TABLE D-8. GEOMETRICAL RELATIONSHIPS FOR SLEWABLE TV CAMERA

Slant Range (R)

$R_{PA} = H/\sin\beta$

$R_{PG} = H/\sin(\beta+\theta_v/2)$

$R_{PF} = H/\sin(\beta-\theta_v/2)$

H = altitude AGL
θ_v = vertical FOV
θ_h = horizontal FOV
β = depression angle
ϕ = azimuth angle

Assumes flat earth and no crab angle

$$R_{PK}, R_{PL} = R_{PA}/\cos(\theta_h/2) = \frac{H}{\sin\beta\cos(\theta_h/2)}$$

$$R_{PB}, R_{PC} = R_{PG}/\cos(\theta_h/2) = \frac{H}{\sin(\beta+\theta_v/2)\cos(\theta_h/2)}$$

$$R_{PD}, R_{PE} = R_{PF}/\cos(\theta_h/2) = \frac{H}{\sin(\beta-\theta_v/2)\cos(\theta_h/2)}$$

Crosstrack Range (T)

$$T_{LK} = 2R_{PA}\tan(\theta_h/2) = 2H\tan(\theta_h/2)/\sin\beta$$

$$T_{CB} = 2R_{PG}\tan(\theta_h/2) = 2H\tan(\theta_h/2)/\sin(\beta+\theta_v/2)$$

$$T_{DE} = 2R_{PF}\tan(\theta_h/2) = 2H\tan(\theta_h/2)/\sin(\beta-\theta_v/2)$$

Alongtrack Range (S)

$$S_{NA} = H/\tan\beta$$

$$S_{NG} = H/\tan(\beta+\theta/2)$$

$$S_{NF} = H/\tan(\beta-\theta/2)$$

$$S_{NF} - S_{NG} = H[\cot(\beta-\theta/2) - \cot(\beta+\theta/2)]$$

Point B

$$Y = \frac{H\{\cos\phi-\sin\phi[\tan(\theta/2)/\cos(\beta+\theta/2)]\}}{\tan(\beta+\theta/2)}$$

$$X = \frac{H\{\sin\phi+\cos\phi[\tan(\theta/2)/\cos(\beta+\theta/2)]\}}{\tan(\beta+\theta/2)}$$

TABLE D-8 (cont'd)

Point C

$$Y = \frac{H\{\cos\phi+\sin\phi[\tan(\theta/2)/\cos(\beta+\theta/2)]\}}{\tan(\beta+\theta/2)}$$

$$X = \frac{H\{\sin\phi-\cos\phi[\tan(\theta/2)/\cos(\beta+\theta/2)]\}}{\tan(\beta+\theta/2)}$$

Point D

$$Y = \frac{H\{\cos\phi+\sin\phi[\tan(\theta/2)/\cos(\beta-\theta/2)]\}}{\tan(\beta-\theta/2)}$$

$$X = \frac{H\{\sin\phi-\cos\phi[\tan(\theta/2)/\cos(\beta-\theta/2)]\}}{\tan(\beta-\theta/2)}$$

Point E

$$Y = \frac{H\{\cos\phi-\sin\phi[\tan(\theta/2)/\cos(\beta-\theta/2)]\}}{\tan(\beta-\theta/2)}$$

$$X = \frac{H\{\sin\phi+\cos\phi[\tan(\theta/2)/\cos(\beta-\theta/2)]\}}{\tan(\beta-\theta/2)}$$

3.3 Raster on FSS

The useful diameter (D) of the flying spot scanner is nine inches. The footprints on the transparency are of a size which will permit their counterparts on the FSS to be enlarged by a factor of 1.25. The FSS raster extremes are shown in Figures D-14a and D-14b.

3.4 Optics

The required magnification (m) is 1/1.25 = 0.8. The existing 150mm focal length (F) lens will be utilized. The FSS phosphor to transparency emulsion distance (Z) can be found by (Figure D-15)

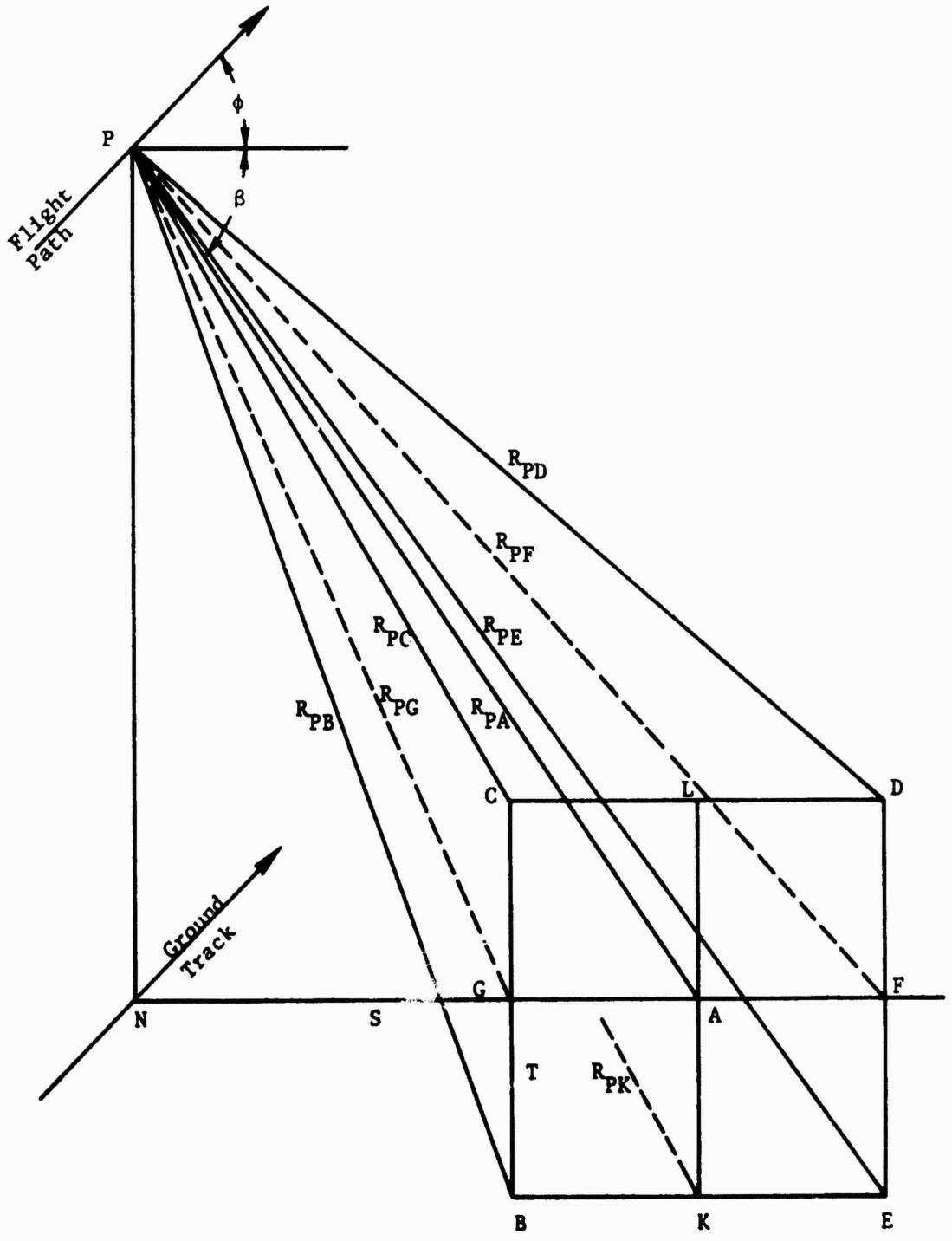

Figure D-12. Viewing Geometry for Slewable TV Camera Simulation

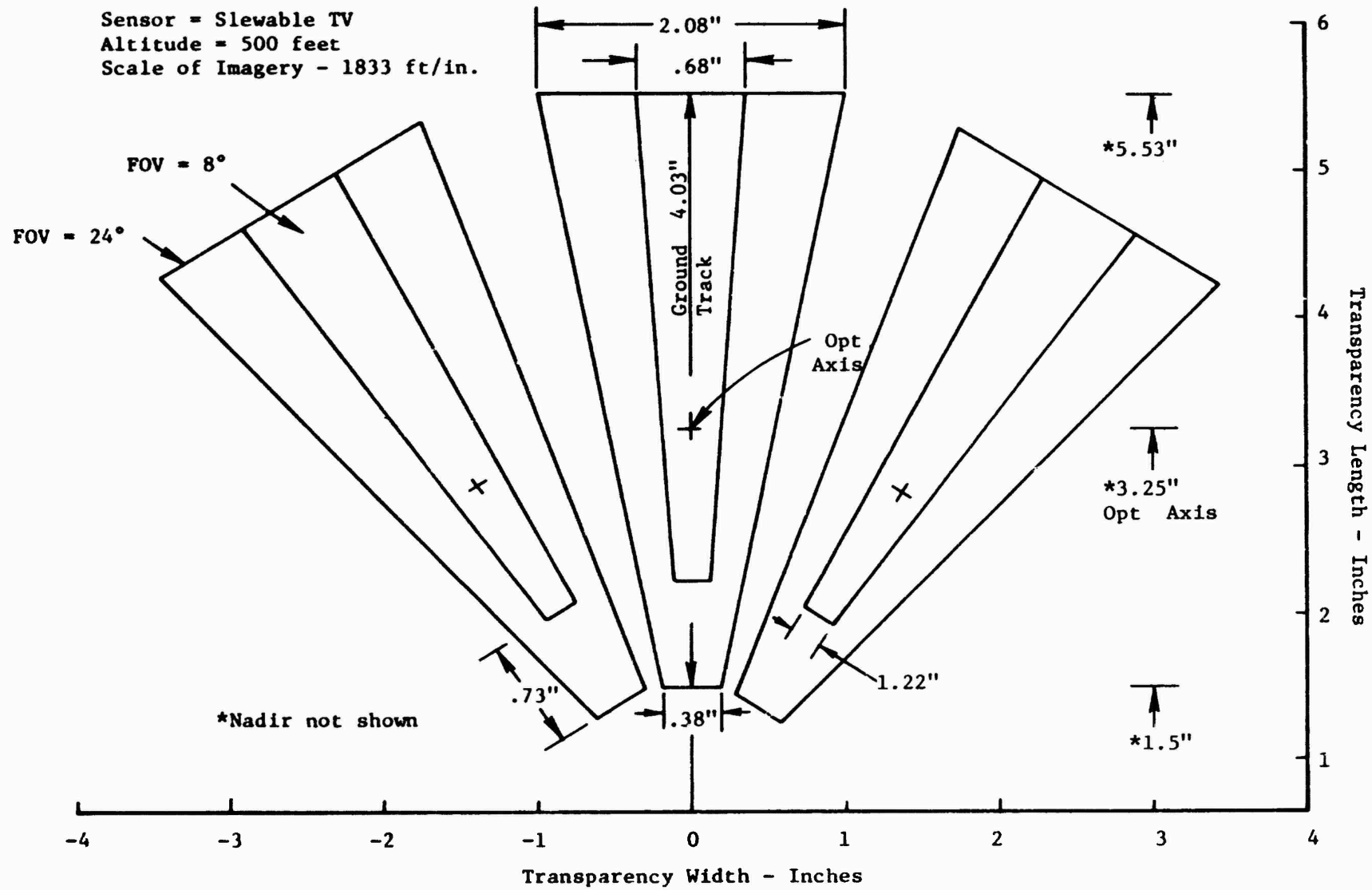

Figure D-13a. Geometry for Slewable TV Camera Footprints on Transparancy (Dep. Angle = 6 deg)

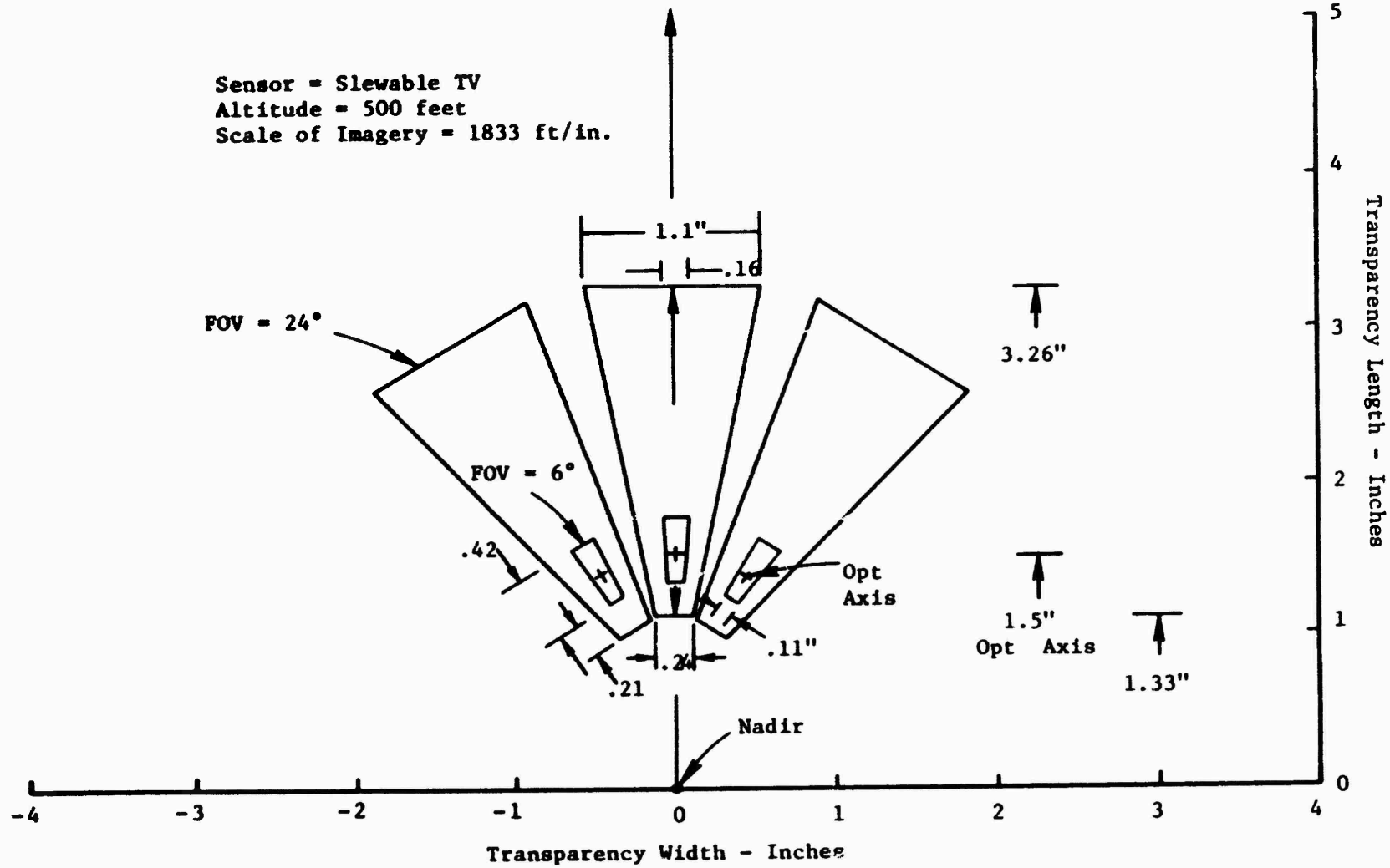

Figure D-13b. Geometry for Slewable TV Camera Footprints on Transparency (Dep. Angle = 18 deg)

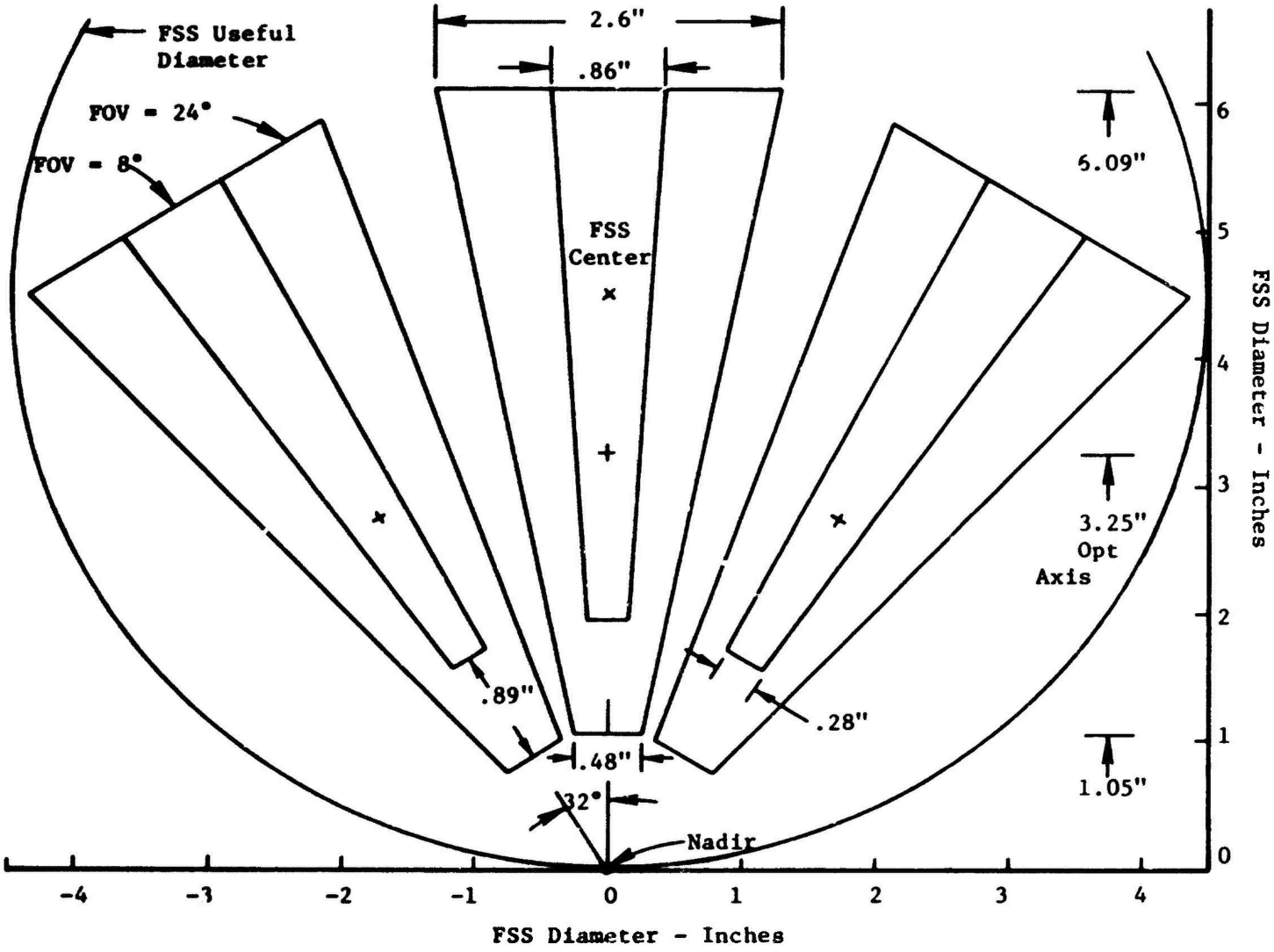

Figure D-14a. Geometry for Slewable TV Camera FSS Rasters (Dep. Angle = 6 deg)

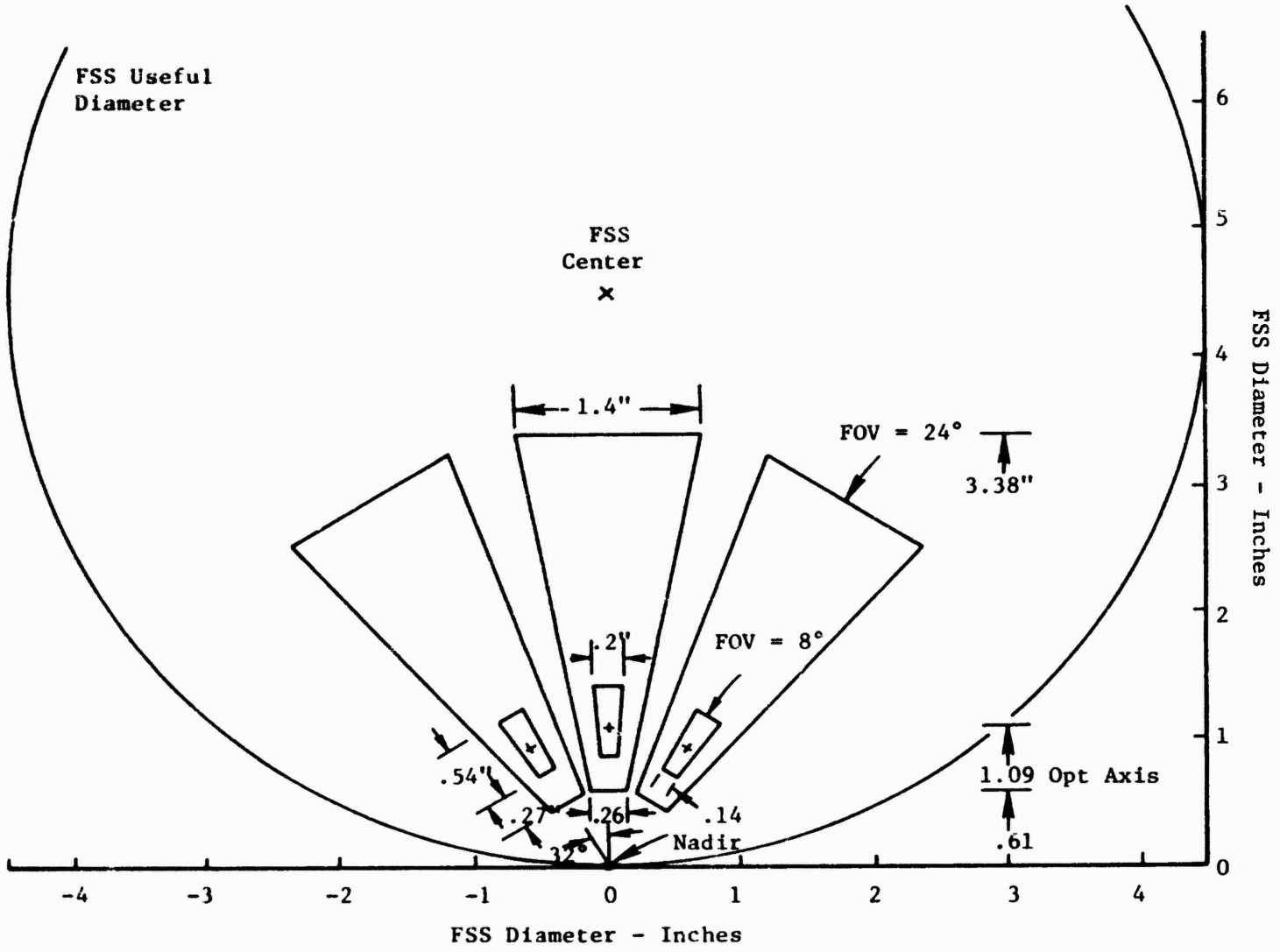

Figure D-14b. Geometry for Slewable TV Camera FSS Rasters (Dep. Angle = 18 deg)

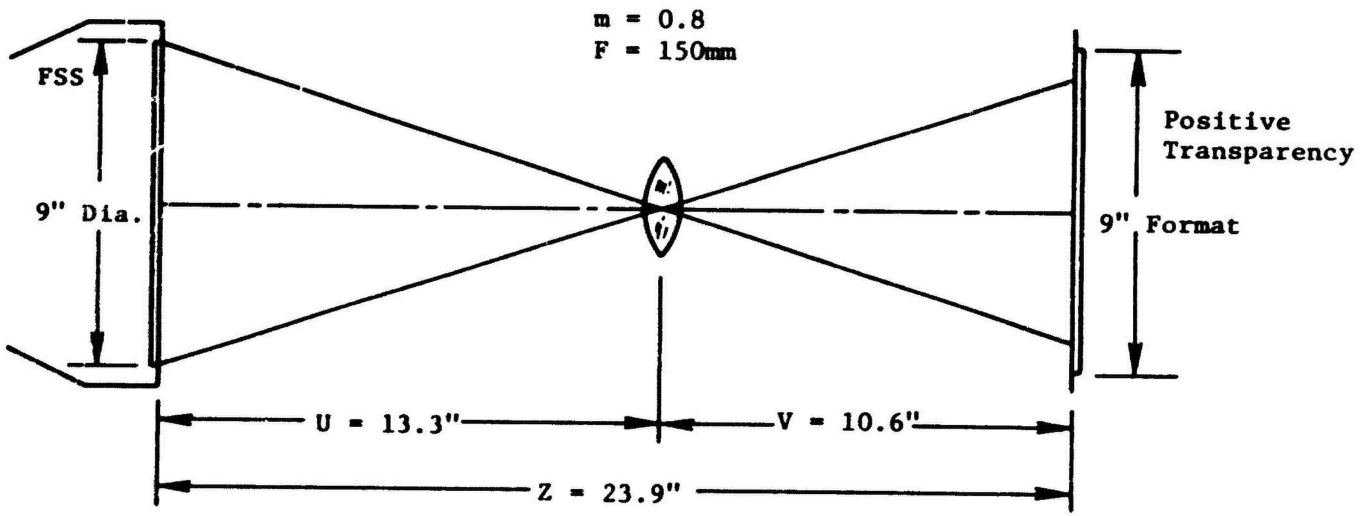

Figure D-15. Optical Geometry for Slewable TV Camera.

$$Z = \frac{F(m+1)^2}{m} \qquad \text{(D-12)}$$

$$= 23.9 \text{ inches}$$

Lens to FSS phosphor distance (U) is related by

$$U = \frac{F}{m} + F \qquad \text{(D-13)}$$

$$= 13.3 \text{ inches}$$

Lens to positive transparency emulsion distance (V) can be found by

$$V = Fm + F \qquad \text{(D-14)}$$

$$= 10.6 \text{ inches}$$

3.5 Transparency Velocity

Transparency velocity (V_t) can be found by dividing the ground velocity (V_g) by the number of feet per inch recorded on the transparency. Thus, a transparency velocity of 0.322 inches per second is required to simulate V_g = 350 knots, and 0.460 inches per second is required to simulate V_g = 500 knots.

REFERENCES

AFM 200-50, Image Interpretation Handbook, Volume 1, NRTSC, December 1967.

Birnbaum, A.H., A Systems Approach to Interpretation Research, U.S. Army Behavioral Science Research Laboratory, Arlington, Virginia, August 1969.

Blackwell, H.R., "Contrast Thresholds of the Human Eye," Journal of the Optical Society of America, 1946.

Brainard, R.W., Resolution Requirements for Identification of Targets in Television Imagery, NA63H-794, North American Rockwell Corporation, Columbus, Ohio, 1965.

Bruns, R.A., Dynamic Target Identification on Television as a Function of Display Size, Viewing Distance, and Target Motion Rate, TP-70-60, Naval Missile Center, Pt. Mugu, California, November 1970.

Erickson, R.A., Television Displays, Naval Weapons Center, China Lake, California, August 1969.

Fowler, F.O. and D.B. Jones, Target Acquisition Studies, OR 11,901, Martin Marietta Corporation, Orlando, Florida, April 1972.

Freitag, M. and S. MacLeod, The Effect of Scene Rotation of Target Acquisition and Tracking, AMRL-TR-74-19, Wright-Patterson Air Force Base, Ohio, March 1974. [AD A008208]

Johnson, J., "Analysis of Image Forming Systems," Proceedings of the Image Intensifier Symposium, Fort Belvoir, Virginia, October 1958.

Kirk, Roger E., Experimental Design: Procedures for the Behavioral Sciences, Brooks/Cole Publishing Company, Belmont, California, 1969. (Pages 63-67 tranformations; 80-01 Scheffes S.)

Krebs, M.J. and C.P. Graf, Real-Time Display Parameters Study, RADAC-TR-73-300, Honeywell Inc., September 1973.

Ludvig, E.J. and J.W. Miller, Joint Project NM 001 015, Kresage Eye Institute and Naval School of Medicine, 1953.

Miller, J.W. and E.J. Ludvig, "The Effects of Relative Motion on Visual Acuity," Survey of Opthamology, Volume 7, 1962.

Naval Weapons Center, Night Displays/One Man Aircraft Compatibility Study, NWC TP 5091, China Lake, California, January 1971.

Self, H.C., Acquisition Slant Ranges for Targets, AMRL-TR-70-96, Aerospace Medical Research Laboratory, Wright-Patterson Air Force Base, Ohio, May 1971. [AD 727772]

Snedecor, George W. and William G. Cochran, Statistical Methods, 6th Ed., Iowa State University Press, Ames, Iowa, 1967. (Pages 296-298 Bartlett's Test of Homogeneity; 349-350 Orthogonal Contrasts.)

Van Den Brink, G., Retinal Summarion and the Visibility of Moving Objects, Institute of Perception, The Netherlands, 1969.

Wallace, A.G., Levine, S.H., Logan, J.H., and Struharik, J.A., Aspect Angle Considerations in Efficiency of Photo Intelligence Extraction, G 839, McDonnell Aircraft Company, St. Louis, Missouri, December 1968.

Winer, B.J., Statistical Principles in Experimental Design, McGraw-Hill Book Company, New York, 1962. (Pages 105-140, single-factor experiments having repeated measures on the same elements; 298-379, multifactor experiments having repeated measures on the same elements.)

*U.S.Government Printing Office: 1977 — 757-001/20